Luis Mayor López

CHARACTERIZATION AND MODELLING OF STRUCTURAL CHANGES IN FRUITS AND VEGETABLE TISSUE SUBMITTED TO DEHYDRATION PROCESSES

Universidade do Porto
FEUP Faculdade de Engenharia
Departamento de Engenharia Química

2006

Luis Mayor López

CHARACTERIZATION AND MODELLING OF STRUCTURAL CHANGES IN FRUITS AND VEGETABLE TISSUE SUBMITTED TO DEHYDRATION PROCESSES

A thesis presented to the Faculty of Engineering of the University of Porto, in partial fulfilment of the requirements for the degree of Doctor of Philosophy in Engineering Sciences

Thesis prepared under the supervision of Dr. Alberto M. Sereno, Associate Professor at the Department of Chemical Engineering of the University of Porto

Universidade do Porto
FEUP Faculdade de Engenharia
Departamento de Engenharia Química

2006

This work was accomplished with the financial support
of the Fundação para a Ciência e a Tecnologia
(Ph. D. Grant SFRH/BD/3414/2000)

Als meus pares,

Rafaela i Lluís

ACKNOWLEDGEMENTS

I would like to express my most special gratitude Professor Alberto Sereno not only for his advice and assistance in this research but also for his support at personal level.

Thanks to Professors Ramón Moreira and Francisco Chenlo, from the University of Santiago de Compostela (Spain); Professors Rosiane Lopes da Cunha and Maria Aparecida Silva, from the University of Campinas (Brasil) and Professor José Pissarra, from the University of Porto (Portugal) for their advice and suggestions to specific parts of this work.

To my colleagues and friends in the Laboratory of Food Engineering and Rheology in FEUP: Marta, Carla, Duarte, Cheng, Fabio and Loïc. It was a pleasure to live and work with you.

To the Department of Chemical Engineering at the Faculty of Engineering of the University of Porto, for hosting and providing resources to carry out this work.

To the Fundação para a Ciência e a Tecnologia for its financial support.

To my friends Lina, Zé, Jaime, Andrea, Ivan, Marta, Ricardo, Claudia, Olga, Serafina, Oscar, Herney, Alis, Mariana, Hiléia, José Miguel and others for all the good moments lived together here in Porto.

To Esperanza for everything.

To my family, for their continuous encouragement in spite of the distance.

ABSTRACT

Osmotic dehydration is a water removal process that consists of placing foods, such as pieces of fruits and vegetables, in a hypertonic solution. The removal of water is accompanied by the simultaneous counter diffusion of solutes from the osmotic solution into the vegetable tissue. Both mass fluxes lead to a decrease of the water activity in the product, increasing its shelf life. It can be used as a single dehydration process or as a pre-treatment of other processes such as drying, pasteurization or freezing.

Heat and mass transfer gradients associated to the process produce changes in the chemical, physical and structural characteristics of the vegetable tissue. The knowledge and prediction of these changes are very important because they affect the quality of the final product, process modelling and design of process equipment.

The objective of this work was the study, characterization and modelling of the physical and structural changes of vegetable tissue during osmotic dehydration.

For this purpose pumpkin fruits were chosen as a food model on the basis of its easy availability, uniformity and typical cellular structure.

Next, the kinetic of osmotic dehydration of pumpkin fruits was studied, varying the chemical composition of the aqueous osmotic solution (binary sucrose solutions, binary NaCl solutions and ternary sucrose/NaCl solutions), the concentration of the osmotic agents, temperature and process time. Water loss, sucrose and NaCl gain ranged 0-80%, 0-19% and 0-16% of the initial sample weight, respectively, depending on the existing experimental processing conditions. A simple model, based on Fick's second law of diffusion, was used to predict the changes of some kinetic parameters (water loss, solids gain, weight reduction and normalized moisture content) as a function of the process conditions, with a reasonable success. Effective coefficients of diffusion for water, sucrose and NaCl ranged 0.29 to 4.22 $x \cdot 10^{-9}$ m^2/s, 0.5 to 1.3 $x \cdot 10^{-9}$ m^2/s and 0.88 to 3.3 $x \cdot 10^{-9}$ m^2/s respectively, depending their value on the existing experimental processing conditions.

After that, the study of some selected physical properties during osmotic dehydration was performed, namely: sorption properties, shrinkage/density/porosity, colour, mechanical properties, and microstructural changes. Sucrose solutions were used in

all such studies, except in the case of shrinkage/density/porosity where binary NaCl solutions and ternary NaCl/sucrose solutions were also tested.

Concerning sorption properties, the sorption isotherms of fresh and osmotically dehydrated pumpkin samples were obtained, and experimental data was satisfactorily fitted to different models found in the literature (GAB, BET and Henderson models among others). When pumpkin parenchyma was osmotically treated, the sorption isotherm was not significantly changed compared with the non treated material. The results indicate that both products, fresh and osmotically-treated, can be stored in the same way.

For the study of porosity changes during dehydration, a new methodology to measure the particle volume of samples with high moisture content by means of a home built gas pycnometer was developed. The gas pycnometer reproducibility of 0.019 %, obtained with dried porous materials, was excellent when compared with a commercial helium pycnometer (0.018%). During the osmotic dehydration studies, shrinkage (ranging from 0 to 73% of the initial volume) was linearly correlated with water loss and weight reduction of samples. Porosity of osmotically dehydrated samples doubled the value for fresh samples. A model based on volume additivity of the chemical components of the material was used to predict particle volume and porosity of samples during dehydration.

Colour changes during osmotic dehydration were not very accentuated, and as an average of all the tested conditions lightness decreased ($\Delta L^* = -4.84$) whereas redness ($\Delta a^* = 2.80$), yellowness ($\Delta b^* = 4.25$) and croma ($\Delta C^* = 4.72$) increased after nine hours of treatment. The results suggested that colour changes are mainly due to pigment concentration (due to water removal) and changes in the internal structure during dehydration. Fractional conversion models showed acceptable correlations of the changes in colour during osmotic dehydration for a*, b* and croma; the colour change rate constants for each parameter were 0.39 h^{-1}, 0.43 h^{-1} and 0.41 h^{-1} respectively.

The mechanical properties of osmodehydrated pumpkin fruits were studied by means of compression tests. Fresh material showed apparent elastic modulus, failure stress and failure strain ranging 0.96-2.53 MPa, 250-630 kPa and 0.42-0.71 respectively. After dehydration and at low moisture contents, the tissue lost its firmness (the apparent elastic modulus decreased drastically), keeping its strength (failure stress showed only a slight decrease) but became more ductile (failure strain increased). Microscopic observation

before and during the compression tests allowed establishing some relations between the textural properties and the microstructure of the vegetable tissue. Firmness seems to be controlled by the turgor pressure of cells, whereas the failure properties are more related with the strength of adhesion of the fibres composing the parenchymatic tissue. Polynomial models were used to relate the changes in the aforementioned mechanical properties with the changes in moisture content during dehydration.

The microstructure of fresh and osmotically dehydrated pumpkin parenchymatic tissue was studied by microscopy observation and image analysis. Fresh pumpkin cells showed average values of 0.015 mm^2, 0.469 mm and 0.136 mm for cell area, cell perimeter and cell equivalent diameter, respectively; and 1.288, 0.831 and 0.871 for cellular elongation, roundness and compactness, respectively. After nine hours of osmotic treatment (in 60% sucrose solutions at 25 ºC), cellular area, equivalent diameter, roundness and compactness decreased, whereas elongation of cells increased and the cellular perimeter was maintained constant along the process. It was observed that the first microstructural changes are located in the external zones of the samples in contact with the osmotic solution, whereas the inner zones of the material only suffer changes in the final stage of the process (six-nine hours). This is likely related with the moisture profiles created in the material during dehydration. Empirical quadratic functions were used to relate the average shape and size parameters with the dehydration parameters water loss, weight reduction and normalized moisture content.

As a final conclusion, the changes in the studied physical properties during osmotic dehydration can be predicted from the process conditions employed (concentration of the osmotic solution, temperature and processing time) by means of the dehydration kinetics model and the proposed models for physical changes, since the latter are either a direct function of the processing conditions (colour changes) or indirectly, a function of dehydration parameters water loss, weight reduction or moisture content.

RESUMO

A desidratação osmótica é um processo de eliminação de água que consiste em introduzir alimentos, nomeadamente frutas e outros vegetais, numa solução hipertónica. A eliminação de água é acompanhada por uma contra difusão de solutos da solução osmótica para o interior do tecido vegetal. Estes fluxos de massa originam uma diminuição da actividade da água do produto, aumentando o seu tempo de vida útil. A desidratação osmótica pode ser utilizada como um único processo de desidratação, ou como um pré-tratamento de outros processos, nomeadamente de secagem, pasteurização ou congelação.

Os gradientes de calor e massa associados ao processo de desidratação osmótica originam modificações nas características químicas, físicas e estruturais do tecido vegetal, sendo o seu conhecimento e previsão muito importantes, na medida em que afectam não só a qualidade do produto final, mas também porque têm que ser considerados aquando da modelização do processo propriamente dito e no desdenho de equipamentos.

O objectivo deste trabalho foi o estudo, caracterização e previsão das alterações físicas e estruturais ocorridas durante a desidratação osmótica do tecido vegetal. Para este propósito escolheu-se para "alimento modelo" a abóbora, já que, para além de estar facilmente disponível no mercado, tem uma estrutura e uniformidade celulares típicas.

Posteriormente, estudaram-se as cinéticas de desidratação da abóbora, variando a composição química da solução osmótica (soluções aquosas de sacarose, de cloreto de sódio e soluções ternárias de sacarose e NaCl), a concentração do agente osmótico, a temperatura e o tempo de processamento. A perda de água, o ganho de sacarose e de NaCl relativamente ao peso inicial da amostra variaram numa gama de 0 a 80%, de 0 a 19% e de 0 a 16%, respectivamente, dependendo das condições de processamento. Um modelo simples, baseado na segunda lei de Fick da difusão, foi utilizado para prever, com razoável sucesso, as alterações de alguns parâmetros cinéticos (perda de água, ganho de sólidos, redução de peso e teor de humidade normalizado) em função das condições de processamento. Os coeficientes de difusão efectiva variaram entre 0.29 e 4.22 $x \cdot 10^{-9}$ m^2/s, para a água, 0.5 e 1.3 $x \cdot 10^{-9}$ m^2/s, para a sacarose e 0.88 e 3.3 $x \cdot 10^{-9}$ m^2/s, para o NaCl, consoante as condições de processo utilizadas.

Numa fase seguinte, estudaram-se algumas propriedades físicas em particular, nomeadamente propriedades de sorção, encolhimento/densidade/porosidade, cor, propriedades mecânicas e alterações microestruturais. Estes estudos foram efectuados utilizando-se soluções de sacarose. No caso concreto do estudo de encolhimento/densidade/porosidade utilizaram-se também soluções aquosas de NaCl e soluções aquosas de NaCl e sacarose.

No que diz respeito às propriedades de sorção, obtiveram-se as isotérmicas de sorção da abóbora fresca e desidratada osmoticamente, tendo os dados experimentais sido ajustados com diferentes modelos publicados na literatura (GAB, BET, Henderson, entre outros). Quando o tecido parenquimatoso de abóbora foi tratado osmoticamente, a isotérmica de sorção não mudou significativamente quando comparada com o material não tratado. Os resultados indicam, portanto, que ambos produtos, fresco e tratado osmoticamente, podem ser armazenados da mesma forma.

Para os estudos de porosidade durante a desidratação, desenvolveu-se uma nova metodologia para a medida do volume de partícula em materiais com humidade elevada, usando um picnómetro de gases. A reprodutibilidade do picnómetro de gases (0.019%), obtida com materiais secos porosos, foi excelente quando comparado com a de um picnómetro de hélio convencional (0.018%). Durante os estudos de desidratação osmótica o encolhimento, que oscila entre 0 e 73% do volume inicial, foi linearmente correlacionado com a perda de água e a redução de peso das amostras. A porosidade das amostras osmoticamente desidratadas duplicou o seu valor relativamente à das amostras frescas. Para a previsão do volume de partícula e a porosidade durante a desidratação utilizou-se um modelo baseado na aditividade de volumes dos componentes químicos do material.

As alterações de cor durante a desidratação osmótica não foram muito marcadas, tendo-se verificado que, para a média de todas as condições experimentadas, a luminosidade desceu ($\Delta L^* = -4.84$), enquanto que os parâmetros a* ($\Delta a^* = 2.80$), b* ($\Delta b^* = 4.25$) e croma ($\Delta C^* = 4.72$) aumentaram, após nove horas de tratamento. Os resultados sugerem que as mudanças de cor são principalmente devidas à concentração de pigmentos (pela eliminação da água) e a mudanças na estrutura interna durante a desidratação. Durante a desidratação, as alterações de cor, nomeadamente, dos parâmetros a*, b* e croma, foram bem correlacionadas com modelos do tipo "fractional conversion"; as constantes de

velocidade de mudança de cor para cada um dos parâmetros foram de 0.39 h^{-1}, 0.43 h^{-1} e 0.41 h^{-1} respectivamente.

As propriedades mecânicas da abóbora desidratada osmoticamente foram estudadas através de testes de compressão. O material fresco mostrou valores para o módulo de elasticidade aparente, tensão de ruptura e deformação de ruptura num intervalo de 0.96 a 2.53 MPa, 250 a 630 kPa e 0.42 a 0.71 respectivamente. Após a desidratação, e para baixo teor de humidade, o tecido perdeu a firmeza (o módulo de elasticidade aparente decresceu drasticamente), mantendo a sua força (a tensão de ruptura mostrou apenas uma pequena diminuição) mas ficou mais dúctil (a deformação de ruptura aumentou). Estabeleceram-se algumas relações entre as propriedades texturais e a microestrutura do tecido vegetal, procedendo-se para o efeito à observação microscópica das amostras antes e durante os testes de compressão. A firmeza parece estar controlada pela pressão de turgor das células, enquanto que as propriedades de ruptura estão mais relacionadas com a força de adesão das fibras que compõem o tecido parenquimatoso. A relação entre as alterações destas propriedades mecânicas e o teor de humidade das amostras foi descrita através de modelos polinomiais.

O estudo da microestrutura da abóbora fresca e osmoticamente desidratada foi efectuado através de observação microscópica e análise de imagem. As células de abóbora fresca mostraram valores médios de 0.015 mm^2, 0.469 mm e 0.136 mm para a área celular, o perímetro celular e o diâmetro equivalente celular, respectivamente, e de 1.288, 0.831 e 0.871 para a elongação celular, redondeza e compactamento, respectivamente. Depois de nove horas de tratamento osmótico (em soluções com 60% de sacarose, a 25 ºC), a área celular, o diâmetro equivalente, a redondeza e o compactamento diminuíram, enquanto que a elongação das células aumentou e o perímetro celular se manteve constante. As primeiras alterações microestruturais foram observadas na zona externa das amostras em contacto com a solução osmótica, enquanto que as zonas internas do material só sofreram alterações nas etapas finais do processo (após seis a nove horas de tratamento). Estes factos estão, provavelmente, relacionados com os perfis de humidade desenvolvidos no material durante a desidratação. Os valores médios dos parâmetros de forma e tamanho celular correlacionaram-se com os parâmetros de desidratação (perda de água, redução de peso e teor de humidade normalizado) através de funções quadráticas.

O trabalho efectuado permitiu concluir, que as modificações nas propriedades físicas estudadas durante a desidratação osmótica podem ser previstas a partir das condições de processamento utilizadas (concentração da solução osmótica, temperatura e tempo de processamento), usando para o efeito um modelo de cinéticas de desidratação e os modelos propostos para as mudanças físicas, já que estas últimas são funções directas das condições de processamento (mudança da cor) ou, indirectamente, função dos parâmetros de desidratação (perda de água, redução de peso ou teor de humidade normalizado).

RESUME

La déshydratation osmotique est un procédé d'élimination de l'eau qui consiste à placer des aliments tels que morceaux de fruits ou légumes, dans une solution hypertonique. L'élimination de l'eau s'accompagne de la contre diffusion simultanée des solutés de la solution osmotique dans le tissu de l'aliment. Les deux flux de masse conduisent à une diminution de l'activité de l'eau dans le produit, et ainsi augmentent sa durée de conservation. Ce procédé peut être utilisé comme un simple procédé de déshydratation ou comme un prétraitement préalable à d'autres traitements tels que séchage, pasteurisation ou congélation.

Les gradients de transferts de masse et de chaleur associés au procédé induisent des changements dans les caractéristiques structurelles, physiques et chimiques du tissu végétal. La connaissance et la prédiction de ces changements sont très importantes car ils affectent la qualité du produit final, la modélisation du procédé et la conception de l'équipement permettant le procédé.

L'objectif de ce travail est l'étude, la caractérisation et la modélisation des changements physiques et structurels du tissu végétal pendant la déshydratation osmotique.

A cet effet, les citrouilles ont été choisies comme fruits models parce qu'elles sont facilement disponibles et possèdent une structure cellulaire uniforme et typique.

Ensuite, la cinétique de déshydratation des citrouilles a été étudiée, en variant la composition chimique de la solution aqueuse osmotique (solutions binaires de sucrose, solutions binaires de NaCl et solutions ternaires de sucrose/NaCl), la concentration en agents osmotiques, la température et la durée du procédé. Suivant les conditions expérimentales utilisées, la perte en eau, le gain en sucrose et en NaCl sont compris entre 0 et 80%, 0 et 19% et 0 et 16%, respectivement, les pourcentages étant relatifs au poids initial de l'échantillon. Un modèle simple, basé sur la seconde loi de diffusion de Fick, a été utilisé afin de prédire, avec un succès raisonnable, les changements de certains paramètres cinétiques (perte en eau, gain en solides, réduction de poids et taux d'humidité normalisé) en fonction des conditions du procédé. Les coefficients effectifs de diffusion de l'eau, de la sucrose et du NaCl sont compris entre 0.29 et 4.22 $x \cdot 10^{-9}$ m^2/s, 0.5 et 1.3 $x \cdot 10^{-9}$ m^2/s et entre 0.88 et 3.3 $x \cdot 10^{-9}$ m^2/s respectivement, suivant les conditions expérimentales utilisées.

Par la suite, l'étude de la variation durant la déshydratation osmotique de certaines propriétés physiques sélectionnées, à savoir, les propriétés de sorption, le rétrécissement, la densité, la porosité, la couleur, les propriétés mécaniques et les changements micro structurels, a été entreprise. Des solutions de sucrose ont été utilisées dans toutes ces études, à l'exception des études de rétrécissement, de densité et de porosité, pourt lesquelles des solutions binaires de NaCl et des solutions ternaires NaCl/sucrose ont également été testées.

En ce qui concerne les propriétés de sorption, les isothermes de sorption des échantillons de citrouille frais et des échantillons de citrouille osmotiquement déshydratés, ont été obtenues. Les données expérimentales ont été ajustées de manière satisfaisante aux différents modèles rencontrés dans la littérature (modèles de GAB, BET et Henderson, entre autres). Lorsque la citrouille « parenchyma » est osmotiquement traitée, l'isotherme de sorption n'est pas significativement affectée en comparaison à l'isotherme du matériau non traité. Les résultats indiquent que les deux produits, le frais et celui traité osmotiquement, peuvent être conservés de la même manière.

En ce qui concerne l'étude des changements de porosité durant la déshydratation, une nouvelle méthodologie a été développée qui emploie un pycnomètre de gaz spécialement construit au laboratoire, et qui permet de mesurer le volume particulaire d'échantillons avec un grand taux d'humidité. La reproductibilité obtenue avec le pycnomètre de gaz est de 0.019 % lorsque des matériaux secs et poreux sont mesurés, ce qui est excellent comparé à la performance d'un pycnomètre commercial à hélium. Durant les études de déshydratation osmotique, le rétrécissement (qui a varié de 0 à 73% du volume initial) s'est trouvé être linéairement corrélé avec la perte en eau et la réduction en poids des échantillons. La porosité des échantillons osmotiquement déshydratés est le double de la porosité des échantillons frais. Un modèle basé sur l'additivité des volumes des composants chimiques du matériau, a été utilisé afin de prédire le volume particulaire et la porosité des échantillons au long de la déshydratation.

Les changements de couleur durant la déshydratation osmotique ne sont pas très accentués, et, en moyenne, pour toutes les conditions testées, la clarté décroît ($\Delta L^* = -4.84$) tandis que le rougeoiement ($\Delta a^* = 2.80$), le jaunissement ($\Delta b^* = 4.25$), et l'intensité chromatique ($\Delta C^* = 4.72$) augmentent après neuf heures de traitement. Les résultats

suggèrent que les changements de couleur sont principalement dus à des variations de concentrations en pigments associées à des changements dans la structure interne au long de la déshydratation. Des modèles de conversion fractionnelle présentent des corrélations acceptables des changements chromatiques pendant la déshydratation osmotique pour a*, b* et l'intensité chromatique; Les constantes de vitesse de changement chromatique pour chacun des paramètres sont respectivement 0.386 h^{-1}, 0.425 h^{-1} et 0.412 h^{-1}.

Les propriétés mécaniques des citrouilles osmotiquement déshydratées ont été étudiées au moyen de tests de compression. Le matériau frais présente un module élastique apparent compris entre 0.96 et 2.53 MPa, une contrainte à la fracture comprise entre 250 et 630 kPa et une déformation à la fracture comprise entre 0.42 et 0.71. Après la déshydratation et pour des taux d'humidité bas, le tissu perd de sa fermeté (le module élastique apparent décroît de manière drastique), tout en conservant sa robustesse (la contrainte à la fracture présente seulement une légère baisse), mais en devenant plus ductile (la déformation à la fracture croît). L'observation microscopique réalisée avant et pendant les tests de compression permet d'établir des relations entre les propriétés texturales et la microstructure du tissu végétal. La fermeté semble être contrôlée par la pression turgescente des cellules, tandis que les propriétés de fracture sont reliées à la force de l'adhésion des fibres qui composent le tissu parenchymateux. Des modèles polynomiaux ont été utilisés afin de relier les variations des propriétés mécaniques susmentionnées avec les variations de taux d'humidité pendant la déshydratation.

La micro structure du tissu parenchymateux de la citrouille fraîche et de la citrouille déshydratée osmotiquement a été étudiée par observation microscopique avec analyse d'image. Les cellules de citrouille fraîche présentent une surface cellulaire moyenne de 0.015 mm^2, un périmètre cellulaire moyen de 0.469 mm, un diamètre cellulaire équivalent moyen de 0.136 mm, une élongation cellulaire moyenne de 1.288, une sphéricité moyenne de 0.831 et une compacité moyenne de 0.871. Après neuf heures de traitement osmotique (dans une solution de sucrose à 60% et à 25 ºC), la surface cellulaire, le diamètre équivalent, la sphéricité et la compacité décroissent, tandis que l'élongation des cellules augmente et que le périmètre cellulaire est maintenu constant pendant le procédé.

Nous avons observé que les premiers changements micro structurels sont localisés dans les zones externes de l'échantillon qui sont en contact avec la solution osmotique,

tandis que les zones intérieures du matériau subissent des changements seulement à l'étape finale (six-neuf heures) du processus. Ceci est probablement associé aux profils d'humidité créés dans le matériau au long de la déshydratation. Des fonctions quadratiques empiriques ont été utilisées afin de relier la forme moyenne et les paramètres dimensionnels avec les paramètres de déshydratation tels que perte en eau, réduction de poids et taux d'humidité normalisé.

En conclusion, les variations des propriétés physiques étudiées pendant la déshydratation osmotique peuvent être prédites à partir des conditions (concentration de la solution osmotique, température et durée de la déshydratation) employées durant le procédé, en utilisant un modèle de cinétique de déshydratation et les modèles proposés pour les variations physiques, puisque ces dernières sont soit une fonction directe des conditions du procédés (variations chromatique), ou indirectement, une fonction des paramètres de déshydratation tels que perte en eau, réduction de poids ou taux d'humidité.

TABLE OF CONTENTS

LIST OF FIGURES

LIST OF TABLES

CHAPTER 1

INTRODUCTION

CHAPTER 1. INTRODUCTION

1.1. Dehydration of foods

1.1.1. Historical background

Dehydration is probably the oldest method of food preservation. The origin of food dehydration came from the prehistory, when man sun dried foods to sustain him in off-season periods. Brennan (1994) reported that around 20.000 BC meat was cut into strips and sun dried in Russia; and "more recently" in ancient Egypt (2800-2300 BC) fruits such as apples, grapes and apricots were dried with the same method. Other traditional dehydrated products have an ancient origin, such as the drying of tea in India (300-400 AD), and the sun drying of different foods (fruits, vegetables, fish, meat) in Japan (710-785 AD) and fish in Norway (900 AD).

It was in the past century when the "art of dehydration" was translated into terms of science and technology. An important advance in the dehydration of foods and other products was made by Sherwood (1929), who in his work "Drying of solids" carried out a rigorous scientific analysis of the mechanisms of drying and considered the drying process as a unit operation differenced from the others. Later efforts in the past century up to date has been done in developing new dehydration techniques and equipment, as well as the understanding of the physical-chemical phenomena involved on them.

Nowadays, the variety of dehydrated food products, produced with different dehydration techniques is considerable. As commented by Mujumdar (1995), the future research on dehydration should be oriented to the improvement of energy conservation, to increase productivity, to a better product quality, to quality control, to new products and new processes, and safer and environmentally superior operations among other aspects.

1.1.2. Definition

The most used definition of the term "dehydration" is the unit operation in which part of the water present in a material is removed by evaporation or sublimation as a result of the application of heat (Brennan, 1994). The term "drying" has been defined as the process of thermally removing volatile substances to yield a solid product (Mujumdar and Menon, 1995). Although the second definition includes not only water but also other substances such as organic compounds, both definitions are used with the same meaning in the dehydration of foods and other materials. These definitions exclude mechanical dewatering methods, such as filtration, centrifugation or expression. Osmotic dehydration, a dewatering technique that is not included in both definitions, has been accepted as a dehydration method because the objectives of this process are basically the same as those found in other food dehydration methods, as explained below.

1.1.3. Objectives of food dehydration

The main objective of food dehydration is to prolong the shelf life of the fresh material. The removal of water leads to a reduction of the water activity (a_w) of the food, which inhibits the growth of microorganisms and reduces enzymatic activity and the rate of undesirable chemical reactions.

In some cases, organoleptic and nutritional qualities of the food are improved after dehydration. In products such as raisins, peanuts, some fish and meat, the consumer is looking for a dehydrated product because its special organoleptic qualities.

The removal of water leads to a reduction of weight and volume in the product. These changes often lead to substantial savings in the cost of packaging, handling, transporting and storage compared with the fresh product.

When the application of heat is adequate, dehydration can have a sanitation effect. Insects and microorganisms can be destroyed during the application of heat and moisture reduction.

Further processing can be improved by dehydration. Processes such as milling, mixing and segregation can be facilitated after dehydration.

1.1.4 Dehydration methods

Several types of dryers and dehydration methods, each one better suited for a particular situation, are commercially used to remove moisture from a wide variety of food products. As discussed by Jayaraman and Das Gupta, (1992), the selection of a particular dryer and dehydrating method depend on a number of factors that include the form of the raw material and its properties, the desired physical form and characteristics of the finished product, the required operating conditions and operation costs.

Several classifications have been proposed according to different criteria. The most common is to classify the drying methods on the basis of the heat transfer mechanism involved in the process. Other common classifications are based on the type of drying vessel (Mujumdar and Menon, 1995), on the operation temperature and pressure (Keey, 1978) and by dividing the methods in adiabatic and non adiabatic (Sokhansanj and Jayas, 1995).

Because these classifications do not easily include methods such as freeze drying or osmotic dehydration, an alternative classification is proposed in this work. The alternative consists in classifying the methods as a function of the physical change that water suffers when leaves the material. Accordingly, three main groups of dehydration methods are presented, as follows: methods in which water is removed by evaporation, methods in which water is removed by sublimation, and methods in which water is removed in liquid state (with no phase change).

1.1.4.1. Methods in which water is removed by evaporation

The necessary sensible and latent heat of evaporation must be supplied to the food, while water or water vapour must move within the food to the evaporating surface and the water vapour must transfer from that surface to the surrounding atmosphere.

a. Heated air is in the drying medium: convective drying methods

During the drying of a wet solid in heated air, the air supplies the necessary sensible and latent heat and also acts as a carrier for the water vapour formed, moving it away from the drying surface and permitting further evaporation to occur. Some systems for drying foods with these methods are cabinet drying, conveyor drying, fluidized bed drying, pneumatic drying and rotary drying. Spray drying is the most common method used for drying food liquids in heated air.

b. The food is placed in contact with a heated surface: Conductive drying methods

If a wet material is placed in contact with a heated surface the necessary sensible and latent heat of evaporation is transferred to the material by conduction and drying can take place. When drying is carried out at atmospheric pressure, the material can be applied in a thin layer onto the heated surface to reduce drying time and thermal damage of the material, as in the drum drying method.

Drying may be also carried out under reduced pressure, so as to decrease temperature of water evaporation and increase the drying rates, as in the case of vacuum driers.

In the azeotropic dehydration, a solvent is added to the food, which forms a low-boiling point azeotrope with water. The azeotrope is removed under vacuum. Boiling

temperature depends on the solvent used and the pressure in the chamber. Ethyl alcohol and ethyl acetate have been used as solvents. No report of commercial application of azeotropic drying was found (Salunkhe *et al*. 1991) but this process has potential application to frozen foods, vegetables and fruits, attaining in some cases very good organoleptic properties, comparable with freeze-dried products (Brennan, 1994).

c. The food is exposed to radiant heat: radiation drying methods

Three types of electromagnetic radiation are used for dehydrating purposes: dielectric, microwave and infrared radiation.

Infrared radiation, which is emitted by hot objects, occupies the wavelength range 0.7 μm to 300 μm. Infrared dehydration is used to remove small amounts of moisture from granular materials such as breadcrumbs, spices and starches. Approximately 48% of solar energy falls within the infrared range of frequencies. Solar drying is widely practised where sufficient sunlight is available.

It is generally accepted that dielectric heating is done at frequencies between 1 and 100 MHz, whereas microwave heating occurs between 300 MHz and 300 GHz (Schiffmann, 1995). The application of these radio waves produces some effects at molecular level in the material, such as ionic conduction and dipolar polarization among others, which converts the electromagnetic energy into heat.

1.1.4.2. Water is removed by sublimation. Freeze drying

This method involves freezing the material, followed by subsequent sublimation of the ice from the frozen state to give a dried product. Sublimation occurs when the water vapour pressure in the immediate surroundings of the frozen material is less than that at the ice front within the material. This water vapour pressure gradient is achieved by placing the

frozen food in a vacuum cabinet and reducing the pressure to levels of the order of 13.5-270 N m^{-2} (Brennan, 1994). Freeze drying is an expensive process, which is often applied to highly valued foods or to heat sensitive products. After dehydration the dried product shows minimal thermal degradation and a highly porous structure with an excellent rehydration capability.

1.1.4.3. Water is removed with no phase change. Osmotic dehydration

Osmotic dehydration is a water removal process common with food materials that consists of placing pieces of the material in a hypertonic solution. Since this solution has higher osmotic pressure and hence lower water activity, a driving force for water removal arises between solution and food, while the natural cell wall acts as semipermeable membrane. As the membrane is only partially selective, there is always some diffusion of solute from the solution into the food and vice versa. The technique is often used as a pre-treatment of other process, to produce intermediate moisture foods with improved shelf life characteristics, or as a pre-treatment to reduce the energy consumption and/or heat damage in other traditional dehydration processes.

1.2. Osmotic dehydration

Osmotic dehydration is used for the partial removal of water from biological tissues by immersion in a hypertonic osmotic solution. The driving force for the transport of water from the tissue into the solution is provided by the higher osmotic pressure of the hypertonic solution. The diffusion of water is accompanied by the simultaneous counter diffusion of solutes from the osmotic solution into the tissue. Since the membrane responsible for osmotic transport is not perfectly selective, other solutes present in the cells can also be leached in the osmotic solution (Giangiacomo *et al*., 1987).

1.2.1. Applications of the osmotic dehydration processes

Osmotic treatments are conducted with the objective of water removal, impregnation with substances from the osmotic solution or a combination of both. The product obtained can be classified as an intermediate moisture food (IMF). This kind of foods has a water activity between 0.6 and 0.9 (Labuza, 1980); some of them are microbiologically stable, but are susceptible to chemical changes (Lewicki and Lenart, 1995). The microbiological stability of the IMF is due to sufficiently low water activity in the material. Dried plums, figs, and raisins, candied fruits, cottage ham and dry sausage are good examples of this type of foods.

In osmodehydrated products, this reduction of water activity is due both to the removal of water and to the addition of humectants (sugars, sodium chloride, polyalcohols). However, the process does not reduce water activity sufficiently to completely hinder the proliferation of microorganisms. The process extends, to some degree, the shelf life of the material, but does not preserve it. Hence, the application of other preservation methods is necessary. However, processing of osmotically dehydrated semiproducts is much less expensive and preserves most of the characteristics acquired during the osmosis. Although most studies of osmotically dehydrated products have been done with vegetables and fruits,

some of them have been also performed with meat (Gerelt *et al*. 2000) and fish (Corzo and Bracho, 2005).

Osmotically treated materials may be processed into finished products by applying just a stabilising operation such as pasteurisation (Forni *et al*., 1993), addition of preservatives and/or acidification (Monsalve-González *et al*. 1993).

Osmotic dehydration has also been used as a pre-treatment to different drying operations, such as freeze drying (Hawkes and Flink, 1978), convective drying (Kim and Toledo, 1987; Mandala *et al*., 2005), vacuum drying (Dixon and Jen, 1977) and microwave drying (Prothon *et al*., 2001). One of the benefits of an osmotic pre-treatment before drying is the energy saving due to the removal of water without phase change (Bolin *et al*. 1983). Estimates of energy consumption per kg of water removed for convective drying of foods were at least twice as much as needed for osmotic dehydration (Lewicki and Lenart, 1995). It also increases sugar to acid ratio, and improves the texture of the material and the stability of pigments during drying and storage (Raoult-Wack, 1994)

Before freezing, an osmotic treatment may be applied with the objective of reducing refrigeration loads by water removal from the tissue and improving storage with the addition of cryoprotectants (Chiralt *et al*. 2001). If the water removal before freezing is considerable, the combined process of osmotic dehydration and freezing has been called osmodehydrofreezing (Tregunno and Goff, 1996). This process has been proposed for the preparation of intermediate moisture fruit ingredients for different applications, such as fruit cubes for dairy products and fruit pastry fillings (Spiess and Behsnilian, 1998).

A pre-treatment to attain concentrations of about 20-24 Brix has been proposed for canned fruit with enhanced natural flavour and better colour and texture stability, by increasing the resistance of the tissue to the following heat treatment (Torreggiani, 1993).

Figure 1.1 shows a synopsis of the state of the art of the applications of osmotic dehydration in food processing. In spite of the wide range of applications described and the

ability of improvement of the overall quality of processed foods showed by osmotic treatments, industrial application on a large scale is still limited. Some of the problems deal with the industrial scaling of the process and the optimization of the osmotic solution management.

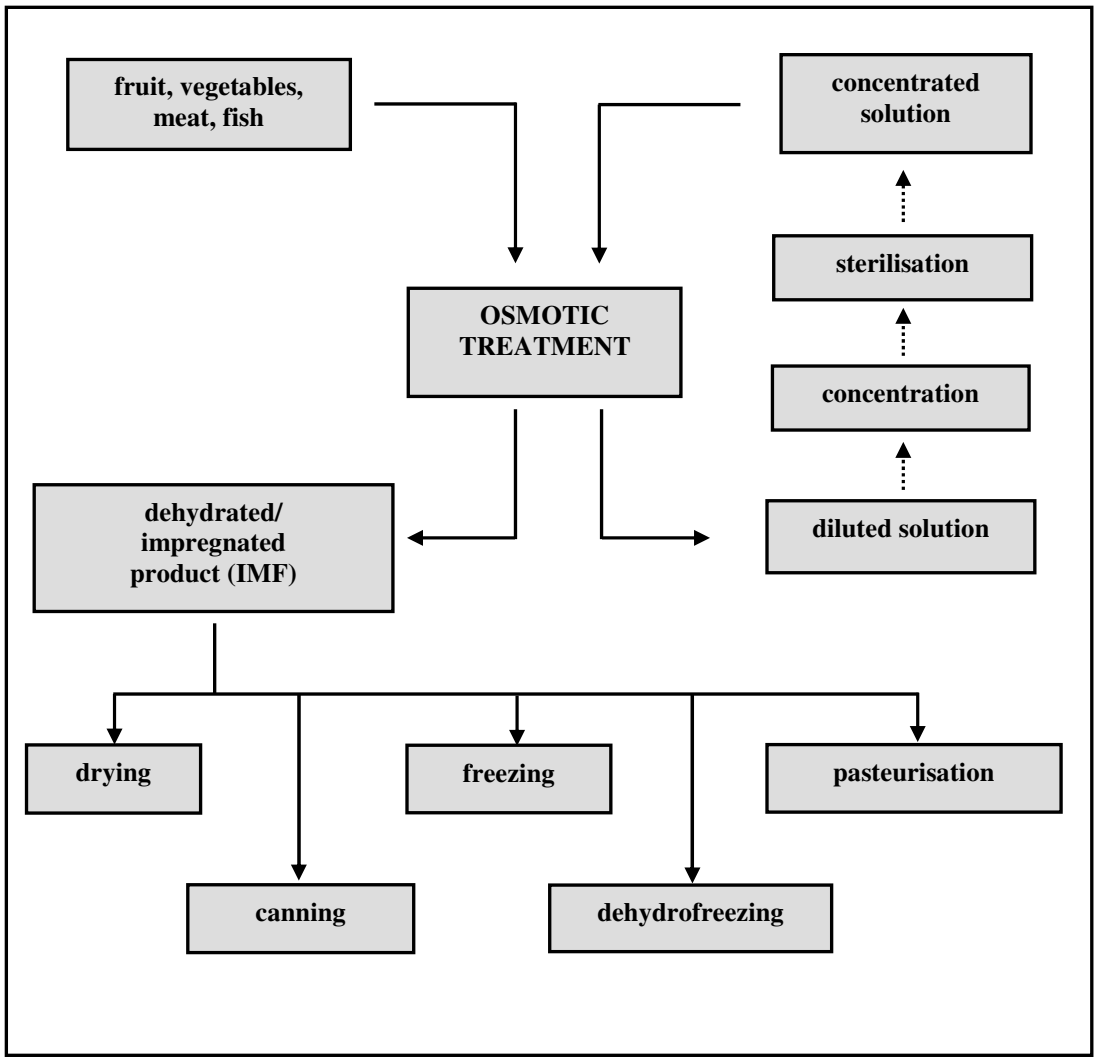

Figure 1.1. Some applications of osmotic treatments in food processing. (Adapted from Spiess and Behsnilian, 1998).

1.2.2. Osmotic dehydration phenomena

1.2.2.1. Osmotic pressure

An osmotic pressure arises when two solutions of different concentration (or a pure solvent and a solution) are separated by a semipermeable membrane (i.e. permeable to the solvent but impermeable to the solute). This situation is illustrated in Figure 1.2 (a). Here the membrane separates two liquid phases, a concentrated phase 1 and a diluted phase 2.

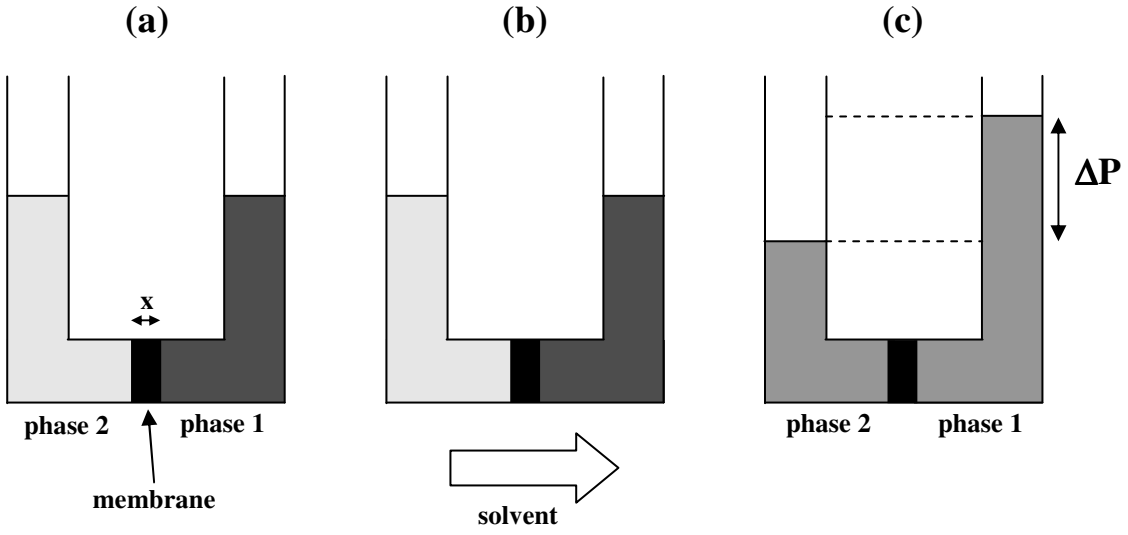

Figure 1.2. Schematic illustration of an osmotic process.

Under isothermal conditions the chemical potential of the solvent in the concentrated phase (phase 1) is given by (Mulder, 1996)

$$\mu_{s,1} = \mu^{o}_{s,1} + RT \ln a_{s,1} + V_s P_1 \qquad (1.1)$$

While the chemical potential of the solvent in the diluted phase (phase 2) is given by

$$\mu_{s,2} = \mu^{o}_{s,2} + RT \ln a_{s,2} + V_s P_2 \qquad (1.2)$$

The solvent molecules in the diluted phase have a higher (more negative) chemical potential than those in the concentrated phase. This chemical potential difference causes a flow of molecules of solvent from the diluted phase to the concentrated phase (the flow is proportional to $-\partial\mu/\partial x$). This is shown in Figure 1.2 (b). This process continues until osmotic equilibrium is reached, i.e. when the chemical potentials of the solvent molecules in both phases are equal (Fig. 1.2 (c)).

$$\mu_{s,1} = \mu_{s,2} \tag{1.3}$$

Combining Eqs. 1.1, 1.2 and 1.3, gives

$$RT(\ln a_{s,2} - \ln a_{s,1}) = (P_1 - P_2)V_s = \Pi \cdot V_s \tag{1.4}$$

This hydrodynamic pressure difference (P_1-P_2) is called the osmotic pressure difference Π. When only pure solvent is situated on one side of the membrane (phase 2), $a_{s,2} = 1$, and Eq. (1.4) becomes

$$\Pi = -\frac{RT}{V_s}\ln a_{s,1} \tag{1.5}$$

if water is the solvent, Eq. (1.5) can be written as

$$\Pi = -\frac{RT}{V_w}\ln a_w \tag{1.6}$$

where a_w is the water activity of the aqueous solution in phase 1.

The phenomenon of osmotic dehydration of foods comes as a consequence of the difference of chemical potential between the water solution inside the cells of the food material and the osmotic solution that surrounds it. The cellular membrane, permeable to

water but not (or partially) permeable to the osmotic agent, acts as the semipermeable membrane needed to create the osmotic effect.

1.2.2.2. Structure of the plant cell

Since most of the osmotic dehydration treatments are carried out with fruit and vegetables, the knowledge of the vegetable tissue structure is important to understand the different mass transfer mechanisms that occur during processing. A simplified explanation of the structure of the plant cell is given in this section. Additionally, a classification of the different plant tissues and some of their relevant characteristics are presented in 1.3.2

Vegetable products undergoing processing come from different parts of a plant, such as roots (carrots), stems (potatoes), leaves (spinach) fruits (apples) or seeds (beans). These parts of the plant are composed by different groups of cells specialized in concrete functions. These specialized groups of cells are called tissues.

The plant cell (Fig. 1.3) is the basic unit of the vegetable tissue. It has two main components: the protoplast and the cell wall. Cellulose is the main component of the cell wall; other components include pectins, hemicelluloses and mineral compounds. The cell wall is permeable to water and low molecular weight compounds and is not a barrier in solute transport from/to cell.

The middle lamella is a layer composed of pectic substances and protein. It is shared by adjacent cells, and its function is acting as cement between the cell walls of adjacent cells.

The cell wall is perforated and the channels are filled with thin strands of protoplasm, assuring the contact between protoplasts of neighbouring cells. These strands are called plasmodesmata.

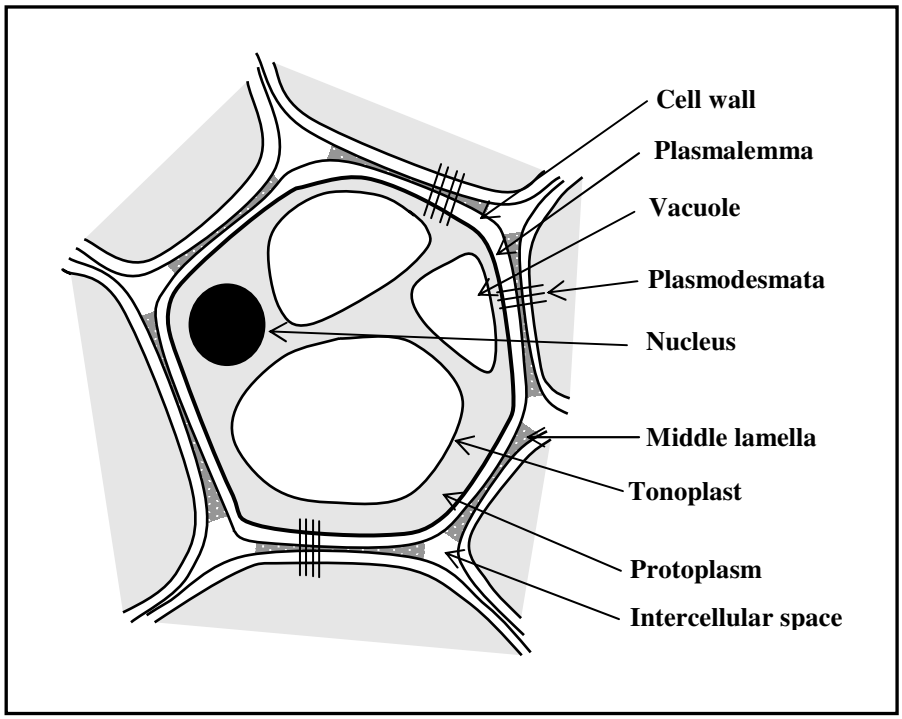

Figure 1.3. A simplified plant cell.

The protoplast is composed of protoplasm enclosed in a membrane called plasmalemma, vacuoles, and other structural elements such as nucleus, plastids and so on. The plasmalemma is a protein-lipid layer that regulates the contact between the protoplast and the environment. It is permeable to water and selectively permeable to other substances. The protoplasm is a colloidal solution of proteins and lipoproteins in water. The vacuoles are suspended in protoplasm and are enclosed in membranes called tonoplasts. They contain a solution of minerals, sugars, and other organic compounds in water.

1.2.2.3. Mass transfer fluxes during osmotic dehydration

From an engineering point of view, the plant material can be considered as a capillary porous body that is divided internally in numerous repeating units. Some capillaries and pores are filled with a solution, while others are empty (contain air). Most capillaries and pores are open, and repeating units (cells) can exchange water between each other (Lewicki and Lenart, 1995).

There are three main potential pathways that water can follow while traversing plant tissue (Shi and Le Maguer, 2002):

a) The apoplastic transport pathway (cell wall pathway), which occurs outside the cell membranes (plasmalemma) and can be defined as water diffusion through cell walls and intercellular spaces between cells

b) The symplastic transport pathway (symplasm pathway), which is inside the plasmalemma and characterized by a fluid transport from one cell directly into another through the small channels of plasmodesmata.

c) The transmembrane transport pathway (vacuolar pathway), which is defined as a water exchange route between the cell interior (protoplasm and vacuole) and the cell exterior (cell wall and intercellular space) across the cell membrane.

It is generally agreed that the cell wall provides the major pathway of water movement in the material. The ratio of volume flows in the apoplastic/simplastic pathways is of the order 50/1 in leaf tissue and lower for the root cortex (Lewicki and Lenart, 1995).

When a cellular solid material is immersed in an osmotic solution, the cells in the first layer of the material contact the osmotic solution and begin to loose water due to the chemical potential gradient between cells and osmotic solution. The cells also begin to shrink due to the water loss. Figure 1.4 shows and schematic representation of the process.

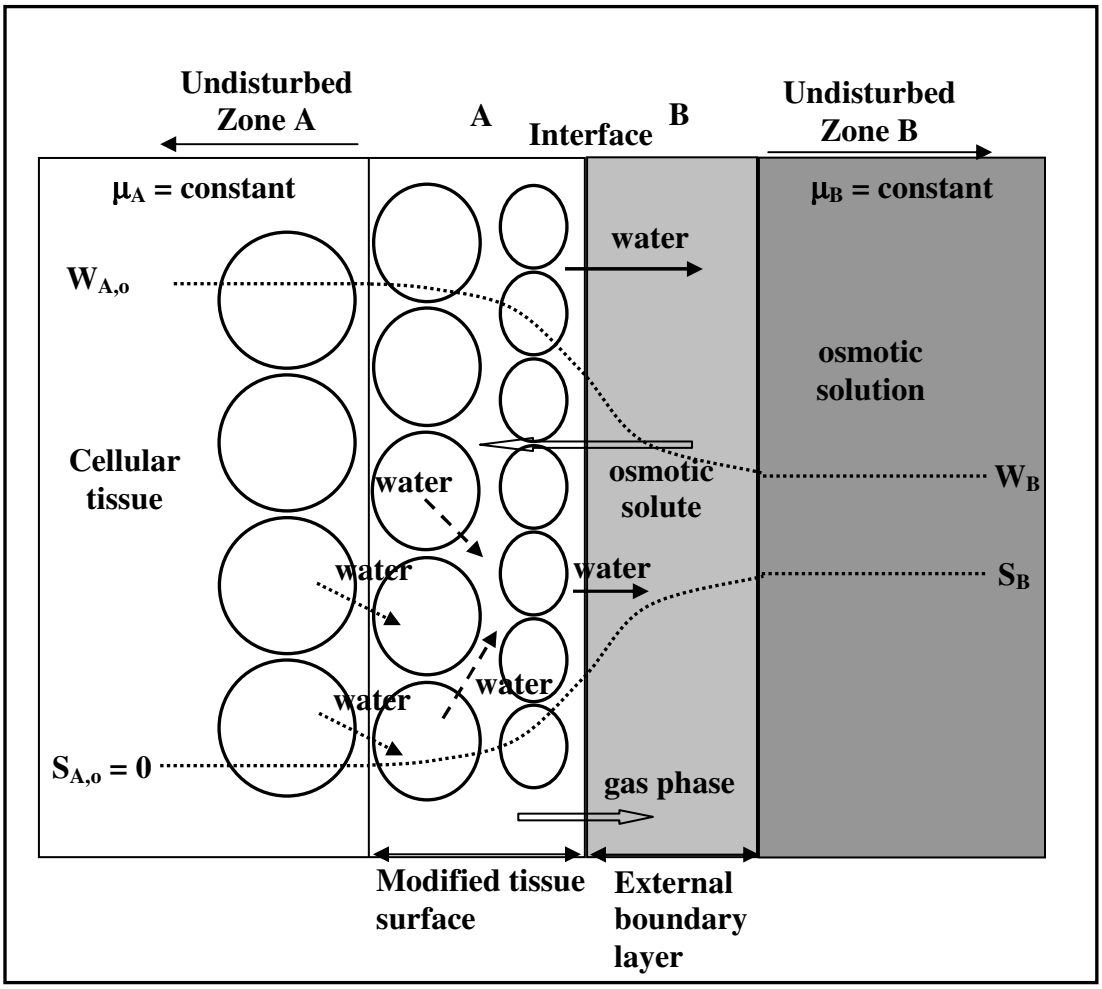

Figure 1.4. Schematic cellular material representation and mass transfer pattern. For water transport: apoplastic transport (continuous arrow), simplastic transport (dotted arrow), transmembrane transport (dashed arrow) (adapted from Shi and Le Maguer, 2002).

In the intercellular spaces initially filled with gas a capillary suction of the osmotic solution will also occur; the gas will be expelled to the osmotic solution or will be compressed during the process. Osmoactive substance will penetrate cell walls by diffusion.

After the cells of the first layer loose water, a chemical potential gradient of water between the first layer and the second layer is established. Then, the cells of the second layer begin to pump water to the cells of the first layer and then they begin to shrink. The

mechanisms of water transfer may be those commented before: apoplastic, simplastic and transmembrane transport. The phenomena of mass transfer and tissue shrinkage spread from the surface to the centre of the material with operation time. Plasmolysis, that is, the detachment of the plasmalemma from the cell wall due to the volume reduction of the protoplast, will also occur when shrinkage is considerable. Due to plasmolysis, the volume between cell wall and plasmalemma increases, and it will be filled with the solution of the intercellular spaces.

In the fresh food material, water transfer occurs through the cell membranes into extracellular space, and then into osmotic solution. Since cell membranes are semipermeable, solute taken up from the solution is only accumulated in the extracellular space. The depth of penetration of the osmotic solute into the tissue depends of several factors, such as the permeability of the solute to the cell membrane, the molecular weight and the temperature. Cells in different layers experience different conditions of water loss, solid gain and tissue shrinkage and plasmolysis; cells in the same layer can be considered in the same physical conditions.

As shown in Figure 1.4., in the undisturbed zone A (food material) the cellular structure is not changed. In section A, water loss, osmotic solute uptake and structural changes (shrinkage, plasmolysis, changes in the volume of gas phase) occur simultaneously. Osmotic solution is accumulated in the extracellular space. Water is transferred from cells into the extracellular space through cell membranes due to the concentration difference between extracellular space and cellular solution. In section B (osmotic solution), water flow and osmotic solute flow occur. The undisturbed zone B is considered as a reservoir of osmotic solution. $W_{A,o}$ is considered the initial water concentration of cell solution and is initially assumed to remain constant in the interior of the food. $S_{A,o}$ is the initial solute concentration inside the solid tissue. It is assumed that there is no osmotic solute inside the solid material at the initial stage. In the osmotic solution reservoir section, water and osmotic solute concentrations, W_B and S_B, remain constant. The consideration of mass transfer modelling is usually based on this mass concentration distribution.

A mixture of various transport mechanisms occurs and the contributions of the different mechanisms to the total transport varies from place to place and changes as dehydration progresses. The transfer process of water and solute out of the food material and uptake of osmotic solutes into the food material are usually described by the following mechanisms (Shi and Le Maguer, 2002):

1. Water and solutes transport by diffusion in osmotic process due to concentration gradients.
2. Water and solutes transport by capillary flow due to differences in total system pressure caused by external pressure, shrinkage and capillarity function.
3. Hydrodynamic flow in pores.
4. Water vapour diffusion within partly-filled pores due to capillary-condensation mechanisms.
5. Water diffusion at pore surfaces due to concentration gradients at the surfaces.

1.2.3. Mass transfer modelling during osmotic dehydration

Osmotic dehydration is a multicomponent transfer process of two simultaneous, countercurrent solution flows and one gas flow. The solution flowing out of the food material is water with dissolved solutes such as organic acids, reducing sugars, minerals, and some flavour and pigment compounds that affect the organoleptic and nutritional characteristics of the final products. Solutes present in the osmotic solution are taken up by the food material. There may be a gas flow out of the intercellular spaces.

Due to the constant moderated temperatures employed, the process can be considered as isothermal, and the main objective of modelling is the prediction of mass fluxes during the process.

The different approaches used during mass transfer modelling in osmotic dehydration can be classified in three groups: empirical, semiempirical and fundamental approach.

1.2.3.1. Empirical approach

In this kind of models, experimental data of both main fluxes, water leaving and osmotic solutes entering the material, are fitted to mathematical equations to obtain some mass transfer coefficients. Often these models are simplified forms of the analytical solution of Fick's second law of diffusion, such as the correlation of the water and solid fluxes with the squared root of time (Hawkes and Flink, 1978; Magee *et al.* 1983, Moreira and Sereno, 2003); asymptotic hyperbolic relations with time (Azuara et al., 1992), or first order kinetics type models (Panagiotou *et al*. 1998). Other models have less fundamental meaning, such as the application of Weibull probabilistic models to osmotic dehydration data (Cunha *et al*., 2001), or the use of response surface methodology, by fitting experimental data to non-linear functions, mostly polynomials relating process conditions with water lost or solids gained by the material (Saurel *et al*., 1994; Bouhon *et al*., 1998).

These models are simple and easy to use, but an important deal of experimental data is needed to obtain their empirical parameters. Besides, they are limited to a specific product and process conditions.

1.2.3.2. Semiempirical approach

The semi empirical approach tries to take into account some phenomena observed during the process but still have a strong empirical component. Raoult-Wack *et al*. (1991[a]) proposed a bicompartmental model for simultaneous water and solute transport in agar gel cubes, in order to explain the formation of a sucrose concentrated layer on the surface of the product. Different mass transfer coefficients for osmotic solute and water were

calculated in the inner and outer compartments, by means of differential system of equations.

Salvatori *et al.* (1999[a]), in the prediction of concentration profiles during osmotic dehydration of apple, proposed the concept of an "advancing disturbance front" that separates two zones: a zone of the tissue near the interface affected by mass transfer mechanisms with a developed concentration profile, and an undisturbed zone where concentrations have not changed from their initial values. The distance of such front to the interface increased linearly with the treatment time. On the basis of this advancing disturbance front concept, a set of empirical equations was fitted to experimental data to predict average and profile composition of the food material during the dehydration process.

In both works the calculation of a number of empirical parameters are required.

1.2.3.3. Fundamental approach

This approach is based on the rigorous analysis of the mass transport phenomena that happens in the process. The simplest models consider only internal resistance to mass transfer, and use Fick's second law of diffusion to obtain effective diffusion coefficients for the diffusing substances (Lazarides *et al*., 1997; Nsonzy and Ramaswamy, 1998; Telis *et al*., 2004).

The water and osmotic solutes transport rates estimated from dehydration data represents an overall mass transport property in the material, which may include several possible mass transfer mechanisms.

Some limitations of the fickian models may come because the flow interactions of the diffusing substances are neglected, and the concentration gradients are the only driving force for the process considered. The different mass transfer pathways available as well as the structure of the material are not taken into account neither. Anyway, models based on

Fick's second law of diffusion proved to be quite successful in predicting mass transfer fluxes during osmotic dehydration.

Other approaches are more complex and take into consideration the cellular structure of the tissue as well as the different mass transfer mechanisms, like diffusion through membranes of different permeability, transport in intercellular spaces (by diffusion, convective movement and capillarity), and occasionally symplastic flow between cells. The difference of the chemical potential of the transferring species is considered as the driving force for the process (Yao and Le Maguer, 1996; Le Maguer *et al.,* 2002). These models are a useful tool to understand all the mass transport phenomena at cellular level during osmotic dehydration, but perhaps too complex from a practical point of view.

1.2.4. Osmotic dehydration processing

The rate and efficiency of the dehydration process are dependent on some variables which are discussed below.

1.2.4.1. Osmotic agents

Osmoactive substances used in food processing must comply with special requirements. They have to be edible with accepted taste and flavour, non-toxic, inert to food components and highly osmotically active (Lewicki and Lenart, 1995). Sucrose, lactose, glucose, fructose, maltodextrins and starch or corn syrups are commonly used in osmotic dehydration of foods (Hawkes and Flink, 1978; Argaiz *et al*., 1994). Honey, glycerol, plant hydrocolloids and sodium chloride were also tested (Bawa and Gujral, 2000; Sereno *et al*. 2001).

Different parameters can be used to asses the quality of the osmotic agent such as: (i) the dehydration efficiency, calculated as the ratio of water loss/solids gained (w/w) in

the material (Lazarides *et al*. 1995[a]); (ii) the capacity of decreasing water activity in the material, (iii) sensory analysis and acceptance of the processed product by the consumer have to be also taken into account (Escriche *et al.* 2002).

Solutions of sugars are most common media used to dehydrate fruits. Among sugars, sucrose is by far the most frequently used substance (Giraldo *et al.* 2003; Mavroudis *et al.* 1998[a]). The WL/SG ratio increases with the molecular weight of the employed sugar. Fructose increases 50% the dry matter content compared with sucrose (Bolin *et al*., 1983); the solids gained by osmodehydrated strawberries were higher with glucose solutions rather than with sucrose solutions of the same concentration (Yang and Le Maguer, 1992). Corn syrups of large molecular size led to a high and negative value of WL/SG ratio, due to a sugar uptake inferior to the leaching of fruit solids (Lazarides *et al*., 1995[a]).

Glycerol and sodium chloride are often used to dehydrate vegetables (Torriga *et al.*, 2001), fish (Walde, 2002) and meat (Gerelt *et al*., 2000).

Combined solutions of sugars and salt are also used to dehydrate some vegetables, meat and fish. It has been found that the addition small quantities of low molecular weight substances such as sodium chloride or lactic acid to sugar solutions improves the removal of water in the material without increasing considerably the solids addition (Lewicki and Lenart, 1995). Calcium chloride, malic acid and calcium lactate have been added to sucrose to improve the texture of osmosed fruits (Hoover and Miller, 1975; Rodrigues *et al*., 2003).

1.2.4.2. Hydrodynamic conditions

Osmotic dehydration can be done in two ways: by a static or a dynamic process. It has been shown that the mass transfer resistance in the static process is higher than the observed in a dynamic process (Moreira and Sereno, 2003); therefore the second way is preferable.

Different mixing methods can be used in the dynamic process. Movement of food particles in a stationary solution (Fig. 1.5), flow of the osmotic solution through a vibrating mixer holding the samples (Fig. 1.6), and the flow of the osmoactive substance through the stationary layer of food pieces (Fig. 1.7), are some designs used for dynamic processing (Lewicki and Lenart, 1995).

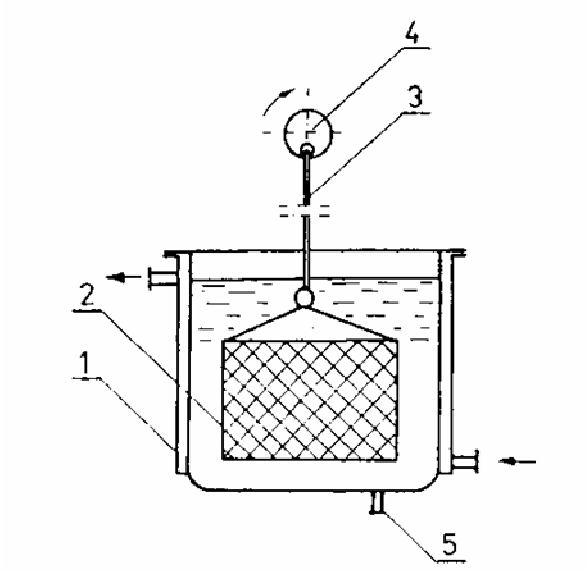

Figure 1.5. Osmotic dehydration with a vibrating basket. (1) Jacketed vessel; (2) basket; (3) shaft; (4) eccentric; (5) spout (adapted from Lewicki and Lenart, 1995).

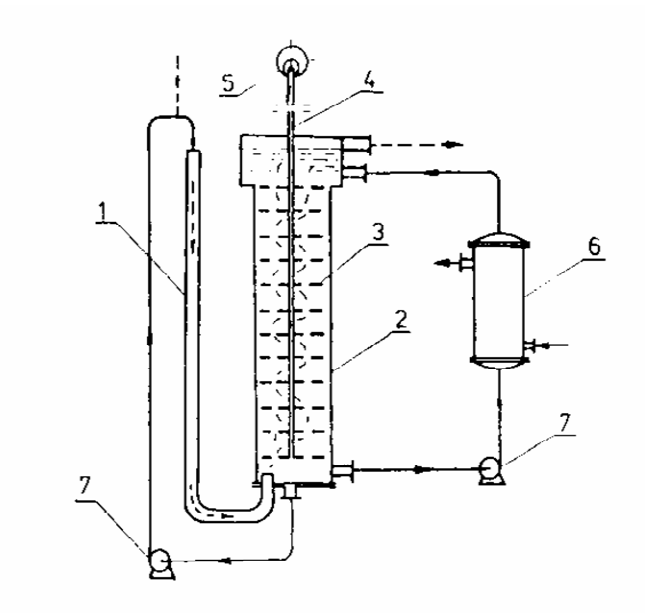

Figure 1.6. Osmotic dehydrator with a vibrating plate mixer. (1) Feed leg; (2) vessel; (3) vibrating mixer; (4) shaft; (5) eccentric; (6) heat exchanger; (7) pump (adapted from Lewicki and Lenart, 1995).

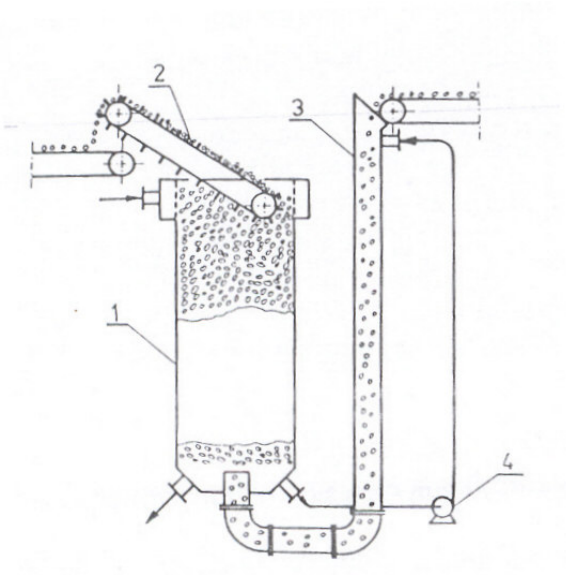

Figure 1.7. Packed bed unit for osmotic dehydration. (1) Vessel; (2) redler conveyor; (3) Feed leg; (4) pump (adapted from Lewiki and Lenart, 1995).

1.2.4.3. Concentration of the osmotic agent

The concentration of the osmotic agent affects the extension of the dehydration, since it affects directly the driving force of the process. The increase of concentration of the osmotic solution leads to a more dehydrated product. Besides, the increase of concentration leads to a higher gain of solids by the material. If a high gain of solids is not desired, a suitable concentration of osmotic agent has to be chosen in order to obtain a good water loss/solids gain ratio.

1.2.4.4. Weight ratio of the solution to food

Since the water removed from the material dilutes the osmotic solution, it is recommended a weight ratio of 1:1 to 1:5 of food to osmoactive solution (Lenart and Flink, 1984). Higher ratios, 1:10 to 1:20, are preferable when negligible dilution effect is desired.

1.2.4.5. Temperature

Temperature affects not only the rate and extension of the process but also influences the chemical composition and properties of the product. The increase of temperature increases the rate of chemical reactions and mass transfer processes as well. Viscosity of the osmotic solution decreases and the diffusion coefficients of the transferring substances increase. If minimal damage of the structure of the food material is desired, temperatures lower than 40-50 ºC are preferable, since at higher temperatures denaturation of cell membranes occurs, loosing their selective permeability and affecting the structure, texture and flavour of the food (Talens, 2002). The use of high temperatures is only indicated when products with high content of osmotic solute are desired (Lazarides and Mavroudis, 1996)

1.2.4.6. Other factors

Shape and size of the material can affect the rate and extension of the process (van Nieuwenhuijzen *et al*., 2001), so the best size and shape has to be chosen in order to fit to technological and consumer requirements.

Reduction of pressure during osmotic dehydration increases the rate of the process. It has been observed that low pressure facilitates penetration of the osmoactive substance into the tissue. Low (pulsed of continuous) pressure increased water loss at the end of the treatment compared with treatments at atmospheric pressure (Fito, 1994; Shi *et al*. 1995).

The characteristics of the fresh material can also affect the dehydration/impregnation process. More impregnation and gain of osmotic solute is expected in highly porous materials than in other with low porosity.

Pretreatment of the material affects the course of the process. During osmotic dehydration of apples, a blanching pre-treatment increased water loss and solids gain (Taiwo *et al*., 2001). Coating strawberries with a polysaccharide edible film before dehydration decreased solids gain, whereas water loss was the same after dehydration, compared with no coated fruits (Matuska *et al*., 2006).

1.2.5. Concluding remarks

Osmotic dehydration is a useful process that allows both dehydration and formulation of raw food materials. With an adequate control of the process conditions, a wide range of composition and organoleptic properties of the product can be attained.

It can be used as a single process (with a short post-treatment) or as a pre-treatment of other food processes, in order to obtain a shelf stable product.

Modelling mass transfer phenomena of the process is necessary for process control and equipment design. Due to the different mass transfer mechanisms occurring during osmotic dehydration and the complex structure of the food materials, mass transfer modelling is not an easy task. Empirical models are suitable but limited to a certain food material and process conditions. Future work has to be done in order to produce fundamental models taking into account the different mass transfer mechanism of the process and the microstructure of the material. Due to the complexity of the fundamental models at microstructural level, further simplifications of these models would be useful for industrial application.

1.3. Physicochemical changes during dehydration processes

1.3.1. Introduction

When a fruit or vegetable is submitted to a dehydration process, heat and mass transfer gradients associated to the treatment produce changes in the chemical, physical and structural characteristics of the vegetable tissue. The knowledge and prediction of these changes are important because they are related with quality factors and some aspects of food processing.

As commented by Perera (2005), the major quality parameters associated with dried food products are colour, visual appearance, shape of the product, flavour, microbial load, retention of nutrients, porosity/bulk density, texture, rehydration properties, water activity and chemical stability, preservatives, freedom from contaminants (pests, insects) as well as freedom from taints and off-odours. Some of these quality parameters are physical properties *per se*, namely colour, shape, bulk density and water activity. Others are related with some physical properties, such as rehydration capability with porosity/bulk density (McMinn and Magee, 1997[a]), texture with mechanical properties and porosity (Gogoi *et al.* 2000), and chemical stability with the physical state of the food components (Avecedo *et al*., 2006).

These physical-chemical changes are also relevant in the design of the food processes and equipment. For example, volume/density changes are important in size and shape classification (Rahman, 2005), and sometimes are needed for modelling heat and mass transfer processes (Balaban, 1989). Mechanical-rheological properties are useful in the design of equipment for handling foods (Rao and Quintero, 2005). Thermal properties are important in the design of process and equipment for blanching, cooking, freezing, drying, etc (Nesvabda, 2005). Water sorption properties are needed for modelling water transfer processes (i.e. dehydration), and for storage and packaging.

The aim of this section is to give a brief description of the chemical, physical and structural changes occurring during dehydration of vegetables. A brief description of the cellular structure of the vegetable tissue will be first presented, followed by the description of some physical-chemical changes.

1.3.2. Vegetable tissue structure

Vegetables are composed of different cellular tissues and organs each one with common and specific functions in the plant. The smaller unit that can be observed is the vegetal cell, which differences form the animal cell mainly because of the existence of a cell wall that gives rigidity to the structure of the tissue, and the existence of the chloroplasts, responsible of the capacity to produce the photosynthetic process. A brief description of the structure of the vegetal cell was already given in the first part of this introduction (1.1.2.2).

Cells are associated in various ways with each other forming coherent masses, or tissues. There are three tissue systems, and their presence in root, stem and leaf reveals both the basic similarity of the plant organs and the continuity of the plant body (Raven *et al*., 1999). The three tissue systems are:

- Dermal tissue system. Forms the outermost layer of cells of the plant body. It is formed by the epidermis tissue and periderm tissue. Their function is to confer mechanical protection to the plant, minimize water loss and aerate the internal tissues.

- Vascular tissue system. Its function is the transport of minerals and nutrients in the plant. It is formed by two tissues: xylem and phloem.

- Ground (or fundamental) tissue system. Formed by three tissues: (i) The parenchymatic tissue. It is by far the most common of the ground tissues. It is involved in photosynthesis, storage and secretion, activities dependent upon living protoplasts. In addition, it may play a role in the movement of water and the transport of food substances in plants. It is located

in the cortex and pith of items and roots, in leaf mesophyll and in the flesh of fruits. (ii) Collenchyma tissue. It supports young growing organs. Its cells are typically elongated with nonlignified primary walls. They are specially adapted for the support of young, growing organs. (iii) Schlerenchyma tissue. Its cells often lack protoplast at maturity, having a thick and often lignified cell wall. They are important strengthening and supporting elements in plant parts. Two types: (iii.1) fibres, composed by generally long, slender cells that commonly occur in strands or bundles; (iii.2) schlereids, with cells variable in shape, often branched. They can be observed in seed coats of many seeds, shell of nuts and the stone endocarp of stone fruits. Schlereids are responsible for the characteristic texture of pears.

Within the plant body the various tissues are distributed in characteristic patterns depending upon the plant part or plant taxon or both. The general pattern is to have the vascular tissue embedded within the ground tissue, with the dermal tissue forming the outer covering (Fig. 1.8 (a)). The main differences in patterns depend largely on the relative distribution of the vascular and ground tissues.

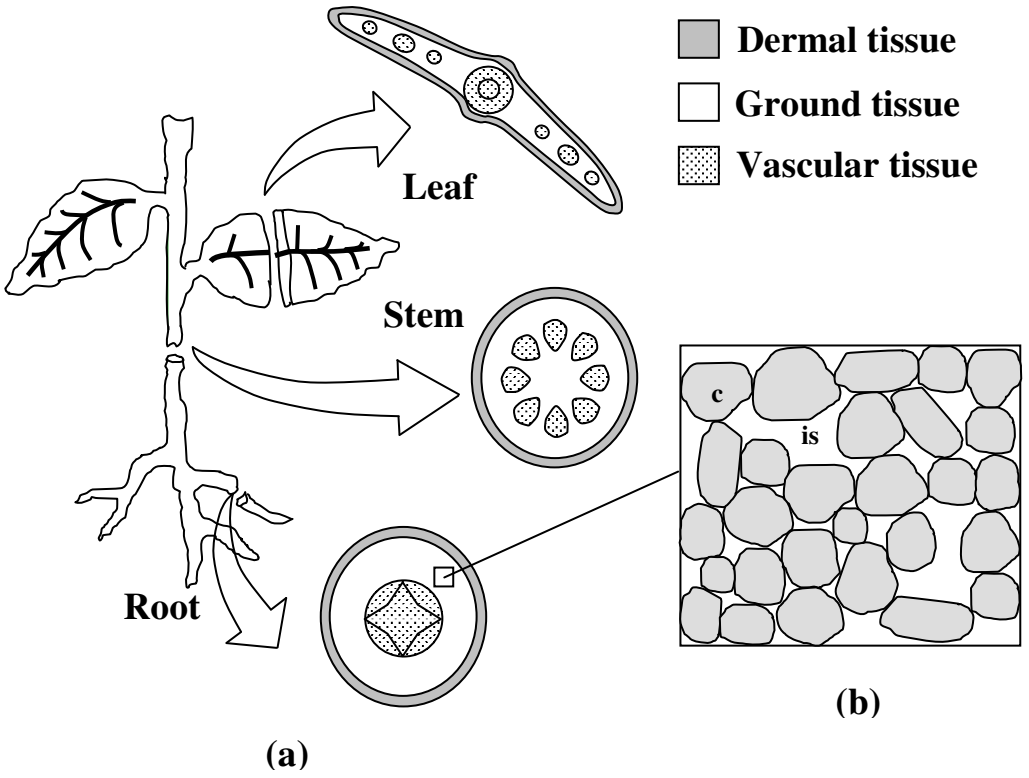

Figure 1.8. (a) Distribution of the different tissue systems in the plant. (b) Detail of parenchymatic tissue. c = cell; is = intercellular space.

Since parenchyma tissue is the most common of the tissues, it has been often used as a model in the study of food and vegetable processing (Mavroudis *et al.* 1998[a]; Prestamo and Arroyo, 1998; Laza *et al*. 2001). Parenchyma cells are loosely arranged in the tissue and some intercellular spaces are formed (Fig. 1.8 (b)). Intercellular spaces form a continuous system of channels that is filled with air (Lewicky and Lenart., 1995).

1.3.3. Physicochemical changes of fruit and vegetable tissue during dehydration

Dehydration is a heat and mass transfer process, in which the heat and mass transfer fluxes produces changes in the physical, chemical and structural properties of the vegetable tissue. The localization of these changes is directly related with the of heat and mass transfer gradients created during dehydration. The type and magnitude of these gradients are a function of the process conditions and the drying technique.

Two main types of developed gradients can be observed, depending on the type of drying process. In the first type, the water is mainly evaporated in the surface of the product, creating a dehydration front from the surface of the material. The tissue can be divided in two zones: a) the dehydrating zone, where water and temperature gradients are significant and where the physical and chemical changes are produced; b) the solid inner core (Suzuki *et al*., 1976), where the material does not suffer dehydration and maintains its initial characteristics.

As the process continues the dehydration front advances from the surface of the tissue up to the inner zone. It is expected that, the faster the drying rate, the more accentuated are these gradients. Figure 1.9 shows a schematic diagram of the heat and mass transfer phenomena in this kind of treatments. Convective drying follows this dehydration pattern. Osmotic dehydration follows a similar pattern, but in this case there is no significant evaporation of water, and a mass flux of osmotic solute from the external solution into the material occurs. Freeze drying also follows this behaviour (Cheng *et al.*,

2002), but in this case water in the dehydration front is removed by sublimation and in the solid core the material has been frozen before drying.

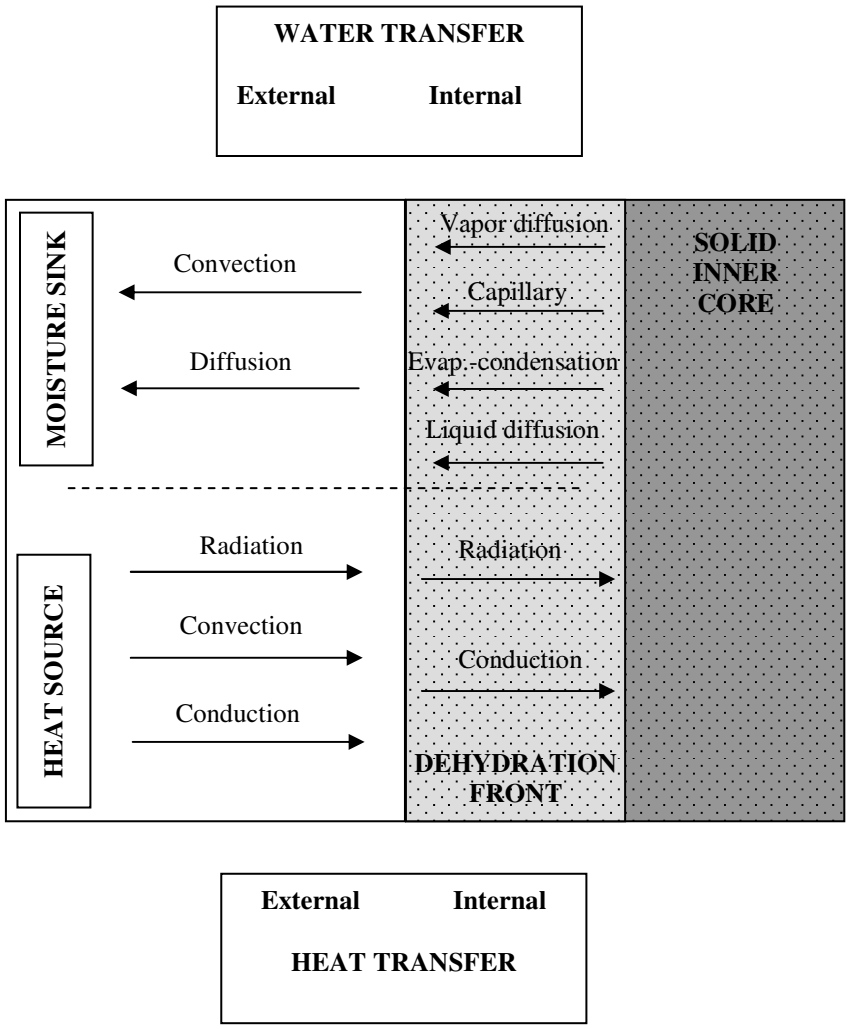

Figure 1.9. Heat and mass transfer processes during dehydration of foods showing a dehydration front (Adapted from Aguilera and Stanley, 1990).

In the second type, evaporation of water happens at any point inside the material, and the same happens with the changes in the physical properties. Microwave drying and puff drying are some examples of this type of behaviour, where internal vaporization is more accentuated than that observed in the first type of drying techniques. The heat and

mass transfer phenomena are similar to those observed in the first type, but here the dehydration front is less marked or not observed (Ahmad *et al*., 2001).

Physical-chemical changes during dehydration can be observed at different structural levels. Some of them are produced at molecular and microstructural level in the plant tissue. Others are observed at macrostructural level. The author has gathered and presented such changes in these two groups.

1.3.3.1. Changes at molecular level and microstructural changes

a. Microstructural changes

Fresh vegetable tissue is composed by cells connected one to each other by the middle lamella. These cells are in turgor pressure, defined as the hydrostatic internal pressure (normally 1-8 bars) exerted by the protoplasm against the plasma membrane and cell wall (Aguilera *et al*., 1998). The turgor pressure gives elastic mechanical characteristics to the vegetable tissue. The cellulose of the cell wall gives rigidity and strength to the tissue, whereas pectins and hemicelluloses of the middle lamella give plasticity and dictate the degree which the cells can be pulled apart during deformations (Lewicki and Pawlak, 2003).

During dehydration, water migrates from the protoplasm through the cell membrane and surrounding wall and across the porous structure of the tissue. High temperatures can denaturise cell membranes; this denaturation can increase the dehydration rates (Aguilera and Stanley, 1990). As a consequence of the water loss and alteration of the membranes, some phenomena can occur in the cellular tissue, namely: shrinkage and deformation of cells, plasmolysis, cell debonding and cell rupture with formation of new cavities. These changes can be observed in Figure 1.10.

When plant tissue is placed in a hypertonic solution (as in the case of osmotic dehydration) water will leave the cell by osmosis. As a result the vacuole and the rest of the protoplast will shrink, causing the plasma membrane to pull away from the cell wall. This phenomenon is known as plasmolysis (Fig. 1.10 (b)) (Raven *et al*., 1999), and it has been observed during osmotic dehydration of potato (Mauro *et al.,* 2002) and strawberry (Ferrando and Spiess, 2001).

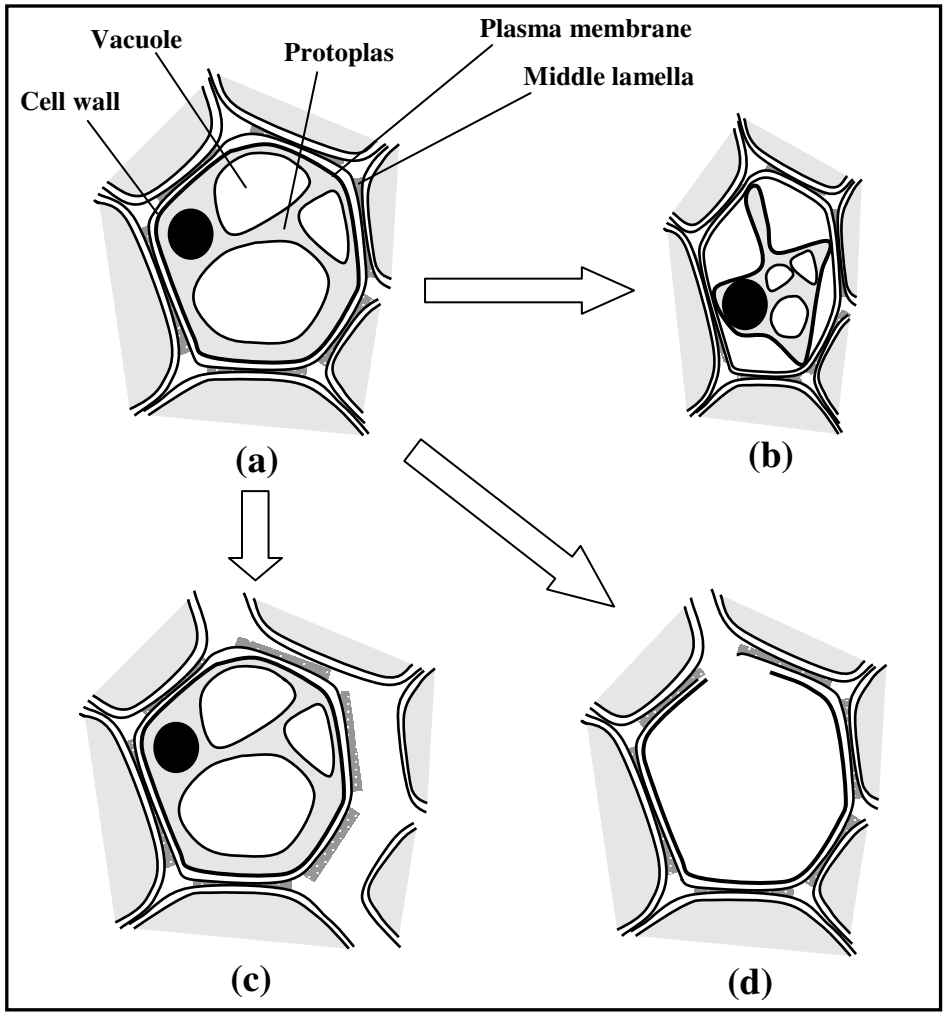

Figure 1.10. Changes of vegetable tissue at microstructural level during dehydration. (a) Fresh cell. (b) Shrinkage and plasmolysis. (c) Cell to cell debonding. (d) Cell rupture and cavity formation.

Plasmolysis is accompanied with a loss in the turgor pressure, shrinkage and deformation of cells (cell wall and plasma membrane), and concentration of the protoplasmatic liquid phase.

Cellular shrinkage during dehydration has been observed during osmotic dehydration of apple (Lewicki and Porzecka-Pawlak, 2005) and convective drying of grapes (Ramos *et al*., 2004)

Other phenomenon that can be observed during dehydration is the detachment of the middle lamella, or cell debonding (Fig. 1.10 (c)). This phenomenon is likely due to the degradation or denaturation of the components of the middle lamella, as well as to the microstress produced in the cellular tissue due to water removal. This phenomenon has an influence on the mechanical properties of the product, as well as in the porosity of the material because intercellular spaces are formed. Cell debonding has been observed during osmotic dehydration of apples (Lewicki and Porzecka-Pawlak, 2005).

Cell rupture, formation of cavities and shrinkage of cells were observed during convective drying, puff drying and freeze drying of apples (Lewicki and Pawlak, 2003). Cell rupture is due to cell membrane and cell wall degradation and microstresses due to water removal. Cell rupture leads to the formation of cavities of different size and shape. This formation of cavities increases the porosity of the product.

b. Phase transitions

Plant tissues are multicomponent and multiphasic systems, which can suffer phase transitions of its components during dehydration. Both first and second order transitions can happen in the typical range of temperatures and pressure in which they are processed.

The most important phase transition suffered during dehydration is the vaporization of water; part of this vaporization occurs at the surface of the material, but in some cases, such as microwave drying, puff drying or in the advanced stages of convective drying,

evaporation can happen at some extent inside the plant tissue. Vaporisation of water inside the cellular tissue may lead to pressure gradients and eventual rupture of cells and formation of new cavities, reducing the apparent density and increasing porosity, as in the case of microwave-dried potatoes (Khraisheh *et al*., 2004) and puff-dried bananas (Hoftsetz *et al*., 2006).

During freeze drying, there is a first transition of water to solid phase, followed by sublimation due to the application of very low pressures. The solidification of water has likely influence on the support of the solid structure of the frozen material during sublimation of water, avoiding its collapse and creating a final porous structure in the dried product. (Karathanos *et al.,* 1993).

Proteins can suffer denaturation in the range of temperatures used during convective drying, and fats can also melt at the adequate temperature. These two transitions are less important in vegetable tissues because of the low protein and fat content. Only in the case of nuts like almonds or peanuts may have those transitions some extension. An exception is enzyme denaturation, which play an important role in the rate and extension of enzyme-controlled chemical reactions.

An important second order transition present in vegetables at changing moisture contents is the glass transition of the sugars present in the protoplasmatic aqueous solution. At a certain temperature called the "glass transition temperature" (T_g) a material in amorphous state changes from the rubbery to the glassy state (Roos and Karel, 1991). This is a typical phase transition of biopolymers. The main substances that suffer these transitions during dehydration of vegetables are monomeric or short chain sugars, such as glucose, fructose, lactose and sucrose. Initially, the soluble sugars are dissolved in the protoplasmatic aqueous solution. If the water removal is fast enough, the sugars cannot reorder to crystallize and form and amorphous concentrated suspension in water, initially in a rubbery and viscous state. As the dehydration continues, it can be observed a transition from the rubbery to the glassy state, called glass transition; here the viscosity of the concentrated solution increases sharply and acquires mechanical characteristics of a solid.

This transition is believed to have a great importance in different physical-chemical phenomena occurring in the vegetable tissue, such as the kinetics of chemical reactions (Acevedo *et al*, 2006), mechanical properties (Payne and Labuza, 2005) and mobility of the solid matrix of the product (Levi and Karel, 1995). Some other changes associated with the glass transition temperature are changes in the free molecular volume, heat capacity, thermal expansion coefficient and dielectric properties (Genin and Rene, 1995).

Some sugars can partially crystallize during dehydration treatments; this fact has been observed during drying of osmotically pretreated fruits (Mandala *et al*., 2005). In starchy vegetables gelatinization of starch can happen in the usual process conditions used during dehydration (Iyota *et al.*, 2001). Other medium and long chain polysaccharides, such as cellulose and pectins, main constituents of the cell wall of the vegetable tissue, do not suffer glass transitions during dehydration (Aguilera *et al*, 1998), as they are likely decomposed before attaining the conditions for the glass transition.

c. Water activity

Water is the main constituent of foods and biological materials. Since the antiquity it is known that the removal of water from a food product extends its shelf life. In the fifties, Scott (1957) and Salwin (1959), independently, suggested that the water activity, a_w (defined at the time as an equilibrium vapour pressure), more than the water content, was the property that controls several chemical reactions and microbiological activity in food products. Figure 1.11 shows a diagram representing the chemical and microbiological changes as a function of the water activity of a typical food product (Labuza, 1970).

Based on the value of water activity it is common to classify food products as "dried", "intermediate moisture content", or "high moisture content", when a_w is less than 0.6 (i.e. cookies, dried pasta), between 0.6 and 0.9 (dried fruits, cured meat, jams), or higher than 0.9 (fresh products), respectively (Labuza, 1980).

Water activity has become, along with the glass transition temperature, one of the most useful parameters that can be used as a reliable guide to predict food spoilage. It is often used as well to determine the drying end point required for a shelf-stable product (Jayaraman and Das Gupta, 1995)

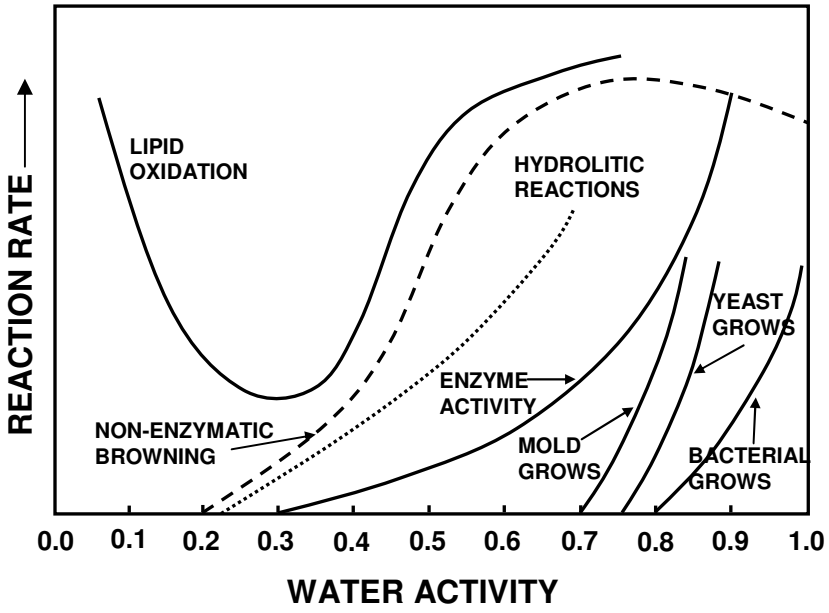

Figure 1.11. Chemical and microbiological changes as a function of the water activity of a food product (adapted from Labuza, 1970).

The most known and used expression to define water activity is

$$a_w = \frac{p_w}{p_w^o} \tag{1.7}$$

where

p_w = equilibrium water vapour pressure in the system

p_w^o = equilibrium water vapour pressure of pure water at the same temperature than the system

In equilibrium conditions, the water activity of a material is related to the relative moisture content of its surrounding atmosphere (RH) by means of the Eq. (1.8)

$$a_w = \frac{RH(\%)}{100} \tag{1.8}$$

The equilibrium relation between the moisture content of a product and the corresponding water activity, at a certain temperature, is described by the sorption isotherm.

Equilibrium sorption data are important for many activities related to food technology, like the prediction of microbiological, enzymatic and chemical activity, selection of packaging materials, design of drying and concentration processes, as well as selection of adequate storage conditions. In all of these cases, the sorption isotherms are required for design purposes.

The shape of a sorption isotherm depends on the structure and composition of the food material, as well as pressure and temperature. It requires experimental determination, since current prediction methods are not able to simulate systems as complex as foods. The sorption isotherms of most foods have a sigmoidal shape, and the isotherm can be divided into three zones as a function of water activity, a_w. At low water activities, physicochemical sorption of moisture is produced, and at higher water activities this is followed by multi-layer adsorption, and finally capillary condensation becomes predominant.

A large number of publications have reported sorption isotherm data for different food products, and some important compilations can be found in the literature (Iglesias and Chirife, 1982; Wolf *et al*., 1985[a]).

The shape and characteristics of a sorption isotherm are related with the chemical composition of the product. When osmotic dehydration is employed, while water removal takes place, the acquisition of osmotic solute occurs in such a way that the composition of

the final product is changed and the characteristics of the moisture sorption isotherm may be modified. Lazarides *et al.* (1995[b]) reported that apples osmotically dehydrated with sucrose solutions resulted in a shift of the sorption isotherm compared with the non-treated material. In other cases, the differences between the sorption isotherms of the osmotically treated and non treated material are not clear, as in the case of pumpkin (*Ambe*r variety) (Palacha *et al*., 1997) or plaintain (Falade *et al*., 2003).

The changes in structure during dehydration also seem to influence in the sorption isotherm. Potatoes dried by two different techniques, freeze drying and vacuum drying, resulted in different sorption isotherms after equilibration of the dried samples in atmospheres of different relative humidity (Mazza, 1982). The freeze-dried product adsorbed more water (for the same relative humidity in the environment) than the vacuum dried material, likely due to the more porous structure obtained by freeze drying, resulting in a product with a higher effective contact area than that obtained with vacuum drying.

d. Chemical reactions

Different chemical reactions can occur during dehydration, affecting the nutritional quality, flavour, taste and physical properties of the product. The type and extension of the chemical reactions depend on the chemical composition of the raw material, process conditions and drying technique. Some of the main chemical reactions produced during dehydration are commented below.

(i) Carbohydrates

Heat treatments can cause interactions between reducing sugars and amino groups of proteins, producing melanoidine pigments and other secondary dark products. This reaction caused browning of the food material and changes in flavour, and is known as the Maillard reaction (Whistler and Daniel, 1985). Maillard browning during dehydration is often observed (Gogus *et al*., 1998; Gupta *et al*., 2002)

Direct heating of carbohydrates produces their thermolysis, leading to a complex group of reactions called "caramelization". These reactions lead to dark-brown flavoured substances. Wilford *et al*. (1997) observed caramelization of sugars in the last stage of drying of prunes.

(ii) Proteins

As commented before, a loss of protein content during dehydration can be due to Maillard reaction. During the initial stage of the drying process some protein losses may be also due to enzymatic degradations (Perera, 2005), and can be related with changes in texture, colour and flavour.

(iii)Lipids

At the beginning of the dehydration treatment lipids may undergo enzymatic hydrolysis, causing off-flavour formation (Nejad *et al*., 2003). At low water activity auto-oxidation of unsaturated fatty acids can occur (Perera, 2005).

(iv) Vitamins

Different factors may be the cause of vitamin losses, such as heating, light exposition and presence of oxygen. In the first stage of the dehydration process, when the moisture content is high and temperature moderate, enzymatic oxidation of vitamins can take place (Perera, 2005). Tocopherol oxidase destroys vitamin E. Lipoxygenases are the major enzymes involved in carotenoid degradation. Ascorbic acid is destroyed during convective drying of potatoes (McMinn and Magee, 1997[b]) by oxidation, both non-enzymatic and enzymatic (ascorbic acid oxidase). Carotenoids (such as vitamin A and beta-carotene) in plant tissue are susceptible to light-induced oxidation, warm temperatures, oxygen, enzymes and storage (Hutchings, 1999). Losses of tocopherols, carotenoids and vitamin C were observed during convective drying of paprika (Ramesh *et al*., 2001). Convective dried carrots showed higher losses of carotenoids and vitamin C compared with

vacuum microwaved and freeze dried samples, due to the high temperature and long time used in the convective treatments (Lin *et al*., 1998). An osmotic step often improves the stability of vitamins and pigments during drying and frozen storage (Torreggiani and Bertolo, 2001).

(v) Other chemical reactions

It is interesting to comment three chemical processes, enzymatic browning, degradation of pigments and degradation of pectic substances. The first two are related to colour change whereas pectic degradation affects the mechanical properties of the plant tissue.

Enzymatic browning, along with Maillard reaction, caramelization and ascorbic acid oxidation are the four types of browning in foods. Enzymatic browning is observed in light-coloured fruits and vegetables, such as apples, bananas and potatoes. This is due to enzymatic oxidation of phenols and quinones which polymerize to form brown pigments and melanines (Richardson and Hyslop, 1985). Enzymatic browning is catalysed by the enzyme poly-phenol oxidase (PPO). Sulphite and blanching pretreatments can reduce enzymatic browning during convective drying (Krokida *et al*., 2000[a]). During osmotic dehydration, the osmotic solution fills intercellular spaces initially with air, reducing the oxygen availability by PPO and decreasing enzymatic browning (Quiles *et al*., 2005).

Some chemical substances present in the cell confer colour to the vegetables, and can be degraded during dehydration. Carotenoids, chlorophylls and anthocyanins are very common pigments present in plant tissue. During dehydration, both enzymatic and nonenzymatic reactions can be expected to be involved in their degradation. Chlorophylls, related to the green colour of vegetables, are mainly converted in pheophytin (Jayaraman and Das Gupta, 1995), changing to a dark olive-brown colour. Anthocyanins impart red colour to plant tissues, and can be degraded during dehydration to greyish colour substances if sulphite pretreatments are not employed (Haard, 1985).

Pectic substances can suffer degradation with the increase of temperature by beta-elimination (Waldron *et al.* 1997). These substances, present in the middle lamella surrounding the cell wall, are responsible of the cell to cell adhesion and their degradation can lead to changes on the mechanical properties of the vegetable tissue. Pectin degradation was observed in different dehydration treatments and products, such as in convective drying of apricots (Femenia *et al*. 1998) and microwave-air dried apple (Contreras *et al*. 2005).

1.3.3.2. Changes at macrostructural level

a. Changes in volume and porosity.

One of the most important physical changes that the food suffers during drying is the reduction of its external volume. Loss of water and heating cause stresses in the cellular structure of the food leading to change in shape and decrease in dimension. During the changes in volume, the ratio air volume to total volume, also know as porosity, can increase, decrease or remain constant depending on the degree of collapse of the inner structure.

The changes in volume and porosity have a direct impact on the quality of the product:

- Changes in shape and loss of volume cause in most cases a negative impression in the consumer. There are, on the other hand, some dried products that have had traditionally a shrunken aspect, a requirement for the consumer of raisins, dried plums, peaches or dates.

- Surface cracking is another phenomenon that may occur during drying. This happens when shrinkage is not uniform during the drying process leading to the formation of unbalanced stresses and failure of the material. Cracking of vegetables has been reported in the drying of some seeds such as soybean (Mensah *et al*., 1984) and corn (Fortes and Okos, 1980).

- Another important consequence of shrinkage/porosity changes is the decrease of the rehydration capacity of the dried product. High degree of shrinkage and low porosity led to dried vegetables with poor dehydration capacity (Jayaraman *et al*., 1990; McMinn and Magee, 1997[a]).

- Porosity change is related to the chemical stability of the dried product, showing influence in reactions like degradation of sugars (White and Bell, 1999) and lipid oxidation (Shimada *et al*., 1991).

- Textural and sensorial properties of foods are related with the density and porosity (Rahman, 2001).

Some authors have reported the importance of taking into account the changes in volume and dimensions when modelling heat and mass transfer phenomena in food processing (Simal *et al*., 1998; Mayor and Sereno, 2004). Porosity has also a direct effect on some properties related to heat and mass transfer modelling, such as mass diffusion coefficient, thermal conductivity and thermal diffusivity (Rahman, 2001).

For all these reasons, the knowledge of the changes in volume and porosity during food dehydration is very important.

(i) Mechanism of shrinkage

Fruits and vegetable tissues are cellular biomaterials that may be considered as consisting of a three-dimensional solid network or matrix holding usually large quantities of an aqueous solution. Biopolymers (mainly celluloses and pectins) are the common structural elements of the solid matrix. The particular structure of the material and the mechanical characteristics of its elements at equilibrium define sample volume and determine its size and shape. When water is removed from the material, a pressure unbalance is produced between the inner of the material and the external pressure,

generating contracting stresses that lead to material shrinkage, changes in shape and occasionally cracking of the product.

(ii) Factors affecting the magnitude of shrinkage

- Volume of removed water

Shrinkage of food materials increases with the volume of water removed, since the more water removed the more contraction stresses are originated in the material. In some cases the mechanical equilibrium is reached when shrinkage of the material equals volume of removed water, as was observed for convective drying of carrots (Krokida and Maroulis, 1997; Lozano *et al*., 1983). In other cases, the volume of removed water during the final stages of drying is larger than the reduction in sample volume, as observed during convective drying of potato (Lozano *et al*., 1983; Wang and Brennan, 1995) and apple (Krokida and Maroulis, 1997; Moreira *et al*., 2000). This behaviour can be explained by the decrease in the mobility of the solid matrix of the material at low moisture contents, as described below.

- Mobility of the solid matrix

The mobility of the solid matrix is closely related to its physical state; high mobility corresponds to viscoelastic behaviour typical of a rubbery state while low mobility corresponds to an elastic behaviour typical of a glassy state. Levi and Karel (1995) found that mobility of the solid matrix is a dynamic process with rates that depend on the difference ($T-T_g$), where T is the temperature of the sample undergoing dehydration and T_g is its glass transition temperature, and that Williams-Landel-Ferry (WLF) equation (Williams *et al*., 1955) applies. Similarly, several authors (Del Valle *et al*., 1998[a]; Karathanos *et al*., 1993) have related the extension of shrinkage in air drying with ($T-T_g$).

At high moistures, when the material is in the rubbery state, shrinkage almost entirely compensates for moisture loss, and volume of the material decreases linearly with

moisture content. At low moisture contents T_g increases, allowing the material to pass from rubbery to glassy state, and the rate and extension of shrinkage decreases significantly. Since no phase transitions of celluloses and pectins are observed at the process conditions used in dehydration processes (Aguilera *et. al*., 1998), transitions from the rubbery to the glassy state of the solid matrix in vegetable tissues are mainly due to transitions of sugars (glucose, fructose, sucrose) present in the aqueous protoplasmatic solution.

This behaviour may explain deviations from linearity observed by several authors in the relative change of sample volume versus the relative change of moisture content (Lozano *et al*., 1983 (0.1 X/X_o, garlic, potato, sweet potato); Ratti, 1994 (0.3 X/X_o, apple, potato), Wang and Brennan, 1995 (0.1 X/X_o, potato)) observed during the final stage of convective drying. When drying process is in the range of low moisture content where phase transition from rubbery to glassy state is going on, rigidity of the material stops shrinkage and parallel pore formation may happen.

Freeze dried products show very little shrinkage compared with vegetables dehydrated using other techniques. During freeze drying ice crystals initially support the structure of the tissue. As dehydration proceeds, water is removed by sublimation at low temperatures and the structure does not shrink due to the high viscosity of the concentrated amorphous glassy state at freeze drying temperatures. The dried product shows a highly porous structure with low shrinkage and no collapse (Karathanos *et al.,* 1993).

- Drying rate

Drying rate has an influence on the extension of shrinkage in the case of dehydration techniques showing a “dehydration front”. If rapid drying rate conditions are used and intense moisture gradients throughout the material are observed, low moisture content of the external surface may induce a rubber-glass transition and the formation of a porous outer rigid crust or shell that fixes the volume and complicates subsequent shrinkage of the still rubbery inner part of the food (Mayor and Sereno, 2004); as a consequence porosity increases. The formation of a shell during drying of gels was verified

experimentally by Schrader and Litchfield (1992), by means of magnetic resonance imaging; similarly, Wang and Brennan (1995), during drying of potatoes, showed light microscopy evidence of this shell formation or ‘‘case hardening’’ effect. If low drying rate conditions are used, diffusion of water from the inner to the outer zone of the material happens at the same rate than evaporation from the surface, no sharp moisture gradients are formed and the material shrinks uniformly until the last stages of drying.

- Internal water vaporization

This effect is important in dehydration techniques with no “dehydration front” or when it is hardly observed. In these drying methods, water vaporization inside the material during dehydration can be significant enough to produce a “puffing effect” of the inner of the tissue. Internal water vaporization creates pressure gradients inside the material, reducing the theoretical shrinkage and creating new pores due to the rupture of cells (Lewicki and Pawlak, 2003). Vacuum-microwave dehydrated carrot resulted in a product with higher density than freeze dried material but with lower density than the convective dried (Lin *et al*., 1998). Puff dried bananas resulted in the formation of a highly porous structure in the material, with lower shrinkage and density than convective dried samples (Hofsetz *et al*., 2006).

- Structure of the raw material

The resistance to shrink of each vegetable tissue depends on its particular structure and chemical composition. Tissues with high moisture content and thin cell walls (i.e. parenchymatic tissue) shrink in more extension than other with less moisture content and thick cell walls rich in celluloses and lignin (sclerenchymatic tissue, vascular tissue). Mulet *et al.* (2000) showed an anisotropic shrinkage in the convective drying of cauliflower stem cylinders, where the decrease of the diameter was much more pronounced than the decrease of the length, due to the presence of oriented fibres making the product stiffer in a preferential orientation. Rossello *et al*. (1997) also found a more accentuated radial than

longitudinal shrinkage during green bean drying; the authors suggested that the fibre orientation of the vegetable was the cause of these differences.

b. Changes in mechanical properties

Dehydration processes lead to changes in the mechanical properties of the material. These changes are important because they are related to the textural and sensorial characteristics of the food, and consequently with the quality and acceptance of the product by the consumer.

The mechanical properties of cellular food materials, such as vegetables and fruits, have been associated with the different levels of structure existing in the material (Waldron *et al*. 1997). At microstructural level, some elements can be pointed as relevant: structure and chemistry of the polymers that make up the plant cell wall, cell wall thickness, turgor pressure of cells and strength and nature of the cell to cell adhesion. At higher structural levels can be cited the structure of the tissue (cellular orientation, quantity of intercellular spaces), and the different types of tissue or organs that make up the vegetable product.

During dehydration, change in turgor pressure of cells, plasmolysis, degradation of the middle lamella, density and phase transition of some components can influence in the mechanical properties of the vegetable tissue. Heating of vegetable tissue causes a loss of firmness due to the disruption of the plasmalemma and an associated loss of turgor (Greve *et al*., 1994[a]). Cell separation due to beta-eliminative degradation of pectic polysaccharides of the middle lamella is also observed (Greve *et al*., 1994[b]).

Several authors have studied the changes in the mechanical properties of food materials during convective drying. In general, during drying the soft product (fresh) transforms into a rigid product (dried) or change from a predominantly plastic to a more elastic behaviour, whereas an accentuated viscoelastic behaviour occurs in the intermediate moisture content (Telis *et al*. 2005).

Lewicki and Jakubczyk (2004) found that the decrease in water content during convective drying caused an increase of the force needed to compress apple slices up to a constant deformation of 20%. Krokida *et al*., (2000[b]), during drying of several vegetables (apple, banana carrot and potato), observed the same behaviour with all the materials during compression tests: failure strain increased with moisture decrease during drying, whereas failure stress initially decreased but a certain moisture content increased with moisture decrease.

Lewicki and Wolf (1995) studied the rheological properties of raisins stored at different water activities. They observed that at low water activity (and low moisture content), the rheological properties of raisins changed dramatically and behaved as brittle bodies, more resistant to compression than fresh ones but easily breakable. They suggested that the transition from the rubbery to a glassy state of the concentrated liquid phase (rich in sugars) at low water activities was the cause of this behaviour.

Other structural changes affecting the mechanical properties of convective dried products can be the changes in the density and tissue alterations (cell rupture, formation of air cavities) during drying.

Some works can be found in the literature about the mechanical behaviour of foods submitted to osmotic dehydration, when used as a pre-treatment or as a single process. Krokida *et al*. (2000[c]) studied the rheological properties of apple and banana pre-dehydrated with glucose solutions and convective dried. Osmo-convective dried samples presented more resistance to rupture (higher values of failure stress and strain) than convective dried ones, for the same moisture content. The authors suggested that this fact was due to the plasticization of the structure and reduction of the elasticity caused by the sugar uptake during the osmotic pre-treatment. Chiralt *et al*. (2001) observed a cryoprotectant effect of sucrose in kiwi and mango. Fruits osmotically dehydrated with sucrose solutions and frozen presented more resistance to compression after thawing than the other non-pretreated frozen samples. In the same work, the authors observed a decrease in the firmness (initial slope of the stress-strain compression curve) in osmotically

dehydrated kiwifruit and mango, compared with fresh products. Failure stress during compression also decreased for kiwi and mango osmodehydrated samples.

c. Colour changes

The changes in colour during dehydration of vegetables are due to different factors. Some of them are physical changes, such as changes in the roughness of the material surface, and changes in density and porosity, changing mainly the lightness and opacity of the dehydrated product (Lewicki and Duszczyk, 1998). Other factor is the removal of water, which leads to the concentration of the pigments in the liquid phase, producing changes mainly in the intensity of the colour perceived by the consumer.

The main recognized cause of the changes in colour is directly associated with chemical reactions occurring during the dehydration process. These reactions can be gathered in two groups: browning reactions and pigment degradation. Browning reactions are Maillard browning, nonenzymatic browning, caramelization and vitamin C oxidation. Browning reactions and pigment degradation have been reviewed in the section of chemical changes during dehydration (1.2.3.1).

Colour of foods is measured by different methods. It can be evaluated by determination of pigment content. This method is used, for example, for determination of colour change due to anthocyanin degradation (Sa and Sereno, 1999), chlorophyll degradation (Weemaes *et al*, 1999) or carotenoid degradation (Minguez-Mosquera and Hornero-Mendez, 1994). The most used method to measure the colour changes during food processing is tristimulus reflectance colorimetry (Francis, 2005), where a white light comes into contact with the food surface, and the reflected light is measured in terms of three colour coordinates. There are different systems of colour coordinates, but the CIELAB system currently seems to have the widest application on foods. In these scale L* is a measure of the lightness, a* measures the redness (-a* greenness) and b* measures

yellowness (-b* blueness). Sometimes, good correlations between pigment content and reflectance colour coordinates are obtained (Ruiz *et al*., 2005).

The changes in colour during dehydration depend on the initial material characteristics, process conditions and dehydration technique. Usually the method which better preserves the initial colour characteristics is freeze-drying (Krokida *et al.,* 2000[d]; Ratti, 2001), due to the low temperatures employed during dehydration, the low mobility of the substances susceptible of chemical reactions and the low availability of atmospheric oxygen for oxidative reactions. Other dehydration method with results in low colour changes is microwave-vacuum drying (Lin *et al*., 1998; Cui *et al*., 2003). Convective drying is probably the dehydration process with the highest colour changes, since involves moderate-high temperatures, long process times and high exposure to oxygen (Krokida *et al*., 2000[d])

During osmotic dehydration, colour changes are not very accentuated, mainly because the low temperatures used and the intermediate moisture contents attained. Enzymatic reactions, leaching of pigmented substances to the osmotic solution, pigment concentration and structural changes can be the main factors causing colour changes in this process. The use of antibrowning agents in the osmotic solution can be useful when enzymatic browning is considerable (Waliszewski *et al*, 2002[ab])

Enzymatic browning can be important at the beginning of the dehydration processes, when temperatures in the material are not excessively high and moisture content is not very low. Blanching before convective drying can reduce colour changes during processing (Krokida *et al*., 2000[a]) The use of an osmotic pre-treatment followed by a conventional drying treatment has been used to attain a better preservation of the colour compared with convective drying (Torreggiani and Bertolo, 2001, Sanjinez-Argandona *et al*. 2005). As commented by Shi *et al*., (1999), the formation of an external crust of osmotic agent limits the contact between the fruit and oxygen, lowering the change in colour caused by oxidative reactions.

1.3.4. Conclusions

The study of physical and structural changes during dehydration is important because they are related with different aspects of food processing, as well as with the quality of the dehydrated product and its acceptance by the consumer.

These changes can be classified in two groups: the changes occurring at molecular and microstructural level and the changes occurring at macrostructural level. They are not independent, and variation in a property can influence in the variation of another property, being most of them interrelated. Figure 1.12 shows a schematic diagram of the changes in chemical and physical properties during dehydration of vegetable tissue and their importance in some food processing and quality aspects.

Physicochemical changes are also dependent on the dehydration technique and process conditions. They have mostly been studied in convective dried materials, whereas there is lack of investigation in other dehydration techniques, being osmotic dehydration one of them.

For these reasons, the study of the physical and structural changes during osmotic dehydration of vegetables is a subject of importance and is the purpose of this dissertation.

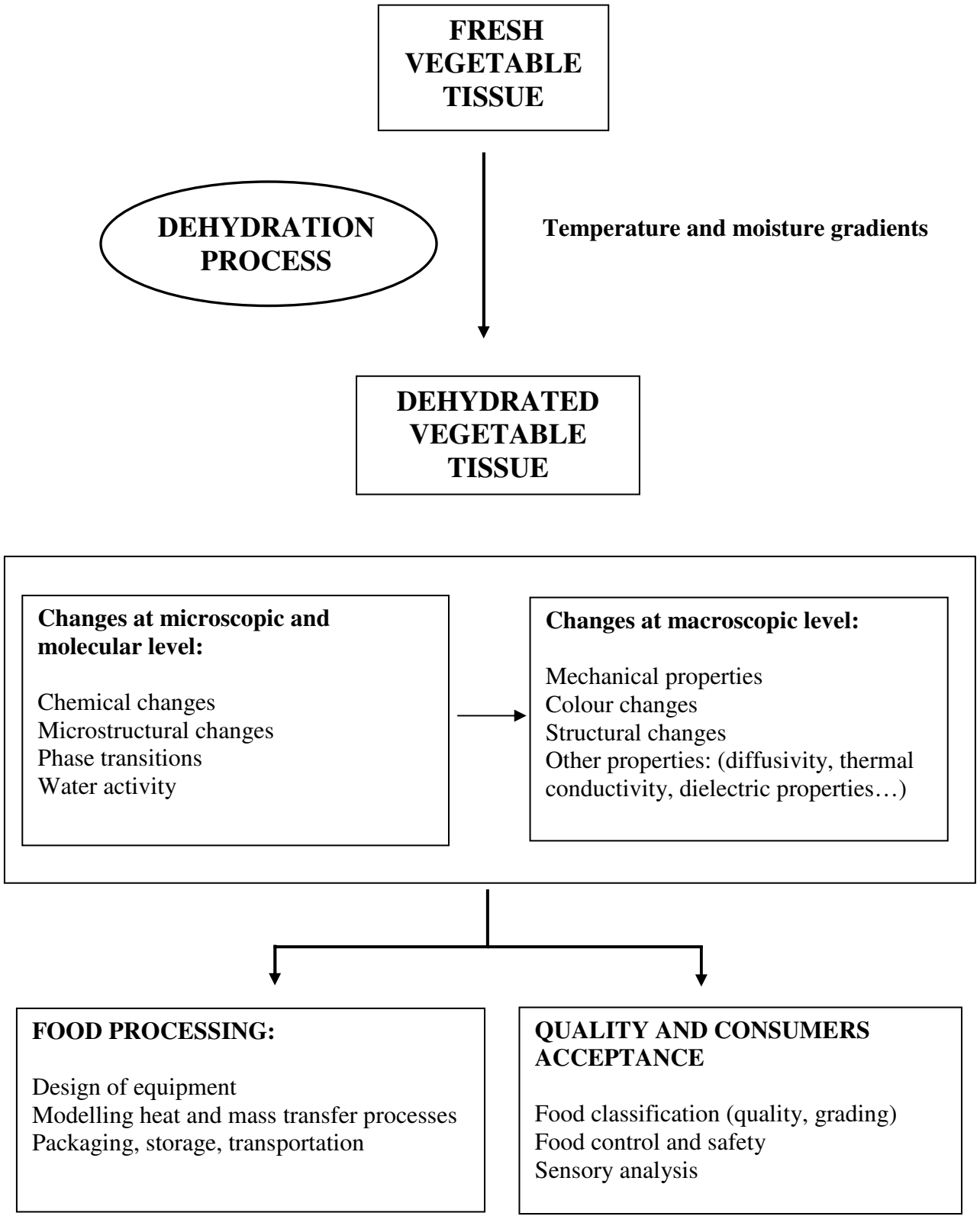

Figure 1.12. Changes in physical and chemical properties during dehydration treatments and their importance in food processing and quality parameters.

1.4. Objectives of the work and structure of the results

The main objective of this thesis is the study of the changes of some physical properties and structure of vegetable tissue submitted to a dehydration process. The dehydration process studied was the osmotic dehydration. Figure 1.13 shows a diagram of the thesis structure,

First of all a vegetable was chosen as a model for these studies (Chapter 2), on the basis of its availability, uniformity and typical cellular structure. The vegetable chosen was pumpkin fruit.

Then the kinetics of osmotic dehydration of the selected vegetable were studied (Chapter 3), varying the process conditions (concentration, temperature and contact time) and the osmotic agent. Three different aqueous solutions were used: binary sucrose solutions, binary NaCl solutions and ternary sucrose/NaCl solutions. A mass transfer model was used in order to relate the process conditions with the different mass transfer fluxes of the dehydration treatment.

Hereafter different physical properties were studied during osmotic dehydration of pumpkin fruits with sucrose solutions, namely sorption properties (Chapter 4), volume, density and porosity (Chapter 5), colour (Chapter 6) and mechanical properties (Chapter 7). In some cases, the experimental determinations were done with methods found in the literature. In others, new experimental methods were implemented. Some models and correlations were employed in order to relate the changes in the physical properties with the process conditions used. After that, the changes in the microstructure of the selected vegetable tissue during osmotic dehydration with sucrose solutions were studied (Chapter 8), by means of microscopy techniques.

Finally, the conclusions of the thesis and perspectives for future work were commented (Chapter 9).

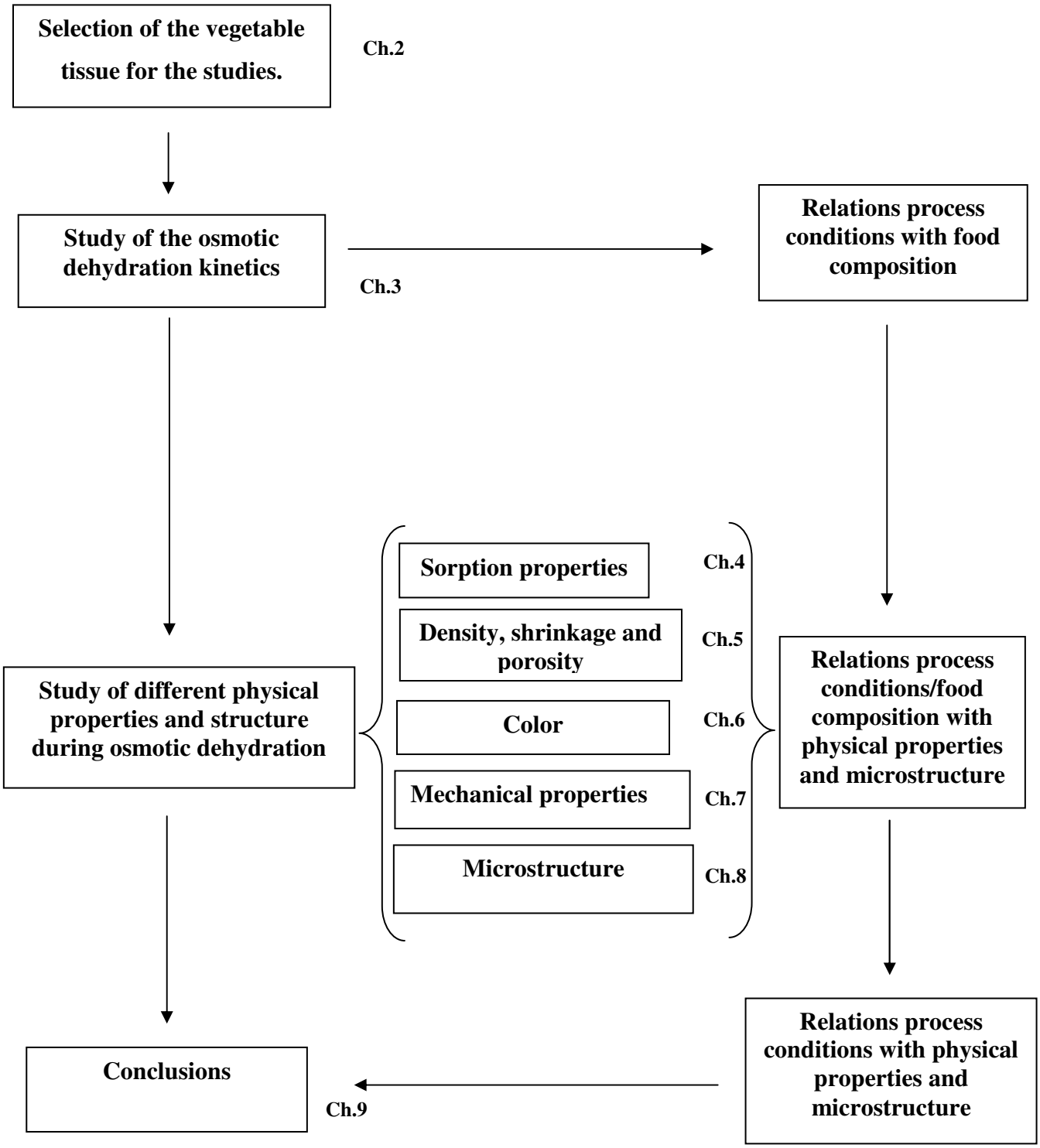

Figure 1.13. Thesis structure.

CHAPTER 2

SELECTION OF A FOOD MODEL: PUMPKIN FRUITS

CHAPTER 2. SELECTION OF A FOOD MODEL: PUMPKIN FRUITS

In this chapter, a brief description of the process of selection of the vegetable chosen as food model, pumpkin fruits, is given. Some general aspects of taxonomy, morphology, composition and production of pumpkin fruits are also revised.

2.1. Selection of a food model

2.1.1. Introduction

In the initial stage of this work, several vegetable products were tested in order to choose one which could serve as food model, namely, a material representative of a wide range of vegetables in their structural and physical properties. For this purpose, the main factor taken into account was the homogeneity of the structure of the fresh product. Other factors were also considered, in order to facilitate the measurement of the more relevant physical properties:

- Maintenance of a minimum structural rigidity during processing.
- Cellular structure with good visibility and definition under the microscope.
- Local availability throughout the year.
- Commercial interest of the product after processing.
- Not yet much studied as represented by literature references.

2.1.2. Materials and methods

Several products were preselected, namely: apple, pumpkin, melon, mango, guava, papaya and courgette.

For the evaluation of the tissue structure, the vegetable was cut and the homogeneity of the flesh was visually assessed.

After the visual evaluation, the flesh of tissue was stained in methylene blue, basic fuchsine and eosin solutions, with different concentrations (0.01, 0.05, 0.1, 0.5, 1 and 5%). The stained tissue was observed under a stereomicroscope (Olympus SZ-11, Tokyo, Japan). Image acquisition and processing was performed as explained in 7.2.3.3.

The structural rigidity after processing was qualitatively evaluated. Three cylinders (1.5 cm diameter, 2.5 cm, height) cut from the flesh of each fruit were immersed in sucrose solutions (60% weight) during 6 hours, and the consistence of the product was assessed by applying a gentle pressure with the fingers and feeling the resistance to compression.

2.1.3. Results and discussion

As expected after the preselection of the materials, all of them showed an acceptable homogeneous structure. Apple and melon showed a structure quite homogeneous in all the regions of the fruit. Pumpkin and mango also showed homogeneous tissues, but in these cases it was observed a fibre-oriented structure. Guava, papaya and courgette showed a homogeneous structure in the external zone of the flesh, but the extension of this homogeneous zone was not very large.

Under microscopical observation, the dyer which offered the best tissue visibility and definition was methylene blue, in a concentration of 0.1%. Figure 2.1 shows some microphotographs of the different observed tissues, stained with methylene blue solutions 0.1%. Methylene blue, a basic thiazine dyer, stains cellulose and other compounds blue in plant tissues (Horobin and Kierman, 2002).

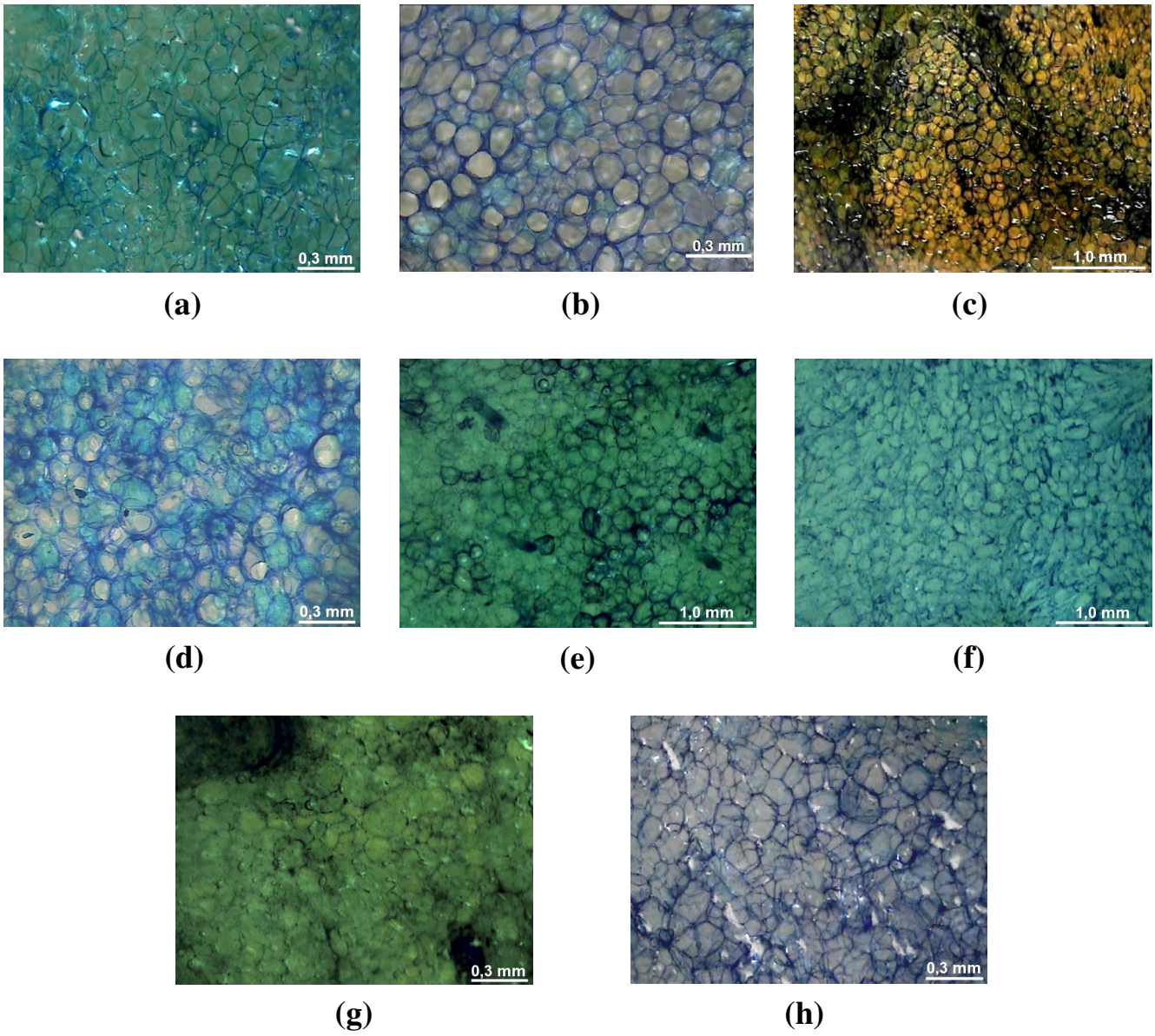

Figure 2.1. Microphotographs of the flesh of different vegetables, stained with a 0.1 % methylene blue solution. (a) Apple. (b) Pumpkin (*Cucurbita Pepo, L.*). (c) Pumpkin (*Cucurbita maxima, L.*). (d) Melon. (e) Mango. (f) Guava. (g) Papaya. (h) Courgette.

The best results for microscopical observation were for apple, pumpkin, melon and courgette; for the other fruit results were also acceptable.

After osmotic dehydration, only melon and papaya showed a very soft and poor consistency after processing. The rest of products remained consistent after dehydration.

Table 2.1 shows the results of the assessment of the different considered factors in the preselected materials. The analyzed factors were qualified as good, acceptable or insufficient.

Table 2.1. Evaluation of the main factors considered in the selection of the food model.

Material	Structural homogeneity	Consistence after processing	Microscopical observation
Apple	Good	Good	Good
Pumpkin	Good-fibrous	Good	Good
Melon	Good	Insufficient	Good
Mango	Good-fibrous	Good	Acceptable
Guava	Good only the external region	Good	Acceptable
Papaya	Good only the external region	Insufficient	Acceptable
Courgette	Acceptable	Good	Good

The best results were obtained for apple and pumpkin. Apple is a widely studied material in food engineering. The scarce literature existent about pumpkin processing, along with the good characteristics observed encouraged us to use it as food model in this work. Furthermore, the typical large size of the fruits of some pumpkin varieties allowed a significant number of samples to be taken from a single source, reducing the usual variability found in natural products.

2.2. Pumpkin fruits: general aspects of composition, properties and production

2.2.1. Introduction

Pumpkins (*Cucurbita* Sp.), also known as squashes or gourds, are vegetables of the family *cucurbitaceae*, a wide family that includes other fruits such as melon, watermelon and cucumber. Pumpkins are annual or perennial climbing or trailing herbs, including about 25 species of which *Cucurbita maxima, Cucurbita moschata* and *Cucurbita pepo* are of economic importance. Each species comprises a large number of varieties yielding fruits of different size and shape.

They are among the most ancient cultivated plants, and several authors have established an american origin for *Cucurbita* species. Seeds and/or rinds of *Cucurbita Pepo* have been found at human settlements dating 7000-9000 BC in Mexico (Robinson and Decker-Walters, 1997). As commented by these authors, aboriginal plant gatherers were probably attracted to these products, particularly by the relatively large and sometimes showy fruits. After fruits were taken back to the settlements, seeds that were purposely discarded, accidentally dropped or partially digested found new life on rubbish heaps, settlement edges or other disturbed areas within the camp. Eventual recognition of the value of the resident cucurbits led to their tolerance, horticultural care and further exploitation. Finally, seeds and, more rarely, vegetative propagules were carried by and exchanged among migrating bands of these incipient cultivators, gradually turning the earliest cultivated cucurbits into domesticated crops. *Cucurbita Pepo* was the first pumpkin specie introduced in Europe, and today is grown throughout the world.

2.2.2. Morphology and anatomy

Pumpkin plants generally have a strong tap root and many secondary roots occurring near the soil surface. The herbaceous or sometimes softly woody stems are typically prostrate, trailing or climbing, angled in cross section, centrally hollow, sap-filled and branched. Primary and secondary branches can reach 15 m in length. Cucurbit leaves

are usually simple (i.e. not divided into leaflets), palmately reined and shallowly to deeply three to seven-lobed. Many cucurbits have large showy flowers which attract pollinating insects. Flowers are unisexual, often white or yellow, but other colours exist. Fruits are extremely diverse in many characteristics, including size, shape, colour and ornamentation. Seeds are usually flat with different colour, size and shape among the varieties. The seed coat encloses a collapsed perisperm, an oily embryo and little or no endosperm. Two cotyledons make up much of the contents of the seed.

The most popular pumpkins in Portugal are the "*abóbora menina*" and the "*abóbora porqueira*", varieties of *Cucurbita Maxima* and *Cucurbita Pepo* respectively ("abóbora" is the portuguese word for pumpkin). Pumpkin species can be distinguished on the basis of peduncle, foliage and seed characteristics (Robinson and Decker-Walters, 1997), and several authors have verified the classification of these two portuguese pumpkin varieties (Vasconcellos, 1949; Gardé and Gardé, 1988).

Figure 2.2. Ready-to-harvest pumpkins in the field.

In this work, the pumpkin used was *Cucurbita Pepo L.* (*porqueira v.*). It was preferred to the other major portuguese variety because of its shorter dehydration time (typically around nine hours) against more than twelve hours of the "*menina*" type, making the experimental work easier. Figure 2.2 shows an image of some ready-to-harvest pumpkins fruits (*porqueira v.*).

2.2.3. Fruit structure

Pumpkin fruit (Figs. 2.3 and 2.4) can be classified as a syncarpous, indehiscent peponium, coming from a gynoecium with three to five carpels. The fruit is composed by the pericarp and seeds. The pericarp (Fig. 2.5 (a and b)) is differentiated in exocarp, mesocarp and endocarp. The different types of cells and tissues forming the parts of a fruit were described in detail by Raven *et al*. (1999). Some relevant characteristics of the pumpkin fruit tissues are described below.

The exocarp is commonly known as the rind, and is composed of cells with highly lignified cell walls, called fibres. Close to the pericarp, there are communicating xylem bundles (Fig. 2.5 (a)) with the function of transporting water and mineral salts to all the parts of the fruit.

The endocarp is composed of some uncompacted parenchymatic bundles close to the seeds (Fig. 2.5 (a)).

In the mesocarp, the tissue is disposed in bundles (also called fibres in other parts of the work), as observed in Figure 2.5 (c). These bundles or fibres (Fig. 2.5 (e)) are formed by sclerenchymatic cells (more lignified) in the centre and parenchymatic cells around them, constituting a circular arrangement. The sclerenchymatic fibrous centre acts as support of the fruit structure. Around this centre, the parenchymatic tissue is compacted with few intercellular spaces; in the limits of the bundle-unit the parenchyma cells are less compacted, with more intercellular spaces and likely with a less efficient middle lamella, delimiting the bundle dimensions.

Figure 2.3. Pumpkin fruit.

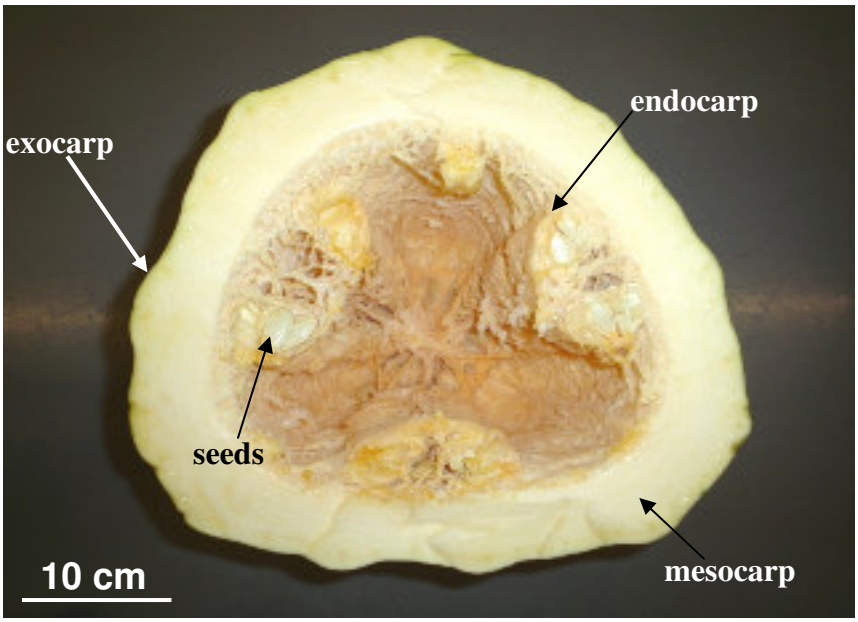

Figure 2.4. Different parts of the fruit (cut perpendicular to the major axis of the fruit).

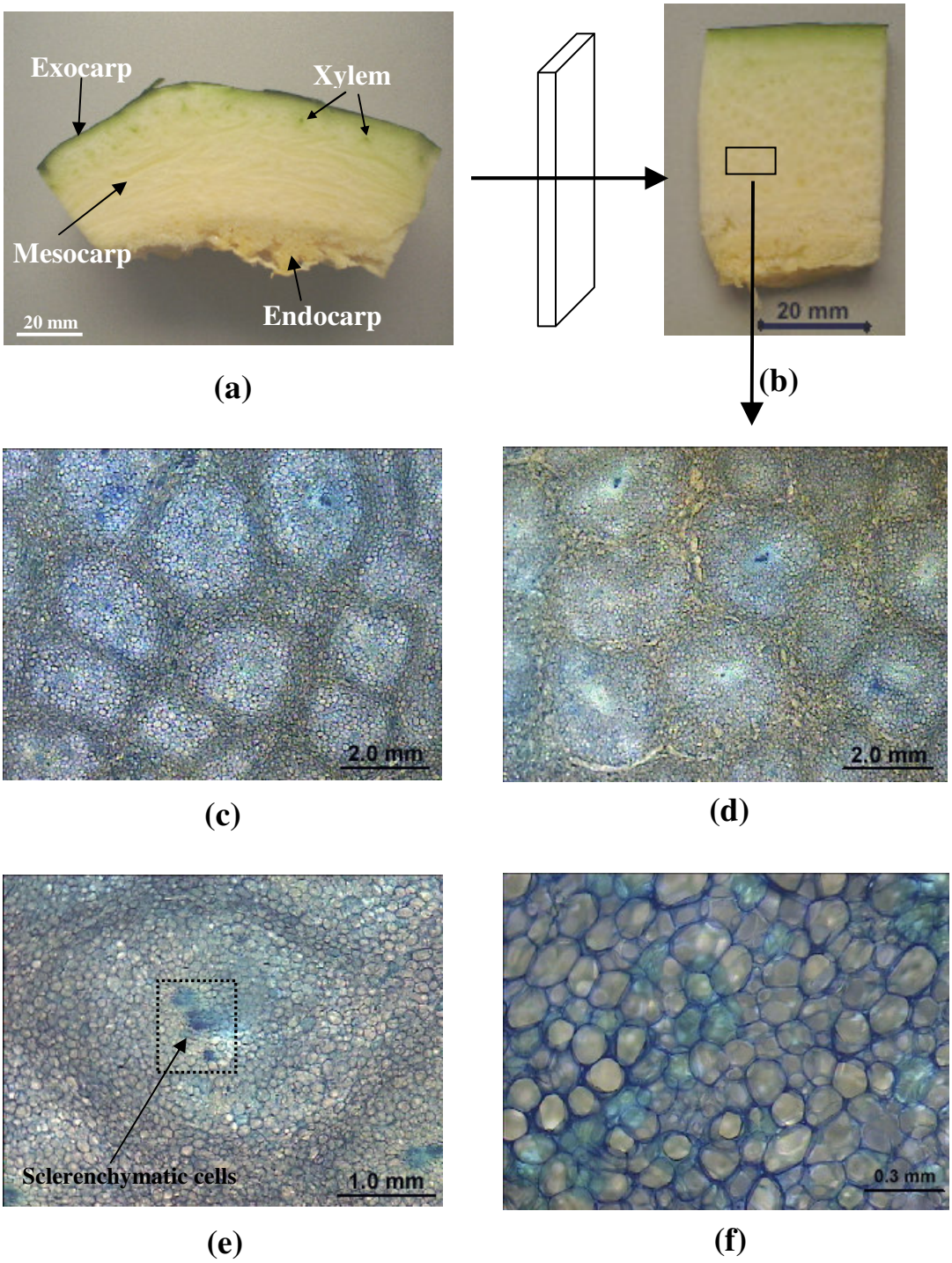

Figure 2.5. Structural elements of the pumpkin pericarp. (a) Pericarp of the fruit. (b) Pericarp cut parallel to the major axis of the fruit. (c) Detail of the mesocarpic tissue structure. (d) Mesocarpic tissue, high degree of ripeness. (e) Mesocarpic bundle. (f) Parenchymatic tissue of the mesocarpic bundle.

Initially, when the fruit is immature, the delimitation of these bundles is not clear, because all the parenchymatic tissue is highly compacted. During the development and maturation of the fruit, the walls of the parenchyma cells in the limits of each bundle become thinner and develop more intercellular spaces, individualizing each bundle-unit (Fig. 2.5 (d)). The parenchymatic tissue is made up of "aquifer parenchyma cells", with low quantity of storage substances and high water content (Fig. 2.5 (f)).

2.2.4. Chemical composition

Table 2.2 shows compositional data of different pumpkin varieties and the composition of the seeds of one of the varieties. These fruits have high moisture content; the second major constituent are carbohydrates followed by proteins, fibre and fat in this order. Moisture content and carbohydrates varies significantly among the different species considered. Carbohydrate content in particular can play an important role in the taste of the fruit. It is interesting to note the relatively high vitamin A content; not as high as in carrot (11000 IU) or spinach (8100 IU), similar to tomato (900 IU), but higher than in beans (280 IU), oranges (200 IU) and apples (90 IU) (Ensminger *et al.,* 1995). Vitamin A along with other carotenoids is responsible for the yellow-orange colour of the fruit flesh.

The most nutritious part of pumpkin fruit is the seed, which is a good source of protein, vegetal fat and minerals.

2.2.5. Economical interest

Pumpkin fruits are consumed both immature and ripe. The flesh of the fruit can be processed in several ways, leading to products of different organoleptic characteristics. These different ways of processing make this fruit an interesting product for the food industry. Teotia (1992) indicates several of such uses:

Table 2.2. Composition of the flesh and seeds of different pumpkin varieties.

	Flesh			Seeds
	Pumpkin	**Summer squash**	**Winter squash**	**Pumpkin**
Moisture (%)	92	93-95	84-88	4
Protein (%)	1.0	0.9-1.2	1.4-1.5	29.0
Fat (%)	0.1	0.1-0.2	0.1-0.3	46.7
Carbohydrates (%)	6.5	3.6-5.1	9.4-14	15.0
Fibre (%)	1.1	0.6	1.4	1.9
Vit. A (IU)	1600	190-460	190-460	70
Vit. C (mg/100g)	9	18-25	18-25	-
Vit. B1,Thiamin	0.05	0.05	0.05	0.24
Ca (mg/100g)	21	28	19-32	51
P (mg/100g)	44	29	31-58	1744
Na (mg/100g)	1	1	1	-
Mg (mg/100g)	12	22.0-23.7	16.5-32.0	-
K (mg/100g)	340	202	217-487	-
Fe (mg/100g)	0.8	0.4	0.6-0.9	11.2
Cu (mg/100g)	0.1	-	0.12	-

Adapted from Robinson and Decker-Walters (1997)

- It can be eaten boiled, fried and baked.
- It has been processed in industry and sold canned or frozen.
- It has been used as an ingredient in baby food products, especially pumpkins with high carotenoids content.
- It can be used in the production of confectionery products: jams, pumpkin sweets, pies.
- It can be used in the production of pickles.
- Finally, powder from dried pumpkin has been used to improve the organoleptic properties of bakery products.

Other parts of the plants are used as well. The seeds are eaten as snacks in some countries (Spain, Mexico, USA). Vegetal oil is extracted for the seeds and can be used for cooking or as a food ingredient. The shoots, leaves and flowers are fresh-eaten as vegetables in salads. The rind and flesh of the fruits can be used to obtain pectic substances, with a potential use as food ingredients (Ptitchkina *et al.* 1994; Jun *et al.* 2006).

The cultivated area and production yield of pumpkin in the world have progressively increased. Results from 1980 to 2005 (FAOSTAT data, 2005), are presented in Figure 2.6. Nowadays, China is the world's leading producer of the major cucurbit crops, not only pumpkins but also other cucurbits such as cucumber, melon and watermelon (FAOSTAT data, 2005). Table 2.3 shows the main producers of pumpkin crops in 2004.

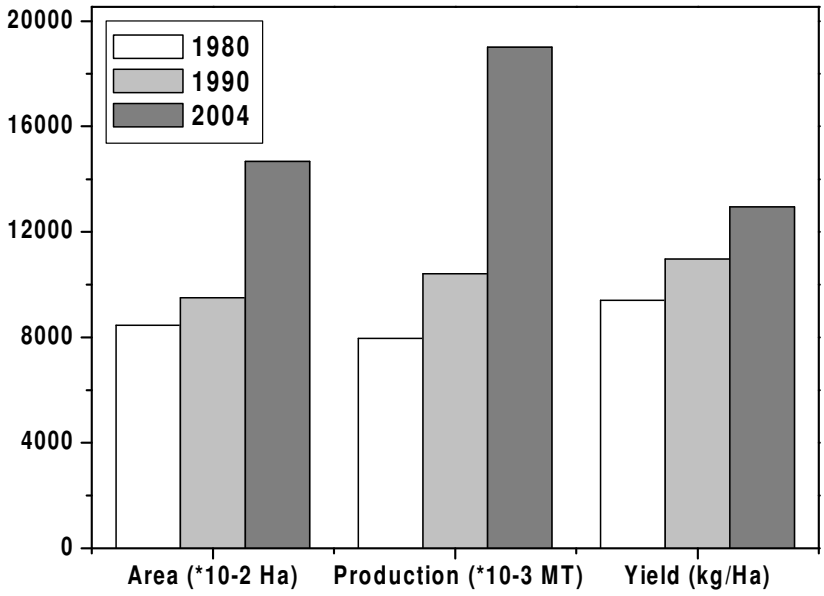

Figure 2.6. Harvested area, production and yield of pumpkin cultivars in the world, during the period 1980-2004.

Table 2.3. Leading producers of pumpkin crops in 2004.

Country	Production (10^3 Ton)
China	5674
India	3500
Ukraine	900
United States	740
Egypt	710
Mexico	560
World Total	19016

Source: FAOSTAT data (2005)

Pumpkin production in Portugal is not high (Table 2.4); far from the production of the major crops (tomato, melon and cabbage) and close to the production of green beans, turnip leaves and strawberries (INE data, 2005). The use of this vegetable in the portuguese diet is not remarkable; it has been traditionally used in soups and confectionery. The fruit is mainly used for animal feed.

Table 2.4. Main vegetables produced in Portugal in 2004.

Ranking	Product	Production (10^3 Ton)
1	Tomato	99
2	Melon	92
3	Cabbage	65
4	Red cabbage	59
5	Lettuce	57
6	Carrot	54
7	Pepper	48
8	Onion	39
9	Broccoli	35
10	Watermelon	27
16	Pumpkin	12

Source: INE data (2005)

Pumpkins are sensitive to low temperature, due to the tropical and subtropical origin of these plants. Pumpkin of the "*porqueira"* variety is available in Portugal from May to December, with important variation in the price of the fruit (from 0.3 to 2.0 euros/kg in 2005). The use of a dehydration process can extend the shelf-life of the fruit, making pumpkin products available all the year.

2.3. Conclusions

Pumpkin fruit is a material that can be used as a vegetable tissue model in food engineering due to its homogeneous "fibre oriented" structure, fruit size, shelf life and low cost.

The use of an osmotic process can be an interesting tool in the production of new processed products based on fresh pumpkin fruits, improving its already good shelf life.

CHAPTER 3

KINETICS OF OSMOTIC DEHYDRATION OF PUMPKIN FRUITS

CHAPTER 3. KINETICS OF OSMOTIC DEHYDRATION OF PUMPKIN FRUITS

3.1. Introduction

The aim of this chapter is to obtain experimental data on kinetics of osmotic dehydration of pumpkin and model such data using a simplified model based on Fick's second law of diffusion. For this purpose, osmotic dehydration experiments were carried out with different osmotic solutions, namely binary sucrose/water solutions, binary NaCl/water solutions and ternary NaCl/sucrose/water solutions. Concentration of the osmotic agents and temperature were varied in the case of binary solutions, whereas for ternary solutions only osmotic solutes concentration was varied.

The mathematical model used includes effective diffusion coefficients for each transferring component: salt, sucrose and water. These coefficients can be used to predict osmotic dehydration kinetics at other conditions than those used in this work. Such coefficients will be obtained with and without shrinkage considerations.

3.2. Materials and methods

3.2.1. Sample preparation

Pumpkin fruits (*Cucurbita Pepo L.*) were purchased from a local producer, and stored at 15-20 ºC in a chamber until processing. Pumpkins with similar initial moisture content (95-97 kg water/100 kg product) and soluble solids (2-4 Brix) were selected for the experiments. Cylinders (25 mm length, 15 mm diameter) from the parenchymatic tissue were obtained employing a metallic cork borer and a cutter. In order to obtain a good structural and compositional homogeneity in the samples, the cylinders were taken from the middle zone of the mesocarp, parallel to the major axis of the fruit, as observed in Figure 3.1.

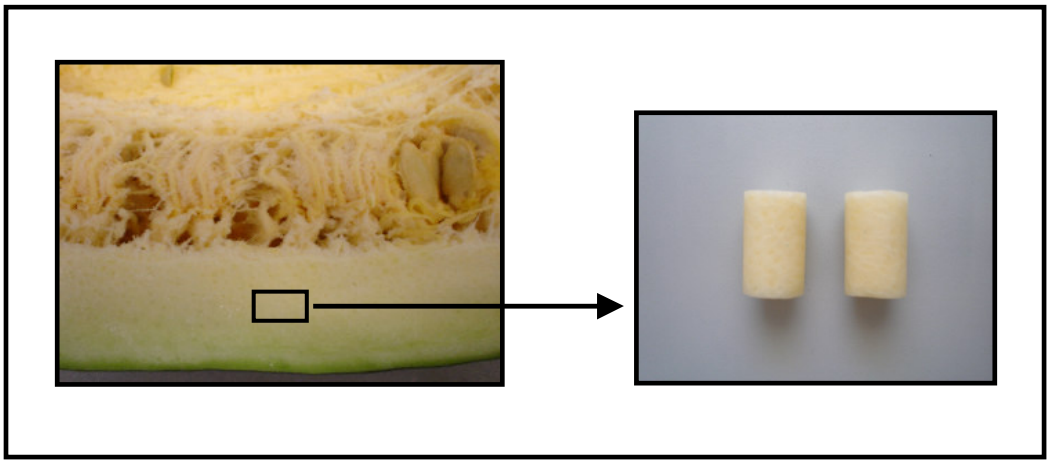

Figure 3.1. Preparation of pumpkin cylinders for the dehydration experiments.

3.2.2. Osmotic solutions and process conditions

As osmotic agents, three different solutions were employed: binary sucrose/water and NaCl/water solutions and ternary sucrose/NaCl/water solutions. The solutions were prepared using distilled water and commercial sucrose and salt.

The levels of temperature and concentration of the osmotic agents were selected using a Uniform Shell Design (Doehlert, 1970).

For binary solutions, temperature ranged from 12 to 38ºC. Sucrose concentration varied from 30 to 60% (w/w) in sucrose solutions, whereas with NaCl solutions the salt concentration ranged 5-25% (w/w). Tables 3.1 and 3.2 show the selected process conditions for osmotic dehydration with sucrose and NaCl solutions respectively.

Table 3.1. Experimental design for dehydration of pumpkin with sucrose solutions.

Coded experimental plan		Actual experimental plan	
X_1	X_2	Sucrose (kg/100kg)	T (ºC)
-1	0	30	25
0	0	45	25
1	0	60	25
-0.5	-0.866	37.5	12
-0.5	0.866	37.5	38
0.5	-0.866	52.5	12
0.5	0.866	52.5	38

Table 3.2. Experimental design for dehydration of pumpkin with NaCl solutions.

Coded experimental plan		Actual experimental plan	
X_3	X_2	NaCl (kg/100kg)	T (ºC)
-1	0	5	25
0	0	15	25
1	0	25	25
-0.5	-0.866	10	12
-0.5	0.866	10	38
0.5	-0.866	20	12
0.5	0.866	20	38

For ternary sucrose/NaCl solutions, temperature was maintained at 25 ºC. Sucrose concentration varied from 32 to 58% (w/w) whereas salt concentration ranged 0-15% (w/w). Table 3.3 shows the selected process conditions for osmotic dehydration in sucrose/NaCl solutions.

Table 3.3. Experimental design for dehydration of pumpkin with sucrose/NaCl solutions.

Coded experimental plan		Actual experimental plan	
X_1	X_3	Sucrose (kg/100kg)	NaCl (kg/100kg)
0	-1	45	0
0	0	45	7.5
0	1	45	15
-0.866	-0.5	32	3.75
0.866	-0.5	58	3.75
-0.866	0.5	32	11.25
0.866	0.5	58	11.25

3.2.3. Experimental set-up for osmotic dehydration tests

The cylinders were put in baskets, which were introduced in stirred vessels containing the osmotic solution. Agitation was conducted using a magnetic stirrer; the speed was chosen according to the kinematic viscosity so as to have a constant Reynolds number (c.a. 3000). Reynolds number was calculated according Eq. (3.1) (Perry and Green, 1999)

$$Re = \frac{N \cdot d^2}{v} \qquad (3.1)$$

The weight ratio of osmotic solution to pumpkin cylinders was 20:1, allowing solution to maintain a constant concentration during the dehydration process. Thermoregulation was obtained by means of a thermostatic bath (±0.2 ºC).

Figure 3.2 shows a schematic picture of the experimental set-up used in the osmotic treatments.

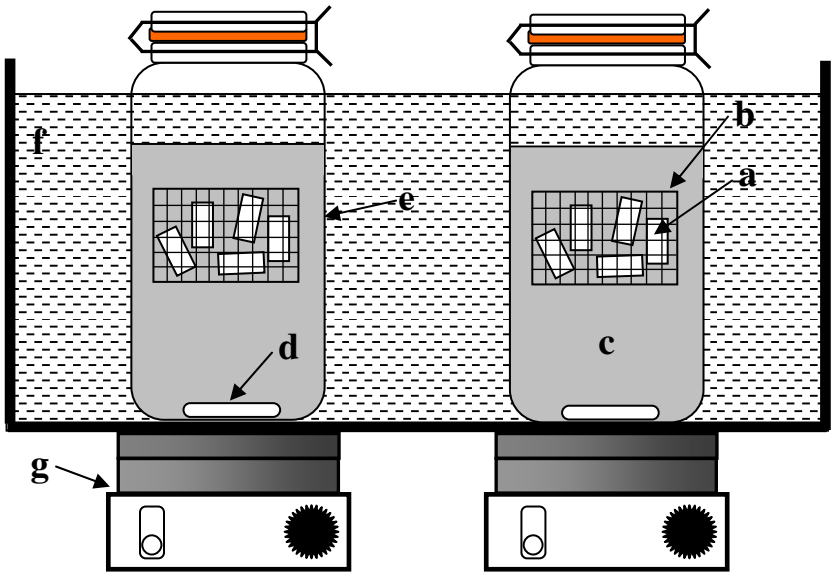

Figure 3.2. Experimental set up for the osmotic treatments. (a) Sample; (b) plastic basket; (c) osmotic solution; (d) magnetic stirrer; (e) hermetic vessel; (f) thermostatic bath; (g) magnetic support.

3.2.4. Experimental determinations

At each contact time (0.25, 0.5, 1, 3, 6 and 9 hours for binary NaCl and sucrose solutions; 0.25, 0.5, 1, 2, 4, and 6 hours for ternary NaCl/sucrose solutions) four cylinders were taken out from the solution and blotted with paper tissue to remove adhered osmotic agent. Then the samples where kept in plastic boxes till experimental determinations.

After the osmotic treatment, each sample was weighed to determine its weight reduction (WR) (Eq. (3.2)). The solids gain (SG) (Eq. (3.3)) were evaluated after vacuum drying at less than 10^4 Pa at 70ºC till constant weight (weight variation less than 0.1% in two consecutive weighing during intervals of two hours of vacuum drying) (AOAC, 1984).

$$WR = \frac{m_o - m}{m_o} \tag{3.2}$$

$$SG = \frac{s - s_o}{m_o} \tag{3.3}$$

It was considered that the flow of solutes from the material to the osmotic solution was negligible, and NaCl and/or sucrose were all the solids gained by the material. Water loss (WL) and normalized moisture content (NMC) were also determined by means of the Eqs. (3.4) and (3.5) respectively

$$WL = SG + WR \tag{3.4}$$

$$NMC = \frac{w \cdot m_o}{w_o \cdot m} \tag{3.5}$$

In the case of binary solutions, solids gain was considered as sucrose gain or NaCl gain, when sucrose solutions or salt solutions were employed in the dehydration experiments, respectively.

In the case of ternary solutions, determination of NaCl content was carried out by means of a conductimetric method. After vacuum drying for the determination of the total solids content, each sample was rehydrated in distilled water during 12 hours. The mixture was grinded, homogenized, filtered and distilled water was added until completing 100mL of solution. Conductimetric measurements were performed in the filtrate with a Crison GLP-32 conductimeter (Crison Instruments S.A., Barcelona, Spain). The equipment was previously calibrated for the range of concentrations of salt and sucrose used in the

experiments. When the mass of NaCl was obtained it was possible to obtain the NaCl gain (NaClG) and the sucrose gain (SucG) by means of the Eqs. (3.6) and (3.7) respectively

$$NaClG = \frac{NaCl - NaCl_o}{m_o} \tag{3.6}$$

$$SucG = SG - NaClG \tag{3.7}$$

3.2.5. Mass transfer model

Mass transfer during osmotic treatments has been successfully modelled using Fick's second Law of diffusion (Lazarides *et al*., 1997; Telis *et al*., 2004), considering external resistance to mass transfer negligible as compared to the internal resistance.

When the Fick's law is applied, other assumptions are usually implicit. One of these is that the volume of the material remains constant during the process. However, most of times water loss and solids gain during the process lead to changes in the volume of the material being dehydrated. Neglecting shrinkage can lead to different values of the effective diffusion coefficients, likely to be overestimated when shrinkage is not considered (Mayor and Sereno, 2004). In spite of this, few works take into account volume variation when modelling osmotic dehydration using Fick's second law (Hough *et al*., 1993; Mauro and Menegalli, 2003).

Another assumption in this work was to consider the finite cylinders as spheres. This is reasonable considering the low ratio length/diameter of the cylinders (sphericity 0.85). Thus, the final mathematical model is simple and the results obtained are more general and can be compared with results of other food materials independently of the geometry used. For this purpose the equivalent radius of the used cylinders was obtained by means of Eq. (3.8), which considers each cylinder as a sphere with the same volume

$$r = \left(\frac{3V}{4\pi}\right)^{\frac{1}{3}} \tag{3.8}$$

With such assumptions, and considering that unsteady state Fickian diffusion governs the process, effective diffusion coefficients can be calculated by means of the analytical solution of Fick's Law applied to spheres. The total amount of each diffusing substance (water, sucrose or NaCl) crossing the sphere surface during a period of time t is given, in these conditions, by (Crank, 1975)

$$\frac{M_t}{M_{eq}} = 1 - \frac{6}{\pi^2}\sum_{j=1}^{\infty}\frac{1}{j^2}\exp\left(\frac{-D_{eff}\, j^2 \pi^2 t}{r^2}\right) \tag{3.9}$$

To take into account the shrinkage of samples, an equation relating changes of their volume with weight reduction was used

$$\frac{\mathrm{V}}{\mathrm{V_o}} = 1 - \mathrm{k}\cdot\mathrm{WR} \tag{3.10}$$

The model proposed by Azuara *et al*. (1992) was used to obtain equilibrium values of WL, SucG and NaClG, when the system was far from the equilibrium conditions. Eq.(3.11) shows the linearized equation of Azuara´s model

$$\frac{t}{M} = \frac{1}{q(M_{eq})} + \frac{t}{M_{eq}} \tag{3.11}$$

The general second order polynomial given below was used to relate equilibrium values of WL, SucG, NaClG and NMC with temperature, sucrose and NaCl concentration in the osmotic solution. Results obtained from Eq. (3.11) were analyzed using the STATISTICA 6.0 software (StatSoft Inc., USA).

$$y = \beta_o + \sum_{i=1}^{k} \beta_i x_i + \sum_{i=1}^{k} \beta_{ii} x_i^2 + \sum_{i=1}^{k-1} \sum_{j=i+1}^{k} \beta_{ij} x_i x_j \quad (3.12)$$

where x_i were the process conditions sucrose concentration, temperature and NaCl concentration and y were the corresponding dependent variables WL, SucG, NaClG and NMC.

In order to obtain the values of effective diffusion coefficients, experimental data were fitted to the mentioned Eq. (3.9). Values of M_t are values of water loss, sucrose gain and salt gain at a time t for water, sucrose and salt effective diffusion coefficients, respectively. Equilibrium values (M_{eq}) were obtained by linear fitting of Eq. (3.11) with experimental data. The values of the equivalent radius (Eq. (3.8)) after each processing time were obtained from their respective volumes by means of Eq. (3.10).

Non linear least square optimization (generalized reduced gradient method) was performed with Eq. (3.9), by means of the ‘‘solver’’ tool of Microsoft® Excel 97 software (Microsoft Corporation). The results allow obtaining the predicted values of WL, SucG and NaClG, and equilibrium values were obtained by means of Eq. (3.12).

3.3. Results and discussion

3.3.1. Osmotic dehydration with sucrose solutions

3.3.1.1. Dehydration kinetics

Figure 3.3 shows experimental data for water loss during osmotic dehydration of pumpkin with sucrose solutions at the process conditions before mentioned. All the process conditions tested showed the same behaviour along the process. Water loss increases fast up to the first three hours of process, then increases less fast till nine hours. For the same temperature of the osmotic solution (30, 45 and 60% sucrose at 25ºC) the water lost by the material increases with the increase of the concentration of the solution. For the same concentration (37.5 % at 12 and 38ºC, or 52.5% at 12 and 38ºC) WL increases with the increase of temperature. The values of WL ranged from 0 to 74% of the initial sample weight, depending on the process conditions employed. Sucrose gain (Fig. 3.4) increases fast up to the first three hours; and then increases in a less accentuated way till the end of process. As in the case of WL, for the same temperature of the solution sucrose gain increases with the solution concentration; and for the same concentration SucG increases with the temperature. Values of sucrose gain vary from 0% to 19% of the initial sample weight, respectively. Normalized moisture content (Fig. 3.5) decreases uniformly along the dehydration process. It decreases faster up to the first three ours of process; after that, due to the water lost and sucrose gained in the pumpkin cylinders, the driving force (difference of chemical potential between soaked material and solution) decreases and also the dehydration rate. As observed in WL and SucG, NMC values decrease with the increase of concentration and temperature of the solution. Moisture content varied from 100% to 57% of the initial value depending on the employed process conditions. Several authors have also observed an increase in WL and SucG with the increase of concentration and temperature of the osmotic solution during osmotic dehydration of vegetables with sugar solutions, as in the case of pumpkin (*Cucurbita Maxima, L.*) (Lenart *et al.*, 1993), pineapple (Saputra, 2001) and carrot (Uddin *et al*., 2004).

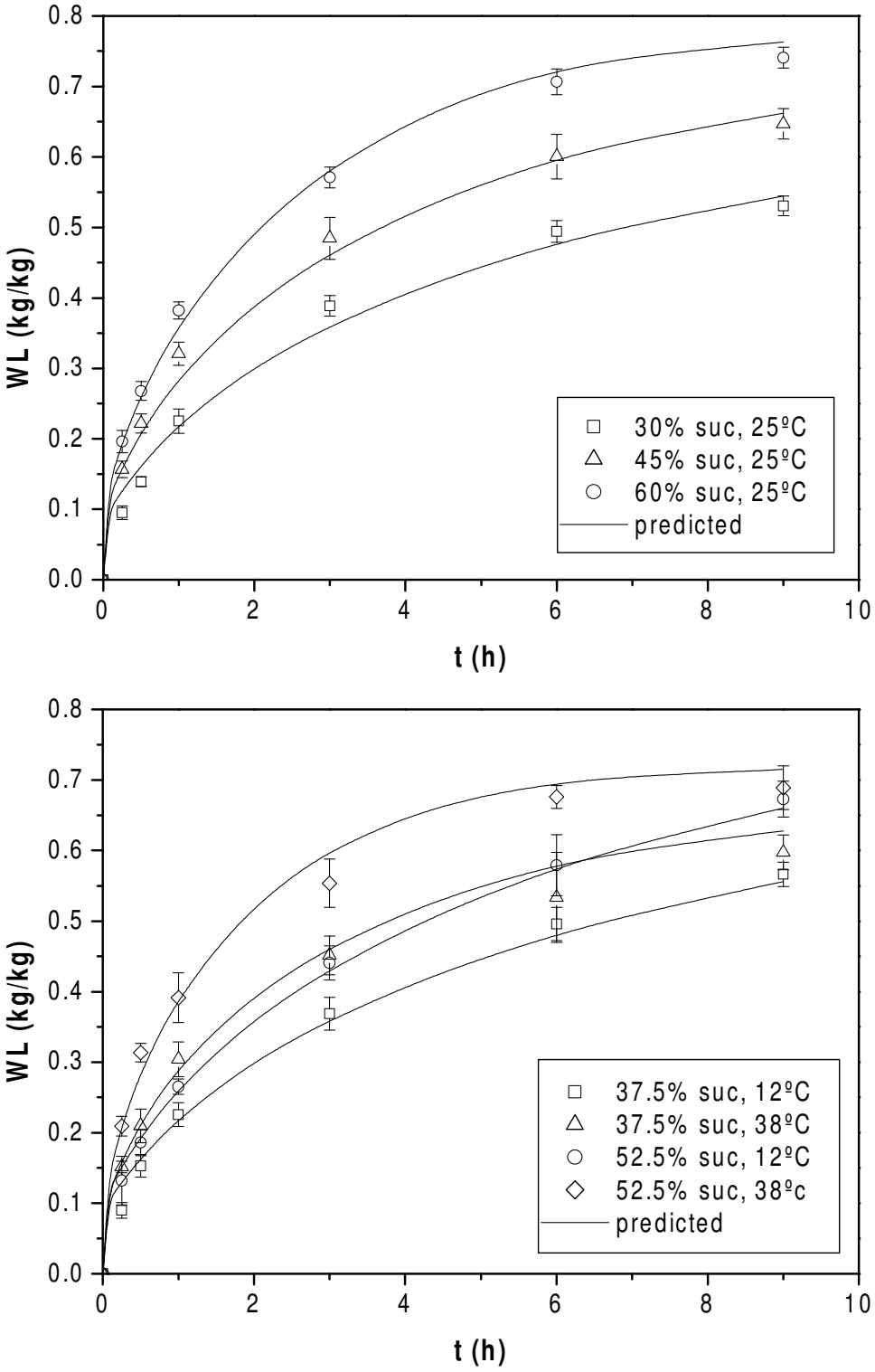

Figure 3.3. Water loss during osmotic dehydration of pumpkin at different sucrose concentration and temperature. Dots represent experimental data and the lines are predicted values with Fick's model considering shrinkage.

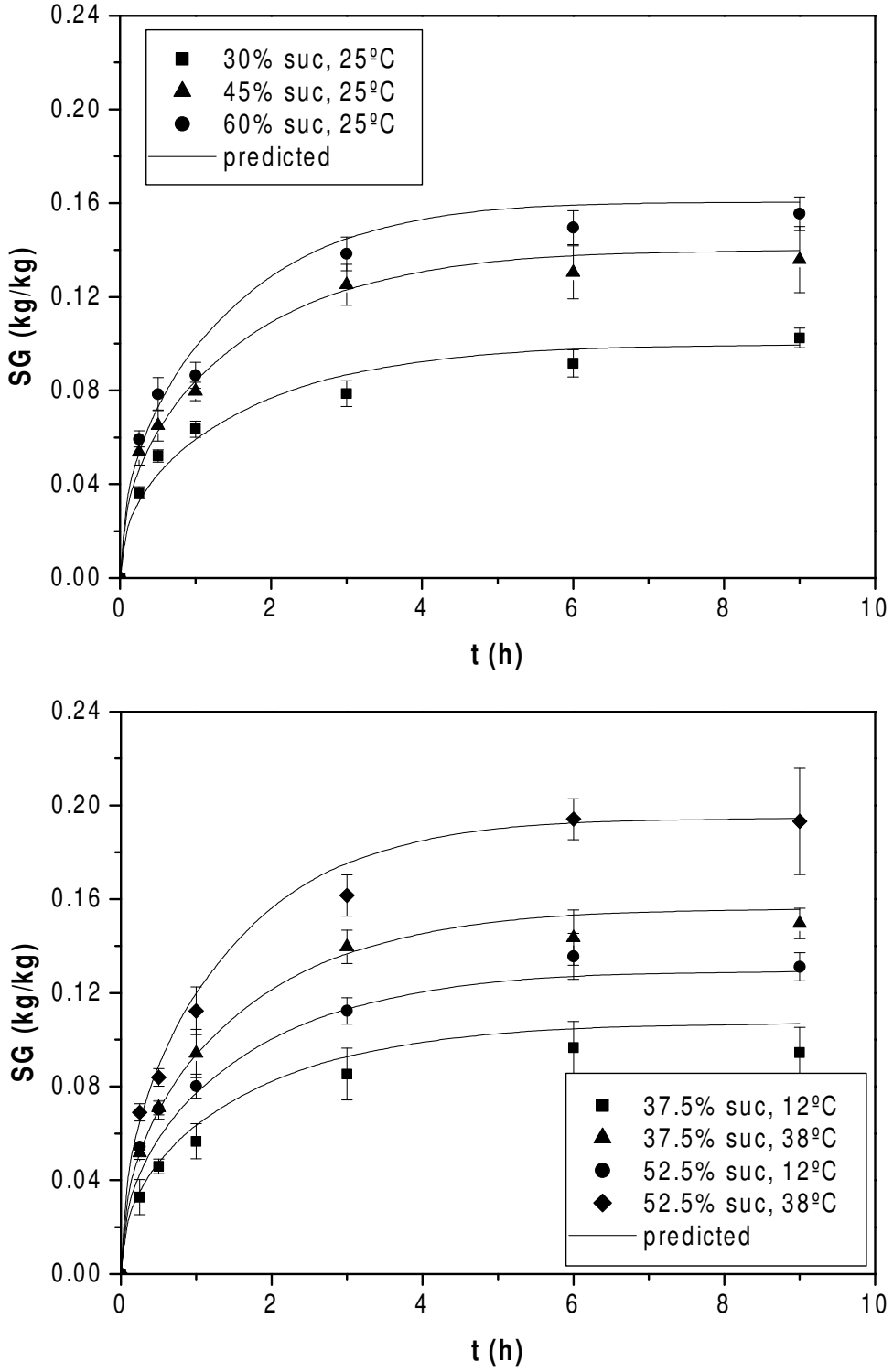

Figure 3.4. Sucrose gain during osmotic dehydration of pumpkin at different sucrose concentration and temperature. Dots represent experimental data and the lines are predicted values with Fick's model considering shrinkage.

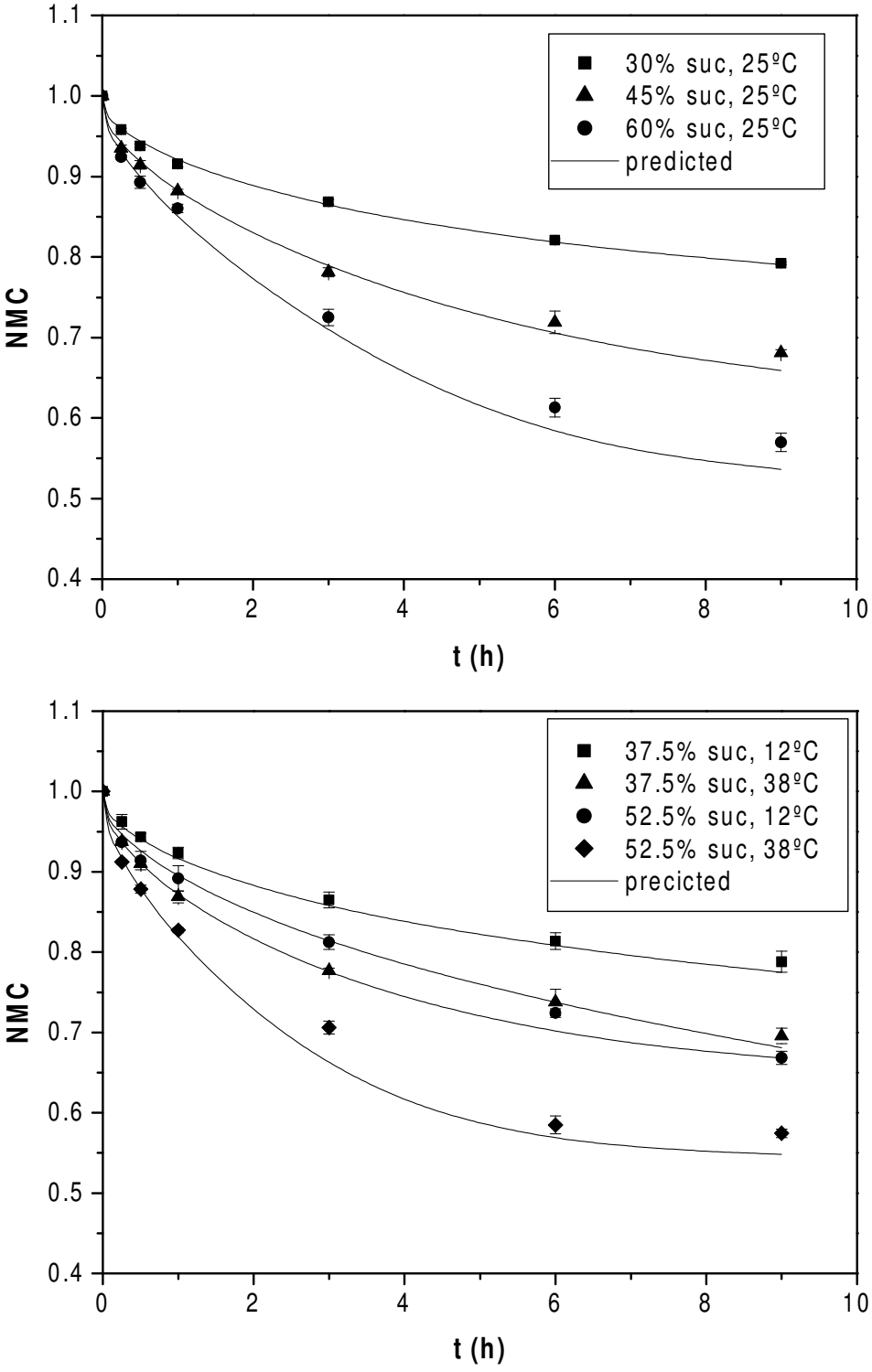

Figure 3.5. Normalized moisture content during osmotic dehydration of pumpkin at different sucrose concentration and temperature. Dots represent experimental data and the lines are predicted values with Fick's model considering shrinkage.

Weight reduction ranged 0-59% during dehydration with sucrose solutions, depending its final value on the conditions used. Weight reduction increases constantly till six hours of process, increasing smoothly till nine hours.

Equilibrium values for WL, SucG and NMC obtained from Azuara's model (Eq. (3.11)) were fitted to the proposed polynomial (Eq. (3.12)). The goodness of fit was evaluated by the correlation coefficient R^2 and the average relative deviation modulus ARD

$$ARD = \frac{100}{n}\sum_{i=1}^{n}\frac{|p_i - p_c|}{p_i} \tag{3.13}$$

Table 3.4. Regression coefficients of Eq. (3.12) for equilibrium values of normalized moisture content (NMC), water loss (WL) and sucrose gain (SucG).

Coefficient	NMC_{eq}	WL_{eq}	$SucG_{eq}$
β_0	1.18083***	0.32230	-0.01375
Linear			
C_{suc}	-0.01444	0.01121	0.00494
T	-0.00334	0.00329	-0.00244
Quadratic			
C^2_{suc}	0.00005	-0.00005	-0.00004
T^2	-0.00004	-0.00003	0.00006
Interaction			
C_{suc}·T	0.00007	-0.00007	0.00004
R^2	0.96	0.92	0.92
ARD	2.19%	0.93%	4.8%

***, **, * Coefficients significant at 0.1%, 1%, and 5% confidence level respectively

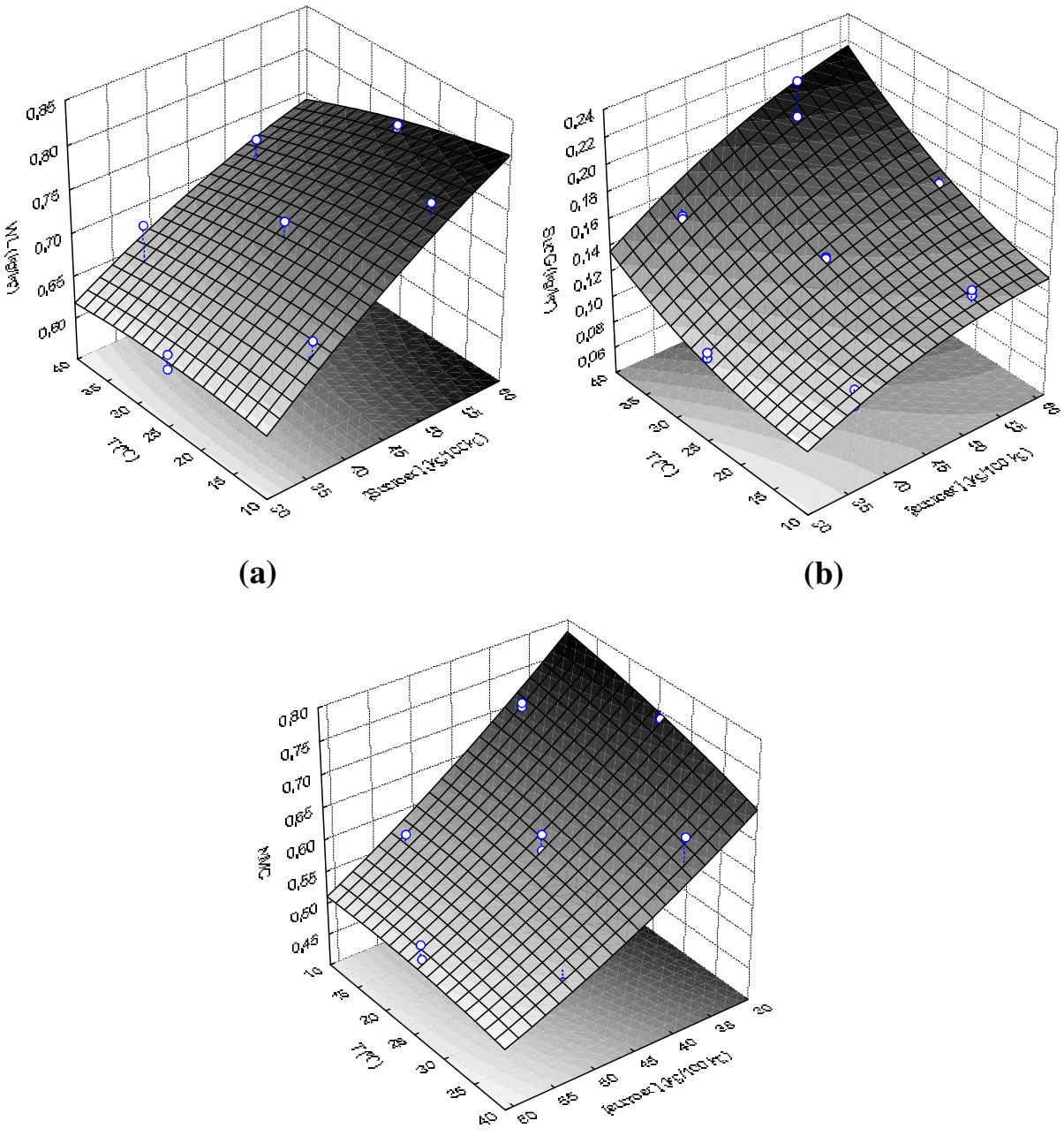

Figure 3.6. Equilibrium values of (a) WL, (b) SucG and (c) NMC for osmodehydrated pumpkin with sucrose solutions. Dots are predicted values from Azuara's model and surfaces are predicted values obtained with equations shown in Table 3.4.

Table 3.4 shows the results of these fits. A good fit was obtained for NMC (R^2 = 0.96, ARD = 0.5%) whereas for WL and SucG the fit was satisfactory, (R^2 = 0.92, ARD = 5.7% for WL; R^2 = 0.92, ARD = 6.2% for SucG).

Figure 3.6 shows the response surfaces obtained using the polynomials described before. Predicted values for WL, SucG and NMC at equilibrium ranged 0.63-0.78, 0.10-0.19 and 0.52-0.75 respectively. Sucrose gained at equilibrium increases with the concentration and temperature of the osmotic solution, being this effect more accentuated at high concentration and temperatures. Equilibrium water loss increases with the concentration of the solution; temperature has no practical effect at low values of solution concentration, but at high concentrations, WL decreases with the increase of temperature. This is likely due to the fact that the more penetration of sucrose in the tissue the less removal of water is necessary to attain the equilibrium state. NMC values decrease with the concentration of the osmotic solution. At low concentrations, NMC increases with temperature.

3.3.1.2. Mass transfer model: evaluation of water and sucrose effective coefficients of diffusion

With the values of radius at each time, obtained from Eqs. (3.8) and (3.10) (see Table 5.7), and the values of WL and SucG, Eq. (3.9) was fitted to experimental data, by means of a nonlinear regression procedure. Four terms of the sum were considered. Effective coefficients of diffusion for sucrose and water were obtained at each process condition, with and without considering shrinkage of samples. Analysis of variance (ANOVA) was performed to assess the influence of concentration and temperature on effective coefficients of diffusion.

No dependence of the effective diffusion coefficient of sucrose was found with the process conditions, and an average value for all the conditions was obtained and used in the calculation of the predicted values. Table 3.5 shows the average values of sucrose

effective coefficients of diffusion, obtained in the fits, with and without shrinkage considerations.

Table 3.5. Effective diffusion coefficients of sucrose.

	$Dx10^9$ Range (m^2/s)	$Dx10^9$ Average (m^2/s)	v.c. (%)
No shrinkage	1.14-1.37	1.28	8.4
Shrinkage	1.10-1.30	1.23	7.1

ANOVA results showed that effective diffusion coefficient for water was found to be dependent in concentration and temperature of the osmotic solutions. For modelling purposes, due to the good fit obtained, nonlinear equations of the form

$$D_{w,eff} = a + b(CT) + c(CT)^2 \quad (3.14)$$

Were used to relate $D_{w,eff}$ with the process conditions. Table 3.6 shows the fit results of Eq. (3.14), with and without considering shrinkage of samples.

Table 3.6. Effective diffusion coefficients of water.

	$a \times 10^{10}$ (m^2/s)	$b \times 10^{14}$ ($m^2 kg_{sol}/s^oC kg_{suc}$)	$c \times 10^{16}$ ($m^2 kg^2_{sol}/s^oC^2 kg^2_{suc}$)	R^2	$Dx10^9$ Range (m^2/s)	ARD
No shrink	3.01	2.74	1.60	0.99	0.36-1.00	7.0
Shrink	2.44	0.53	1.50	0.99	0.29-0.84	6.3

The values of effective diffusion coefficients of water and sucrose are in the range of those observed in the osmotic dehydration of different vegetable products with sucrose solutions (Rastogi and Raghavarao, 1997; Nsonzi and Rawasmany, 1998; Rodrigues *et al*., 2003).

As can be observed, values of effective coefficients of diffusion for water are lower than those found for sucrose. It would be expected, comparing molecular weights, lower values for sucrose. Rastogi and Raghavarao (1997) found similar diffusion coefficients for

water and sucrose during osmotic dehydration of banana with sucrose solutions. In some cases were observed higher diffusion coefficients for sucrose; as in the case of osmotic dehydration of papaya (Mendoza and Schmalko, 2002; Rodrigues *et al*. 2003), or pear (Park *et al*., 2002). Saurel *et al.* (1994) during osmotic dehydration of apple with polyethylene glycols (PEG) found that fructose leakage and the rate of water loss decreased with the increase of the molecular weight of the PEG used as osmotic agent. They suggested that the increase of molecular weight favoured the formation of a dense inner layer composed mainly by the osmotic agent at the surface of the samples. This layer acts like a barrier that can reduce the total flux (as in the case of fructose) or decrease the rate of transfer (as in the case of water) of compounds from the material to the solution.

During osmotic dehydration of vegetables with sucrose solutions, sucrose also accumulates in the outer regions of the material. Salvatori *et al.* (1999[b]), during osmotic dehydration of apple, showed that even at long process time (34 hours) sucrose gained remained close to the surface of the material, whereas water profiles evolved more deeply in the tissue. The accumulation of sucrose in the outer regions can produce, as in the case observed by Saurel *et al*. (1994), a dense layer which difficult the water transfer from the material to the solution, explaining the low values of the effective coefficient of diffusion for water observed in this work.

Figures 3.3-3.5 show experimental and predicted values (with shrinkage) of WL, SucG and NMC for osmotic dehydration of pumpkin at different process conditions. Average relative deviation values were 7 and 6 % with and without considering shrinkage respectively, indicating than the model fits slightly better with experimental data when shrinkage is considered.

3.3.2. Osmotic dehydration of pumpkin with NaCl solutions

3.3.2.1. Dehydration kinetics

Figures 3.7 and 3.8 show experimental data for WL and NaClG during osmotic dehydration of pumpkin with NaCl solutions. For all process conditions tested, most significant changes in WL and NaClG occur during the first 3 hours of the process; and in the interval from 6 to 9 hours a pseudo-equilibrium between the liquid phase inside the food material and the osmotic solution is reached. For the same temperature, WL increases with the concentration of NaCl in the solution. The gain of salt also increases with the concentration of the osmotic solution. At the end of the treatments, no tendencies with temperature were observed for both WL and NaClG. Values of water loss and salt gain vary during the process from 0 up to 45% and 0 up to 16% of the initial sample weight, respectively.

Observing NMC values in Figure 3.9, temperature of the osmotic solution seems to affect the rate of dehydration, but has little effect (higher temperature leads to a slightly more dehydrated product) in the extension of the process. On the contrary, concentration on the osmotic solution seems to have no effect in the dehydration rate but the increase of NaCl in the solution leads to a more dehydrated final product. Moisture content varied from 100% to 78% of the initial value depending on the employed process conditions. Chenlo *et al.* (2006[a]), during osmotic dehydration of chestnuts with NaCl solutions, observed that temperature had no significant effect on water loss, salt gain and moisture content of dehydrated samples; they suggested that the fact could be related with the low viscosity of the osmotic medium (Chenlo *et. al*., 2002), and the high mechanical resistance of the chestnut which restricted the thermal relaxation of the solid matrix.

Weight reduction ranged between 0-37% along the process. For all the process conditions tested, WR increased considerably up to 3 hours, after that time it was practically constant till the end of the osmotic treatment.

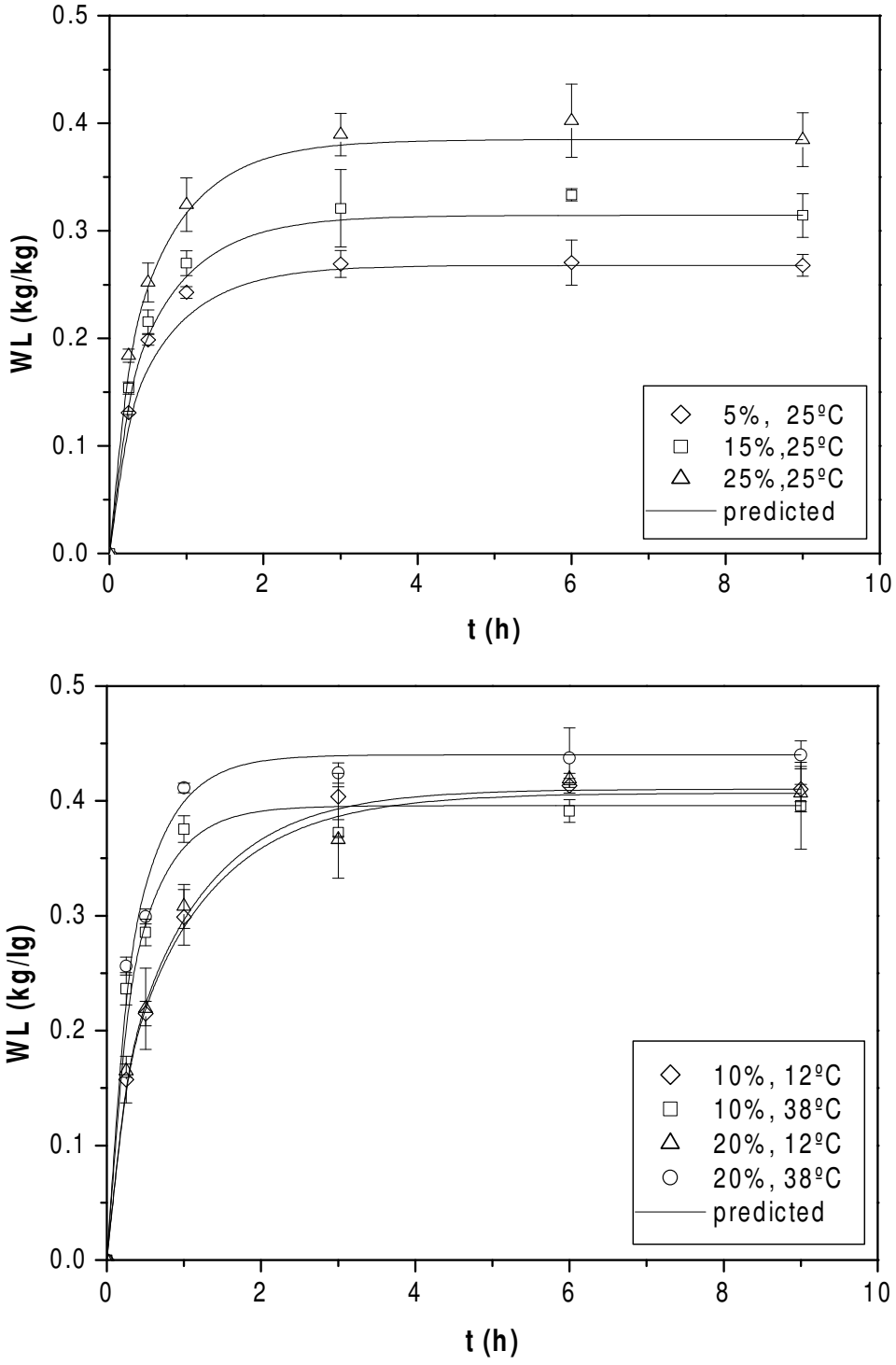

Figure 3.7. Water loss during osmotic dehydration of pumpkin at different NaCl concentration and temperature. Dots represent experimental data and the lines are predicted values with Fick's model considering shrinkage.

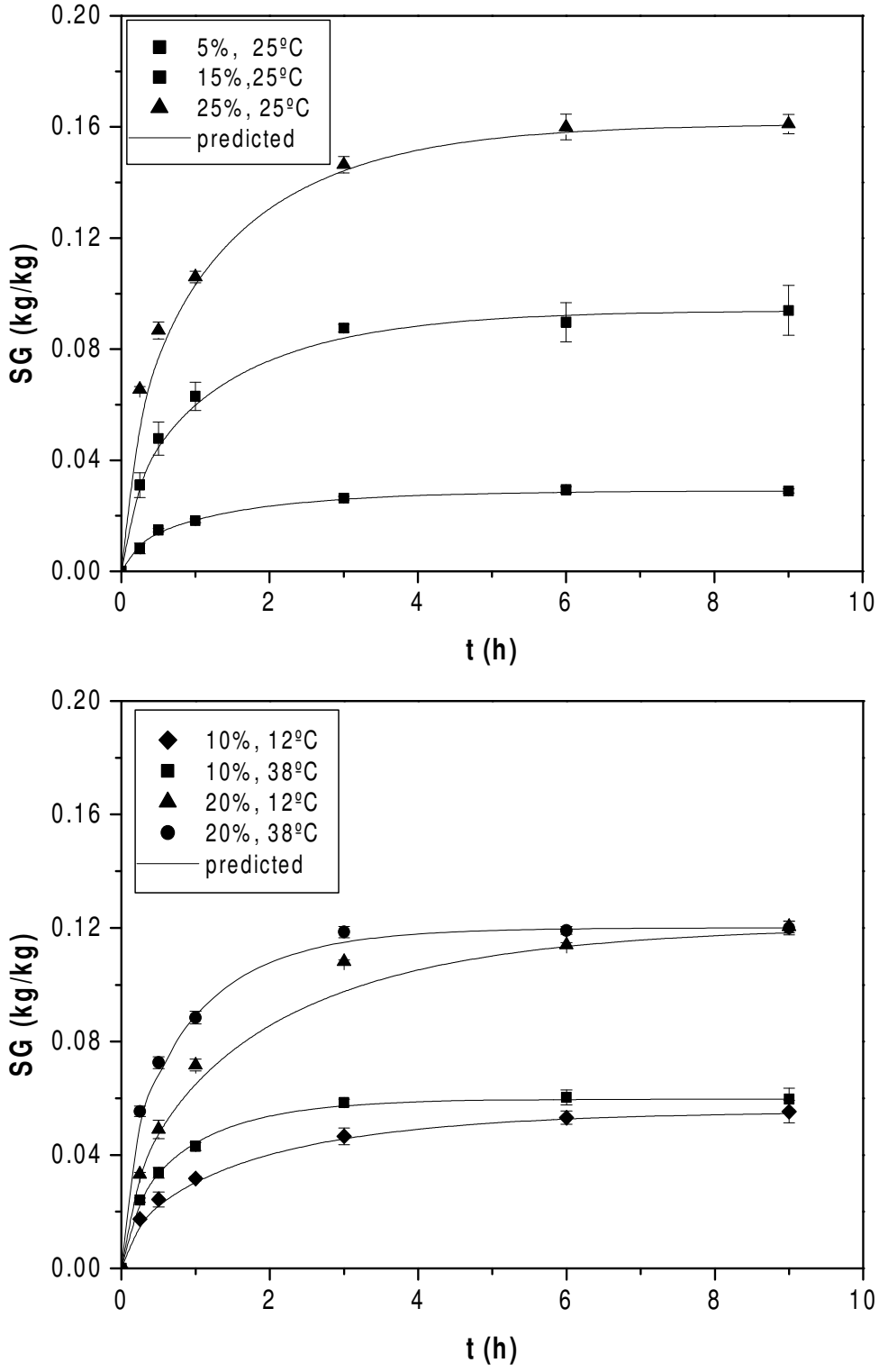

Figure 3.8. NaGl gain during osmotic dehydration of pumpkin at different NaCl concentration and temperature. Dots represent experimental data and the lines are predicted values with Fick's model considering shrinkage.

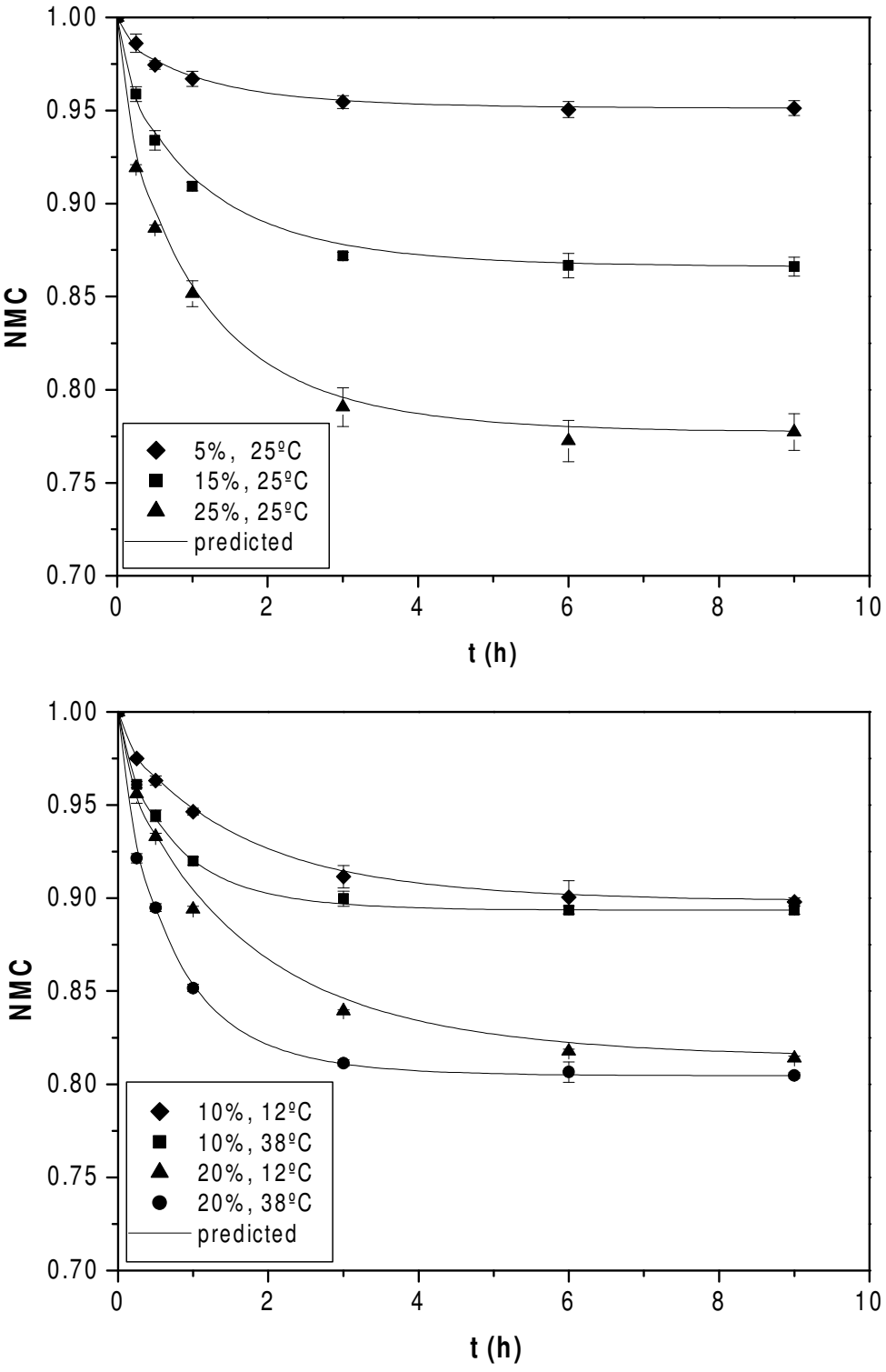

Figure 3.9. Normalized moisture content during osmotic dehydration of pumpkin at different NaCl concentration and temperature. Dots represent experimental data and the lines are predicted values with Fick's model considering shrinkage.

Equilibrium values for WL, NaClG and NMC obtained from Azuara's model (Eq. (3.11)) were fitted to the proposed polynomial (Eq. 3.(12)). Table 3.7 shows the results of these fits. For NaCl gain (R^2 = 0.98, ARD = 6.2%) and normalized moisture content (R^2 = 0.99, ARD = 0.5%) the fit is adequate. For water loss (R^2 = 0.83, ARD = 5.7%) it is less good, suggesting that the model only shows a tendency of the water loss behaviour as a function of temperature and concentration and is not recommended for predictive purposes. Then, predicted values of water loss at equilibrium were obtained from the equations of solids gain and normalized moisture content at equilibrium.

Table 3.7. Regression coefficients of Eq. (3.12) for equilibrium values of normalized moisture content (NMC), water loss (WL) and NaCl gain (NaClG).

Coefficient	**NMC_{eq}**	**WL_{eq}**	**$NaClG_{eq}$**
β_0	0.96232***	0.55643***	-0.01209
Linear			
C_{NaCl}	-0.00806***	0.00720	0.00362***
T	0.00263***	-0.02466***	0.00173**
Quadratic			
C^2_{NaCl}	-0.00005*	0.00012	0.00005
T^2	-0.00006***	0.00051***	-0.00004***
Interaction			
C_{NaCl}*T	0.00002	-0.00021**	0.00006***
R^2	0.99	0.83	0.98
ARD	0.5%	5.7%	6.2%

*****, **, * Coefficients significant at 0.1%, 1%, and 5% confidence level respectively**

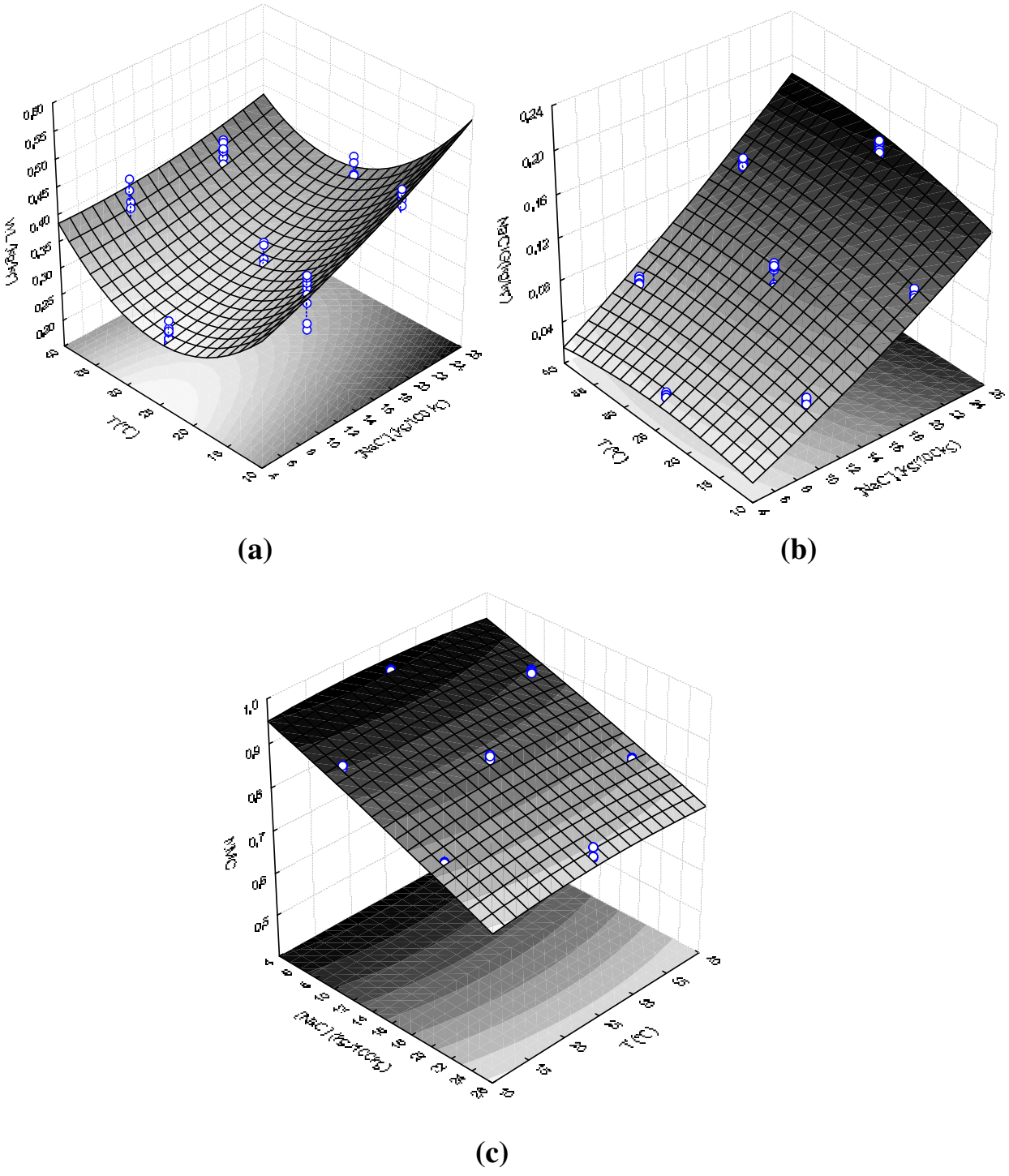

Figure 3.10. Equilibrium values of (a) WL, (b) NaClG and (c) NMC for osmodehydrated pumpkin with NaCl solutions. Dots are experimental values whereas surfaces are predicted values obtained with equations shown in Table 3.7.

Figure 3.10 shows the response surfaces obtained using the polynomials described before. Predicted values for WL, NaClG and NMC at equilibrium ranged 0.27-0.47, 0.03-0.17 and 0.77-0.95 respectively. NaCl gain at equilibrium increases with the concentration of the solution. Temperature has a slight effect, more accentuated at high temperatures, increasing the salt gained. Initially, water loss decreases with the increase of temperature, shows a minimum around 25ºC, and then increases till 40 ºC; the increase of concentration leads to the increase of water loss at equilibrium. Temperature does not have a significant influence on NMC values at the end of the process. Only concentration of the solution has effect on the values of NMC; the increase of concentration decreases NMC values.

3.3.2.2. Mass transfer model: evaluation of water and NaCl effective coefficients of diffusion

Equation (3.10) (see Table 5.8) was used to calculate the changes in volume during the process, and the equivalent radius (Eq. (3.8)), was introduced in Eq. (3.9) in order to consider shrinkage. ANOVA results showed that water and NaCl coefficients were dependent on the temperature, but no significant dependence on concentration of osmotic solution was observed. However, it was observed a linear relationship between diffusion coefficients and process temperature. It was also observed that values of effective coefficients of diffusion were systematically lower when shrinkage was considered in their calculation.

Linear functions of the type

$$D_{eff} = a + bT \tag{3.15}$$

can be used for evaluating the effect of temperature on effective diffusion coefficients. Table 3.8 shows the values of a and b parameters for salt and water with and without shrinkage considerations.

Table 3.8. Parameters of Eq. (3.15) to evaluate D_{eff} with T.

		$a \cdot 10^{10}$ (m^2/s)	$b \cdot 10^{11}$ (m^2/sK)	R^2	$D \cdot 10^9$ Range (m^2/s)
No Shrinkage	D_{NaCl}	6.22	4.61	0.95	1.20-2.50
No Shrinkage	D_w	7.99	11.55	0.93	2.0-4.6
Shrinkage	D_{NaCl}	4.19	4.07	0.95	0.88-1.92
Shrinkage	D_w	7.53	9.13	0.97	1.88-4.22

An Arrhenius type equation of the form

$$D_{eff} = D_P exp\left(\frac{-E_a}{R(T+273.1)}\right) \tag{3.16}$$

can be also employed to relate effective diffusion coefficients with temperature. Table 3.9 shows the values of the coefficients D_P and E_a for the Arrhenius type equation. Values of salt coefficients of diffusion are very close to those reported for several authors in the salting process of pickling cucumbers (Schwartzberg and Chao, 1982). Effective water coefficients of diffusion are in the range of those observed for different food products (Zogzas *et al*., 1996).

Table 3.9. Values of Eq. (3.16) to evaluate D_{eff} with T.

		$D_P \cdot 10^6$ (m^2/s)	Ea (kJ/mol)	R^2	$D \cdot 10^9$ Range (m^2/s)
No Shrinkage	D_{NaCl}	4.12	19.28	0.96	1.18-2.32
No Shrinkage	D_{water}	51.3	23.75	0.96	2.23-5.15
Shrinkage	D_{NaCl}	8.22	21.53	0.96	0.91-1.94
Shrinkage	D_{water}	46.7	24.00	0.96	2.00-4.66

Values for activation energy are similar to those reported by Lazarides *et al.* (1997) during osmotic dehydration of apple in sucrose solutions, and in the range of the values of activation energy for water diffusivity observed for different food materials (Zogzas *et al*., 1996).

Predicted data of WL and SG were obtained with effective coefficients of diffusion obtained from Eq. (3.15). P values were 3.5 and 12.8 % with and without considering shrinkage respectively, indicating than the model fits better with experimental data when shrinkage is considered. Figures 3.7-3.9 show experimental and predicted values (considering shrinkage) for osmotic dehydration of pumpkin at different process conditions.

3.3.3. Osmotic dehydration with ternary NaCl/sucrose solutions

3.3.3.1. Dehydration kinetics

Figure 3. 11 shows the changes in sucrose gain (SucG) during osmotic dehydration of pumpkin with the ternary solutions employed. Initially, for all the process conditions, the flow of sucrose inside the material is fast till two hours, after that increases uniformly till the end of process. Sucrose gain increases with the concentration of sucrose in the solution.

When no NaCl is present in the solution (see 0% NaCl, 45% sucrose), the gain of sucrose attain its highest values. Medina-Vivanco *et al.* (2002), during osmotic dehydration with ternary sucrose/NaCl solutions of fish (tilapia fillets), also observed higher sucrose gain in binary sucrose solutions compared with ternary NaCl/sucrose solutions with the same sucrose concentration. When NaCl is present, for low concentration of sucrose in the solution (32%), sucrose gain increases with the increase of NaCl in the solution. At higher sucrose concentrations (45 and 58%) the effect is not clear; and it can be said that NaCl concentration has no effect on sucrose gain. The same work of Medina-Vivanco *et al.* (2002), and the work of Bouhon *et al*. (1998), during osmotic dehydration with ternary sucrose/NaCl solutions of a protein-polysaccharide food system, observed that the concentration of NaCl in the solutions had no effect on the sucrose entered in the material.

At low sucrose concentrations the gain of sucrose is not high; the presence of NaCl can avoid in more extension than at higher sucrose gain values the formation of a dense shell of sucrose in the surface of the material (see comments in 3.3.1.2) which difficults the transfer of sucrose in the inner of the food and the flow of water to the solution. Then at these conditions higher NaCl concentration can promote higher gains of sucrose. Values of sucrose gain ranged 0-13% of the initial sample weight.

NaCl gain (Fig. 3.12) ranged from 0-6% of the initial weight. The increase of NaCl in the material is fast till two hours, then increases very smoothly till the end of the process. NaCl gain increases with the concentration of NaCl in the solution.

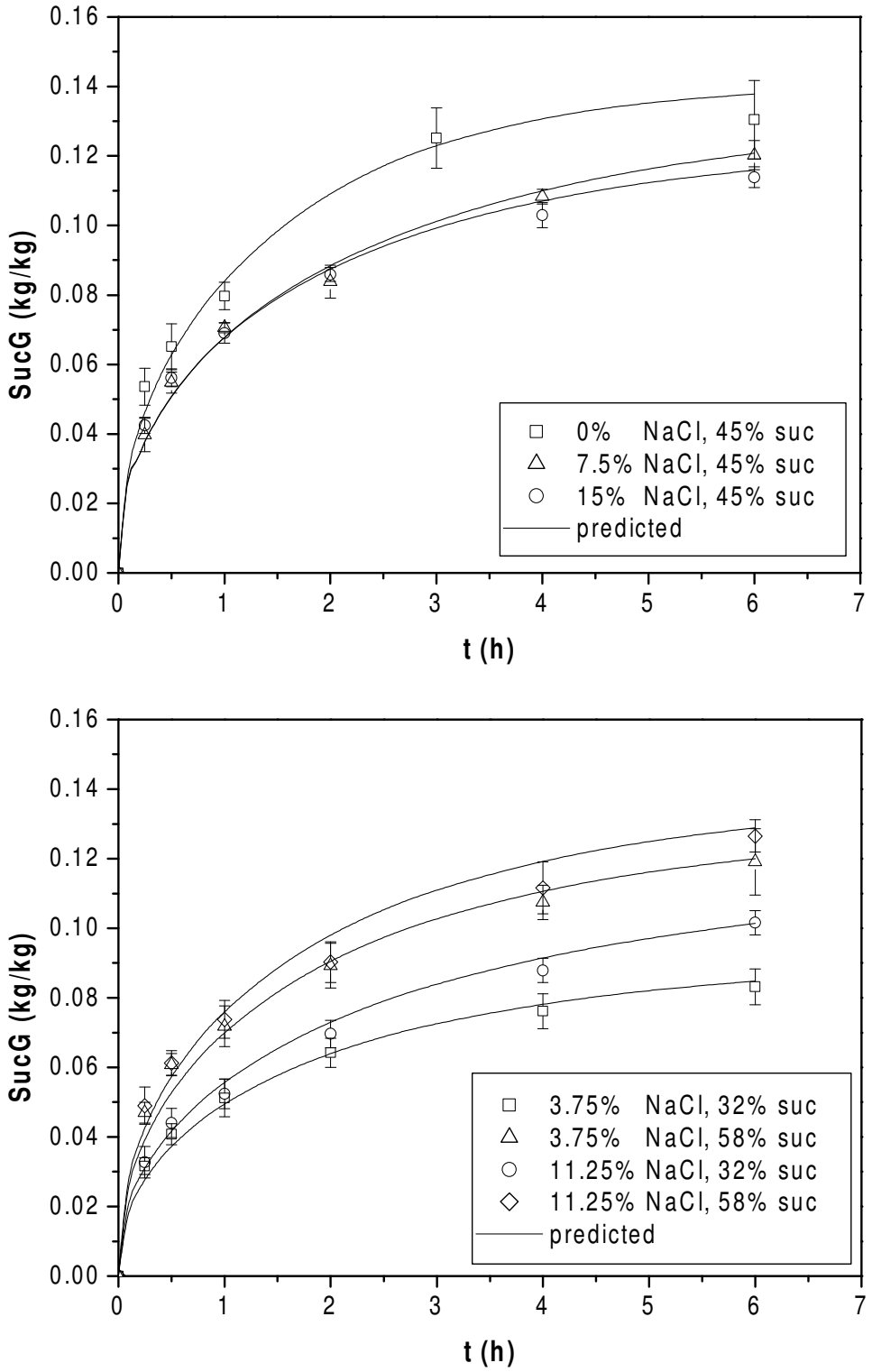

Figure 3.11. Sucrose gain during osmotic dehydration of pumpkin at different NaCl and sucrose concentrations, at 25 ºC. Dots represent experimental data and the lines are predicted values with Fick's model with constant dimensions.

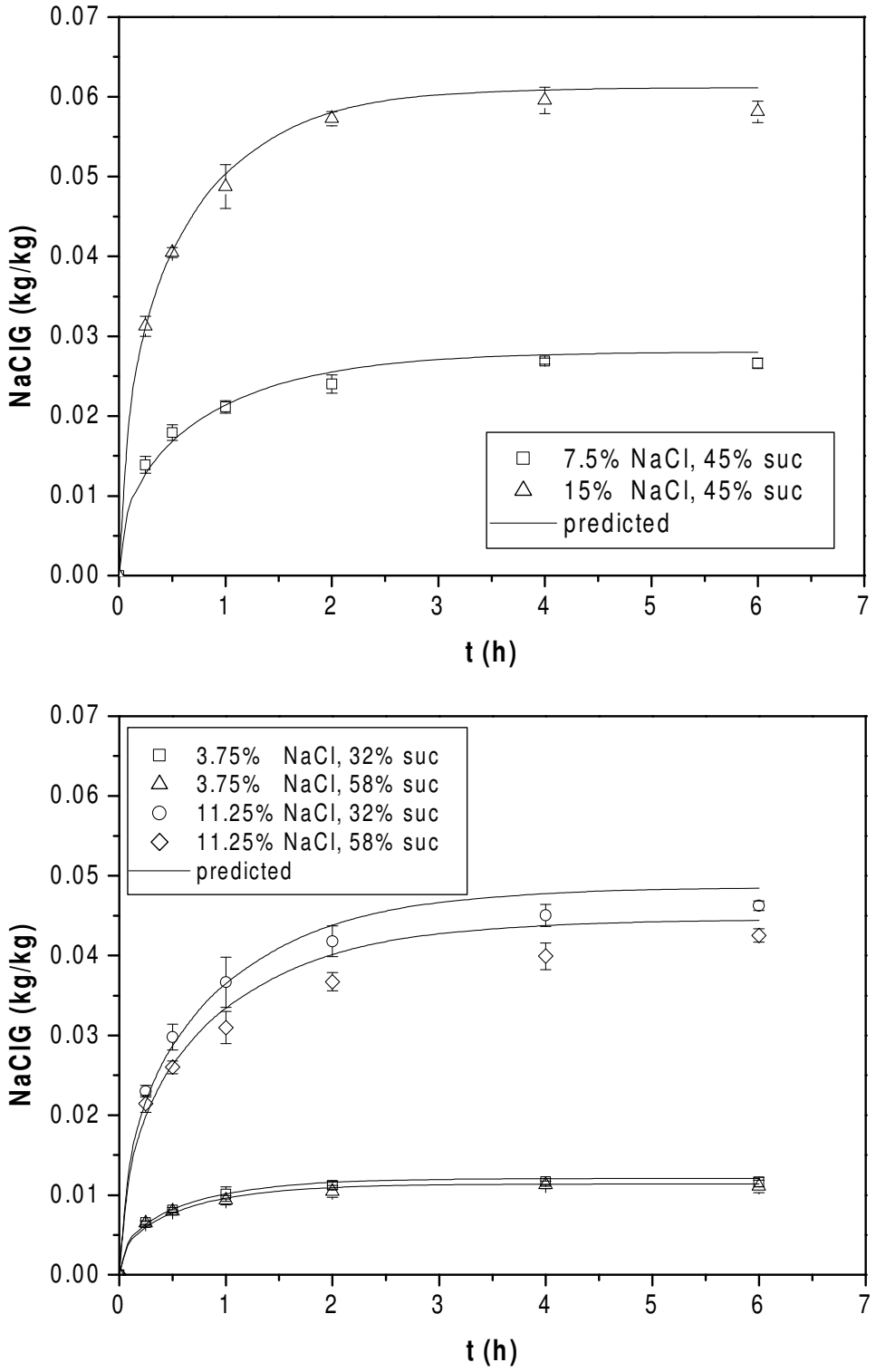

Figure 3.12. NaCl gain during osmotic dehydration of pumpkin at different NaCl and sucrose concentrations, at 25°C. Dots represent experimental data and the lines are predicted values with Fick's model with constant dimensions.

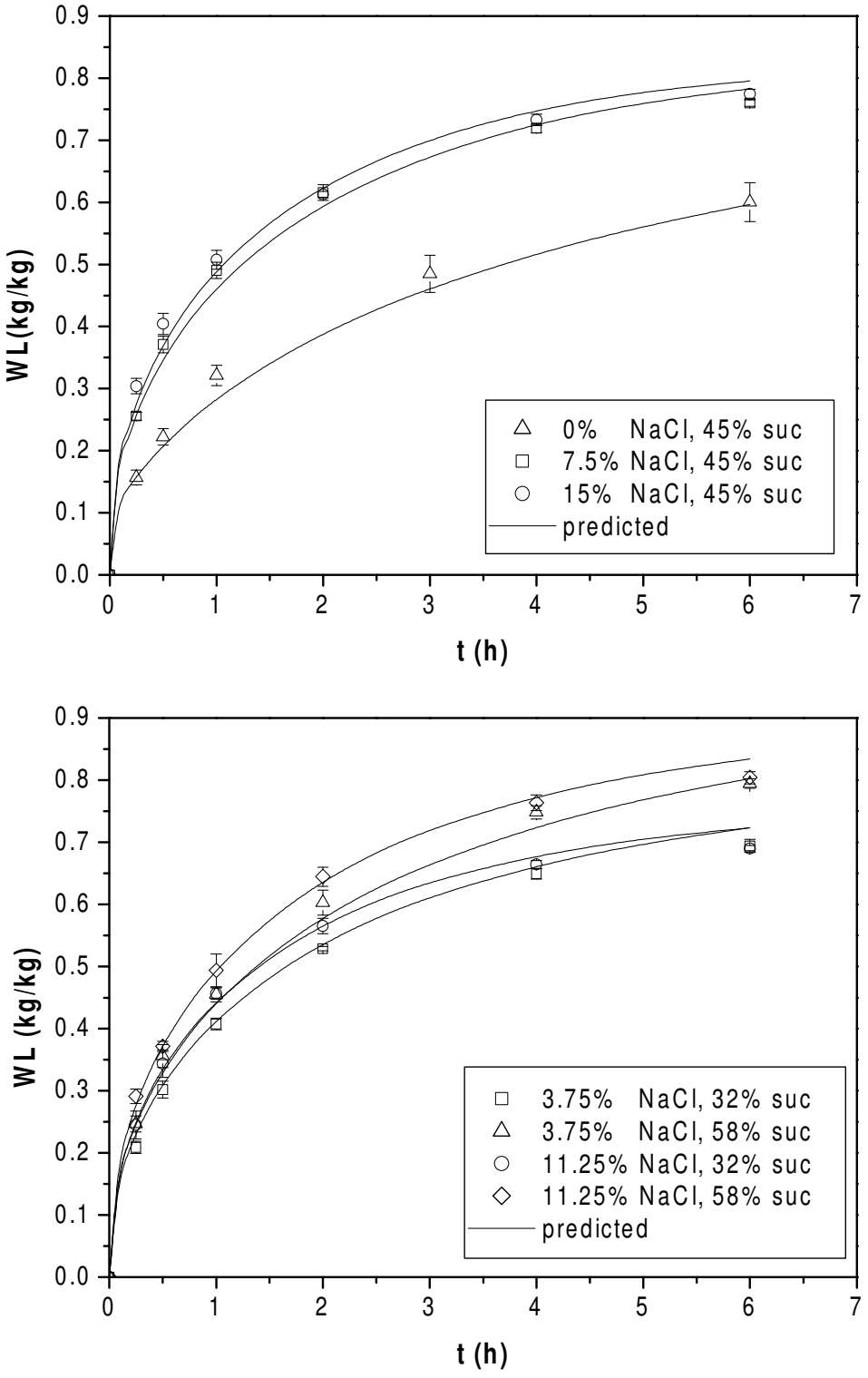

Figure 3.13. WL during osmotic dehydration of pumpkin at different NaCl and sucrose concentrations, at 25ºC. Dots represent experimental data and the lines are predicted values with Fick's model with constant dimensions.

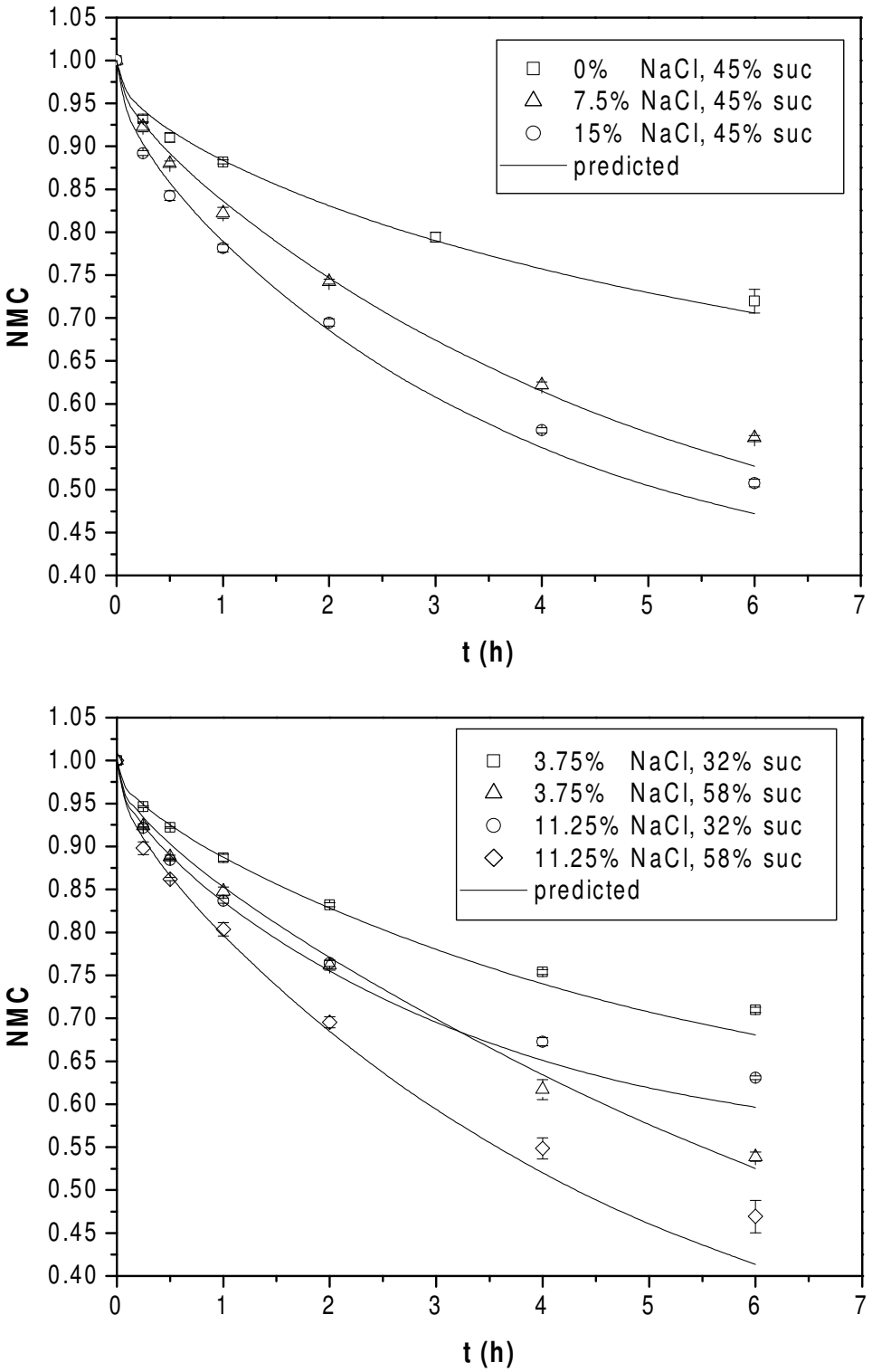

Figure 3.14. Normalized moisture content during osmotic dehydration of pumpkin at different NaCl and sucrose concentrations, at 25ºC. Dots represent experimental data and the lines are predicted values with Fick's model with constant dimensions.

At low concentration of NaCl in the solution, sucrose concentration has no effect on NaClG values; at high NaCl concentration (11.25%) the salt gain decreases if sucrose concentration increases. Medina-Vivanco *et al.* (2002) observed that sucrose concentration had no effect on NaCl gain, whereas Bouhon *et al*. (1998) observed a decrease of NaClG when sucrose concentration increased.

Water loss (WL) (Fig. 3.13) increased fast up to two hours and then increased uniformly up to the end of the process. Values of WL ranged from 0-80% of the initial sample weight. The lowest values of water loss were obtained when the binary 45% sucrose solution was used. When NaCl was present in the solution, water loss increased when sucrose concentration increased; salt concentration was found to have no significant effect on water loss.

Normalized moisture content (Fig. 3.14) decreased fast till two hours and after that decreases is a less accentuated way but constantly till the end of process. Values of NMC ranged 100-47% of the initial moisture content. The increase of both concentrations of NaCl and sucrose in the solution lead to a more dehydrated product.

Table 3.10 shows the results of the fits of Eq. (3.13) with equilibrium values of WL, SucG, NaClG and NMC. NaCl gain (R^2 = 0.99, ARD = 1.8%) resulted in an excellent fit, whereas for WL (R^2 = 0.95, ARD = 1.3%), SucG (R^2 = 0.93, ARD = 3.1%) and NMC (R^2 = 0.96, ARD = 5.6%) the fit was adequate.

Figure 3.15 shows predicted and experimental values of WL, SucG, NaClG and NMC at equilibrium. Water loss at equilibrium is strongly influenced by sucrose concentration in the osmotic solution; the increase of sucrose concentration increases the water loss at equilibrium. A slight effect of NaCl concentration can be observed at low sucrose concentrations, increasing water loss when the concentration of salt decreases.

NaCl gain at equilibrium increases with the concentration of the salt in the solution. At high NaCl concentration the concentration of sucrose has a slight effect on NaClG: salt

content at equilibrium decreases with the increase of sucrose concentration in the solution. Sucrose gain increases with concentration of sucrose; the increase of salt in the solution initially increases sugar gain, reaches a maximum value at 8-10% NaCl and then decreases with the increase of salt concentration.

Table 3.10. Regression coefficients of Eq. (3.12) for equilibrium values of normalized moisture content (NMC), water loss (WL), sucrose gain (SucG) and NaCl gain (NaClG).

Coefficient	NMC_{eq}	WL_{eq}	$SucG_{eq}$	$NaClG_{eq}$
β_0	1.09713**	0.58626**	-0.10007	0.00791
Linear				
Csal	-0.01581	-0.01148	0.01207**	0.00589***
Csuc	-0.01574	0.00872	0.00682*	-0.00077*
Quadratic				
$Csal^2$	0.00016	0.00034	-0.00044*	-0.00003
$Csuc^2$	0.00004	-0.00005	-0.00006	0.00001*
Interaction				
Csal*Csuc	0.00016	0.00010	-0.00007	-0.00002*
R^2	0.96	0.95	0.93	0.99
ARD	5.6%	1.3%	3.1%	1.8%

*****, **, * Coefficients significant at 0.1%, 1%, and 5% confidence level respectively**

NMC decreases with the increase of sucrose and salt in the osmotic solution; the increase of both osmotic agents increases the concentration gradients of NaCl and sucrose between the material and the solution increasing the transfer of both components into the vegetable tissue. Furthermore, the increase of these components decreases the water activity of the solution favouring the transfer of water from the material to the solution.

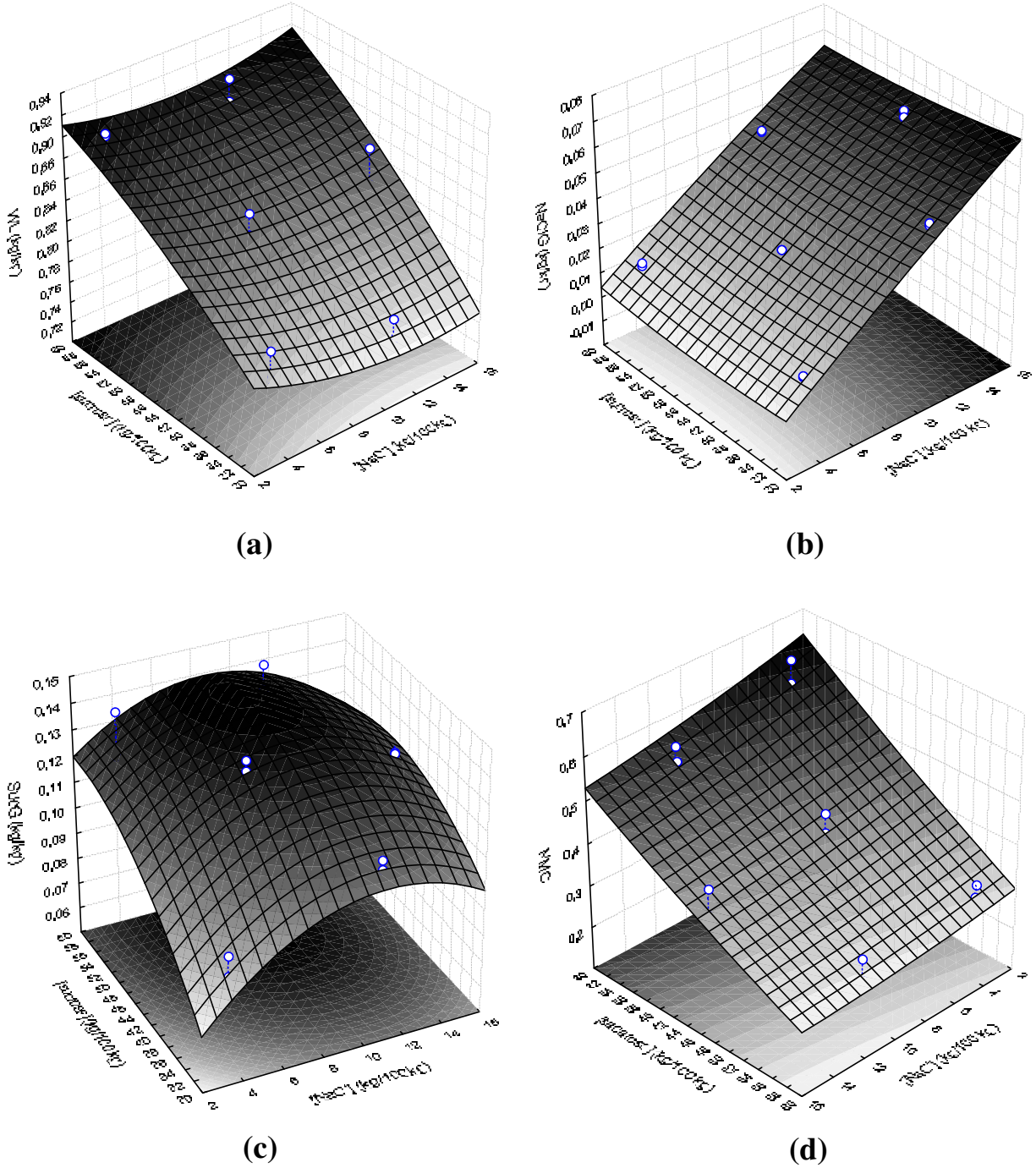

Figure 3.15. Equilibrium values of (a) WL, (b) NaClG, (c) SucG and (d) NMC for osmodehydrated pumpkin with NaCl/sucrose solutions. Dots are experimental values whereas surfaces are predicted values obtained with equations shown in Table 3.10.

3.3.3.2. Mass transfer model: evaluation of water, sucrose and NaCl effective coefficients of diffusion

Effective diffusion coefficient of water was found to increase with salt concentration and decrease with sucrose concentration in the solution. A good fit was obtained with an equation of the type

$$D_{w,eff} = a + b\left(\frac{C_{NaCl}}{C_{suc}}\right) + c\left(\frac{C_{NaCl}}{C_{suc}}\right)^2 \quad (3.17)$$

Table 3.11 shows the fit results with and without considering shrinkage. Eq. (3.10) (see Table 5.9) was used to consider shrinkage of samples during the treatments.

Table 3.11. Fit results for effective coefficients of diffusion of water in NaCl/sucrose solutions.

	a x 10^9 (m^2/s)	b x 10^9 (m^2/s)	c x 10^9 (m^2/s)	R^2	Dx10^9 Range (m^2/s)	ARD
No shrink	0.61	3.99	-5.51	0.93	0.58-1.4	6.4
Shrink	0.48	2.61	-2.99	0.94	0.47-1.03	4.5

Telis *et al*. (2004), during osmotic dehydration of tomatoes with ternary sucrose/NaCl solutions, also observed that effective diffusion coefficient of water increased with the increase of NaCl concentration and the decrease of sucrose concentration in the osmotic solution. As commented in this work for binary sucrose solutions (see 3.3.1.2), the formation of a surface layer of sucrose can hinder the water loss from the sample. The presence of NaCl in the solution can produce two effects favouring the water transfer: first of all the increase of NaCl in the solution decreases its water activity, increasing the driving force for water removal; secondly, the presence of NaCl can avoid the formation of the above mentioned surface layer of osmotic solute.

A quadratic model as a function of salt concentration was used to predict effective diffusion coefficient for NaCl

$$D_{NaCl,eff} = a + b\,C_{NaCl} + c\,C_{NaCl}^2 \qquad (3.18)$$

Table 3.12 shows the fit results of Eq. (3.18) with and without considering shrinkage.

Table 3.12. Fit results for effective coefficients of diffusion of NaCl in NaCl/sucrose solutions.

	a x 10^9 (m^2/s)	**b x 10^9 (m^2kg_{sol}/skg_{NaCl})**	**c x 10^9 ($m^2kg^2_{sol}/skg^2_{NaCl}$)**	**R^2**	**Dx10^9 Range (m^2/s)**	**ARD**
No shrink	6.19	-0.75	0.04	0.95	2.6-4.1	5.8
Shrink	4.83	-0.54	0.03	0.94	2.1-3.3	5.1

Concerning effective coefficients of diffusion of sucrose, a polynomial as a function of sucrose and salt concentration (Eq. (3.19))

$$D_{suc,eff} = a + bC_{NaCl} + cC_{suc} + dC_{NaCl}^2 + eC_{suc}^2 + fC_{NaCl}C_{suc} \qquad (3.19)$$

was acceptably fitted to experimental values. Table 3.13 shows the fit results obtained with and without considering shrinkage respectively.

Values of D_w ranged (0.58-1.40)*10^{-9}, D_{NaCl} ranged (2.60-4.11)*10^{-9}, and D_{suc} ranged (0.75-1.23)*10^{-9}, all values without considering shrinkage. These values were in the range of those observed by Azoubel and Murr (2004) and Telis *et al*. (2004) in the osmotic dehydration of tomato with ternary sucrose/NaCl solutions.

Table 3.13. Fit results for effective coefficients of diffusion of sucrose in NaCl/sucrose solutions.

Coefficient ($x10^9$)	No shrinkage	Shrinkage
a (m^2/s)	2.4022**	1.6439*
b (m^2kg_{sol}/kg_{NaCl})	-0.1621***	-0.1622***
c (m^2kg_{sol}/kg_{suc})	-0.0423	-0.0155
d ($m^2kg_{sol}^2/kg_{NaCl}^2$)	0.0050**	0.0049***
e($m^2kg_{sol}^2/kg_{suc}^2$)	0.0004	0.0001
f($m^2kg_{sol}/kg_{NaCl}kg_{suc}$)	0.0016*	0.0014*
$Dx10^9$ range (m^2/s)	0.75-1.23	0.5-1.1
R^2	0.88	0.92
ARD	6.3%	2.9%

*****, **, * Coefficients significant at 0.1%, 1%, and 5% confidence level respectively**

Average percent relative deviation between predicted and observed values of SucG, NaClG, WL and NMC was 7.0 and 3.2% with and without considering shrinkage of samples respectively, suggesting that the prediction of the different mass transfer fluxes with the proposed model is adequate. Figures 3.11-14 show experimental and predicted values of SucG, NaClG, WL and NMC using the proposed model, when no shrinkage of samples was considered.

A better fit, as in the case of osmotic dehydration with binary solutions of sucrose and NaCl, would be expected when shrinkage was considered. The better fit observed with constant dimensions can be attributed to the fact that in ternary solutions other non-diffusional mechanisms of mass transfer can have an important contribution in the global mass transfer of the process. In this way, the shape of the kinetic curves is fairly different of the shape of a pure diffusional process, the consideration of dimensional changes is not so necessary, and the diffusion coefficients have a more empirical meaning.

3.3.4. WL/SG ratio

The WL/SG ratio has been used for assessing the quality of the osmotic agent, or water removal efficiency (Lazarides *et al*., 1995[a]; Sereno *et al.,* 2001). High values of this ratio are related with good dehydrating agents, whereas low values correspond to good soaking or infusing agents. Table 3.14 shows maximum values of WL/SG ratio for different osmotic agents and different products, in an advanced degree of dehydration (WL>0.4). A wide range of this ratio for the different osmotic agents and different products used may be observed. Several factors can influence the value of this ratio, namely: process conditions (type of osmotic agent, solution concentration, contact time, temperature, etc.) and physicochemical properties of raw material (initial moisture content, density, etc). An important factor seems to be the molecular weight of the osmotic agent. Agents with high molecular weight (Corn Syrup, PEG) leads to significantly higher WL/SG ratios compared with the other osmotic agents. This can be due to the low diffusivity of substances with high molecular weight.

In this work, the highest values of this ratio were obtained with 37.5% sucrose at 12ºC for binary sucrose solutions, 10% NaCl at 12 ºC for binary NaCl solutions, and 3.75% NaCl, 32% sucrose at 25ºC for ternary NaCl/sucrose solutions. Although the highest ratio was obtained for binary NaCl solutions, the ternary solutions may be preferable for dehydration purposes, since the ratio of 8.67 for NaCl solutions is obtained with a removal of water of 40% of the initial weight, and for ternary solutions the ratio is similar (7.39) but the water removed in this case is 65%.

Table 3.14. WL/SG ratio (WL>0.4), for different vegetable products and osmotic agents.

Osmotic agent	Material	WL	WL/SG	Reference
NaCl	Apple	0.50	2.55	Azuara *et al.* (1996)
	Potato	0.40	1.77	Azuara *et al*. (1996)
	Pumpkin	0.40	8.67	This work
NaCl/Sucrose	Pumpkin	0.65	7.39	This work
Sucrose	Agar gel	0.55	2.20	Raoult-Wack *et al.* (1991[b])
	Apple	0.39	4.13	Kowalska and Lenart (2001)
	Apple	2.5*	7.57	Lazarides *et al.* (1995[a])
	Apple	0.45	4.50	Panagiotou *et al* (1998)
	Apple	0.71	8.91	Azuara *et al.* (1996)
	Banana	0.42	4.67	Panagiotou *et al.* (1998)
	Carrot	0.40	6.73	Kowalska and Lenart (2001)
	Kiwifruit	0.46	4.60	Panagiotou *et al*. (1998)
	Potato	0.70	10.51	Azuara *et al.* (1996)
	Pumpkin	0.52	8.09	Kowalska and Lenart (2001)
	Pumpkin	0.57	6.00	This work
Corn Syrup (42 DE)	Apple	3.91*	23.7**	Lazarides *et al*. (1995[a])
PEG (20000 Da)	Agar Gel	0.85	170	Raoult-Wack *et al.* (1991[b])

*** (g Water loss/g initial dry matter) ** (Syrups of 18-38 DE gave negative solid gain values)**

3.4. Conclusions

Kinetics of water loss and solids gain during osmotic dehydration of pumpkin were obtained, varying the type of osmotic agent, its concentration and the temperature of the osmotic solution.

For binary sucrose solutions, water loss and sucrose gain varied in a range from 0-74% and 0-19% of the initial sample weight, respectively. Moisture content decreased up to 57% of the initial value (97%). For binary NaCl solutions, Water loss and NaCl gain varied in a range from 0 up to 45 %n and from 0 up to 16 % of their initial mass, respectively. Moisture content decreased up to 78% of the initial value. For ternary NaCl/sucrose solutions, water loss ranged 0-80%, sucrose gain 0-13% and NaCl gain 0-6% of the initial sample weight respectively. Moisture content decreased until 47% of the initial value. Although the highest WL/SG ratio was obtained with binary NaCl solutions, they are not very recommended to obtain low moisture content products, but can be used, for example, to produce a pickle type vegetable. Ternary NaCl/sucrose solutions lead to a high WL/SG ratio, and the water removal is considerable, so they are preferred if the removal of water is the objective of the process.

Diffusion coefficients obtained considering shrinkage during the process resulted in systematically lower values than those obtained with constant dimensions. Effective coefficients of diffusion for water, sucrose and NaCl ranged $(0.29\text{-}4.22)\cdot10^{-9}$ m^2/s, $(0.5\text{-}1.3)\cdot10^{-9}$ m^2/s and $(0.88\text{-}3.3)\cdot10^{-9}$ m^2/s respectively considering shrinkage, depending their value on the employed process conditions. In binary sucrose solutions, effective diffusion coefficient for sucrose was found to be not dependent with concentration neither temperature of the solution, whereas the coefficient for water was dependent for both concentration of the solution and temperature. Effective coefficients of diffusion for NaCl and water in binary NaCl solutions were linearly dependent with the temperature of the solution, whereas they were independent of the concentration. Regarding ternary solutions, both water and sucrose effective coefficients of diffusion were dependent of sucrose and

NaCl concentrations, whereas NaCl coefficient of diffusion was only dependent with concentration of NaCl.

For binary solutions of water and sucrose, relative deviations between experimental and predicted values were lower when shrinkage was considered. For ternary solutions, relative deviations were lower when constant dimensions were considered.

The experimental and predicted values showed in general a good agreement indicating that the model is adequate. In this way, the proposed model allows the simulation of mass transfer processes during osmotic dehydration, and consequently it can be used as a useful tool in the design and control of the corresponding industrial operation.

CHAPTER 4

SORPTION PROPERTIES OF FRESH AND OSMOTICALLY DEHYDRATED PUMPKIN FRUITS

CHAPTER 4. SORPTION PROPERTIES OF FRESH AND OSMOTICALLY DEHYDRATED PUMPKIN FRUITS

4.1. Introduction

One of the aims of this chapter is to determine the effect of sucrose impregnation of pumpkin on its sorption isotherm. Another objective is to establish the effect of temperature on the desorption isotherm of parenchyma, since this variable is of great importance, taking into account the temperatures used during storage and processing. Temperature affects the mobility of the water molecules and also the corresponding dynamic equilibrium (Al-Muhtaseb *et al*., 2004). Pumpkin seeds are a source of oils and other oligocomponents (Mandl *et al*., 1999). In this chapter, its desorption isotherm at 25 ºC was experimentally determined and compared with bibliographic data for other seed products.

An important number of mathematical models have been proposed to describe sorption isotherms, and can be found in the literature. In this part of the work, a selection the most common models with two (BET, Halsey, Harkins, Henderson, Kühn, Mizrahi, Oswin and Smith), three (Chirife and GAB) and four (Peleg) parameters were considered. The mathematical expressions of each model are collected in Table 4.1. In general, most of them are empirical or based on semitheoretical assumptions.

Table 4.1. Sorption models used to fit experimental data.

Model		Equation	
BET	(Brunauer *et al*., 1938)	$X_e = \frac{a\,b\,a_w}{(1-a_w)\,(1+(b-1)\,a_w)}$	(4.1)
Chirife	(Chirife *et al*., 1983)	$X_e = \frac{1}{a}\left[\ln\left(\frac{b}{RT}\right) - \ln(-\ln(a_w)\right]$	(4.2)
GAB	(van den Berg, 1984)	$X_e = \frac{a\,b\,c\,a_w}{(1-c\,a_w)[1+(b-1)\,c\,a_w]}$	(4.3)
Halsey	(Halsey, 1948)	$X_e = \left[\frac{-a}{\ln(a_w)}\right]^{(1/b)}$	(4.4)
Harkins	(Boente *et al*., 1996)	$X_e = \frac{1}{\sqrt{a+b\ln(a_w)}}$	(4.5)
Henderson	(Henderson, 1952)	$X_e = \left[\frac{\ln(1-a_w)}{a}\right]^{(1/b)}$	(4.6)
Kühn	(Boente *et. al*., 1996)	$X_e = a + \frac{b}{\ln(a_w)}$	(4.7)
Mizrahi	(Boente *et al*., 1996)	$X_e = a\left[\frac{a_w}{(1-a_w)} + \frac{b}{(1-a_w)}\right]$	(4.8)
Oswin	(Oswin, 1946)	$X_e = a\left[\frac{a_w}{1-a_w}\right]^b$	(4.9)
Peleg	(Peleg, 1993)	$X_e = a\,(a_w)^b + c(a_w)^d$	(4.10)
Smith	(Smith, 1947)	$X_e = a - b\ln[1-a_w]$	(4.11)

4.2. Materials and methods

4.2.1. Sample preparation

Pumpkins (*Cucurbita pepo L.*), stored at 5 ºC and at similar stages of ripeness, were selected for the equilibrium experiments. Cylinders with fixed dimensions (length: 25 mm; diameter: 15 mm) were obtained from parenchyma tissue using a cork borer. The initial moisture content (from 95% to 97%, wet basis), and Brix (from 3 to 4 Brix) of the samples were used as control values for the fresh pumpkin. Pumpkin seeds were carefully separated from the fruit and stored. The seeds were cut into slices before the equilibrium experiment. In both cases, the moisture content was determined in a vacuum oven at 70 ºC and 104 Pa (AOAC, 1984) until a constant weight was achieved, as described in 3.2.4.

4.2.2. Osmotic dehydration

Some of the cylinders of pumpkin parenchyma were immersed into a sucrose solution (60% w/w) with agitation at 25 ºC for 3 h as explained in 3.2.3. After this contact with the solution, the tissue was partially dehydrated and acquired different contents of osmotic solute.

4.2.3. Equilibrium experiments

Experiments with fresh and osmotic dehydrated parenchyma and raw seeds were carried out in the same way. Each experimental equilibrium moisture content was determined using a gravimetric technique: the static equilibrium method (Wolf *et al.*, 1985[b]).

Saturated salt solutions with water activity ranging from 0.08 to 0.94 at 25ºC were prepared with pure salts and distilled water, according to Greenspan (1977) specifications. The salts selected were KOH, LiCl, $MgCl_2$, K_2CO_3, $Mg(NO_3)_2$, NaBr, $SrCl_2$, NaCl,

$(NH_4)_2SO_4$, KCl, $BaCl_2$ and KNO_3. Values for the water activity of the salt solutions at each temperature were obtained from the literature (Greenspan, 1997; Bell and Labuza, 2000), and where no data were found, they were experimentally measured with a Novasina Thermoconstanter apparatus (Novasina, Switzerland). The values of water activity are shown in Table 4.2. Each saturated salt solution was introduced in a hermetic container. For water activities above 0.65, some thymol crystals were put in the sorption container to avoid microbial growth.

Table 4.2. Water activity of the selected saturated salt solutions at the three working temperatures.

Salt	Water activity		
	5 ºC	**25 ºC**	**45 ºC**
KOH	0.143	0.083	0.059
LiCl	0.113	0.113	0.112
$MgCl_2$	0.336	0.328	0.311
K_2CrO_3	0.431	0.432	0.430
$Mg(NO_3)_2$	0.589	0.529	0.469
NaBr	0.635	0.576	0.519
$SrCl_2$	0.771	0.709	0.630
NaCl	0.757	0.753	0.745
$(NH_4)_2SO_4$	0.824	0.810	0.796
KCl	0.877	0.843	0.817
$BaCl_2$	0.950	0.902	0.910
KNO_3	0.963	0.936	0.870

All measurements were done in triplicate using ca. 2 g of pumpkin for each sample. Each sample was introduced in a little glass flask (25 mL) which was introduced in the hermetic container with the salt solution. These containers were introduced and maintained in chambers with controlled temperature at 5 ºC, 25 ºC and 45 ºC (±1ºC).

Samples were kept in the containers till observing weight variation less than 0.4% during a week. When equilibrium was reached (after eight weeks, approximately), the equilibrium moisture content of the samples was determined as described in 3.2.4.

4.2.4. Data analysis

Non-linear least square regression analysis was used for evaluating the parameters of the selected model with the software package Tablecurve™, AISN Software. The goodness of fit was determined using the correlation coefficient, the average residual (A) and percent average relative deviation (ARD) and the standard deviation (S). Each parameter is given by Eqs. (4.12) to (4.14), respectively, as:

$$A = \sum_{i=1}^{n} \left[\frac{X_{ei}^{cal} - X_{ei}^{\exp}}{n} \right] \tag{4.12}$$

$$ARD(\%) = \frac{100}{n} \sum_{i=1}^{n} \left| \frac{X_{ei}^{cal} - X_{ei}^{\exp}}{X_{ei}^{\exp}} \right| \tag{4.13}$$

$$S = \sqrt{\sum_{i=1}^{n} \left[\frac{\left((X_{ei}^{cal} - X_{ei}^{\exp}) - A \right)^2}{n - y - 1} \right]} \tag{4.14}$$

where X_{ei}^{cal} and X_{ei}^{exp} are the calculated and experimental equilibrium moisture content values, n is the number of experimental data and y the number of the parameters of the model, respectively.

4.3. Results and discussion

4.3.1. Equilibrium data

Experimental equilibrium data for pumpkin parenchyma at 5 ºC, 25 ºC and 45 ºC are shown in Figure 4.1. The equilibrium moisture content at each water activity is the

mean value of three replications. All isotherms show an increase in equilibrium moisture content with increasing water activity, at each temperature.

The shape of each isotherm is a very light sigmoidal curve of somewhere between type II and type III following Brunauer's classification (Brunauer *et al*., 1940). Taking into account the composition of pumpkin parenchyma tissue (82.7% carbohydrate and 9.6% protein, both values measured on a dry basis) (Teotia, 1992), the sorption isotherm is very similar to the corresponding average sorption isotherms of glucose and fructose (the main sugars present in the pumpkin with similar composition values), and the end is also similar to the sucrose isotherm (included in Fig. 4.2) (Makower and Dye, 1956).

Moisture content increases considerably at high water activity values. This fact is related to the crystalline sugars' transition to the amorphous state (Weisser *et al*., 1982).

Practically no effect of temperature on the sorption isotherm is observed. The dependence with temperature is clearer at higher temperatures and when a wide range of temperatures are studied. These results indicate that, over the range of temperatures studied, the pumpkin tissue exhibits similar hygroscopicities. When low temperatures are employed, no physical or chemical changes are produced, and the energy levels reached are insufficient to allow great water mobility. This behaviour is also shown for other products (Chen, 2002). As sorption characteristics have practically no dependence on temperature, this fact indicates that pumpkin can be stored in the same atmosphere at any temperature within the studied range (these are common conditions for storing).

Figure 4.2 shows the equilibrium desorption data for fresh pumpkin parenchyma and that partially dehydrated by osmotic dehydration using a sucrose solution. During soaking, the composition of the pumpkin is changed, not only through water loss, but also by acquisition of solutes from the osmotic solution. The osmotic agent acquisition and water removal kinetics of pumpkin with 60% Brix sucrose solution at 25 ºC are shown in Figure 4.3.

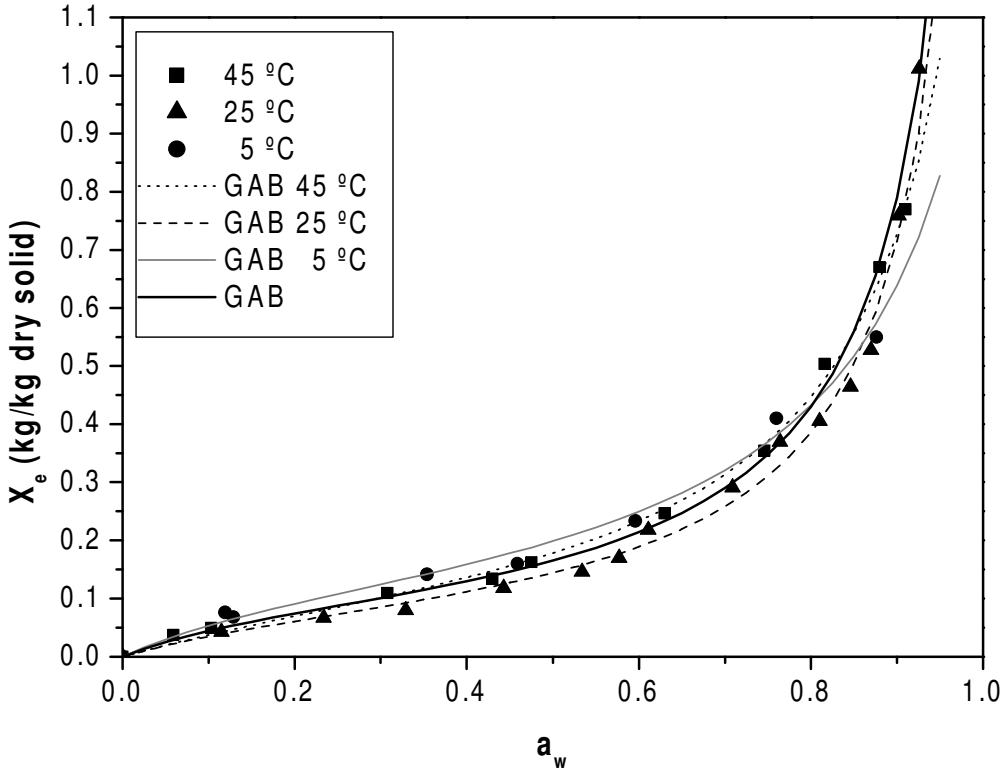

Figure 4.1. Experimental equilibrium data at different temperatures and GAB sorption isotherms (Eq. (4.3)) for fresh pumpkin parenchyma.

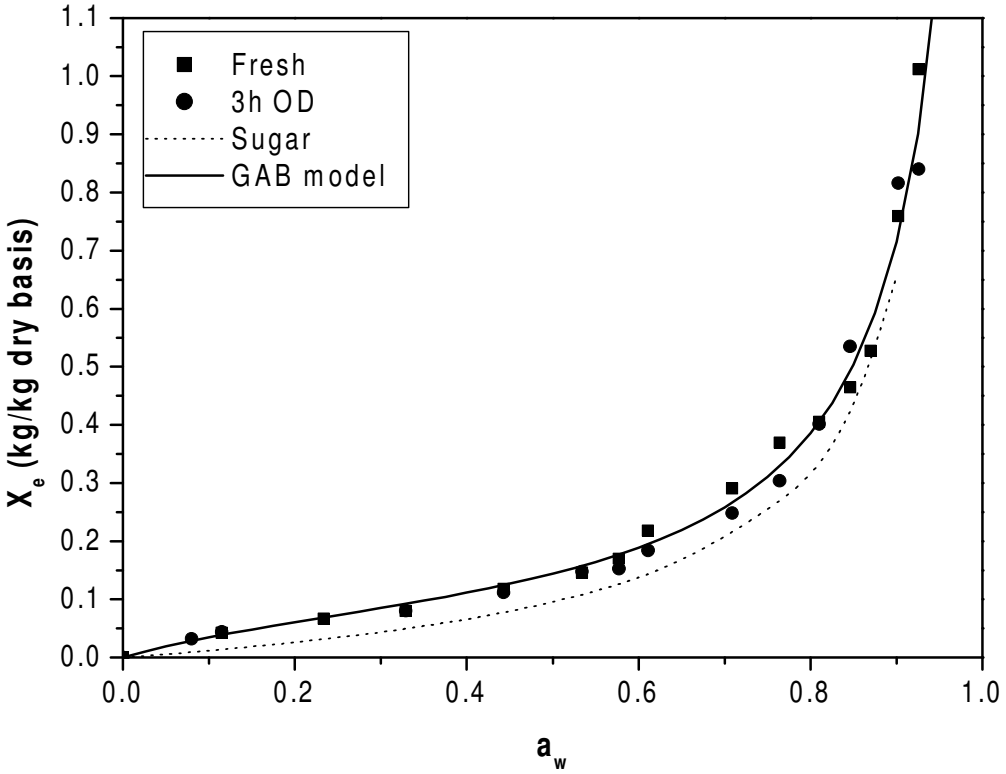

Figure 4.2. Experimental equilibrium data for fresh and osmotically-treated (OD) pumpkin parenchyma tissue with sucrose solution, with the GAB model (Eq. (4.3)) and the sucrose isotherm (Makower and Dye, 1956) also plotted at 25 ºC.

Both processes are fast and 0.095 kg sucrose/kg initial wet mass was gained by the pumpkin after three hours. The uptake of solids is more rapid over the first hour, after that it slows down because a pseudo-equilibrium is achieved, but the water loss continues to be fairly rapid (reaching 0.58 kg water/kg initial wet basis) after three hours. The sorption isotherms of these pre-osmotic products are very similar. In Figure 4.2, the sorption isotherm of pure sucrose is shown for comparison (Makower and Dye, 1956), and the equilibrium data for the pumpkin impregnated with sucrose over three hours correlates closely to the sucrose sorption isotherm, although the values of equilibrium moisture content are slightly higher, probably due to the presence of proteins and other more hygroscopic compounds in the pumpkin (Falade *et al*., 2003). Taking into account the previous considerations, it is reasonable to assume that the sorption isotherms are very similar, and from a practical point of view this means that all pumpkins can be dried, stored and preserved in the same way.

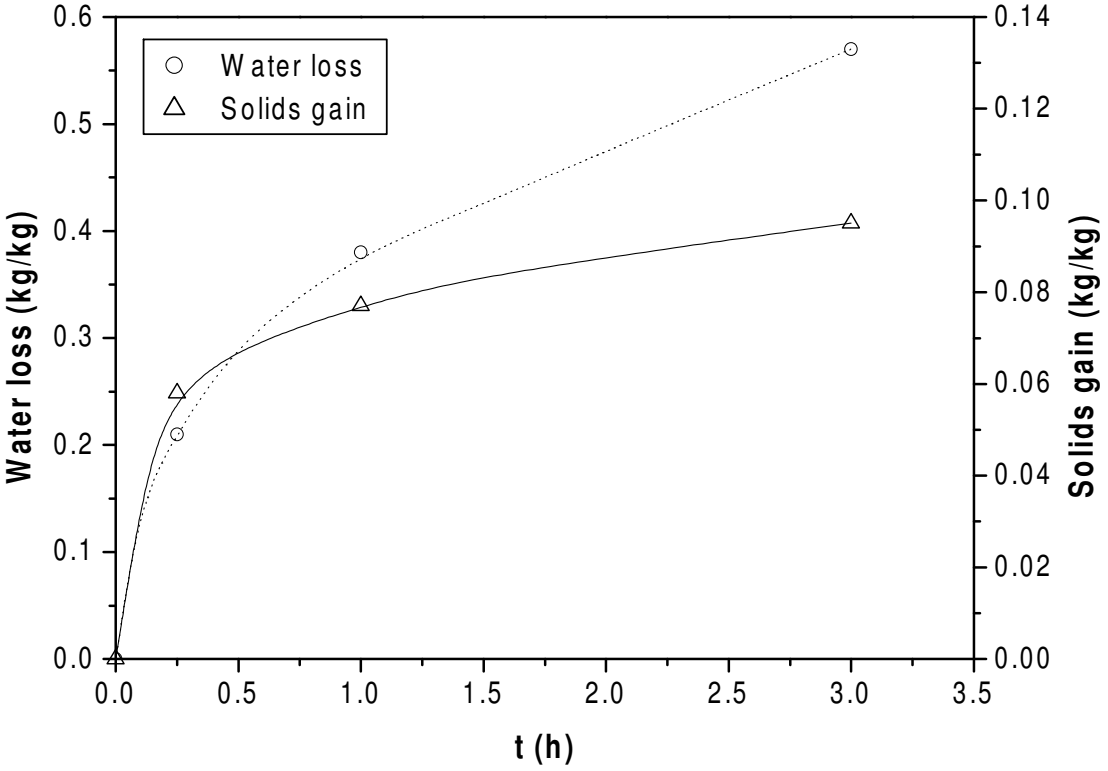

Figure 4.3. Water loss and solid gain kinetics for the simultaneous dehydration/sucrose impregnation of pumpkin parenchyma with 60 Brix sucrose solution at 25 ºC.

Figure 4.4 shows equilibrium experimental data for the sorption isotherm of pumpkin seeds. The shape classification of the isotherm is type II. The high oil concentration in the seeds facilitates a lower equilibrium moisture content compared to parenchyma tissue at the same water activity. The results obtained are similar to those found for seeds of other food materials reported by other authors (Marcos *et al*., 1997).

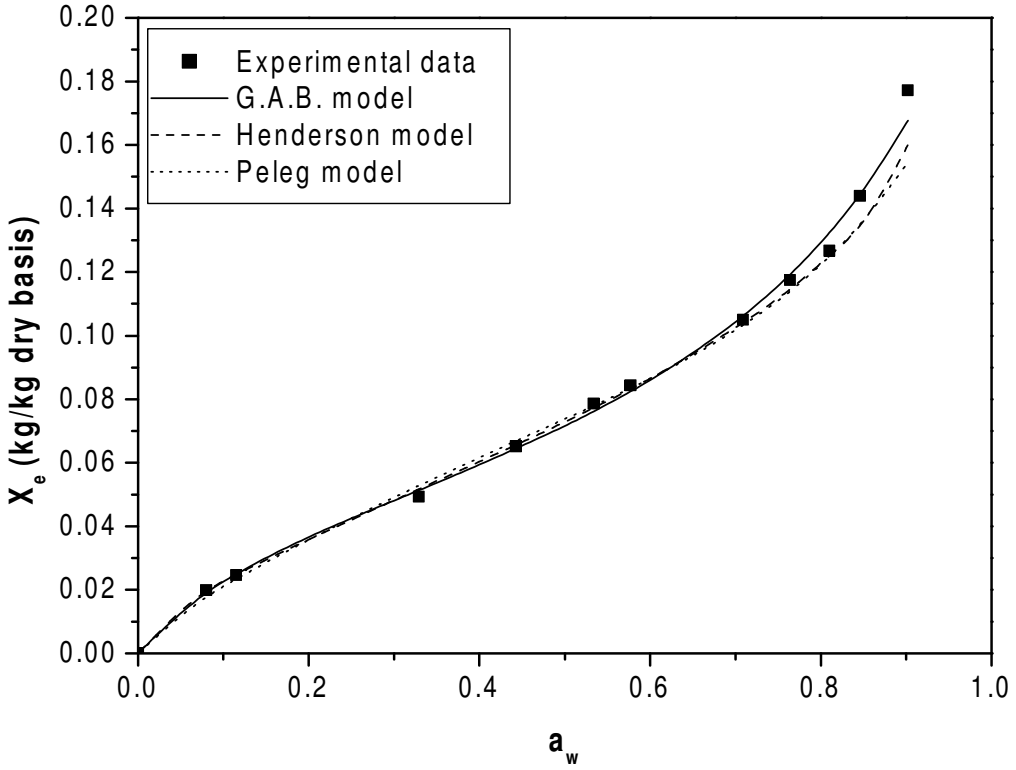

Figure 4.4. Experimental equilibrium data and several models for the sorption isotherm of pumpkin seed at 25 ºC.

4.3.2. Modelling of sorption isotherms

The experimental data were modelled using several models found in the literature. Taking into account that equilibrium moisture content did not depend on the temperature for the pumpkin parenchyma in the studied range for the osmotic pretreatment, the modelling incorporated all of the experimental data in order to obtain a single equation valid over the interval of interest. This equation is very useful from a practical point of

view. The values of the fit parameters for each model and their associated statistics are collected in Table 4.3.

Table 4.3. Estimated values for the fit parameters (and associated statistics) for sorption models applied to sorption data for pumpkin parenchyma, in the range 5 - 45 ºC.

Model	*a*	*b*	*c*	*d*	R^2	*ARD(%)*	*A*	*S*
BET(a_w< 0.4)	0.078	31.864			0.966	17.28	0.033	0.020
Chirife	2.080	-0.803	-0.002		0.975	15.47	0.029	0.017
GAB	0.096	0.976	8.063		0.974	12.95	0.029	0.017
Halsey	0.076	1.236			0.975	15.29	0.029	0.017
Harkins	2.088	-38.702			0.959	31.90	0.037	0.025
Henderson	-2.759	0.705			0.972	20.69	0.030	0.018
Kühn	0.045	-0.077			0.965	19.43	0.034	0.020
Mizrahi	0.074	0.171			0.957	32.91	0.058	0.029
Oswin	0.164	0.705			0.974	14.70	0.029	0.018
Peleg	0.366	1.000	1.617	12.047	0.982	16.17	0.032	0.019
Smith	-0.004	0.311			0.958	26.48	0.051	0.027

Several models gave similar results when fitting the experimental data; from this point of view, the Halsey and Oswin models with two parameters (simpler models) and the Chirife and GAB models with three parameters may be recommended. The values of the fit statistics for each model are satisfactory, taking into account the wide range of application of these equations. Specifically, the GAB model (also known as the kinetic model based on a multilayer and condensed film) is considered to be the most versatile, and it has been adopted by many researchers to model sorption isotherms of many food materials, due to the physical meaning often attached to its parameters.

Table 4.4 shows the fit parameters and associated statistics for the GAB model at each considered temperature.

Table 4.4. Estimated values for the fit parameters (and associated statistics) for the GAB model applied to sorption data for pumpkin parenchyma at several temperatures.

T(ºC)	*a*	*b*	*c*	R^2	*ARD(%)*	*A*	*S*
5	0.134	0.887	5.831	0.993	4.23	0.009	0.002
25	0.089	0.976	4.990	0.990	5.02	0.011	0.003
45	0.116	0.928	3.553	0.997	3.53	0.009	0.002

Table 4.5. Estimated values for the fit parameters (and associated statistics) for sorption models applied to sorption data for pumpkin seeds at 25 ºC.

Model	*a*	*b*	*c*	*d*	R^2	*P(%)*	*A*	*S*
Chirife	-2.307	-1.296	0.613		0.993	4.07	0.003	0.004
GAB	0.057	7.443	0.729		0.995	2.90	0.002	0.004
Halsey	0.0015	2.299			0.951	14.69	0.008	0.007
Karkins	14.219	-263.370			0.968	13.07	0.007	0.006
Henderson	-47.548	1.614			0.996	2.30	0.002	0.003
Oswin	0.072	0.353			0.981	10.37	0.006	0.004
Peleg	0.125	0.776	0.079	6.843	0.995	4.14	0.003	0.003
Smith	0.022	0.060			0.960	11.31	0.008	0.006

The results are in the typical range for this type of product (Iglesias and Chirife, 1982, Vázquez *et al*., 2003) and the quality of the fits is good (but useful only for each temperature). Figure 4.1 shows the GAB model fits at each temperature (values of the parameters are shown in Table 4.4), as well as the GAB model for all experimental data (values of the parameters are shown in Table 4.3). Also, for comparison, the average GAB model is plotted in Figure 4.2.

The results from modelling the sorption isotherm for pumpkin seeds are collected in Table 4.5. Analyzing the results, the Henderson, GAB and Peleg models are the best. Figure 4.4 shows the sorption isotherms obtained with these models.

4.4. Conclusions

The shape of the desorption isotherm of fresh pumpkin parenchyma tissue is intermediate between types II and III (slight sigmoidal shape); for seeds it is clearly type II. Over the range of the low temperatures studied, the isotherms for parenchyma tissue show no clear dependence on the temperature. The equilibrium data are satisfactorily fitted by several models. Specifically, the parameter a (corresponding to the monolayer moisture content, an important value for correct preservation) of the GAB model, resulted in values of 0.096 and 0.057 (kg water)/ (kg dry solid) for parenchyma and seed, respectively. The equilibrium values for the moisture content of both parenchyma and seed have water activity values that are very similar (0.30–0.35), indicating that both products can be stored in the same atmosphere.

When pumpkin parenchyma is osmotically treated, the sorption isotherm is not significantly changed because the self-dried composition of pumpkin is practically a mixture of sugars (glucose and fructose, monosaccharides of sucrose). With more sucrose content, the pumpkin has a sorption isotherm similar to the sucrose sorption isotherm, but with a higher equilibrium moisture content, probably due to the presence of proteins in the pumpkin. The results indicate that both products, fresh or osmotically-treated, can be stored in the same way.

CHAPTER 5

DENSITY, SHRINKAGE AND POROSITY CHANGES DURING OSMOTIC DEHYDRATION OF PUMPKIN FRUITS

CHAPTER 5. DENSITY, SHRINKAGE AND POROSITY CHANGES DURING OSMOTIC DEHYDRATION OF PUMPKIN FRUITS

5.1. Design, installation and calibration of a gas pycnometer for particle density measurement of high moisture materials

5.1.1. Introduction

One of the most important parameter of macroscopic structure of porous media is the porosity, generally defined as the ratio of pore or void volume and the bulk volume of the porous sample (Dullien, 1992). Depending on the typical form of the material and the type of void spaces considered, it is common to add an "adjective" to define porosity in a more precise way, as "effective", "interparticle", "intraparticle", "particle", "powder" (Keey, 1992).

In many aspects the quality of porous products is dependent on their porosity and the understanding of porosity behaviour during the processing of such products is a true concern in many research fields, as in foods (Krokida and Maroulis, 1997; Rahman, 2001), in inorganic catalysts (Silva and Miranda, 2003) and in a general way in powder processing (van der Wel, 1998).

In the case of foods, Rahman (2001) pointed out the following aspects as dependent on material porosity:

- Prediction and understanding of heat and mass transfer phenomena in several food processing operations, such as drying, smoking, blanching, frying, and extrusion among others.
- Mechanical and textural properties of foods are often correlated to porosity.
- Sensory properties of foods are affected by porosity.
- Pore characteristics are a key factor in many food products' quality.

Determination of porosity requires the knowledge of the total or bulk volume and the void volume included in the material matrix; their difference is also known as the particle volume. Measurement of the bulk or total volume is a relatively easy task and has been performed by means of different experimental procedures (Prothon *et al*., 2003); such as volume displacement of a liquid, dimensional determinations, and buoyant force measurements. Difference methods have been proposed to measure the particle volume; these methods often implies changes in the structure and/or composition of the material; such as the measurement of the volume of ground and degasified samples (Nieto *et al*. 2004) and liquid infiltration by application of a vacuum pulse (del Valle *et al*., 1998[b]; Mavroudis *et al*., 2004). Helium stereopycnometry and mercury porosimetry have also been used but they require sample dehydration (Karathanos *et al*. 1993; Krokida and Maroulis, 1997).

Some authors have proposed empirical and semiempirical equations for prediction of porosity (Krokida and Maroulis, 1997; Moreira *et al*., 2000; Rahman, 2003). Few papers have proposed methods to measure particle volume in solids with high moisture content, and consequently, porosity of these solids (Lozano *et. al*., 1980; Mavroudis *et. al*., 1998[b]).

Following the procedure described by Day (1964) and Mavroudis *et al*. (1998[b]), a special designed gas pycnometer described in this work was successfully built and used to measure the particle volume of solids with any moisture content and as a consequence to determine the porosity of such solids, if bulk volume is also known. The performance of this pycnometer was compared with other methods used to measure the particle volume of solids.

5.1.2. Definitions

Some definitions, previously reported by other authors (Lozano *et al*., 1980; Zogzas *et al*., 1994), are associated with the different measured properties in this work. In all these definitions it is assumed that the material to be analyzed is made up of a solid matrix (sm),

water (w) and a gas phase. The gas phase is present in open (op) and closed (cp) pores. The open or interconnected pores, as defined by Dullien (1992), are the pores connected among them and with the external surface of the material. Thus the total (bulk) volume of the material can be defined as

$$V_T = V_{sm} + V_w + V_{op} + V_{cp} \tag{5.1}$$

the particle volume is the volume of the sample excluding the volume of the open pores, but including the volume of closed pores.

$$V_p = V_{sm} + V_w + V_{cp} \tag{5.2}$$

finally, the substance volume is the volume of the material excluding the air phase volume

$$V_{sb} = V_{sm} + V_w \tag{5.3}$$

as a consequence, definitions of three different densities: bulk, particle and substance density can be given by substituting in Eq. (5.4) V_i by total (bulk) volume, particle volume and substance volume respectively.

$$\rho_i = \frac{m}{V_i} \tag{5.4}$$

two different types of porosity can be described: total porosity, as the ratio of air phase volume (that is, open and closed pores volumes) to total (bulk) volume

$$\varepsilon_T = \frac{\rho_{sb} - \rho_b}{\rho_{sb}} = \frac{V_T - V_{sb}}{V_T} \tag{5.5}$$

and open pore porosity, also called effective porosity (Dullien, 1992), as the ratio of the volume of pores connected to the outside to the total (bulk) volume

$$\varepsilon_{op} = \frac{\rho_p - \rho_b}{\rho_p} = \frac{V_T - V_p}{V_T} \quad (5.6)$$

In this work a procedure is proposed to determine the particle volume of solids moist and dry, allowing the calculation of the particle density and open pore porosity, if the bulk density of such materials is known. In the next section a detailed description of the proposed apparatus used to measure such volume is made.

5.1.3. Description of the gas pycnometer

The apparatus used in this study was a gas pycnometer home built at the Laboratory of Rheology and Food Engineering, Department of Chemical Engineering, University of Porto. The pycnometer measures the change in pressure experienced by a given amount of compressed gas filling a constant volume reference chamber when it expands into a second chamber containing a sample of the material.

Basically, the difference between the gas pycnometer presented in this work and a commercial helium pycnometer is in the sequence of the chambers, since in the latter the gas compression is done in the sample chamber followed by its expansion into a reference chamber. Such sequence of operations implies that when the solid contains moisture, even in small quantities, its partial vaporization occurs during the gas expansion, changing the composition of the solid sample and affecting the pressure in the system. Since it is pressure what is actually measured by the instrument, any variation in pressure measurement will be reported as a volume variation. Thus, the commercial helium pycnometers are only recommended to measure the volume of bone dry solids (Webb and Orr, 1997; Micromeritics, 2005; Quantachrome, 2005).

A schematic diagram of the experimental gas pycnometer described is shown in Figure 5.1 and a photograph in Figure 5.2.

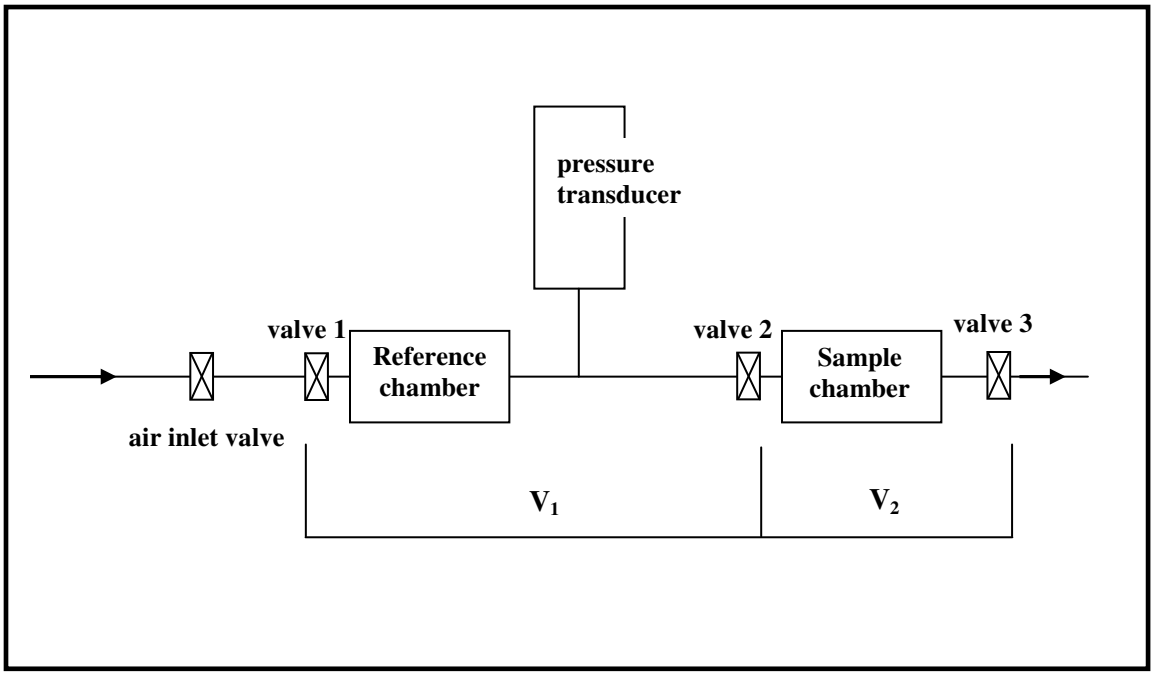

Figure 5.1. Schematic diagram of the gas pycnometer.

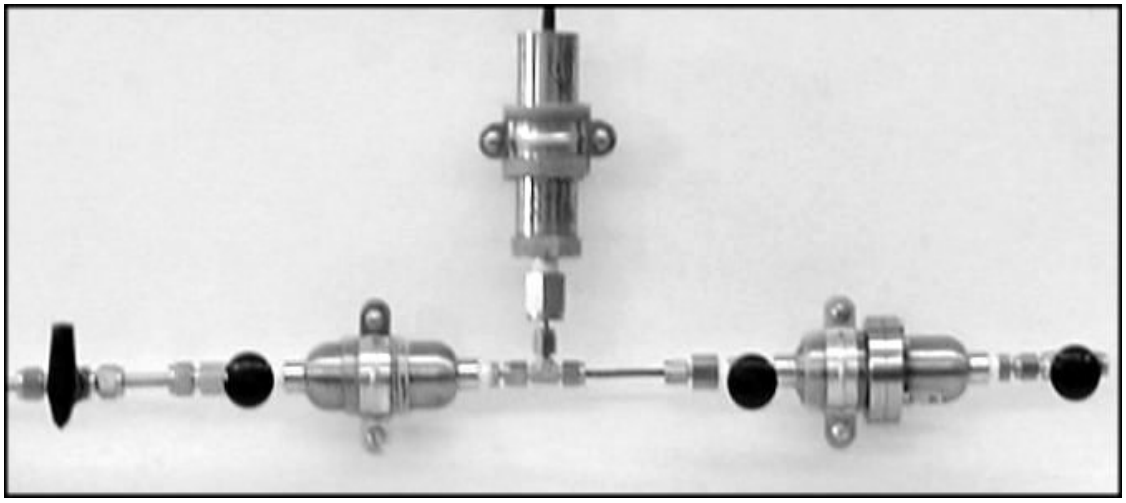

Figure 5.2. Picture of the gas pycnometer.

This gas pycnometer consists of two well defined volumes, four valves, one pressure transducer and one thermocouple. The first volume V1(ca. 44 cm3) includes the reference chamber and all piping connections between valve 1 and valve 2. The pressure transducer and the thermocouple are placed after the reference chamber and before valve 2. The second volume V2 (ca. 47 cm3) includes the sample chamber and all piping connections between valves 2 and 3. The pressure transducer measures the absolute pressure within a range of 0-7 bar (0-0.7 MPa) and resolution of 0.001 bar (100 Pa). Although the apparatus was located in a room with controlled temperature, a thermocouple was installed to check any variation in the temperature during the analysis. The K-type thermocouple was connected to a digital display with resolution of 0.1 ºC. The gas used in the experiments was compressed air.

5.1.4. Gas pycnometer operation and calibration

To obtain reliable measurements the apparatus must be always operated in two subsequent modes: (i) calibration and (ii) analysis. In the calibration mode, the measurements are done using a calibration cylinder made of nonporous steel, having a known constant volume, in order to evaluate V1 and V2. In the analysis mode, the calibration cylinder is substituted by the sample.

Operation steps:

Calibration

1. With empty pycnometer and valves 1 and 3 closed measure pressure and temperature (P_{atm} and T_{atm}).
2. Close valve 2 and open valve 1 controlling the pressure to the desired value.
3. After equilibration, measure P_1 and T_1.
4. Open valve 2 and after equilibration measure P_2 and T_2.
5. Open valve 3 to exhaust the air.
6. After equilibration measure ambient pressure and temperature with calibration cylinder in the sample chamber and valves 1 and 3 closed.

	7. Repeat steps 2 to 5 at least 3 times.
Analysis	8. Replace calibration cylinders by the sample of porous material with unknown volume. 9. Measure the ambient pressure and temperature with sample material in the sample chamber and valves 1 and 3 closed. 10. Repeat steps 2 to 5 at least 5 times.

It is considered that the system has reached the mechanical equilibrium when no pressure change was recorded for 1 minute. It is also assumed that the volume of the solid matrix and liquid phase are incompressible in the range of pressures used (up to seven bars).

Calibration of the pycnometer is very important and consists in the determination of the reference (V1) and sample (V2) empty volumes. As air is the gas used in the experiments and pressure up to seven bars was reached, the ideal gas equation and the Beattie-Bridgeman equation for air (Hougen *et al*., 1954) were used to describe air behaviour, but no significant differences between them were found. So, the ideal gas equation was used for all the calculations.

Eqs. (5.7)-(5.13) correspond to step 1-4 described above, that is, with empty pycnometer. The ideal gas model applied to step 1 provides Eqs. (5.7) and (5.8)

$$P_{atm}V_1 = n_{1e}RT_{atm} \tag{5.7}$$

$$P_{atm}V_2 = n_{2e}RT_{atm} \tag{5.8}$$

temperature and pressure measured in step 3 are related by Eq. (5.9) meanwhile Eq. (5.10) represents step 4.

$$P_1V_1 = n_1RT_1 \tag{5.9}$$

where n_1 corresponds to the amount of air in V_1, that is, the air that entered after opening valve 1 plus the amount of air initially in V_1 at atmospheric pressure.

$$P_2(V_1 + V_2) = (n_1 + n_{2e})RT_2 \tag{5.10}$$

re-arranging Eqs. (5.9) and (5.10),

$$\frac{V_1}{V_1 + V_2} = \frac{n_1}{n_1 + n_{2e}} \frac{T_1}{T_2} \frac{P_2}{P_1} \tag{5.11}$$

making $A = \frac{T_1}{T_2} \frac{P_2}{P_1}$ and inverting Eq. (5.11), (5.11a)

$$\frac{V_1 + V_2}{V_1} = \left(1 + \frac{n_{2e}}{n_1}\right) \frac{1}{A} \tag{5.12}$$

combining Eqs. (5.8) and (5.9) with Eq. (5.12) and solving with respect to V_1:

$$V_1 = V_2 \left(\frac{P_{atm}}{P_2} \frac{T_2}{T_{atm}} - 1 \right) \frac{A}{A - 1} \tag{5.13}$$

Eqs. (5.14)-(5.22) correspond to step 6-7, that is, with the calibration cylinder inside the sample chamber

$$P'_{atm}(V_2 - V_k) = n_{2k} R T'_{atm} \tag{5.14}$$

repeating steps 2 and 3 with the calibration cylinder in the pycnometer, Eq. (5.15) can be written

$$P'_1 V_1 = n'_1 R T'_1 \tag{5.15}$$

where $n_1^{'}$ corresponds to a new amount of air contained in V_1, that is, the air that entered volume V_1 after opening valve 1 plus the air initially present in V_1 at atmospheric pressure. Letting the air expand to fill the sample cell, the following relation is obtained:

$$P_2^{'}\left(V_1+V_2-V_k\right)=\left(n_1^{'}+n_{2k}\right)RT_2^{'} \tag{5.16}$$

dividing the members of Eq. (5.15) by the corresponding members of Eq. (5.16),

$$\frac{V_1}{V_1+V_2-V_k}=\frac{n_1^{'}}{n_1^{'}+n_{2k}}\frac{T_1^{'}}{T_2^{'}}\frac{P_2^{'}}{P_1^{'}} \tag{5.17}$$

making $B=\dfrac{T_1^{'}}{T_2^{'}}\dfrac{P_2^{'}}{P_1^{'}}$ and inverting Eq. (5.17), (5.17a)

$$\frac{V_1+V_2-V_k}{V_1}=\frac{n_1^{'}+n_{2k}}{n_1^{'}}\frac{1}{B} \tag{5.18}$$

combining Eqs. (5.14) and (5.15) with Eq. (5.18) and re-arranging

$$\frac{V_1}{V_2-V_k}=\left(\frac{P_{atm}^{'}}{P_2^{'}}\frac{T_2^{'}}{T_{atm}^{'}}-1\right)\frac{B}{B-1} \tag{5.19}$$

or

$$V_2=\frac{V_1}{\left(\dfrac{P_{atm}^{'}}{P_2^{'}}\dfrac{T_2^{'}}{T_{atm}^{'}}-1\right)\dfrac{B}{B-1}}+V_k \tag{5.19a}$$

substituting Eq. (5.13) into Eq. (5.19) and solving for V_2

$$V_2 = \frac{V_k}{1 - \frac{E}{G}\frac{F}{H}} \tag{5.20}$$

where

$$E = \frac{P_{atm}}{P_2}\frac{T_2}{T_{atm}} - 1 \qquad F = \frac{A}{A-1} \qquad G = \frac{P'_{atm}}{P'_2}\frac{T'_2}{T'_{atm}} - 1 \qquad H = \frac{B}{B-1} \tag{5.21}$$

comparing Eqs. (5.21) with Eq. (5.13), V_1.can be rewritten as:

$$V_1 = V_2 EF \tag{5.22}$$

During calibration, the gas pycnometer is operated according to the steps 1-6 and Eqs. (5.20) and (5.22) are used to calculate V_1 and V_2.

The next equations are used to obtain the sample particle volume. With the unknown sample volume in the sample chamber and valves 1 and 2 closed (system at atmospheric pressure), Eq. (5.23) is obtained

$$P_{atm}\left(V_2 - V_S\right) = n_{2S} R T_{atm} \tag{5.23}$$

after steps 2 and 3 with the sample,

$$P_{1S} V_1 = n_1^* R T_{1S} \tag{5.24}$$

where n_1^* corresponds to the amount of air in V_1, that is, the air that entered after opening valve 1 plus the air mass initially in V_1 at atmospheric pressure when the sample is in the gas pycnometer.

Expanding the air into the sample cell,

$$P_{2S}\left(V_1 + V_2 - V_S\right) = \left(n_1^* + n_{2S}\right)RT_{2S} \tag{5.25}$$

combining Eqs. (5.23)-(5.25) and re-arranging, the expression for the sample volume can be found

$$V_S = \frac{V_1\left(\frac{P_{1S}}{P_{2S}}\frac{T_{2S}}{T_{1S}} - 1\right)}{\left(\frac{P_{atm}}{P_{2S}}\frac{T_{2S}}{T_{atm}} - 1\right)} + V_2 \tag{5.26}$$

in the case that an isothermal operation can be considered,

$$V_S = V_1\left(\frac{P_{1S} - P_{2S}}{P_{atm} - P_{2S}}\right) + V_2 \tag{5.27}$$

It is observed that in Eq. (5.27) only pressure differences are involved and thus gauge pressures (p) can be used instead of absolute pressures, leading to

$$\frac{V_2 - V_S}{V_1} = \frac{p_{1S} - p_{2S}}{p_{2S}} \tag{5.28}$$

for a non-isothermal situation in which gauge pressures are measured, a suitable equation can also be found from Eq. (5.26).

The same principle used in this work was used by Day (1964) to determine the interstitial volume of seeds in chambers with volume of 1000 cm^3 and pressures slightly higher than the atmospheric. Eq. (5.28) is identical than the one obtained by Day (1964), that used gauge pressures in his final equation. Mohsenin (1970, 1986) cited Day's paper and presented the initial derivation, where absolute pressures are considered, and a final equation similar to Eq. (5.28) without specifying that in such equation gauge pressures need to be used. Mavroudis *et al*. (1998[b]) also used the same principle to determine particle

volume and porosity during osmotic dehydration of apples. They presented an identical equation but they didn't specify whether they used absolute or gauge pressures.

When absolute pressure is measured, Eq. (5.26) or (5.27) must be used, since these equations take into account the amount of air contained initially in the chambers, before the compression. For the same reason, Eqs. (5.13) and (5.19) must be used for the calibration. Table 5.1 illustrates what happens if the adequate equations are not used, that is, if absolute pressure is measured but the amount of air contained in the chamber at atmospheric pressure is not considered in the calculations.

Table 5.1. Volume of reference and sample chambers with applied pressure.

Absolute Applied Pressure (P_1), MPa	**Reference chamber (V_1), cm^3**		**Sample chamber (V_2), cm^3**	
	Eq. (5.13)	**n_{2e}=0 in Eq. (5.12)**	**Eq. (5.19)**	**n_{2k}=0 in Eq. (5.18)**
0.3489	44.5	87.3	46.6	50.5
0.5042	44.3	70.4	46.6	49.3
0.6550	44.3	63.2	46.5	48.6

5.1.5 Comparative performance tests of the gas pycnometer

5.1.5.1. Methodology

In order to assess the reliability of the gas pycnometer used, the particle volume of different solid samples was measured. The samples used were a non-porous metallic cylinder, glass spheres and a sintered sand cylinder.

The results were compared with the particle volume values obtained using other methods. Callipers were used to determine the dimensions of the non-porous metallic cylinder, and the particle volume was obtained from such dimensions. Liquid pycnometry

was used to determine the volume of the glass spheres. A helium pycnometer (AccuPyc 1330^{TM} from Micromeritics®) was used to measure the particle volume of the sintered sand cylinder.

After the performance of the pycnometer was assessed, particle density and porosity of a moist biological material (apple) was measured at different moisture contents.

Apples (*Golden Delicious* variety) were purchased in a local market, and stored in a refrigerator at 4 ºC until use. An electric slicing machine was used to produce slices cut perpendicularly to the apple axis with a thickness of 2.60±0.1 mm; from those slices, discs with diameter of 25.7±0.1 mm were subsequently cut with a cork borer. To obtain samples of different moisture contents, samples were partially dried in an oven at 70ºC under natural convection; they were removed from the oven at different drying times and their mass, dimensions, particle volume and bulk volume were determined. Dimensions were measured with a calliper. Particle volume was determined with the gas pycnometer presented in this work.

Bulk volume was obtained by two different methods: from the dimension values, using callipers (experiment 1) and measuring buoyant forces (Lozano *et al*., 1980) using n-heptane as liquid (experiment 2). From the bulk and particle volume, and using Eq. (5.6), porosity was calculated.

The equipment shown in Figure 5.3 was used to determine the bulk volume of the samples. This equipment consists in (Fig. 5.3 (a)):

1) Balance (Sartorius MA30, Sartorius GM Goettigen, Germany), with a precision of ±0.001g.
2) Aluminium support.
3) Table.
4) Steel wire for holding the sample.
5) Beaker with n-heptane.

An aluminium support is put on the balance. The support passes through the table board through two holes made in it. A steel wire is hanged on the support. This steel wire has in one end a spiral shape where the sample is introduced. For the volume determination, both sample weights in air and immersed in n-heptane are required.

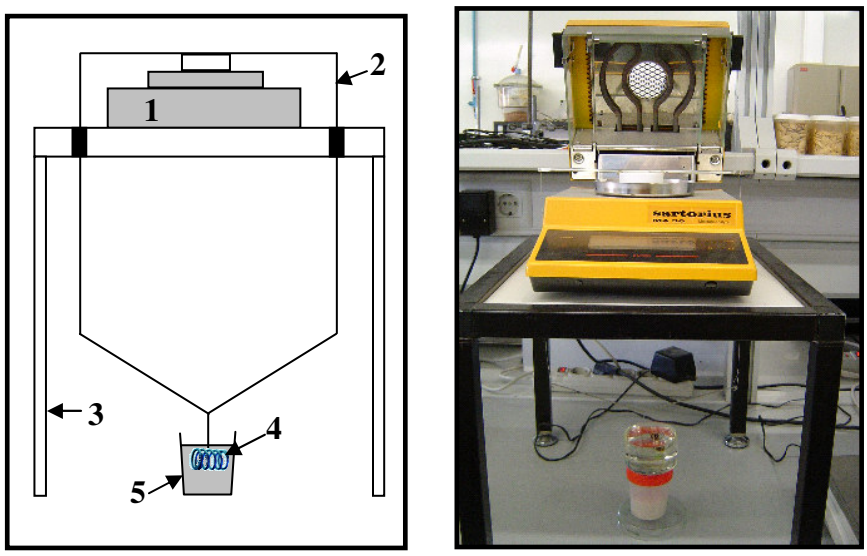

(a) (b)

Figure 5.3. Equipment used for the bulk volume measurements. (a) Schematic diagram; (b) Photograph.

Making a balance of forces in the system

$$\beta - w_S = \rho_f \cdot g \cdot V_f - \rho_{b,S} \cdot g \cdot V_{b,S} \qquad (5.29)$$

where β is the buoyant force, equal to the weight of displaced fluid; w_S is the sample weight; ρ_f and $\rho_{b,S}$ the density of the fluid and bulk sample density respectively; and V_f and $V_{b,S}$ the volume of the displaced fluid and the sample bulk volume, respectively. When the sample is totally immersed in the fluid $V_f = V_{b,S}$, and

$$\beta - w_S = V_{b,S} \cdot g \cdot (\rho_f - \rho_{b,S}) \qquad (5.30)$$

when the sample in weighed in air (air is the fluid)

$$\beta - w_S = weight\ in\ air = V_{b,S} \cdot g \cdot (\rho_{air} - \rho_{b,S}) \tag{5.31}$$

similarly, when the sample is weighed in n-heptane (heptane is the fluid)

$$\beta - w_S = weight\ in\ heptane = V_{b,S} \cdot g \cdot (\rho_{hep} - \rho_{b,S}) \tag{5.32}$$

making Eq. (5.31) – Eq. (5.32)

$$-(m_{air} \cdot g - m_{hep} \cdot g) = V_{b,S} \cdot g \cdot (\rho_{air} - \rho_{hep}) \tag{5.33}$$

where m_{air} and m_{hep} are the sample masses (kg) obtained in the balance when weighed in air and in heptane respectively. Considering that ρ_{air} (20ºC, 1 atm) ≅ 1.2 kg/m^3, and ρ_{hep} (20ºC) ≅ 682 kg/m^3, it is possible to neglect the air density from the above equation; rearranging, Eq. (5.34) is obtained

$$V_{b,S} = \frac{m_{air} - m_{hep}}{\rho_{hep}} \tag{5.34}$$

which can be used to measure the bulk or total volume of the sample.

The measurement procedure has two steps:

1) Measurement of the volume of the wire holding the sample. The wire holding the sample is weighed in air and after that weighed in n-heptane. From the two measurements the volume of the wire immersed in heptane is calculated with Eq. (5.34).

2) Measurement of the sample bulk volume. The sample is introduced in the spiral wire and weighed in air; after that wire and sample)are immersed in n-heptane at the same level as in point 1 and weighed. Applying Eq. (5.34) the volume of the sample and wire is obtained; then subtracting the wire volume obtained in the first step the sample bulk volume is determined.

The volume of a glass cylinder was measured with this method and with a liquid pycnometer. The difference of the volume measured with the two methods was less than 2% (with no significant differences), so good results are obtained with this method of measurement.

Concerning particle volume measurements with the proposed gas pycnometer, for all series of tests the effect of the applied pressure was studied as well as different modes of opening valve 2, namely fast, slowly and by steps. The sensitivity of the results with respect to pressure and temperature uncertainty of the measurements was also assessed. In the case of tests involving apple, mass of samples was determined before and after the analysis in order to check any possible weight loss.

Moisture content of apple samples was determined by vacuum drying till constant weight as explained in 3.2.4.

5.1.5.2. Results and discussion

The calibration procedure was repeated in different occasions, totalling more than 50 times in order to verify the reproducibility of the results. The volume that contains the sample chamber (V2) was found to be 46.505±0.009 cm^3 with reproducibility of 0.019%. The reproducibility of a helium gas pycnometer (AccuPyc 1330TM from Micromeritics®) was determined as 0.018%, slightly higher than the reproducibility indicated by the manufacturer, typically to within ± 0.01% (Micromeritics, 1997). In spite of the difference between the accuracy of the pressure transducers used in both pycnometers, the

reproducibility of the gas pycnometer studied in this work is excellent when compared to a commercial one.

The results obtained for the different solids tested in the gas pycnometer are shown in Table 5.2. Such results are quite good when compared with other methods.

All tests were performed using different applied pressures of 0.20; 0.25; 0.30; 0.35; 0.50 and 0.65 MPa and similar results were obtained in all cases.

The operating mode of valve 2 has a slight influence in the results. When slow or step opening were used the measured volume was slightly smaller than when the valve was opened very quickly, apparently suggesting that in the former a more intense air penetration in the solid is observed. Nevertheless, it is too difficult to control and reproduce the way the valve is opened in the slow or step modes, when this is conducted manually, leading to increase the standard deviations of the results for such runs.

The sensitivity of the results with respect to the uncertainty in pressure and temperature measurements is presented in Table 5.3. As expected the higher the pressure the lower the deviation in the measured volume. This is the reason why higher pressures, around 0.65 MPa, were used for the analyses described, leading to the results presented in Tables 5.2 and 5.4.

Some tests were done using samples of fresh *Golden Delicious* apple (M = 87% w.b.). All values of porosity were between 22.5 and 24.5% in agreement with results presented by Hills and Remigereau (1997) in the range of 20% to 25% as well as with the values determined by Lozano *et al*. (1980) (M = 88% w.b.).

If any water was lost in moist samples, then a weight loss would be observed during the analysis. Some weight loss (less than 1%) was in fact detected for samples of fresh apple only due to their high moisture content (87% wb). Such loss may be considered

negligible compared to the loss of about 5% observed during the same time for control samples resting on the laboratory bench.

Table 5.2. Comparison of tests performed in the gas pycnometer and with other methods of particle volume analysis.

Material	**Volume (cm^3)**					**Relative deviation (%)**
	gas pycnometer		**other methods**[1]			$\frac{\lvert V_{om} - V_S \rvert}{V_{om}} x100$
	V_S	**σ**	**V_{om}**	**σ**	[1]**Method**	
Non-porous metallic cylinder	29.390	0.019	29.4053	0.0004	Callipers	0.05
Glass spheres	19.635	0.015	19.486	0.005	Liquid pycnometry	0.76
Sintered sand cylinder	2.80	0.02	2.811	0.003	Helium pycnometer	0.39

Table 5.3. Sensitivity of the results related to the accuracy of the pressure and temperature measurements.

P_1 (MPa)	**ΔP_2 (MPa)**	**ΔV_S (cm^3)**	**ΔT (^oC)**	**ΔV_S (cm^3)**
0.20	± 0.0001	±0.10	± 0.1	±0.054
0.25	± 0.0001	±0.07	± 0.1	±0.045
0.35	± 0.0001	±0.04	± 0.1	±0.038
0.50	± 0.0001	±0.03	± 0.1	±0.034
0.65	± 0.0001	±0.02	± 0.1	±0.032

Table 5.4. Porosity of *Golden Delicious* apple at different moisture content.

Experiment 1			Experiment 2		
Moisture content ($kg_{water}/kg_{dry\ solid}$)	**Porosity (%)**	**Standard deviation for the porosity**	**Moisture content ($kg_{water}/kg_{dry\ solid}$)**	**Porosity (%)**	**Standard deviation for the porosity**
6.452	24.38	0.005	6.452	22.67	0.009
5.428	31.35	0.002	5.242	25.71	0.003
4.735	33.79	0.005	4.485	27.65	0.004
3.844	39.20	0.005	3.619	30.53	0.011
3.086	42.08	0.004	2.914	34.31	0.003
2.588	47.32	0.005	1.886	40.74	0.005
1.959	47.25	0.010			

Figure 5.4 shows particle and bulk density of dehydrated apple samples at different moisture contents. As can be observed, the values for particle density obtained in experiments 1 and 2 are similar, whereas values of bulk density show differences due to the different experimental method used to obtain the bulk volume of samples.

Figure 5.5 presents the porosity of *Golden Delicious* apples with different moisture contents, which were obtained in the drying experiments. The difference between the results of experiment 1 and 2 are directly associated to the different ways used to obtain the bulk volume, since there was no difference between their particle volumes. The results for porosity are in good agreement with those obtained by Lozano *et al*. (1980) for *Granny Smith* apples, as can be observed in Figure 5.5. Each point in Figure 5.4 is the average value of five runs and all points are presented in Table 5.4 with the corresponding standard deviation.

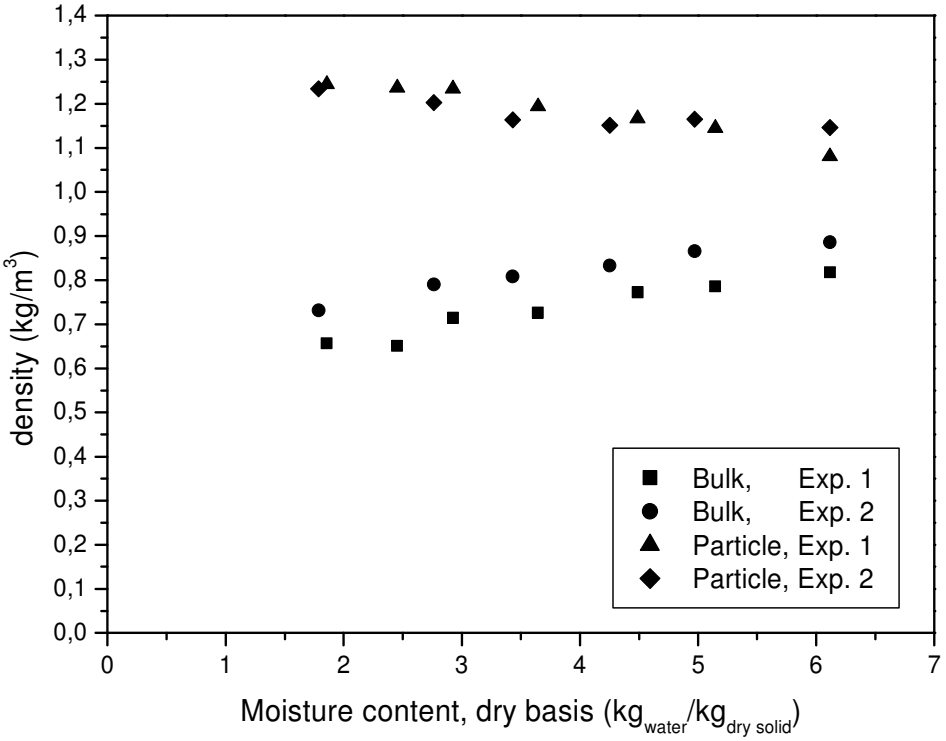

Figure 5.4. Particle and bulk densities of *Golden Delicious* apple at different moisture contents.

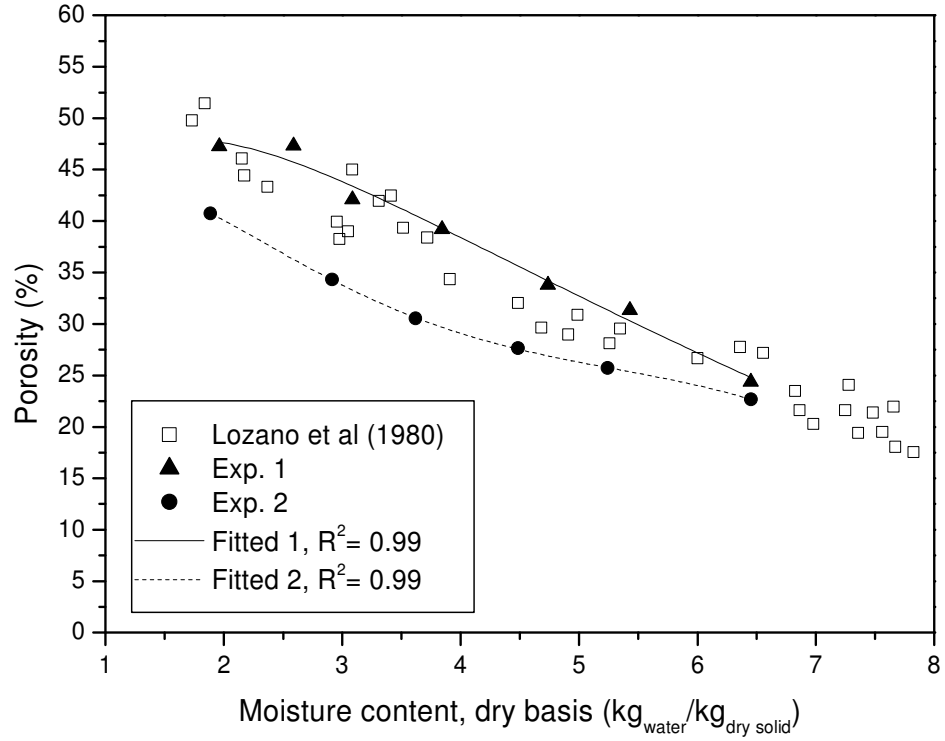

Figure 5.5. Porosity of *Golden Delicious* apple at different moisture contents.

5.1.6. Conclusions

The gas pycnometer described in this work was successfully used to determine particle volume of solids with high moisture content, that is, the volume occupied by the solid matrix, water and closed pores. Therefore the porosity and particle density of foods and other solids with high moisture content can be easily and accurately obtained from measurements using this method with the proposed mathematical models and associated with a precise pressure sensor.

The gas pycnometer can be easily built offering reliable results of particle volume for solids with high moisture content.

Further investigation needs to be done in order to verify the influence of the air humidity in the pressure measurements and in the sample weight loss. The operation mode of the expansion valve should as well be further investigated to assure reproducible results.

5.2. Shrinkage, density, porosity and change in shape during osmotic dehydration of pumpkin fruits

5.2.1. Introduction

The aim of this part of the work is to present experimental data on volume, density and porosity changes during osmotic dehydration of pumpkin fruits. Some of these data were obtained with the methods implemented in the first part of this chapter. Dimensional and morphological changes of the pumpkin samples were also studied by means of image analysis. Predictive models and correlation for these changes were proposed.

5.2.2. Materials and methods.

5.2.2.1. Sample preparation

The procedure explained in 3.2.1 was used in the preparation of samples for the dehydration experiments.

5.2.2.2. Dehydration experiments.

The studies of changes in bulk volume and bulk density were performed in osmotic solutions of different composition (binary sucrose and NaCl solutions and ternary NaCl/sucrose solutions) at different concentration of the osmotic solution and temperature (see Table 5.5).

The studies of particle volume and particle density were carried out in sucrose solutions and convective dehydrated samples.

Image analysis was performed on samples osmodehydrated with 60% sucrose solutions at 25ºC.

For all these studies the samples were removed for analysis at different process times (Table 5.5), then they were gently blotted with adsorbing paper to remove excess osmotic solution (in the case of osmotic treatments) and kept in plastic boxes till experimental determinations.

All the measurements were done in triplicate, except for the image analysis where the results are the average of six samples.

Table 5.5 shows a synopsis of the experiments performed in this chapter.

Table 5.5. Experiments for the studies of subchapter 5.2.

Dehydration treatment	**Process conditions**	**Experimental determinations**	**Sampling times (h)**
Osmotic dehydration Sucrose solutions	Table 3.1	A, B, C	0.083, 0.25, 0.5, 1, 1.5, 2, 2.5, 3, 4, 6 and 9 h.
	60% sucrose, 25 ºC	A, D	0.5, 1, 3, 6 and 9h
Osmotic dehydration NaCl solutions	5% NaCl, 25 ºC 20% NaCl, 12 ºC 10% NaCl, 38ºC	A,B	0.083, 0.5, 1, 2, 2.5, 3, 4, 5, 6 and 8h
Osmotic dehydration NaCl/sucrose solutions	3.5% NaCl, 58% suc. 7.5% NaCl, 45% suc. at 25ºC	A, B	0.083, 0.25, 0.5, 1, 1.5, 2, 2.5, 3, 3.5, 4, 5 and 6h
Convective drying	Oven drying at 70ºC	A, B, C	0.5, 1, 1.5, 2, 2.5, 3, 3.5, 4, 5, 6 and 8 h

A = Kinetic parameters (WL, SG, WR, NMC); B = bulk volume; C = particle volume; D = image analysis

5.2.2.3. Experimental determinations

The volume of each sample was calculated from the resultant buoyant force on the sample when immersed in n-heptane, as explained in 5.1.5.1. After this measurement, particle volume was obtained with the gas pycnometer presented in 5.1.

Weight reduction (WR), water loss (WL), solids gain (SG) and normalized moisture content (NMC) were obtained by means of the procedure explained in 3.2.4.

Since the soluble solids of pumpkin flesh are mostly sugars, soluble solids of fresh samples were determined with a refractometer (Abbe-3L refractometer, Bausch & Lomb, Rochester, NY, USA), thermo stated at 20 ºC. The clear juice was extracted by pressure and analyzed directly in the refractometer

To study change of dimension and shape, one rectangular slab of ca. 0.5-1mm of thickness was gently cut parallel to the height of the cylinders at the maximum section area as shown in Figure 7.1 (a), with a razor blade. One face of the slab was stained with a solution of methylene blue 0.1 % (Mayor *et al*., 2005) during 15 s. After that the sample was ready for observation under the stereomicroscope. Image acquisition and processing was performed as explained in 7.2.3.3.

Image analysis of the isolated sample contour (Fig. 5.6 (b)) was performed with the image analysis software “Image Tool” (free software available from Health Science Centre, University of Texas, San Antonio, Texas).

Several geometrical parameters of the samples, previously considered by other authors (Reeve, 1953, Lewicki and Pawlak, 2003, Mayor *et. al* 2005) were analyzed:

1) Surface area.
2) Perimeter of the contour.

3) Length of the major axis: the length of the longest line that can be drawn through the object.

4) Length of the minor axis: the length of the longest line that can be drawn through the object perpendicular to the major axis.

5) Roundness, defined as

$$Roundness = \frac{4\pi Area}{perimeter^2} \tag{5.35}$$

6) Elongation: the ratio of the length of the major axis to the length of the minor axis.

7) Compactness, defined as

$$Compactness = \frac{\sqrt{\frac{4area}{\pi}}}{major\ axis\ length} \tag{5.36}$$

8) In order to determine the linear dimensions, five measurements at different zones of the cylinders were done for the diameter and length (Fig. 5.6). Average values of these dimensions were obtained from the five measurements.

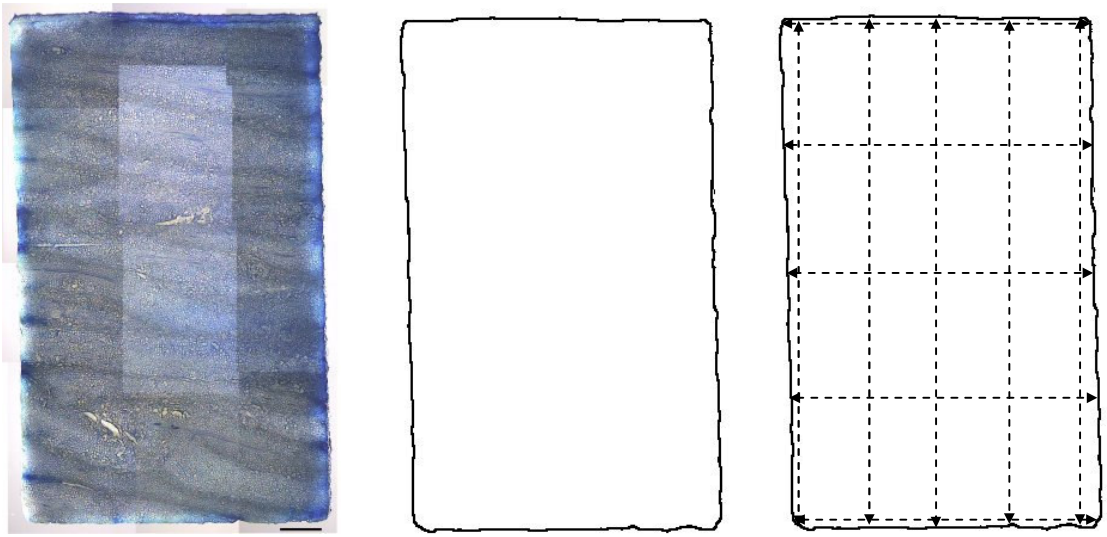

Figure 5.6. Procedure for the determination of the average diameter and length of the pumpkin cylinders. (a) Sample photograph. (b) Contour. (c) Dimension measurements (horizontal line in (a) corresponds to 2mm length).

5.2.3. Results and discussion.

5.2.3.1. Shrinkage during dehydration.

Figure 5.7 shows experimental shrinkage data of pumpkin cylinders along the different processing conditions tested versus water loss, weight reduction and normalized moisture content respectively. Plots on the left correspond to osmotic dehydration with sucrose solutions, whereas plots on the right correspond to osmotic dehydration with different osmotic agents and convective drying. Shrinkage of osmodehydrated samples varied from 0 to 73% of their initial volume, depending on the process conditions used. In the case of convective dried samples, shrinkage at the end of the drying attained values near to 95% of the initial volume.

Observing Figure 5.7 (a), there is a linear decrease of volume versus water loss during osmotic dehydration. The decrease is more accentuated in the case of NaCl solutions, followed by sucrose solutions and NaCl/sucrose solutions. No effect of process conditions concentration and temperature is observed for the same osmotic agent, as shown in Figure 5.7 (a) for sucrose solutions. Nieto *et al.* (2004), observed a linear decrease of sample volume with the loss of water during osmotic dehydration of apple; the decrease was more accentuated at the same water loss, for the samples osmodehydrated with glucose solutions compared with sucrose solutions. Mavroudis *et al.* (1998[b]) during osmotic dehydration of apples (var. *Granny Smith*) with sucrose solutions also observed a linear decrease of volume with the decrease of water in the material; they observed no effect of process temperature on shrinkage.

Convective dried samples also showed a linear decrease of the volume with the loss of water, but in this case the decrease is more accentuated than in the case of different osmotic agents. For the same water loss, the solids gained during osmotic dehydration compensate the volume reduction caused by the removal of water and shrinkage is less than the observed in convective drying.

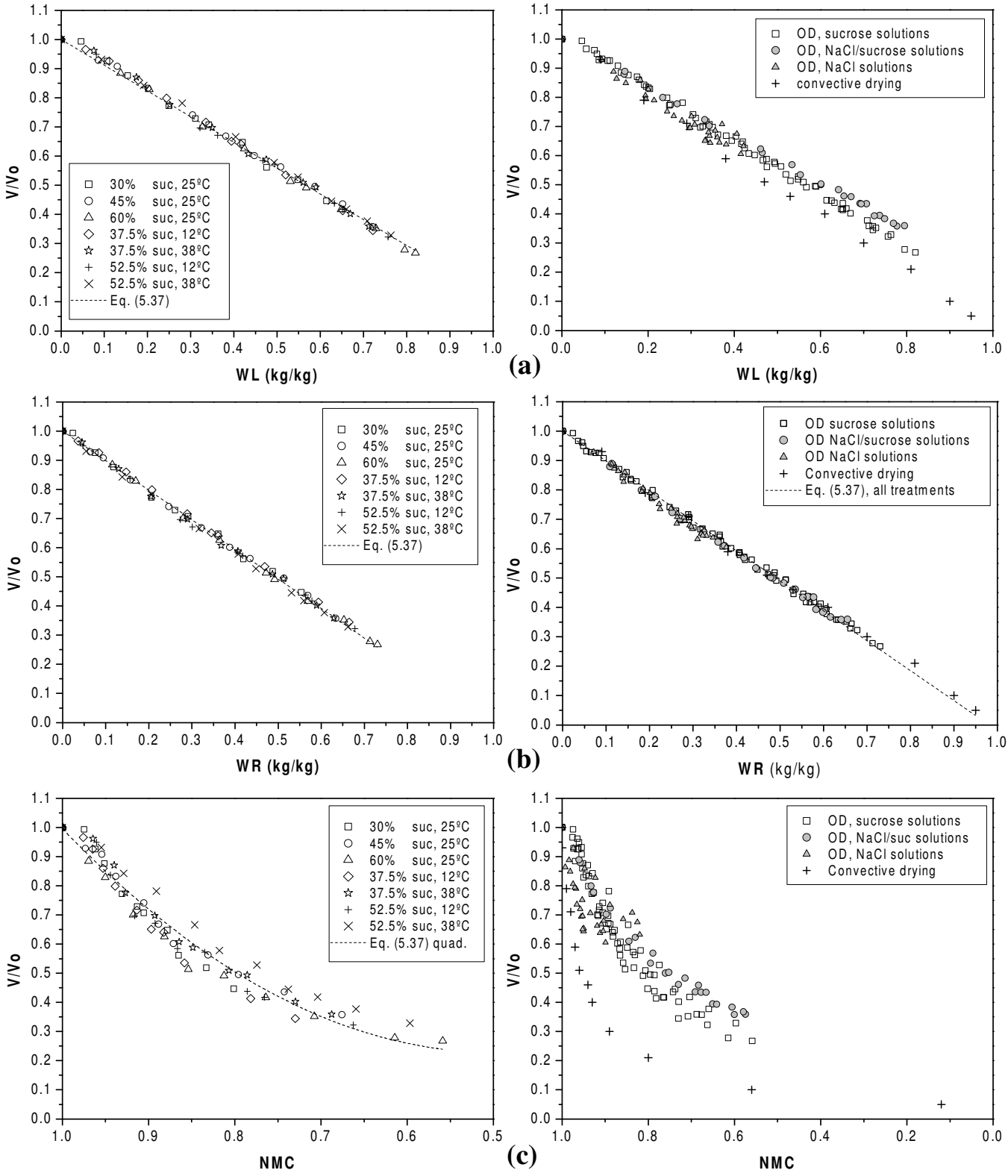

Figure 5.7. Shrinkage during dehydration of pumpkin cylinders versus (a) water loss, (b) weight reduction and (c) normalized moisture content. Left figures correspond to osmotic dehydration with sucrose solutions, whereas figures on the right correspond to osmotic dehydration with different osmotic solutions and convective drying.

If shrinkage is presented against weight reduction (Fig. 5.7 (b)), a linear decrease of volume with weight reduction can be seen, independently of the process conditions and dehydration process.

Moreira and Sereno (2003) during osmotic dehydration of apple with sucrose solutions found that independently of the process conditions (concentration and temperature of the osmotic solutions and hydrodynamic conditions) a simple linear relation between weight reduction and changes in volume could be observed. During convective drying, this linear behaviour of shrinkage against weight reduction (and consequently against water loss) is often reported (Lozano *et al.,* 1983; Zogzas *et al*., 1994).

Shrinkage of osmodehydrated and convective dried samples shows a nonlinear decrease with moisture content (Fig. 5.7 (c)). For convective dried samples this decrease is more accentuated, for the same reason as commented for the representation against water loss.

The volume change along dehydration is supposed to be mainly due to the volume of removed water from the material. As commented before, in the case of osmotic dehydration this effect is partially compensated by the volume gained by the sample due to the acquisition of solids from the osmotic solution. Variation in the volume of the gas phase inside the vegetable tissue also contributes to this change, increasing or decreasing the theoretical shrinkage produced by the removal of water. An ideal shrinkage could be defined as the shrinkage resulting as a consequence of the change in volume due to the water loss and the solids gained in the material only, supposing that the volume of the initial solids of the material remains constant. Assuming volume additivity, change in volume was calculated from experimental data of water loss, sucrose gain and NaCl gain and the density values 0.9971, 1.5805 and 1.2700 g/cm^3 for water (25ºC), sucrose and NaCl respectively (Lide, 2005). The assumption that volumes are additive is acceptable for the calculations, since excess volume of binary solutions of sucrose and NaCl and ternary NaCl/sucrose solutions obtained comparing experimental data from other authors is of the order of 1%, rarely exceeding 2%, as showed in Table 5.6.

Table 5.6. Excess volume of the osmotic solutions employed in the experiments.

Aqueous solution	Concentration range (*m*)	Excess volume (%)	Experimental data
Sucrose	0-4.5 *m*	Av. -0.3%	Lide (2005)
		Int. [-0.02, -0.76%]	Chenlo *et al*. (2002)
NaCl	0.-4.5 *m*	Av. -1.45%	Chenlo *et al.* (2002)
		Int. [-0.59, -2.51%]	
NaCl/sucrose	0.5-4.5 *m* NaCl	Av. -1.05%	Chenlo *et al.* (2002)
	0.5-4.5 *m* sucrose	Int. [-0.40, -2.11%]	

Figure 5.8 shows the "ideal shrinkage" of pumpkin cylinders dehydrated with binary solutions of sucrose and NaCl and convective dried, versus the actual shrinkage observed in the samples.

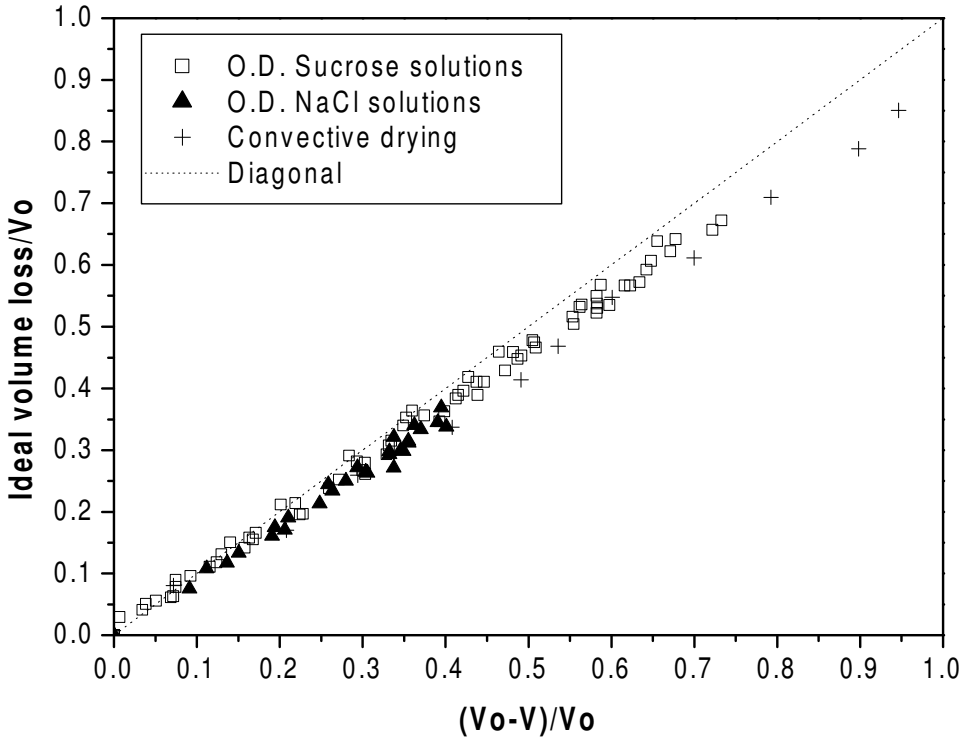

Figure 5.8. Ideal volume loss versus actual volume loss during osmotic dehydration of pumpkin fruits with binary sucrose and NaCl solutions and convective drying.

It is observed that, for each of the three dehydration treatments, the volume lost by the material is higher than the volume change caused by the mass fluxes occurring during dehydration. This higher loss of volume than expected is related with the decrease of the volume of the air phase and collapse of the material. Barat *et al.* (2001), during the osmotic dehydration of apples with sucrose solutions, observed that the decrease of total volume was higher than the decrease of the liquid phase volume in the samples. Several phenomena can be the cause of this material collapse, such as capillary forces caused by the removal of water and loss of turgor pressure in the cells, creating stresses in the system and leading to a higher shrinkage than the expected due to the change in the volume of the liquid phase in the material.

Shrinkage of pumpkin during dehydration can be correlated with water loss, weight reduction and moisture content by means of empirical equations. A polynomial of the form

$$\frac{V}{V_o} = 1 + aX + bX^2 + cX^3 \tag{5.37}$$

where X can represent water loss, weight reduction, or normalized moisture content, was fitted to experimental data on shrinkage. Results of the fits are shown in Tables 5.7 to 5.12, and some of them are shown in Figure 5.7. The fits were made considering each osmotic agent alone, considering all the osmotic treatments together, convective drying alone, and all the dehydration treatments together (convective drying and osmotic dehydration).

Table 5.7. Parameters of Eq. (5.37) for sucrose solutions.

X	a	b	c	R^2	ARD (%)
WL(linear)	-0.88	-	-	0.99	1.65
WR(linear)	-1.01	-	-	0.99	1.44
NMC (quadratic)	-3.08	3.07	-	0.96	5.96
NMC (cubic)	-1.74	-0.18	1.94	0.97	5.26

Table 5.8. Parameters of Eq. (5.37) for NaCl solutions.

X	a	b	c	R^2	ARD (%)
WL(linear)	-0.94	-	-	0.96	2.4
WR(linear)	-1.09	-	-	0.99	1.19
NMC (quadratic)	-2.24	2.10	-	0.49	9.48
NMC (cubic)	16.04	-37.82	21.74	0.71	6.38

Table 5.9. Parameters of Eq. (5.37) for NaCl/sucrose solutions.

X	a	b	c	R^2	ARD (%)
WL(linear)	-0.82	-	-	0.99	1.18
WR(linear)	-1.02	-	-	0.99	1.96
NMC (quadratic)	-2.58	2.55	-	0.99	2.59
NMC (cubic)	-2.17	1.50	0.66	0.99	2.67

Table 5.10. Parameters of Eq. (5.37) for convective drying.

X	a	b	c	R^2	ARD (%)
WL, WR (linear)	-1.00	-	-	0.99	2.86
NMC (quadratic)	-4.55	4.35	-	0.59	43.99
NMC (cubic)	-6.34	9.19	-3.11	0.63	48.61

Table 5.11. Parameters of Eq. (5.37) for osmotic dehydration.

X	a	b	c	R^2	ARD (%)
WL(linear)	-0.87	-	-	0.99	3.13
WR(linear)	-1.02	-	-	0.99	1.81
NMC (quadratic)	-2.75	2.70	-	0.90	8.70
NMC (cubic)	-1.74	0.22	1.49	0.91	8.09

Table 5.12. Parameters of Eq. (5.37) for all the dehydration treatments.

X	a	b	c	R^2	ARD (%)
WR (linear)	-1.02	-	-	0.99	2.43

For WL and SG the linear fit is satisfactory. For normalized moisture content, both quadratic and cubic models are acceptable (except for OD with NaCl solutions and convective drying); being the cubic fit the one which gave slightly better results. These equations are very useful since they allow the prediction of shrinkage data independently of the process conditions (concentration and temperature) used.

5.2.3.2. Bulk density, particle density and porosity.

Similar trend of change of bulk density, particle density and porosity were observed versus WL and WR of samples along processing. For NMC the observed trend was not as clear as in the case of water loss and weight reduction (data not shown). Figure 5.9 shows the changes in normalized bulk density (ρ_b/ρ_{bo}), normalized particle density (ρ_p/ρ_{po}) and normalized porosity ($\varepsilon/\varepsilon_o$) against weight reduction. Reduced values were used in order to minimize the variability of the initial values. Table 5.13 shows the average values of some physicochemical characteristics of raw pumpkin parenchymatic tissue.

Table 5.13. Some physicochemical properties of raw pumpkin flesh.

Property	Average value	Range
Moisture content (%)	95.57	[94.44-96.92]
Soluble solids (%)	3.22	[2.14-3.63]
Insoluble solids (%)	1.21	[0.78-1.97]
Bulk density (kg/m^3)	0.89	[0.86-0.92]
Particle density (kg/m^3)	1.04	[1.003-1.07]
Porosity (%)	14.79	[10.22-18.18]

The variation of bulk density (Fig. 5.9 (a)) during osmotic dehydration with sucrose solutions was not very large, amounting to about 5% during the treatments. Similar variation was observed for osmotic dehydration with NaCl solutions. Higher variation was obtained for ternary NaCl/sucrose solutions (ca. 10%) and convective drying (ca. 13%). Similar behaviour is observed for all the treatments during dehydration; bulk density of the samples initially increases, reaching a maximum value and decreases or fluctuates till the end of the process. Nieto *et al*. (2004), during osmotic dehydration of apples with sucrose and glucose solutions, observed an increase of bulk density of apple samples in the beginning of the treatments (around the first hour of treatments) for both osmotic agents, and then bulk density suffered fluctuations until the end of the processes.

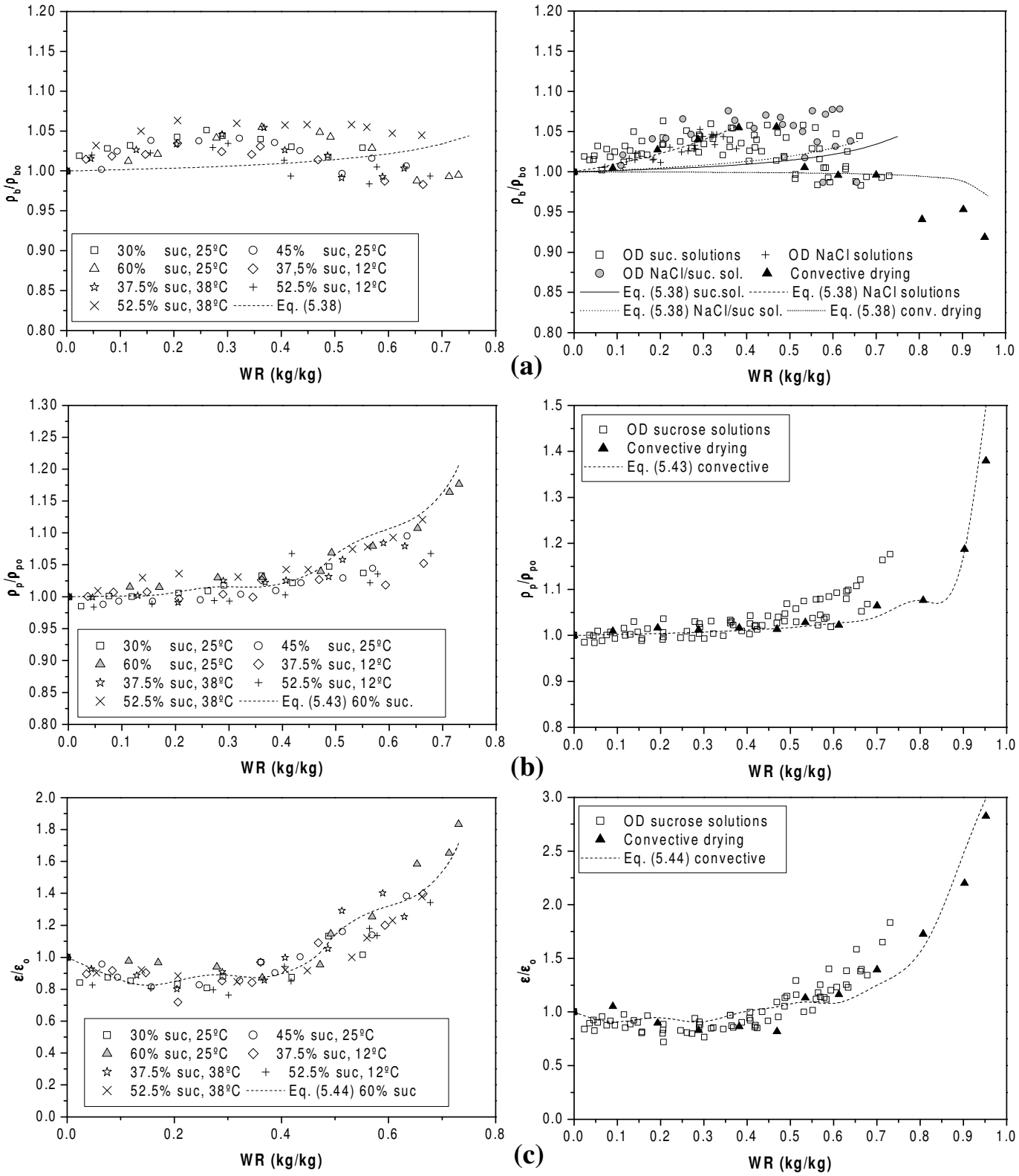

Figure 5.9. Changes in density and porosity during dehydration of pumpkin cylinders versus weight reduction: (a) bulk density (b) particle density and (c) porosity. Left figures correspond to osmotic dehydration with sucrose solutions, whereas figures on the right correspond to osmotic dehydration with different osmotic solutions and convective drying.

During convective drying of different fruits and vegetables, Lozano *et al*. (1983) and Krokida and Maroulis (1997) observed that the change in bulk density during the treatments was different for each food material tested. In some cases bulk density increases (banana, carrot), in other cases decreases (apple), and still in other cases initially increases, reach a maximum value and then decreases (sweet potato, garlic) (as happened with pumpkin in this work) along the dehydration process. This different behaviour could be associated with different physical-chemical characteristics of the raw material, such as chemical composition, initial porosity or the presence of soft/rigid structures, which can lead to different type of stresses when processing. It is reasonable to think that for osmotic dehydration the characteristics of the initial material also influence in the change in bulk density as observed for convective drying of vegetables. The type and amount of solid gained by the material is another important factor in the change of bulk density during osmotic dehydration.

Bulk density changes can be predicted by means of Eq. (5.38):

$$\frac{\rho_b}{\rho_{bo}} = \frac{1-WR}{V/V_o} = \frac{1-WR}{1-aWR} \tag{5.38}$$

where a is the regression coefficient obtained for Eq. (5.37) when shrinkage data and weight reduction are correlated. For each osmotic agent and for convective drying different linear equations, correlating shrinkage with weight reduction, were used. Average relative deviations between experimental and predicted density values were 2.4 % (Max.: 5.6%; Min.: 0%) for sucrose solutions; 1.3% (Max.: 4.8%; Min.: 0%) for NaCl solutions; 3.2% (Max.: 6.0%; Min.: 0%) for NaCl solutions and 2.9% (Max.: 6.1%; Min. 0%) for convective drying. Figure 5.9 (a) shows predicted values for bulk density for these different treatments.

Particle density (Fig. 5.9 (b)) during osmotic dehydration with sucrose solutions increases slowly at the beginning of the process, but near 50% of weight reduction the increase is more pronounced. No significant differences are observed among the process

conditions tested. Particle density increases as a result of the compositional change of the wet solid matrix during dehydration; initially the percentage of water is high, but during dehydration the percentage of more dense substances (sucrose, cellulose) increases leading to the increase of particle density. For convective dried samples, the behaviour is similar, but initially the increase of particle density is very low, and at 60% of weight reduction particle density values increase till attaining a value around 40% higher at the end of the process. During osmotic dehydration of apple with sugar solutions, a progressive increase of particle density along the process was observed (Nieto *et al.,* 2004). For convective dried vegetables, a slow increase of particle density was observed at the beginning of the process and after that the increase was more pronounced till the end of the process (Krokida and Maroulis, 1997).

An attempt to predict particle density during dehydration can be performed, if the composition of the material is known. Particle density, as defined in Eq. (5.4), is the ratio of sample mass to particle volume. The particle volume can be calculated from the masses and densities of each component in the material. For pumpkin parenchymatic tissue, fresh material is composed by water, insoluble solids, soluble solids and a gas phase. So the particle volume (without the gas phase) can be defined as

$$V_{po} = V_w + V_{is} + V_{ss} \tag{5.39}$$

in terms of masses of the components and densities, Eq. (5.39) can be rewritten as

$$V_{po} = \frac{m_w}{\rho_w} + \frac{m_{is}}{\rho_{is}} + \frac{m_{ss}}{\rho_{ss}} \tag{5.40}$$

For pumpkin osmodehydrated with sucrose and NaCl solutions, the particle volume changes not only by the water loss but also for the gain of sucrose and /or NaCl, so the particle volume of osmodehydrated pumpkin tissue can be defined as

$$V_p = V_w + V_{is} + V_{ss} + V_{suc} + V_{NaCl} \tag{5.41}$$

in terms of masses and densities

$$V_p = \frac{m_w}{\rho_w} + \frac{m_{is}}{\rho_{is}} + \frac{m_{ss}}{\rho_{ss}} + \frac{m_{suc}}{\rho_{suc}} + \frac{m_{NaCl}}{\rho_{NaCl}} \tag{5.42}$$

Lozano *et al.* (1980) considered the insoluble solids of apple tissue as cellulose. In this work the same assumption was considered. Soluble solids in pumpkin are mainly fructose and glucose in the same proportion, so an average value of the densities of fructose and glucose was taken as the density of initial soluble solids. Values of the different densities used in the calculations are shown in Table 5.14.

Table 5.14. Density values used in Eq. (5.40) and Eq. (5.42).

Component	Density (g/m^3)	Reference
Water	0.997 (25ºC)	Lide (2005)
Fructose	1.665	Lide (2005)
Glucose	1.562	Lide (2005)
NaCl	2.170	Lide (2005)
Sucrose	1.581	Lide (2005)
Cellulose	1.550	Lozano *et al.* (1980)

Figure 5.10 shows predicted values of particle volume for fresh and dehydrated pumpkin fruits with sucrose solutions and convective drying versus experimental data obtained with the gas pycnometer. This prediction is quite good, leading to a relative deviation of the predicted values of 2.63% on average.

Finally, normalized particle volume can be obtained by means of Eq. (5.43)

$$\frac{\rho_p}{\rho_{po}} = \frac{1 - WR}{V_p / V_{po}} \tag{5.43}$$

where V_{po} and V_p can be obtained with Eq. (5.40) and (5.42) respectively.

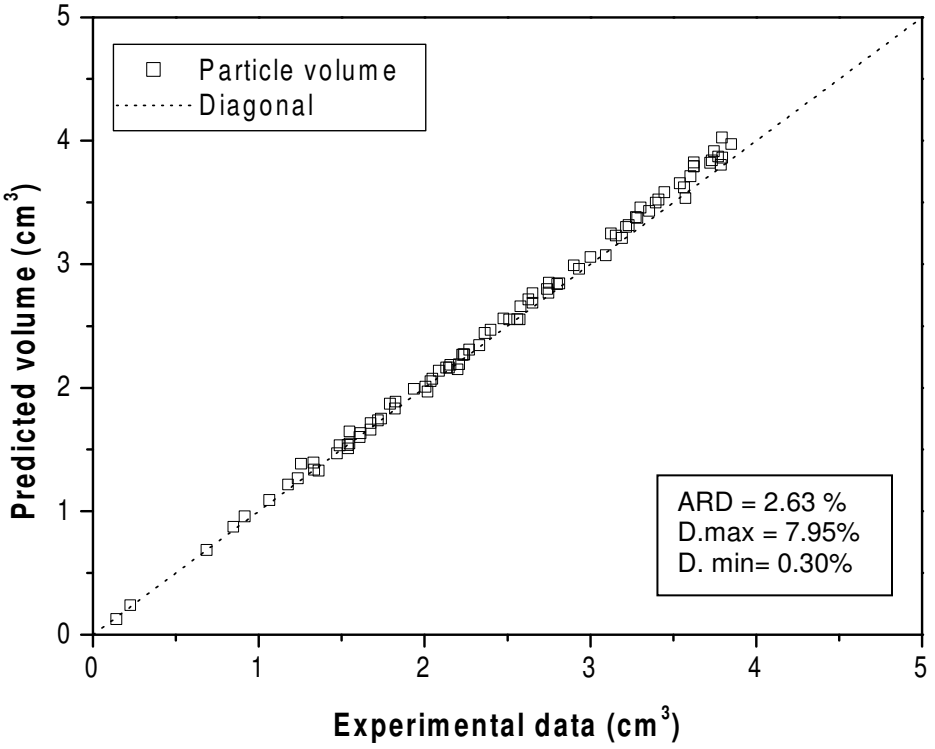

Figure 5.10. Experimental (gas pycnometer) data and predicted values (Eqs. (5.40) and (5.42)) of particle volume for fresh and dehydrated pumpkin with sucrose solutions and convective drying.

Average relative deviation between experimental data and predicted values obtained with Eq. (5.43) was 2.02%, proving that the model gives a good prediction of experimental data. Figure 5.9 (b) shows predicted values of reduced particle density for osmotic dehydration with 60% sucrose solutions at 25 ºC and convective drying at 70 ºC; as observed, the prediction is quite good.

Porosity of dehydrated pumpkin with sucrose solutions (Fig. 5.9 (c)) slightly decreases up to intermediate values of weight reduction (c.a. 0.4); after that point porosity increases until it doubles the value for the fresh material (with 60% sucrose solutions at 25ºC). No effect of the process conditions on porosity is observed when representing reduced porosity against weight reduction or water loss. For convective drying the behaviour is similar; at the beginning of the process porosity suffers fluctuations but at

weight reduction around 0.5 porosity starts to increase and at the end of the process almost triplicates ($\varepsilon/\varepsilon_o$ = 2.8, WR = 0.95) its initial value.

Mavroudis *et al*. (1998[b]) observed an increase of porosity of osmodehydrated apple at the end of the process. Giraldo *et al.* (2003) showed that in the osmotic dehydration of mango, porosity of dehydrated samples initially decreased and then after that increased during the process. The initial decrease of porosity in the sample can be associated with the fast initial impregnation of the tissue with the osmotic solution, with enters into the external pores of the material by capillary forces and other mass transfer mechanisms. After that, as commented in 3.3.1, the accumulation of sucrose in the external surface of the material creating a dense layer hinders the further penetration of the osmotic solution, and can difficult the exit of gas from the material to the solution, favouring the increase of porosity in the material.

Porosity change during convective drying of foodstuffs have different behaviour during processing, as shown by Lozano *et al*. (1983) and Krokida and Maroulis (1997); in some cases it decreases (sweet potato); in others it initially decreases and then increases (pear) and in still other cases it increases during the whole drying process (apple, banana). As commented for bulk density change, this different behaviour can be associated with the initial structural and compositional characteristics of the raw material, as well as the operating process conditions.

Figure 5.11 shows the relative volume changes of total volume, particle volume and air volume during osmotic dehydration of pumpkin with 60% sucrose solutions at 25 ºC and convective drying. Initially, in both treatments the three volumes decrease during dehydration. In this initial stage (0-0.5 WR) the relative decrease of air volume is higher than the other two volume decreases. The relative decrease of particle volume and total volume is the same with OD while with convective drying, total volume decreases more than particle volume. Air volume decreases more in convective drying up to 50% of weight reduction. At WR= 0.5, in OD the particle volume starts to decrease in percentage more than total volume, and air volume suffers fluctuations but practically remains constant until

the end of the process. In convective drying, around a weight reduction of 50% the volume of air phase remains constant till WR = 0.6, and then again decreases until the end of process; total volume decreases less than particle volume from 50% of weight reduction until the end of the process.

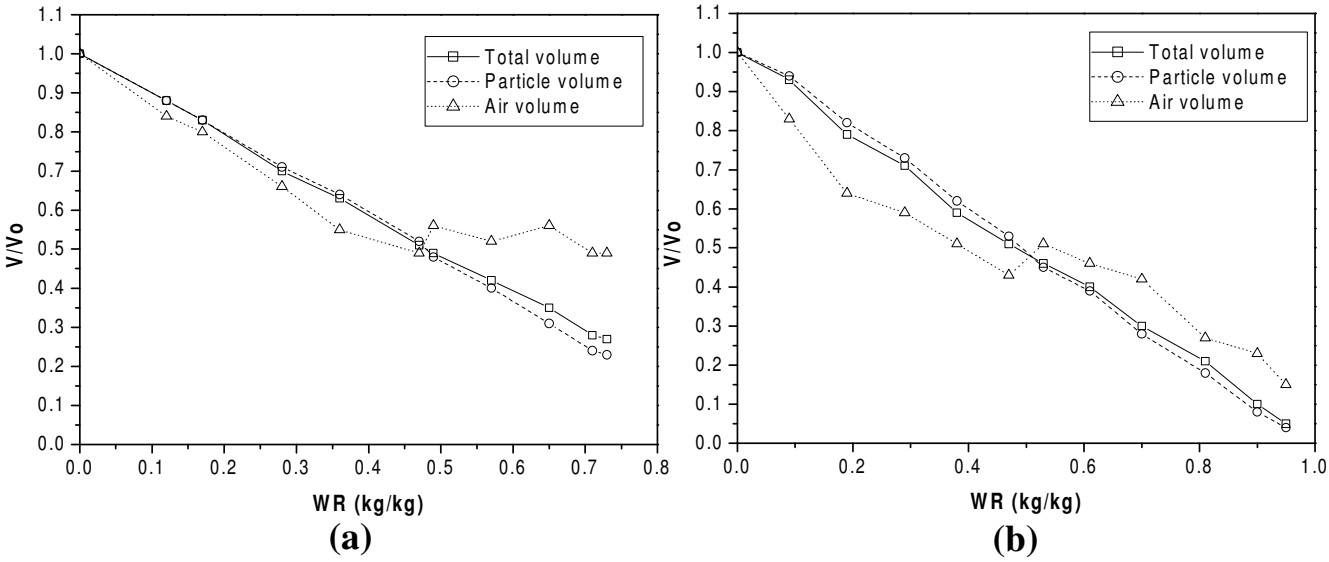

Figure 5.11. Relative volume changes for total volume, particle volume and air volume during dehydration of pumpkin cylinders in (a) 60% sucrose solutions at 25ºC and (b) convective drying at 70ºC.

It seems that the gas phase is better retained in the osmotic treatment than in convective drying; as commented before, the formation of a dense layer of osmotic agent in the surface of the material can be the cause of this phenomenon.

Porosity, defined as

$$\varepsilon = 1 - \frac{V_p}{V_T} \tag{5.44}$$

can be predicted obtaining V_p from Eqs. (5.40) and (5.42), and V_T with Eq. (5.37). Average relative deviation in the prediction of porosity values was 14.5%. Figure 5.9 (c) shows

experimental and predicted values of reduced porosity for osmotic dehydration of pumpkin with 60% sucrose solutions and convective drying.

5.2.3.3. Sample shape analysis.

Figure 5.12 shows the contour of cylinders dehydrated with sucrose solutions (60%, 25ºC), at different process times. It can be observed a constant decrease of area and dimensions during the process. The shape of the cylinders also changes during dehydration. Shrinkage is stronger at mid-length and mid-thickness of the cylinder, whereas at the edges shrinkage is less pronounced; this "corner effect" is clearly observed in the most dehydrated cylinder (Fig. 5.12. (f)). Del Valle *et al.* (1998[a]) also reported this effect during dehydration of apple cylinders, and Mulet *et al.* (2000) during convective drying of potato cubes.

Due to the irregularities of the diameter and length observed in the cylinders during processing, an average value was obtained measuring these linear dimensions in five different parts of the sample. As observed in Figure 5.13, no significant differences were found in the decrease of length and diameter during the process, so it can be said that shrinkage is isotropic. Trujillo *et al.* (2007) found similar results during the convective drying of beef meat discs (L/D ≈0.25).

However, Mulet *et al.* (2000) showed an anisotropic shrinkage in the convective drying of potato (L/D ≈ 4.6) and cauliflower stem (L/D ≈ 1.7) cylinders, observing a higher decrease of the diameter than that observed in the length at the same moisture content for both products. In the case of potato cylinders, the authors suggested that the high L/D ratio favoured the formation of an inner core along the axis length maintaining the shape along this axis. In the case of cauliflower stems, where the decrease of the diameter was much more pronounced than the decrease of the length, the presence of oriented fibres made the product stiffer in a preferential orientation and the shrinkage was less than radial.

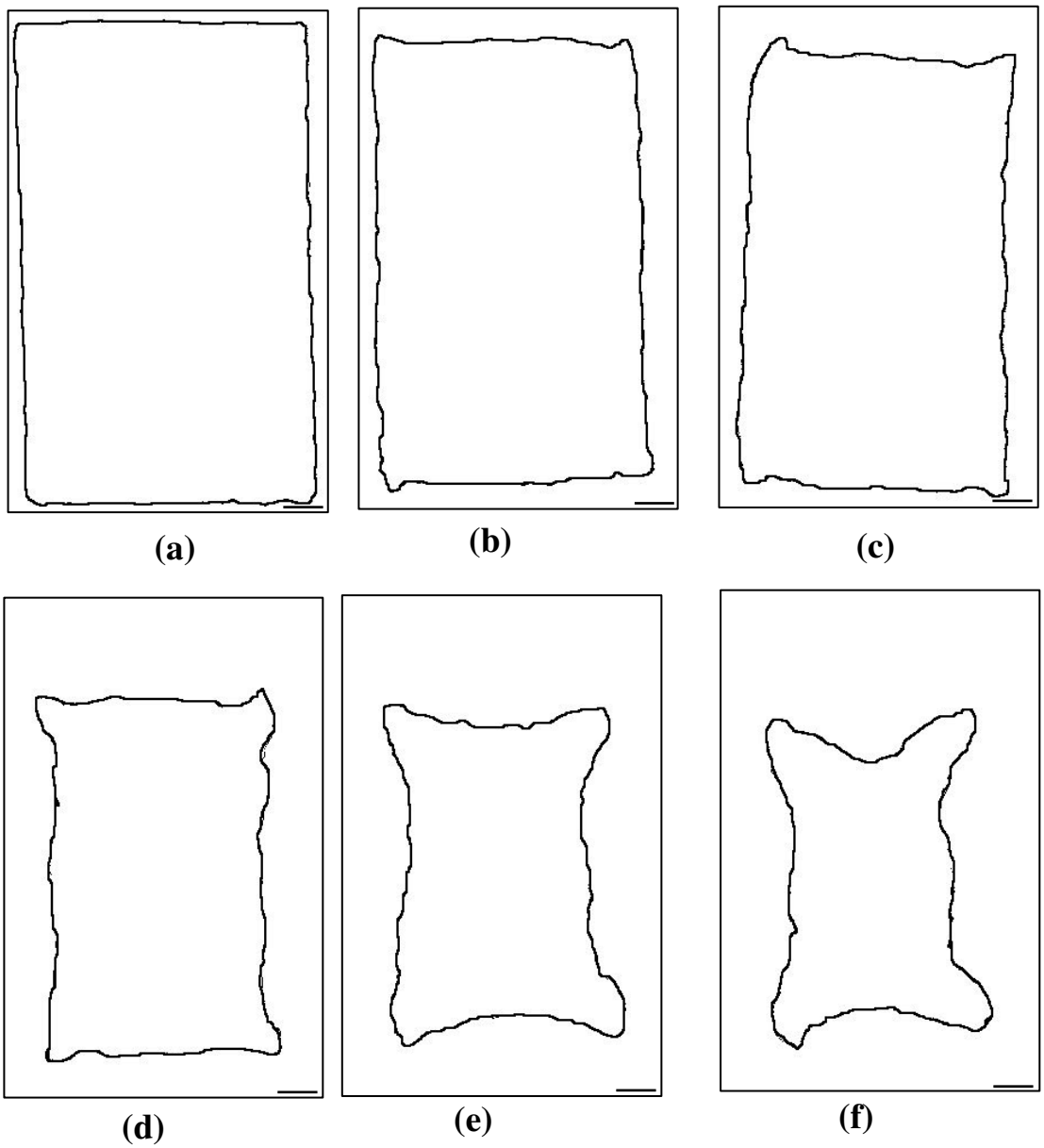

Figure 5.12. Changes in shape and dimensions during osmotic dehydration of pumpkin cylinders in 60% sucrose solutions at 25ºC, at different process times. (a) Fresh material. (b) 0.5 h. (c) 1 h. (d) 3 h. (e) 6 h. (f) 9 h. The horizontal line at the bottom right of each image corresponds to 2mm length.

Based on those results, it can be concluded that two important factors can affect the shrinkage isotropicity: the existence of preferential pathways of mass transfer (due to geometric and structural features) and the homogeneity of the structure of the material (due to structural features).

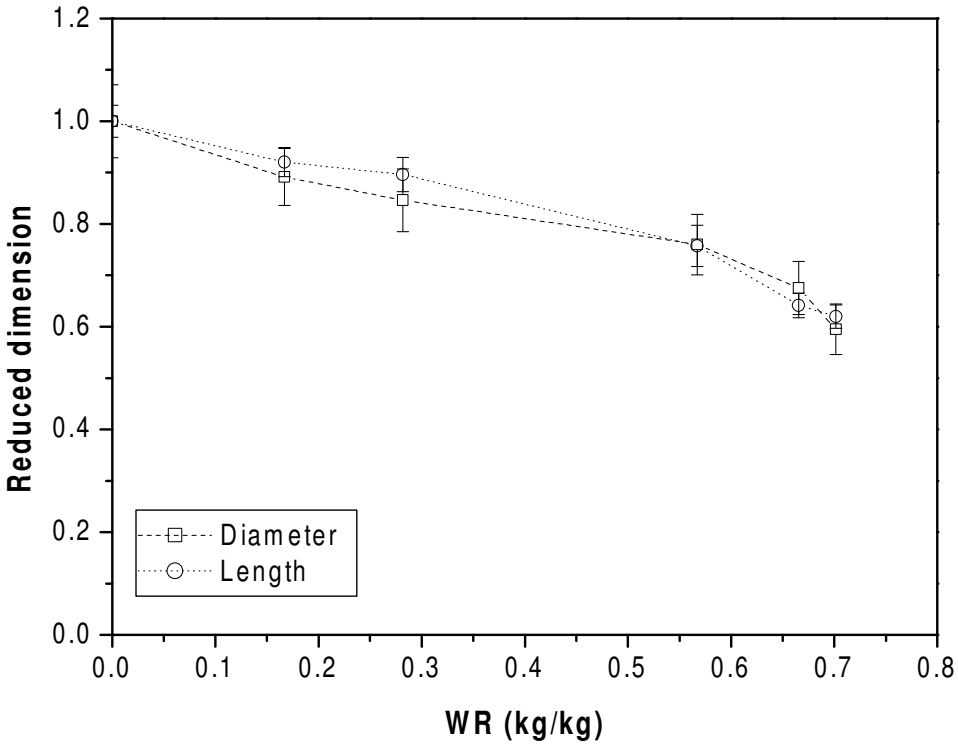

Figure 5.13. Relative changes in dimensions of osmodehydrated pumpkin cylinders (60% sucrose, 25°C) versus weight reduction.

Figure 5.14 shows the relative changes in the shape factors studied as a function of weight reduction. The average initial values of the shape factors were 1.657, 0.670 and 0.749 for elongation, roundness and compactness respectively. If elongation is equal to 1, the object is a circle or square, if the value increases the object becomes more elongated. Roughness and compactness give an idea of the circularity of the object. Both shape factors range from 0 to 1; when the value is one, the object is a perfect circle, when their value decreases from one the object becomes less circular and less round.

As can be observed, elongation slightly increases, whereas roundness and compactness decrease during dehydration. It is often reported a decrease of roundness during dehydration of foods, as in the case of convective drying of apple discs (Mayor *et al*., 2005; Fernandez et *al.* 2005) or apricot cubes (Riva *et al*. 2005).

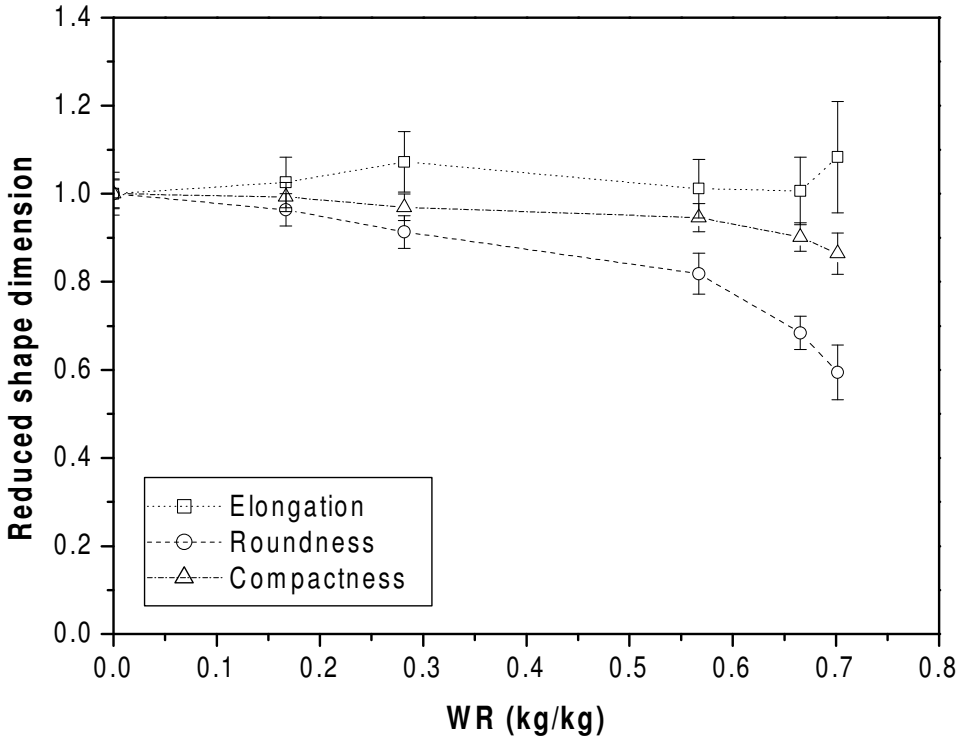

Figure 5.14. Changes in shape factors during osmotic dehydration (60% sucrose, 25ºC) of pumpkin cylinders versus weight reduction.

The tissue suffers deformations as a consequence of the water removed in the material; in this way roundness and compactness decrease during dehydration. The increase in the elongation is mainly due to the "corner effect" observed during the treatment, reducing the value of the minor axis length (minimum value of the diameter of the cylinder) but maintaining the value of the major axis length (distance between two opposite corners of the cylinder).

5.2.4. Conclusions.

Shrinkage of samples due to dehydration was observed with all processing methods studied. This is a very important effect on dehydration, which may be both desired and undesired according with the type of product and its further use.

Shrinkage of pumpkin during osmotic dehydration ranged form 0 to 73% of the initial volume of the samples, depending on the process condition used. For convective drying, shrinkage at the end of the treatment reached 95% of the initial volume. Independently of the process conditions (concentration and temperature of the osmotic solution), shrinkage of samples decreased linearly with the water loss and the weight reduction during processing. Linear equations relating change of volume vs. water loss and weight reduction were obtained with a good fit. For convective drying the same behaviours were observed, but the decrease of shrinkage versus water loss was more accentuated. A general equation correlating shrinkage versus weight reduction was obtained for both osmotic dehydration and convective drying at any process condition, with an excellent fit.

Bulk density did not change considerably during dehydration; differences between maximum and minimum values were around 5% for osmotic dehydration with binary sucrose and NaCl solutions, 10% for ternary NaCl/sucrose solutions and 13% for convective drying. For all the dehydration treatments, bulk density initially increases in the samples, then reaches a maximum value and after that decreases or fluctuates till the end of the process. Predicted values of bulk density were obtained by means of an equation relating weight reduction of samples and shrinkage with bulk density. Average relative deviations of the predicted values were always lower than 3.2% for all the treatments, proving the adequacy of the model.

For all the treatments, particle density increases slowly at the beginning of the process, and at certain weight reduction (50% for osmotic dehydration with sucrose solutions and 60% for convective drying) the increase is more pronounced, attaining at the end of process an increase of 20% and 40% of the initial value for osmotic dehydration (60% sucrose, 25ºC) and convective drying respectively. Particle density was predicted

from weight reduction and particle volumes predicted from the chemical composition of the material. Average relative deviation between experimental and predicted values was 2%, proving that the model was adequate.

The change in porosity also followed the same behaviour during osmotic dehydration and convective drying. Initially porosity decreases up to a point (WR = 0.4 for OD and 0.5 for convective drying) where porosity starts to increase till the end of the treatment, duplicating the initial value in the case of osmotic dehydration with sucrose solutions and almost triplicating the initial value for convective drying. Average relative deviation of predicted porosity values was 14.5%.

A similar relative decrease of the average values of the diameter and length of the samples along the dehydration process was observed, suggesting that shrinkage was isotropic.

As a consequence of the deformations suffered by the cylinders during dehydration, elongation increased and roundness and compactness decreases after processing.

CHAPTER 6

COLOUR CHANGES DURING OSMOTIC DEHYDRATION OF PUMPKIN FRUITS

CHAPTER 6. COLOUR CHANGES DURING OSMOTIC DEHYDRATION OF PUMPKIN FRUITS

6.1. Introduction

This chapter shows experimental data on colour changes during osmotic dehydration of pumpkin fruits. In order to compare the results with those obtained in other mass transfer processes, experimental data on colour changes during water soaking and convective drying of pumpkin fruits were also studied. Enzymatic browning in contact with air was also observed and compared with apple enzymatic browning. Some models were used so as to obtain predicted values of colour changes during osmotic dehydration.

6.2. Materials and methods

6.2.1. Sample preparation

The procedure explained in 3.2.1 was used in the preparation of samples for the different processes, but in this case discs (diameter 30 mm, height 9 mm) were employed instead of cylinders. The dimensions of the discs were chosen in order to have the same surface area/volume ratio (A/V = 0.35) as the cylinders used in Chapter 3.

6.2.2. Sample processing

Osmotic dehydration of pumpkin was performed in sucrose solutions, with the process conditions (concentration and temperature) showed in Chapter 3, Table 3.1. At different process times (0, 0.5, 1, 3, 6 and 9 hours) seven samples were removed from the osmotic solutions, blotted with paper to remove the excess of adhering osmotic solution, and kept in plastic boxes till experimental determinations.

Convective drying was carried out in an oven at 70ºC, under natural convection. The samples were put in plastic wire nets allowing heat and mass transfer from the whole external surface of the discs, and then they were introduced in the oven. Seven samples were removed from the oven at 0.5, 1, 3, 6 and 8 hours, and kept in plastic boxes till experimental determinations.

Soaking of pumpkin discs in water was performed with the same experimental procedure and equipment as commented in 3.2.3, but in this case distilled water was used instead of an osmotic solution. Temperature of the process was 25 ºC. Seven samples were removed from the soaking medium at 0.25, 0.8, 1.5, 3, 6 and 9 hours for the experimental determinations.

Samples of pumpkin and apple (*Golden Delicious*) with the same shape and dimensions as the other experiments were used to observe the enzymatic browning in contact with air. The colour and water loss of samples was determined immediately after the preparation of samples and after nine hours in the laboratory bench.

Two runs were performed for each process.

6.2.3. Experimental determinations

CIE L*a*b* colour coordinates were measured with a tristimulus reflectance colorimeter (Fig. 6.1) (MINOLTA CR-300, Radiometric Instrument Operations, Osaka, Japan) where L* value is a measure of lightness, a* is a measure of redness (-a* greenness) and b* of yellowness (-b* blueness).

Before measurements, the colorimeter was calibrated with a white ceramic plate. Three measurements were taken on surface of the disc, and the parameters L*, a*, and b* were obtained. The average values of these parameters were obtained from the three measurements.

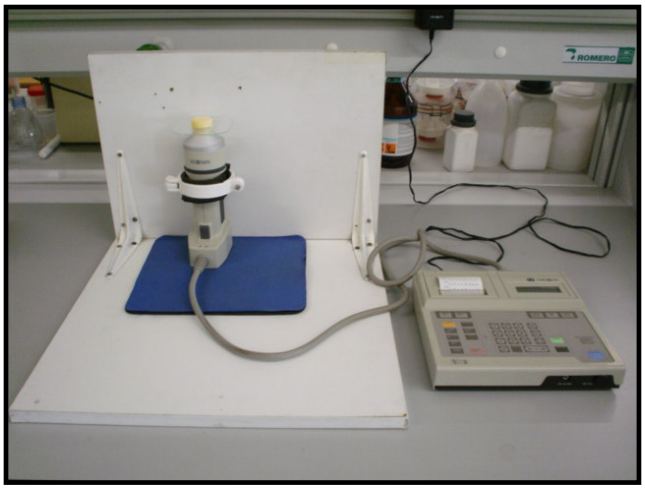

Figure. 6.1. Reflectance colorimeter.

From the L*, a* and b* values it was possible calculate the psychometric coordinates hue (h*) and croma (C*) by means of the Eqs. (6.1) and (6.2) respectively

$$h^* = arctg\frac{b^*}{a^*} \tag{6.1}$$

$$C^* = \sqrt{a^{*2} + b^{*2}} \tag{6.2}$$

Likewise, the total colour differences ΔE between fresh and processed material can be calculated by means of the Eq. (6.3)

$$\Delta E = \sqrt{(\Delta a^*)^2 + (\Delta b^*)^2 + (\Delta L^*)^2} \tag{6.3}$$

Kinetic parameters WR, WL, SG and NMC were determined as explained in 3.2.4.

6.3. Results and discussion

6.3.1. Fresh material

Pumpkin flesh showed a yellow to orange homogeneous colour. This colour has been associated to a complex making-up of carotenoids, such as alpha-carotene, beta-carotene and monohydroxy and polyhydroxy carotenoids (Francis and Clydesdale, 1975).

Table 6.1 shows the average values of the studied colour parameters. As can be observed, variation coefficients are mainly due to the differences in colour among the fruits used in the experiments, since the colour in each pumpkin is pretty homogeneous, showing variation coefficients within fruits lower than those observed for the total of samples.

Table 6.1 Colour characteristics of fresh pumpkin fruits.

parameter	average	interval	v.c. (%)	v.c., within fruits (%)
L*	75.43	[69.43-83.58]	4.27	[0.38-2.76]
a*	5.04	[0.69-8.65]	47.58	[2.52-23.97]
b*	32.06	[25.79-36.90]	10.15	[1.07-6.86]
hue	1.41	[1.34-1.55]	4.32	[0.18-1.59]
croma	32.53	[26.50-37.74]	10.58	[1.10-6.67]

The colour differences among fresh fruits can be associated to the different degree of ripeness attained in each fruit.

Each run was performed with samples taken from the same fruit; since the colour within a single fruit is essentially homogeneous it is expected a minimum influence of the natural colour variability of the fresh material on the changes observed during processing. In order to minimize the effect of the colour variation initially observed among fruits, the

increment of each colour parameter was used in the presentation of the results instead of the absolute value.

6.3.2. Enzymatic browning of pumpkin and apple in contact with air

After nine hours in contact with air at room temperature, pumpkin samples didn't show change in their visual aspect, only a slight shrinkage due to water loss (17% of the initial weight). Figure 6.2 shows the changes in colour parameters after maintaining the samples in the laboratory bench nine hours. It can be observed that the changes in the colour parameters for pumpkin are very small, only L* and ΔE present some change, whereas the other parameters practically are maintained constant; these changes may be due to the slight water loss due to evaporation.

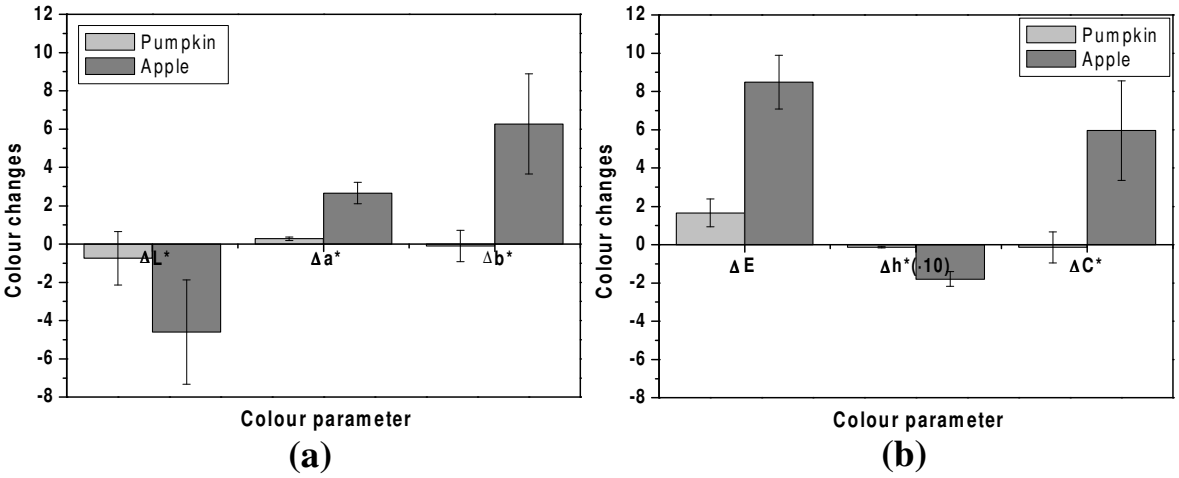

Figure 6.2. Changes in colour parameters for pumpkin and apple tissue in contact with air: (a) L*, a* and b* changes; (b) ΔE, h* and C* changes.

Apple samples after nine hours in contact with air at room temperature (WL = 17%) looked darker and presented some brown areas, a typical aspect of vegetables suffering enzymatic browning. Enzymatic browning of apples is widely reported in the literature (Lozano *et al*., 1994; Monsalve-Gonzalez *et al.,* 1995). Figure 6.2 shows the changes in

colour parameters for apple: lightness and hue decrease, whereas a*, b*, ΔE and C* increase.

Since no significant changes in colour were observed in pumpkin fruits after nine hours in contact with air, it was concluded that enzymatic browning in pumpkin parenchymatic tissue is not produced.

6.3.3. Water soaking

After soaking pumpkin samples in distilled water for nine hours, the samples gained water amounting to 14 % of their initial weight (WL = -14), to a normalized moisture content of 1.005. The water gain is in the same magnitude as the water loss observed in pumpkin left in air nine hours but (WL = 17%).

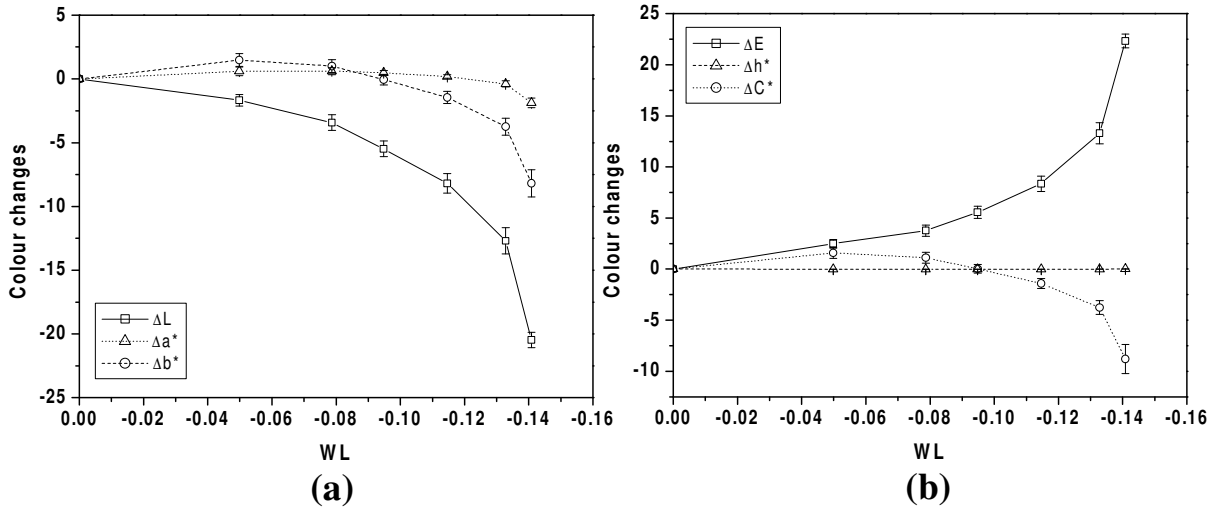

Figure 6.3. Changes in colour parameters for water soaked pumpkin: (a) L*, a* and b* changes; (b) ΔE, h* and C* changes.

Figure 6.3 shows the colour changes during water soaking of pumpkin samples. It can be observed a decrease in L*, a*, b* and C*, hue does not show important changes (Δh*= 0.02 at the end of the process) whereas the total colour changes (ΔE) increase during

the process. It would be expected similar (but opposite) changes in colour compared with samples left in air, since the change of water content is similar but opposite. However the colour changes in water soaked samples was much more pronounced.

Since enzymatic browning is expected to be negligible, the changes in colour may be attributed to changes in the concentration of pigments (more diluted due to the water gain) and changes in the structure of the material. The dilution effect can explain the decrease in a*, b* and croma values, whereas hue is basically unchanged. The important decrease in lightness is likely related with the changes in the structure of the pumpkin tissue, since no chemical degradations are expected and the dilution effect is moderate. The main change observed during water soaking is the filling of air pores by water, decreasing the porosity and air phase of the product. This change in porosity can lead to change in the light reflection characteristics of the material, producing in this case a decrease in the lightness of the samples.

6.3.4. Convective drying

After eight hours of convective drying at 70 ºC, the samples lost water 74% of the initial weight, and the normalized moisture content was 0.136.

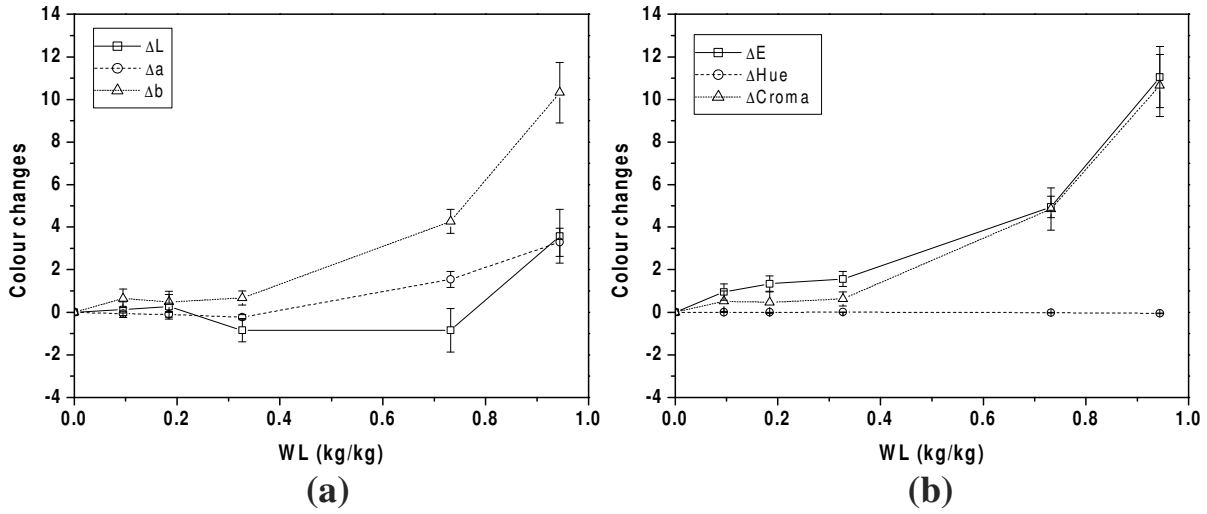

Figure 6.4. Changes in colour parameters for convective dried pumpkin: (a) L*, a* and b* changes; (b) ΔE, h* and C* changes.

Figure 6.4 shows the changes in colour during convective drying of pumpkin discs. Lightness increases with the decrease of moisture content in the samples, whereas a* and b* suffer fluctuations during the process and at the end increase. Hue values show a slight decrease ($\Delta h^* = -0.05$ at the end of the process) whereas total colour change and croma values increase along the process. The increase of a* and b* values during convective drying have been observed in different vegetables (Krokida *et al*., 1988). Changes in colour during convective drying have been associated to non-enzymatic browning (Krokida *et al*., 2000[e]), pigment concentration and changes in the internal structure of the vegetable tissue (Lewicki and Duszczyk, 1998).

6.3.5. Osmotic dehydration

As an example of the colour changes during an osmotic process, Figure 6.5 shows the colour changes during osmotic dehydration of pumpkin with 60% sucrose solutions at 25 ºC. The changes in colour are not very pronounced, showing total colour changes lower than those observed in water soaking and in convective drying.

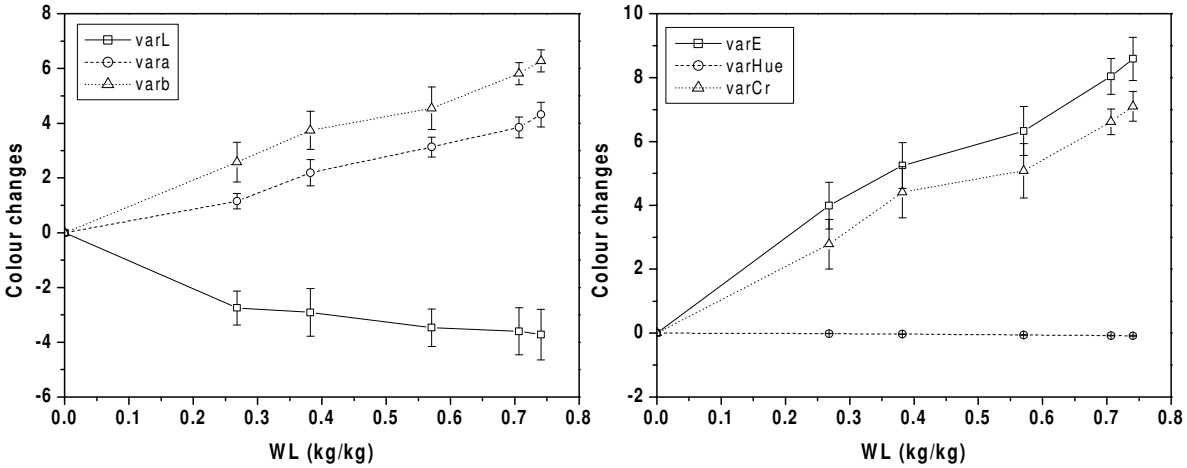

Figure 6.5. Changes in colour parameters for osmotically dehydrated pumpkin with 60% sucrose solutions at 25 ºC: (a) L*, a* and b* changes; (b) ΔE, h* and C* changes.

It is observed an increase in a* and b* values, probably due to the concentration of the pigments in the tissue during the osmotic process. Lightness decreases along the process; this behaviour is also observed in the water soaked samples and can be also attributed to the changes in the structure and opacity of the samples due to the impregnation of the pores in the tissue with the osmotic solution, mainly in the external surface. Hue variation is not very pronounced (Δh^*=-0.09 at the end of the process). Croma increases as a consequence of the pigment concentration, as in the case of convective dried pumpkin.

As commented in Chapter 1, colour changes during osmotic dehydration of fruits and vegetables are moderate, due to the low temperatures used and the intermediate moisture contents attained. These changes can be higher when enzymatic reactions occur during the process.

It is often observed a decrease in lightness during osmotic processes. In some cases this change is partially explained by enzymatic browning occurring during dehydration, as in the case of osmotic dehydration of banana with sucrose solutions (Waliszewski *et al*, 1999); the addition of chitin or EDTA in the osmotic solution reduced the enzymatic activity and the decrease in lightness (Waliszewski *et al*, 2002[ab]). In other cases, such as osmotic dehydration of cactus pear fruits (Moreno-Castillo *et al*., 2005) and apricots (Riva *et al*., 2005), is not so clear the relation of lightness decrease and enzymatic browning. As observed in this work, lightness also decreases without enzymatic activity, and it can be attributed to changes in the light reflection characteristics of the material due to structural changes.

The changes in a* and b* parameters during osmotic dehydration do not show a clear trend. In the two aforementioned works for cactus pear fruit and apricot osmotic dehydration the changes in a* and b* values did not show a clear tendency and the colour changes were mainly due to change in lightness during the processes. The results of our work show an increase of both colour coordinates, likely due to the pigment concentration during dehydration. Figure 6.6 shows the change in croma versus the water loss in pumpkin discs, after the different studied processes.

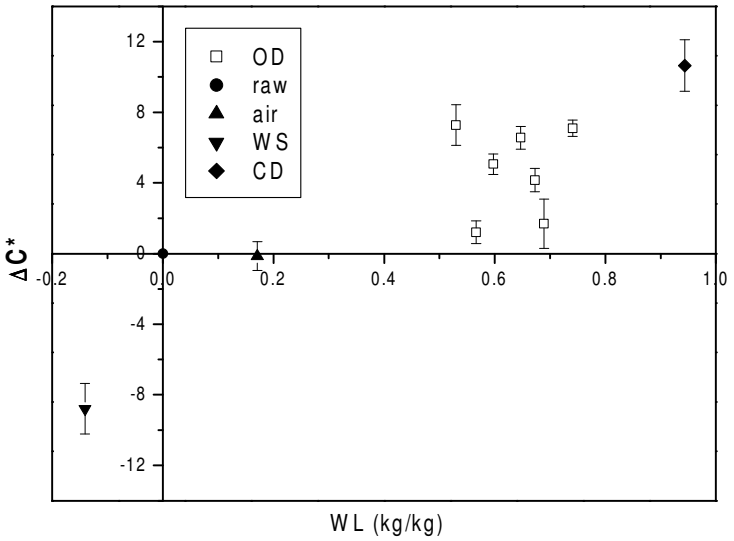

Figure 6.6. Croma changes versus water loss after the different studied processes: OD: osmotic dehydration. Raw: fresh material. Air: left in air nine hours. WS: water soaked. CD: convective dried.

It can be observed that croma, which is a measurement of the colour intensity, increases linearly with the water loss independently of the type of process. This result suggests a strong relationship between water loss and colour intensity, likely due to pigment concentration.

All the process condition tested during osmotic dehydration show the same behaviour of the colour parameters versus water loss commented before (Fig. 6.5), but no effect of concentration and temperature of the osmotic solution on the extension of these changes were observed. Table 6.2 shows the values of the colour parameters at the end of the process for the different process conditions tested. For all the colour parameters, the values obtained at different process conditions are similar and no trend with concentration of the solution and temperature is observed. It can be said that, as an average, $\Delta L^* = -4.84$,

Δa*= 2.80, Δb*= 4.25, ΔE = 7.39, Δh*= -0.06 and ΔC*= 4.72 after osmotic dehydration of pumpkin with sucrose solutions.

Table 6.2. Colour variation after osmotic treatments (nine hours) with sucrose solutions at different concentration (% w/w) and temperature (ºC).

C	T	ΔL*	Δa*	Δb*	ΔE	Δh*	ΔC*
30	**25**	-5.53±0.93	3.09±0.44	7.06±1.04	9.91±0.91	-0.06±0.01	7.27±1.16
45	**25**	-3.33±0.62	2.94±0.38	5.49±0.81	6.70±0.87	-0.05±0.01	6.56±0.64
60	**25**	-3.72±0.92	4.32±0.45	6.28±0.40	8.59±0.68	-0.09±0.01	7.10±0.47
37.5	**12**	-5.52±0.92	1.72±0.36	0.99±0.60	5.89±0.87	-0.05±0.01	1.20±0.65
37.5	**38**	-7.39±1.17	2.11±0.56	4.81±0.77	9.02±0.70	-0.03±0.01	5.07±0.57
52.5	**12**	-3.50±0.95	3.44±0.66	3.51±0.54	6.16±0.57	-0.08±0.01	4.16±0.66
52.5	**38**	-4.86±1.21	1.96±0.58	1.59±1.42	5.48±1.40	-0.04±0.01	1.69±1.39
Average		-4.84±0.96	2.80±0.49	4.25±0.80	7.39±0.86	-0.06±0.01	4.72±0.79

Table 6.3. Correlation matrix (r values) for the linear relationship between colour change and the dehydration kinetics parameters.

variable	ΔL*	Δa*	Δb*	ΔE	Δh*	ΔC*
SG	-0.66	0.76	0.65	0.75	-0.75	0.66
WL	-0.66	0.88	0.75	0.81	-0.88	0.77
NMC	0.57	-0.83	-0.68	-0.72	0.83	-0.69
WR	-0.64	0.89	0.76	0.82	0.90	0.79

As can be observed in Table 6.3, some relationships between colour changes and dehydration parameters can be established. As expected, Δa*, Δb*, ΔE and ΔC* increase with the increase in water loss and the decrease in moisture content, and ΔL* and Δh* decreases with the increase in water loss and the decrease in moisture content. However, the relations are not enough strong (maximum r attained 0.90, corresponding to R^2= 0.81) to use linear models for predictive purposes. The increase of the degree in the polynomials did not show improvements in the correlation coefficients.

Zero order and first order kinetic equations were not found to be adequate for modelling purposes. However, fractional conversion models were found to be adequate in the modelling of some colour parameters during osmotic dehydration. These kind of models are often used for modelling colour changes in food processing (Avila and Silva, 1999; Weemaes *et al*., 1999), and are equations of the form

$$\frac{Y - Y_e}{Y_o - Y_e} = \exp(-kt) \qquad (6.4)$$

where:

Y is the colour parameter

Y_o and Y_e are the corresponding initial and equilibrium values

k is the colour change rate constant (h^{-1}) for each colour parameter

t is the dehydration time (h)

Table 6.4. Fit results for the fractional conversion model.

parameter	k (h^{-1})	R^2	ARD (%)
L*	0.38	0.18	1.68
a*	0.39	0.87	6.96
b*	0.43	0.79	2.91
ΔE*	0.44	0.64	24.95
h*	0.42	0.78	0.70
C*	0.412	0.84	2.94

Experimental data were fitted to Eq. (6.4) and the rate constant for each colour parameter was obtained. Since no dependence of the equilibrium values of the colour parameters was observed on concentration and temperature of the osmotic solution, an average value of all the process conditions (see Table 6.2) was used to obtain predicted values.

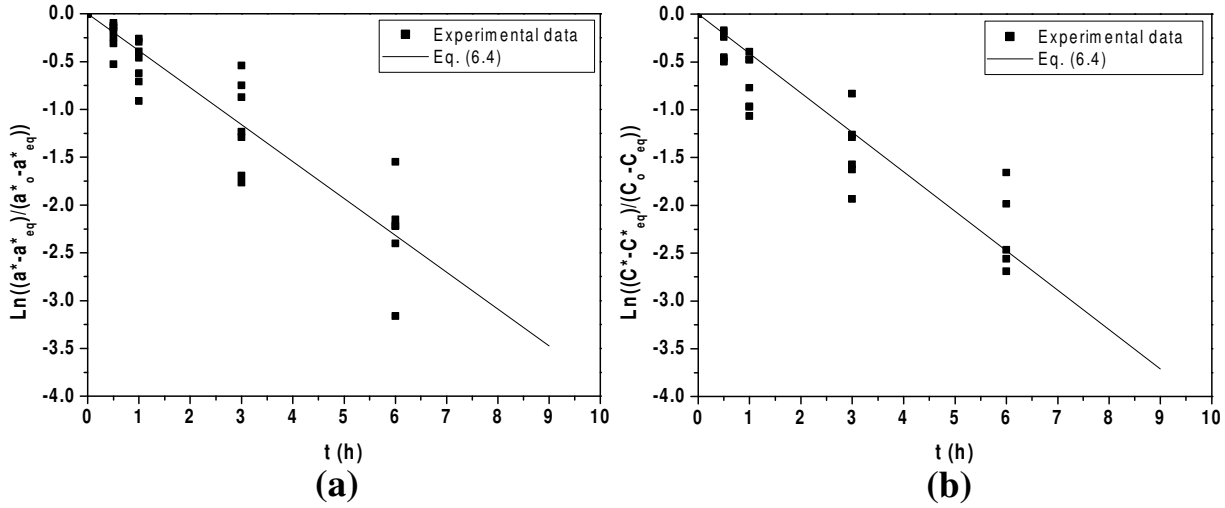

Figure 6.7. Logarithmic plot of the first term of Eq. (6.4) versus time and fit results for (a) a* and (b) croma.

Observing R^2 values and average relative deviations, the fit for a*, b*, hue and croma was acceptable, whereas in the other colour parameters the fit was not so satisfactory. Figure 6.7 shows the experimental data and fit results for a* and croma.

Predicted values for a*, b*, hue and croma can be obtained from those of the fresh material, the equilibrium value (Table 6.2), the colour change rate constant of the corresponding colour parameter and process time. As observed in Table 6.4, relative deviation between experimental and predicted values was always lower than 7% for these colour parameters, showing that in spite of the low values of R^2 obtained in the fits they can be considered acceptable.

6.4. Conclusions

Pumpkin fruits show a yellow to orange homogeneous colour. The colour differences among fruits can be associated to the different degree of ripeness attained in each fruit.

Enzymatic browning was not observed in pumpkin samples in contact with air. Due to the low availability of air in the osmotic processes, it can be said that enzymatic browning of pumpkin during osmotic dehydration is not presented.

Water soaking decreases L*, a*, b* and C* values, whereas convective drying increases L*, a*, b* and C* values. Accordingly, the change in lightness seems to be associated to changes in the internal structure (i.e. porosity) of the material during processing, changing the opacity and the light reflection characteristics. The changes in a*, b* and C* parameters are likely related to changes in the pigment concentration. Water soaking showed higher colour changes than those observed during convective drying, mainly due to the change in lightness.

The changes in colour observed during osmotic dehydration were lower than those observed in water soaking and convective drying. Osmotic dehydration decreases lightness and increases a*, b* and C* values after processing. The formation of a dense layer of osmotic agent in the surface of the material can be the cause of the decrease in lightness, whereas the increase in the concentration of pigments (as in convective drying) due to water removal may be the cause of the increase of a*, b* and C* parameters.

They were observed correlations between colour changes and kinetic parameters (WL, SG, NMC, and WR) but not enough good for predictive purposes. Fractional conversion models showed acceptable correlations of the changes in colour during osmotic dehydration for a*, b*, hue and croma.

CHAPTER 7

MECHANICAL PROPERTIES CHANGES DURING OSMOTIC DEHYDRATION OF PUMPKIN FRUITS

CHAPTER 7. MECHANICAL PROPERTIES CHANGES DURING OSMOTIC DEHYDRATION OF PUMPKIN FRUITS

7.1. Introduction

The aim of this part of the work was to study the changes in the mechanical properties of pumpkin subjected to osmotic dehydration. For comparison purposes, mechanical properties of pumpkin soaked in water (as an "opposite" process to dehydration) were also studied. The relations between the structure of the vegetable tissue and the mechanical properties were studied by microscopic observation of fresh and processed samples before and during the compression tests.

7.2. Materials and methods

7.2.1. Preparation of samples

The procedure explained in 3.2.1 was used in the preparation of samples for the different processes.

7.2.2. Processes

Samples were processed by osmotic dehydration in binary sucrose/water solutions. Process conditions, selected to cover a range of temperature (10-40ºC) and sucrose concentration (30-60% w/w sucrose) are described in Table 3.1. Experimental set-up and dehydration procedure are described in 3.2.3. Two runs were performed for each process condition.

Soaking of pumpkin cylinders was performed in distilled water at 25ºC, in the same stirred vessels as those used for the osmotic treatments. Two runs were also performed for water soaked cylinders.

7.2.3. Experimental determinations

7.2.3.1. Compositional analysis

At different process times (0, 0.5, 1, 3, 6 and 9 hours), four cylinders were removed from the processing vessel, blotted with paper tissue and analyzed for weight reduction (WR), solids gain (SG), water loss (WL) and normalized moisture content (NMC), as described in 3.2.4.

7.2.3.2. Texture measurements

At different process times (0, 0.5, 1, 3, 6 and 9 hours for osmotic dehydration and 9 hours for water soaking), 15-20 cylinders were removed from the stirred vessels and used for textural measurements. Cylinders of 15 mm length were gently cut from the initial (fresh or processed) ones, removing the top and bottom using a razor blade, as described in Figure 7.1 (b). The diameter of the resulted cylinder was measured with a calliper. These cylinders were used in compression tests.

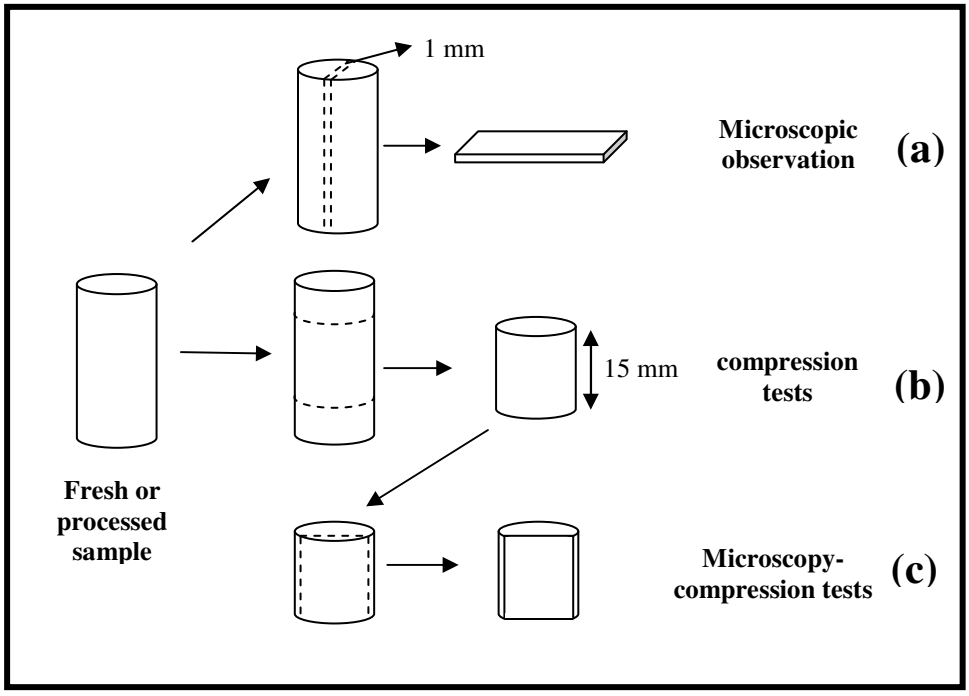

Figure 7.1. Preparation of samples for different experimental determinations: (a) microscopic observation, (b) compression tests, and (c) simultaneous microscopic observation-compression tests.

Uniaxial compression was performed in a TA.XT2 texture analyzer (Texture Technologies Corp., USA), with a flat-end cylindrical probe (35 mm. diameter). The probe was lubricated to avoid the effects of the plate-sample friction during compression. Compression tests were done at 0.5 mm s^{-1} deformation rate until 90 % of sample deformation. From the force-deformation data at each deformation time, it was possible to calculate Hencky strain (Eq. (7.1)) and true stress (Eq. (7.2)) (Calzada and Peleg, 1978)

$$\varepsilon = \int_{L}^{L_o} \frac{dL}{L} = Ln\frac{L_o}{L} \tag{7.1}$$

$$\sigma = \frac{\mathrm{F}}{\mathrm{A(t)}} \tag{7.2}$$

where L and L_o are the height of the cylinder at a time of compression t and t=0, respectively, F is the compression force and A(t) is the contact area of compression at a time t. Contact area at each time was obtained from the measured diameter of the cylinder before compression and the height at each time, assuming constancy of sample volume during compression.

Apparent modulus of elasticity (E_{ap}) was calculated from the slope of the initial linear zone (values of strain less than 0.15) of the stress-strain curve. Stress-strain curves show in practice an initiating effect resulting from a non-ideal flat surface of samples, due to the manual incision. Because of this, E_{ap} was taken from the slope of the curve after this initiating effect (Keetels *et al.*, 1996). Failure stress (σ_F) and failure strain (ε_F) were determined from the first peak of the stress-strain curve. The work at rupture or toughness, defined as the energy absorbed by the material up to the rupture point per unit of volume of the cylinder, was obtained from the area of the stress-strain curve till the rupture point

$$W = \int_{\varepsilon_o}^{\varepsilon_F} \sigma \cdot \varepsilon \cdot d\varepsilon \tag{7.3}$$

Figure 7.2 shows a typical compression curve for a vegetable product, where the mentioned mechanical parameters are indicated. Toughness corresponds to the grey area under the curve.

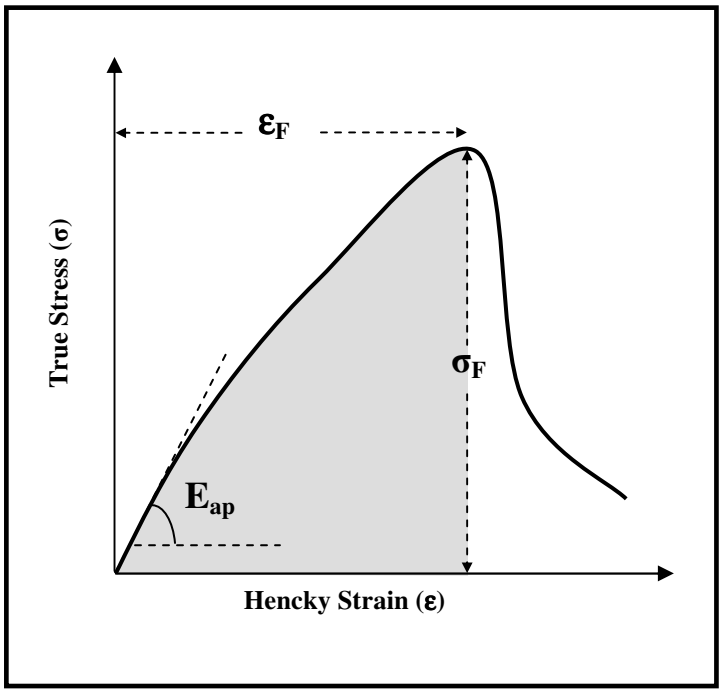

Figure 7.2. Typical compression curve for a vegetable product.

Since texture is not uniform among fruits, values of the four parameters presented above were normalized as the ratio between values for treated cylinders and the fresh counterparts (Rodrigues *et al*., 2003).

7.2.3.3. Microscopic analysis

At the same sampling times for the textural measurements, two samples were removed from the stirred vessels for microscopic observation. One rectangular slab of ca. 1mm of thickness was gently cut parallel to the height of the cylindrical samples at the maximum section area as shown in Figure 7.1 (a), with a razor blade. One face of the slab

was stained with a solution of methylene blue 0.1 % (Mayor *et al*., 2005) during 15 s. After that the sample was ready for observation under the stereomicroscope.

Microimages of stained samples were obtained under a stereomicroscope (Olympus SZ-11, Tokyo, Japan). The samples were put on a thin glass plate under the objective; a source of light was located under the plate so as to work in transmitted light mode. A digital colour videocamera (SONY SSC-DC50AP, Tokyo, Japan) was attached to the microscope and connected to a personal computer. Image acquisition was done with an interface (PCTV videocard, Pinnacle Systems GmbH, Munich, Germany). Images were calibrated with a stage micrometer of 2 mm length and divisions of 0.01 mm interval (Leitz Wetzlar, Germany). The images were processed using Microsoft Photo Editor 3.0 (Microsoft Corporation) software. Figure 7.3 shows the equipment used for observation of pumpkin samples with the stereomicroscope.

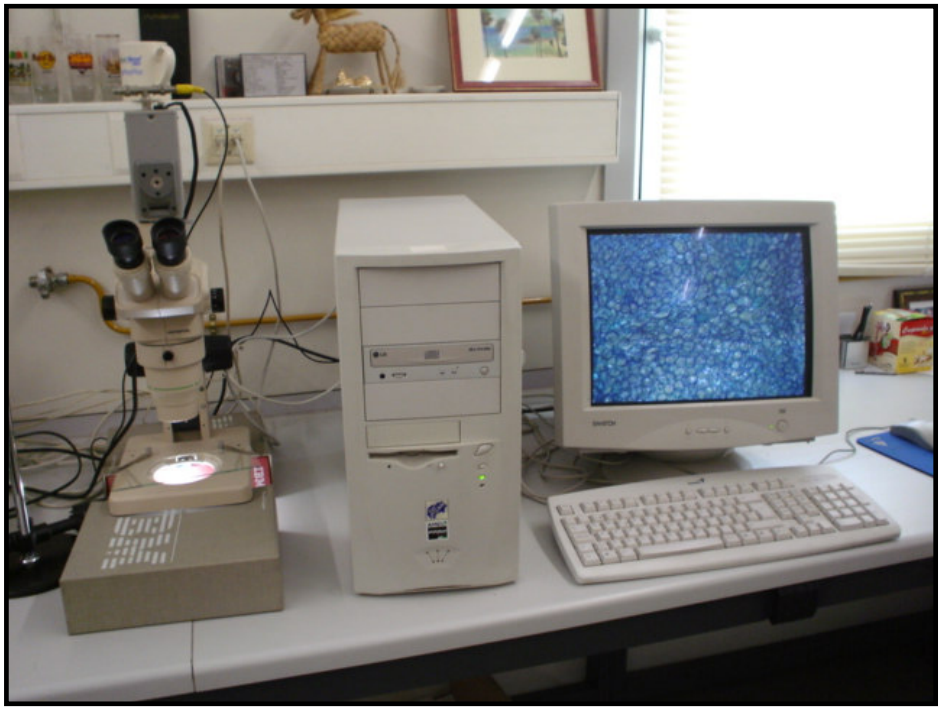

Figure 7.3. Equipment for microscopical observation with the stereomicroscope.

7.2.3.4. Simultaneous microscopic observation/compression tests

At the same sampling times of the textural measurements, two samples were removed from the stirred vessels for simultaneous microscopic observation/compression tests.

Samples were cut in the same way as for the textural measurements, but after that an additional cut was made parallel to the sample axis (Fig. 7.1 (c)), in order to have a flat surface that allows the visualization of the structural changes during compression. This flat surface was stained in the same way as in microscopic analysis (7.2.3.3).

The experimental set-up shown in Figure 7.4 was used for the for the simultaneous microscopic observation/compression experiments. A sample (a) was compressed in the texture analyzer (b). During the compression test, a stereomicroscope (c) attached to a videocamera (d) followed the changes of the tissue structure during the compression. Both texture analyzer and video camera were connected to a personal computer (e), for further combined simultaneous analysis of force, structure images and compression time.

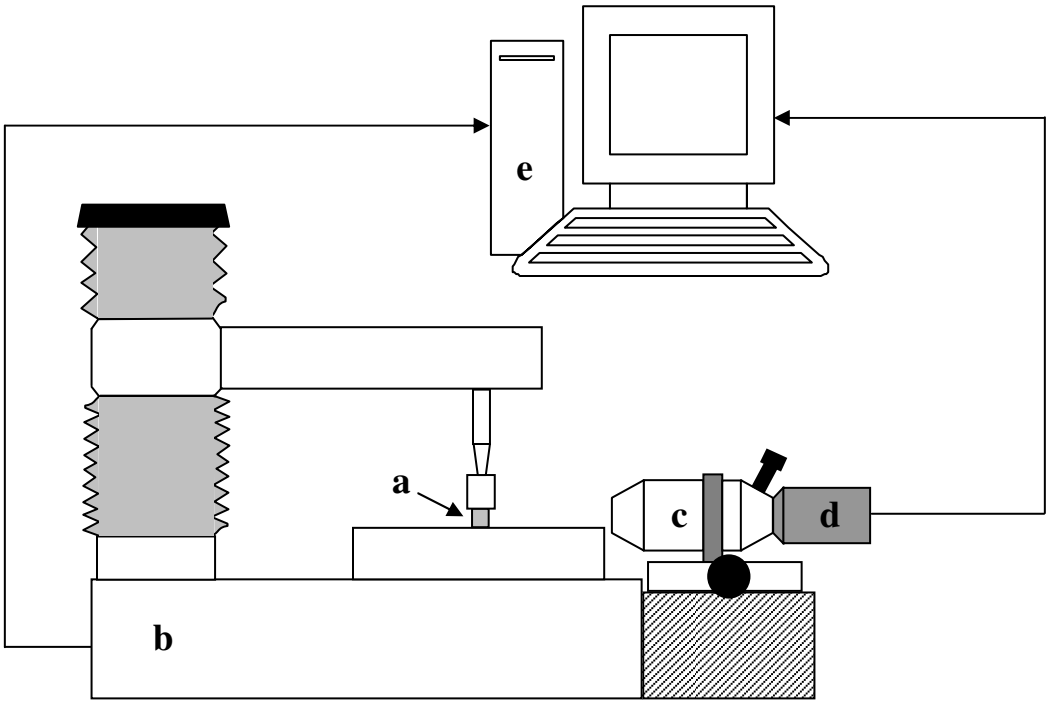

Figure 7.4. Experimental set-up for the simultaneous microscopic observation-compression tests: (a) Sample; (b) Texture analyzer; (c) Stereomicroscope; (d) Digital video-camera; (e) Personal computer.

From the digital video files some images at selected times were obtained using Microsoft Windows Movie Maker 5.1 software (Microsoft Corporation), and were related with the corresponding stress-strain curve

In order to determine the stress values of the compression curve, constant volume of samples was assumed as in 7.2.3.2, but in this case, the area of the cut section of the cylinder must be subtracted (Fig. 7.5) . Initial contact area of compression can be calculated by means of Eq. (7.4)

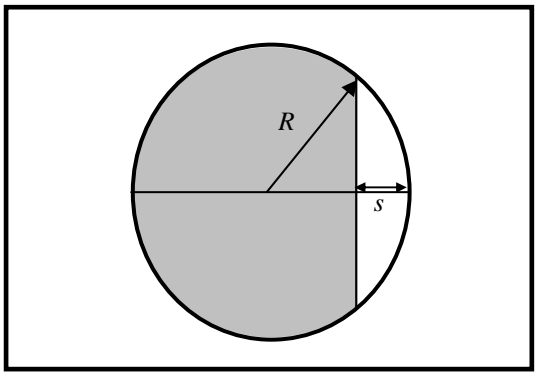

Figure 7.5. Initial area considered for stress calculations (grey area) in the simultaneous microscopy observation-compression tests.

$$A = \pi R^2 - (2Rs - s^2)ar\cos\left(1 - \frac{s}{R}\right) \qquad (7.4)$$

7.3. Results and discussion

7.3.1. Fresh material

Figure 7.6 shows a typical compression-decompression stress-strain curve for fresh pumpkin. The behaviour under compression up to the rupture zone is the typical of other vegetables and fruits. Initially, a linear stress-strain relationship is observed, followed by a

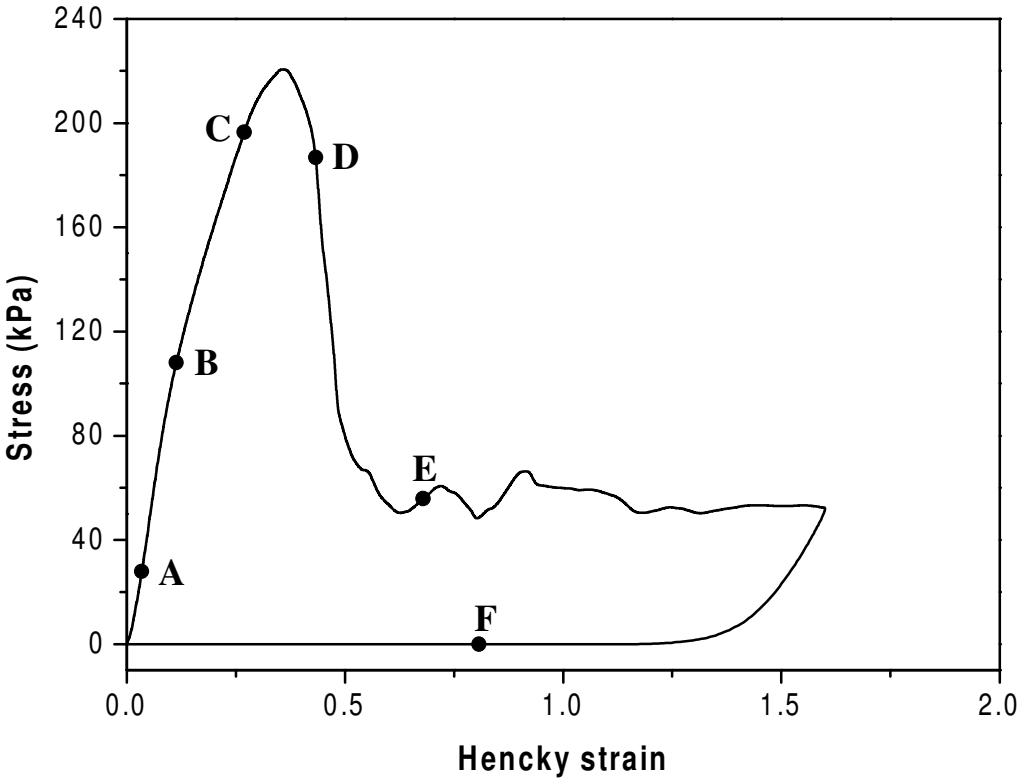

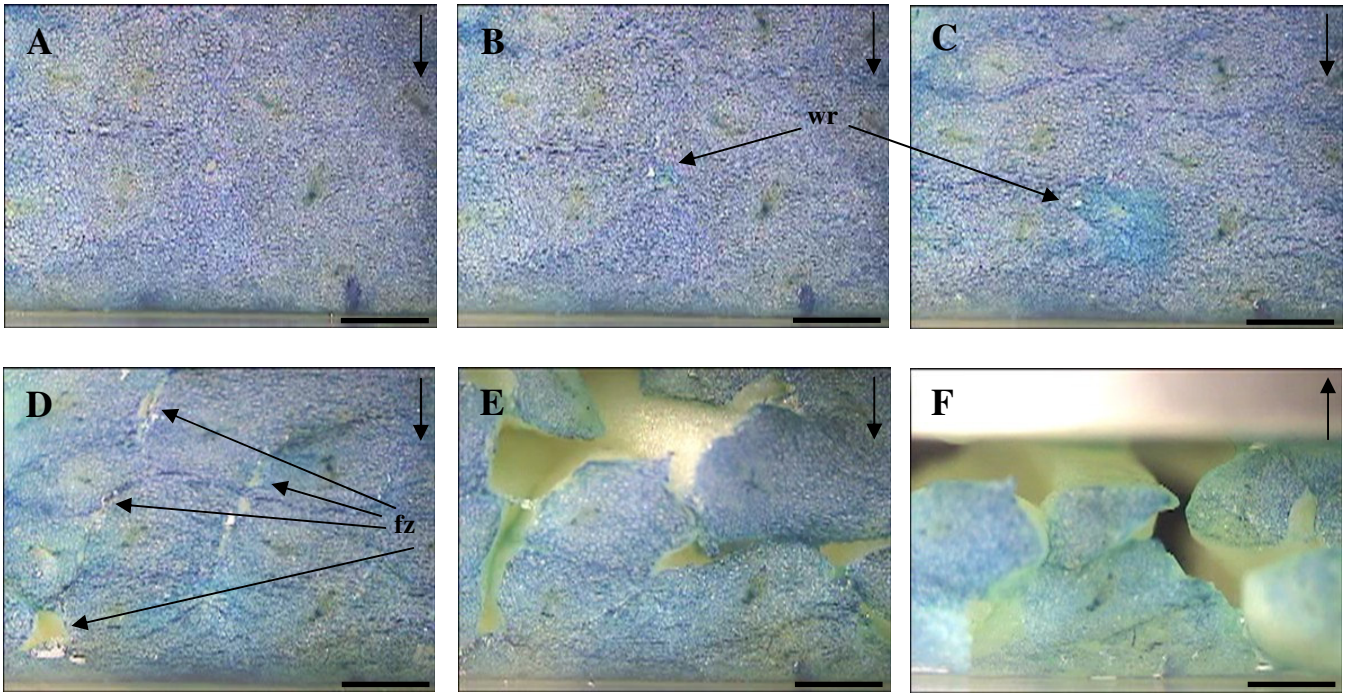

Figure 7.6. Typical compression-decompression stress-strain curve for fresh pumpkin. A,B,C,D,E and F points in the curve correspond to A,B,C,D E and F microphotographs, respectively. The top right arrow indicates the direction of the compression probe. Bottom right horizontal line is one mm length. Water release = wr; failure zone = fz.

nonlinear region where is also observed an increase of the stress with the strain, up to a critical point (the failure point) where the stress attains a maximum value and starts to decrease. This behaviour has been observed in several vegetables, such as apples (Rebouillat and Peleg, 1988), kiwifruit and strawberries (Chiralt *et al*. 2001) and potatoes (Luscher *et. al*., 2005).

Figure 7.7 (b) shows a microphotograph of the section of a fresh pumpkin cylinder. A fibre oriented structure of the parenchymatic tissue can be observed (see comments in 2.2.3). In order to avoid any influence of the fibre orientation on the mechanical properties, compression was performed perpendicular to the fibres during all the tests.

In Figure 7.6 are also shown online-microphotographs taken during the compression test. Point A corresponds to the linear region of the compression curve, where compression of the intercellular spaces and cells can be observed. Point B corresponds to the nonlinear region before rupture. The changes occurring in the material in this region can be considered irreversible; an incipient release of water out of the tissue due to compression is observed, probably due to the fracture of cells or coming from intercellular spaces. Although microfractures occur in the tissue, these do not cause in general the failure of the structure, but the linearity initially observed disappears. In point C water release and compression of fibres are more accentuated. After the failure point (point D), pumpkin tissue fails in the zone of fibre adhesion. After compression (point F), the tissue has been partially separated in its fibres.

Several factors may have influence on the mechanical properties of vegetables, such as density and composition of the material, turgor pressure of cells, cell adhesion and mode of fracture (Waldron *et al*. 1997). Vegetable tissue can fail in two modes: cell wall rupture and/or cell-cell debonding trough the middle lamella (Edwards, 1999), the thin layer composed by pectin polysaccharides which surrounds the cell wall and acts as cement among cells. In the case of pumpkin tissue, these two failure modes can exist, but there is a preferential failure pathway for the rupture: the connection zones among the fibres of the material. In these zones, parenchymatic tissue is less compacted, with more intercellular

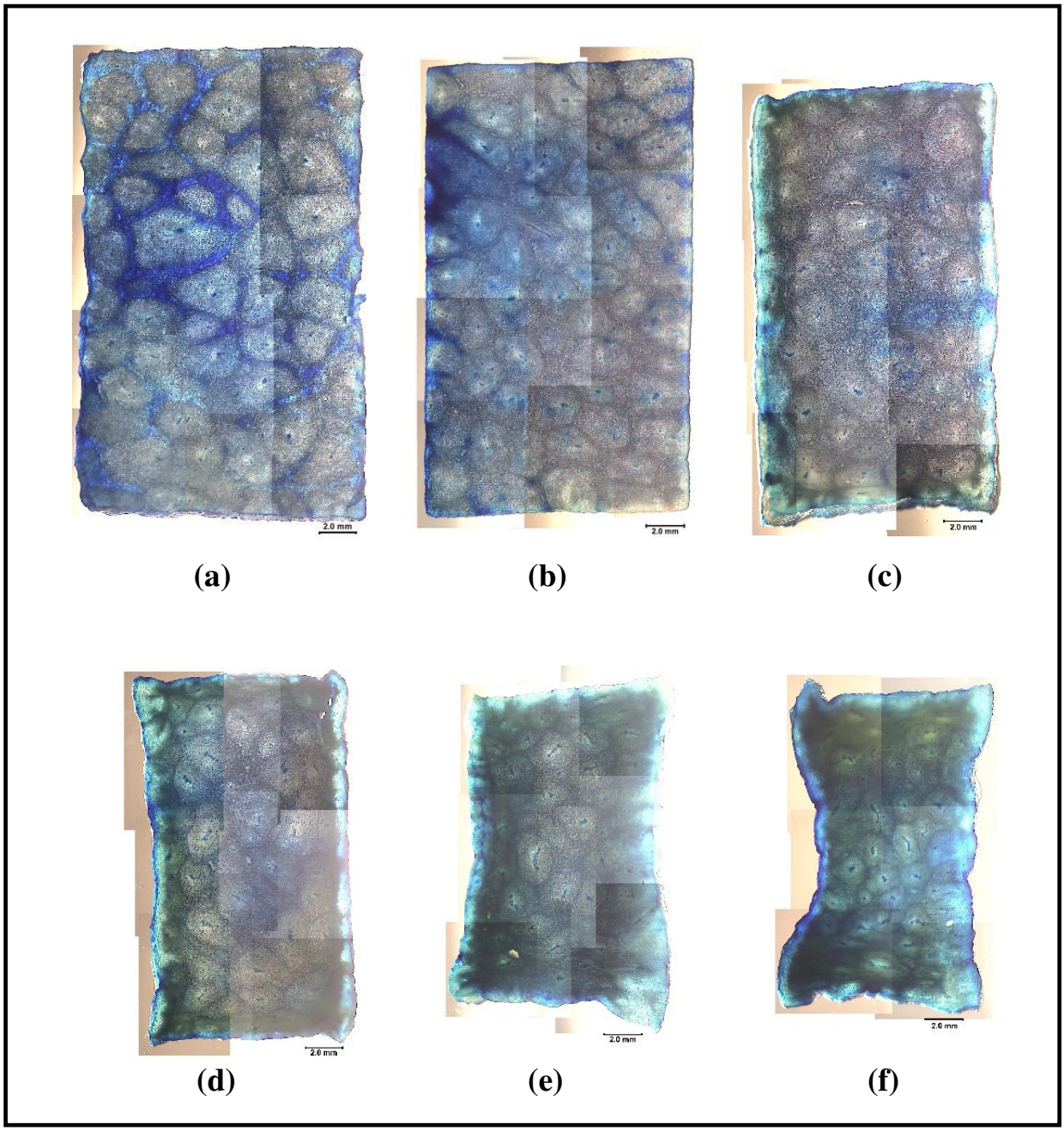

Figure 7.7. Structural changes during osmotic dehydration (OD) in 60% sucrose solutions at 25ºC and water soaking of pumpkin tissue. (a) Water soaking, nine hours. (b) Fresh material. (c) OD one hour. (d) OD three hours. (e) OD six hours. (f) OD nine hours. Horizontal line at the bottom right of each image is two mm length.

spaces and likely with a less efficient middle lamella, delimiting the fibre dimensions. It can be said that the failure mode for fresh pumpkin is "fibre debonding".

For the strain-stress curves, the values of apparent modulus of elasticity, Hencky strain at failure, true stress at failure and toughness were obtained. These values ranged 0.96-2.53 MPa for apparent elasticity modulus, 0.42-0.71 for failure strain, 250-630 kPa for failure stress and 83-285 kJ/m^3 for toughness in fresh pumpkin. The variability of these values was mainly due to the variability among fruits, since coefficients of variation for these parameters were always less than 15% within the same fruit.

Table 7.1 shows the values of apparent modulus of elasticity, failure stress and failure strain for fresh pumpkin (this work) and for other vegetable products found in the literature.

Table 7.1. Some mechanical properties of different fresh vegetable products.

Material	Apparent Modulus (MPa)	Failure strain	Failure stress (kPa)	Reference
Carrot	-	0.45	1855	Kohyama *et. al*. (2004)
Pumpkin	0.96-2.53	0.42-0.71	250-630	This work
Potato	-	0.5-0.6	500-600	Luscher *et a*l. (2005)
Apple	1.5-2.3	0.12-0.25	160-280	Rebouillat and Peleg (1988)
Mango	0.1-0.3	0.1-0.65	20-40	Chiralt *et. al*. (2001)
Kiwifruit	0.2	0.18-0.26	20-40	Chiralt *et. al*. (2001)
Sweet cherry	0.12-0.16	0.24-0.27	32-38	Vursavus *et al*. (2006)

Although a strict comparison can not be done because the compression experiments were performed with different conditions in all these works (deformation rate, lubrication), the results are different enough to establish some differences among these vegetable products. Comparing the values of this table, pumpkin tissue shows a firm structure (high values of elastic modulus) similar to apples and firmer than mango and kiwifruit. It also presents a high ability to resist force during compression (high values of failure stress) similar to potatoes but bigger than those showed by apple, mango, kiwifruit and cherry. It is also a ductile product (high values of failure strain).

7.3.2. Osmotically dehydrated samples

As an example of osmotic treatment, Figure 7.8 (a) shows the stress-strains curves of pumpkin samples osmotically dehydrated with 60% sucrose solutions at 25 ºC. As can be observed, the slope of the initial linear zone of the curves decreases with moisture content, and consequently the apparent modulus of elasticity also decreases. Chiralt *et al*. (2001) also observed a decrease in the apparent modulus after osmotic dehydration with sucrose solutions of kiwifruit, strawberries and mango. In dehydration processes, water loss can lead to the decrease of turgor pressure in the cells and even plasmolysis (Mauro *et al*., 2002). This decrease in turgor pressure leads to the decrease of the apparent modulus of elasticity, as observed by Scanlon *et al*. (1996) during the immersion of potato tissue in mannitol solutions of different concentration.

Hencky strain at failure increases with the decrease in moisture content. This increase of strain at failure after osmotic dehydration was also observed for kiwifruit (Chiralt *et al.*, 2001) and mango (Torres *et al*., 2006). Failure stress initially decrease during dehydration, but at a certain moisture content (NMC=0.82) failure stress starts to increase with the decrease of moisture content till the end of the process.

Krokida *et al*., (2000[b]), during convective drying vegetable products, observed a similar behaviour of the stress and strain at failure during the drying process for all the materials. The shift in the behaviour of failure strain was produced at NMC = 0.73, 0.86, 0.83 and 0.86 for apple, banana, potato and carrot respectively. They attributed this behaviour to the fact that at certain moisture content some important changes in the tissue structure occur, such as crystallization of cellulosic components of the cell walls. Another phenomenon which can difficult the failure of the material is the transition to a glassy state of the concentrated liquid phase at certain moisture contents.

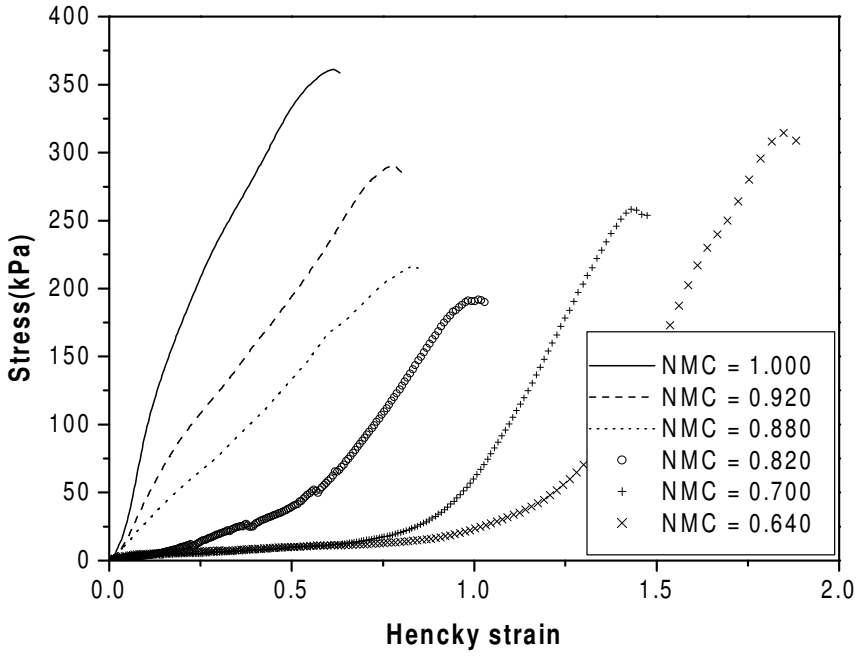

(a)

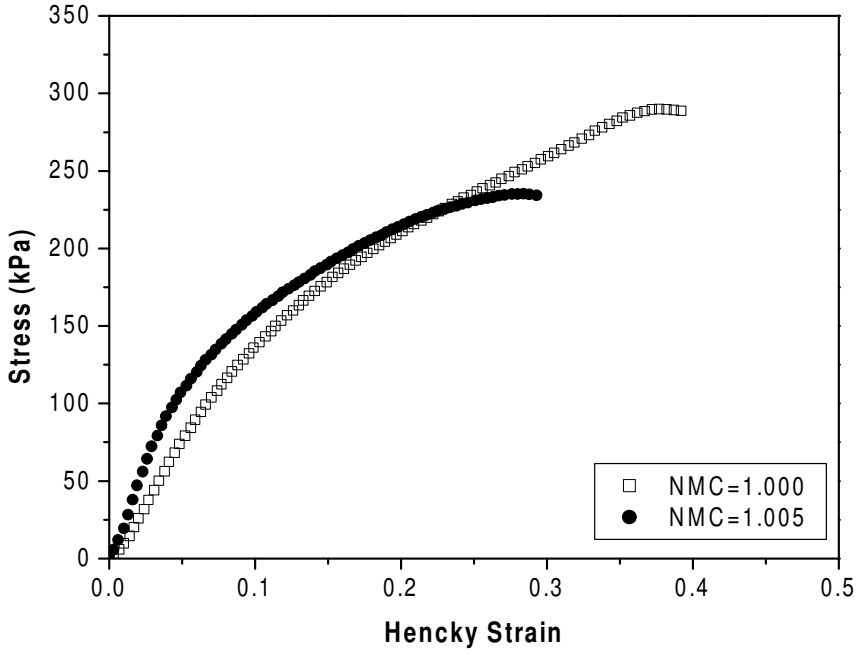

(b)

Figure 7.8. Compression curves for fresh and processed pumpkin at different moisture contents. (a) Osmotic dehydration with 60% sucrose solutions at 25ºC. (b) Water soaking.

In osmotically dehydrated products, the decrease of moisture content is not enough to produce glass transitions of their chemical components, so the reasons for the changes in the behaviour of failure stress along the process should be looked for in other facts, as discussed as follows.

Figure 7.7 shows the microstructure of fresh and osmotically dehydrated (60% sucrose, 25ºC) cylinders at different process times. Initially, the fresh tissue (Fig. 7.7 (b)) shows a homogeneous and fibre-oriented structure. The high values observed in the apparent initial modulus during compression (Fig. 7.8 (a), NMC =1), may be associated to the natural turgor pressure of the cells. The material fails at a certain stress and strain by the contact zone of its fibres, as observed in Figure 7.6.

At nine hours of dehydration process, the structure of the sample has changed considerably (Fig. 7.7 (f)); the volume has decreased as a consequence of the loss of water, and the delimitation of the fibres is not so clearly observed, likely because they are more compacted. Figure 7.8 (a) (NMC= 0.640) shows the compression curve of a sample osmotically dehydrated during nine hours (60% sucrose, 25 ºC). It is observed a dramatic decrease of the initial modulus, probably due to the decrease of the turgor pressure in the cells. The material also shows more ability to resist the failure (failure strain slightly decreases but failure strain increases considerably) compared to fresh material; this fact may be due to the compacting of the fibres during dehydration.

Between these two situations, a monotonic evolution for the mechanical properties from the fresh to the more dehydrated product should be expected. In Figure 7.8 (a), this behaviour is observed for the apparent elastic modulus (continuous decrease) and failure Hencky strain (continuous increase), but not for failure stress, which shows a minimum around NMC=0.82. The existence of structural profiles in the samples during dehydration may explain this behaviour. It can be observed, along the dehydration process, two different structural zones in the material: a dehydration front, where dehydration process occurs, which penetrates in the tissue during the treatment; and a solid core, with the same physical, chemical and structural characteristics than the fresh material, which decreases

along the osmotic treatment. The advance of the dehydration front and decrease of the solid core can be observed in Figure 7.7. For the sample osmotically dehydrated during one hour (Fig. 7.7 (c)) the dehydration front is observed in the outer region of the cylinder, whereas the solid core is located in the inner of the sample. At nine hours (Fig. 7.7 (f)), the material seems to be dehydrated in all the zones and the solid core is practically inexistent. The dehydration front, where the cells have lost their turgor pressure and the fibres are more compacted, probably has similar mechanical characteristics than the material dehydrated at nine hours: low firmness, similar failure stress and higher failure strain compared with fresh material. However, the solid core has the mechanical characteristics of the fresh material: firm, strong, and brittle.

When a sample showing structural profiles is submitted to a compression test, initially the dehydration front is compressed, and at a certain strain the solid core starts also to compress. Since the soft (low firmness) and ductile dehydration front penetrates in the sample during dehydration, firmness decreases and Hencky strain increases with the decrease in moisture content of samples. The compression, at a certain strain value, attains the solid core, and the material fails in this more brittle zone. Since the solid core decreases during dehydration, the failure stress decreases. The lowest value of failure stress is observed for NMC=0.82 (55% of the value for fresh material). From this moisture content, the remaining solid core changes and tends to be similar to the dehydrated samples at nine hours; then the failure stress stars to increase up to the end of the process which attains a value of 80% of the value for fresh material.

Figure 7.9 shows online-microphotographs taken during the compression test of an osmotically dehydrated (60% sucrose, 25 ºC) pumpkin cylinder during three hours. It is observed that the release of water is more intense than in the case of the fresh material, probably due to the plasmolysis of cells during the osmotic process. As can be seen, the material fails in the central zone of the cylinder, where the less ductile zone (solid core) of the material is found. This failure in the solid core was verified for all the osmodehydrated samples that developed moisture profiles, at different moisture contents.

No significant influence of solution concentration and process temperature on mechanical parameters was observed, and in a general way their behaviour during dehydration can be explained as a function of changes in moisture content. The changes of the studied mechanical properties with moisture content, for osmotic dehydrated samples, are shown in Figures 7.10 and 7.11. The average variation coefficients were 15%, (ranging 1-35%) for apparent elastic modulus, 36% (17-56%) for normalized failure strain, 22% (14-33%) for normalized failure stress and 34% (22-55%) for normalized toughness. This dispersion of data is pretty acceptable considering the high number of replicates; each point is the average of 30-40 samples (two runs each one with 15-20 samples).

Apparent modulus of elasticity decreases with moisture content up to NMC = 0.8, then the modulus attains a residual value and remains practically constant. Failure strain increases uniformly with the decrease of moisture content, till triplicate its initial value at the lowest moisture content achieved (NMC = 0.62). Failure stress and toughness initially decrease with moisture content until a critical moisture content (somewhere between NMC= 0.8-0.85) where these values decrease to 50% of the initial value; then increase up to the end of the process until attaining, for NMC = 0.62, the 75% and 90% of the initial value for failure stress and toughness respectively.

Polynomial equations with the form

$$Y = a_0 + a_1(NMC) + a_2(NMC)^2 + ... + a_n(NMC)^n \qquad (7.5)$$

were fitted to experimental data on normalised apparent elastic modulus, normalised failure strain, normalised failure stress and normalised toughness; the results of the fits are presented in Table 7.2. The selection of the polynomial order was performed by a backward elimination procedure using the statistical software STATISTICA 6.0 (Statsoft Inc., USA).

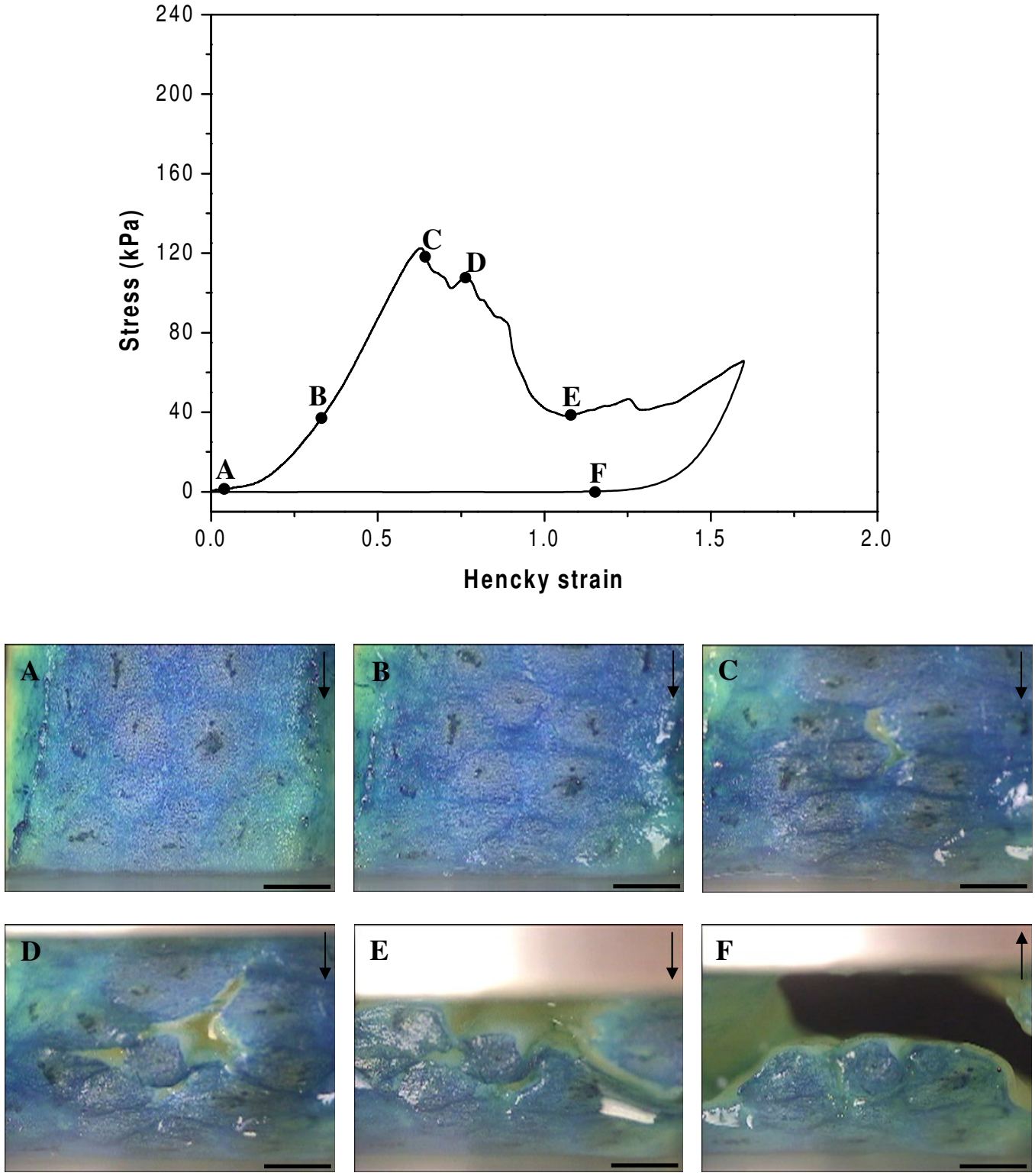

Figure 7.9. Typical compression-decompression stress-strain curve for pumpkin osmotically dehydrated in 60% sucrose solutions during three hours. A,B,C,D,E and F points in the curve correspond to A,B,C,D E and F microphotographs, respectively. The top right arrow indicates the direction of the compression probe. Bottom right horizontal line is one mm length.

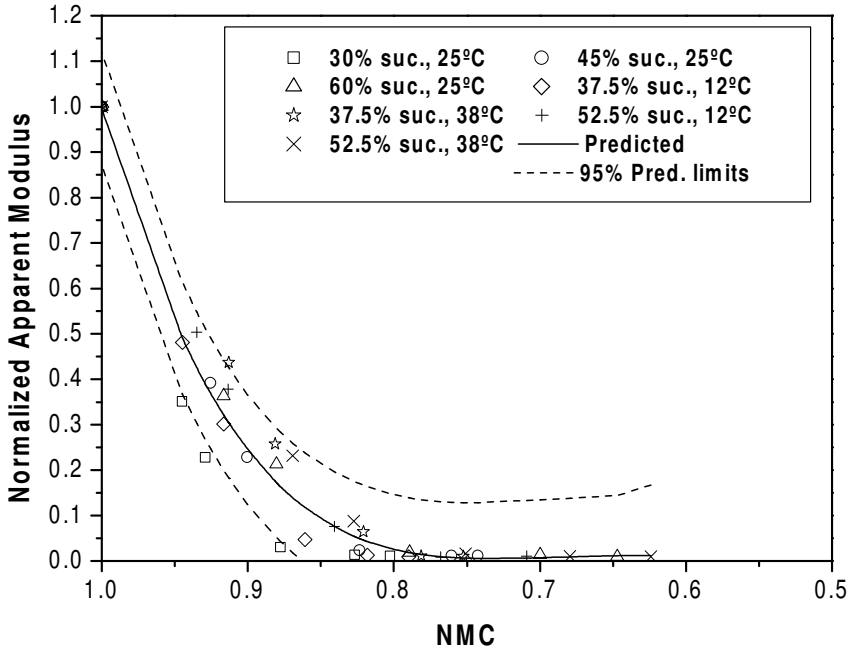

(a)

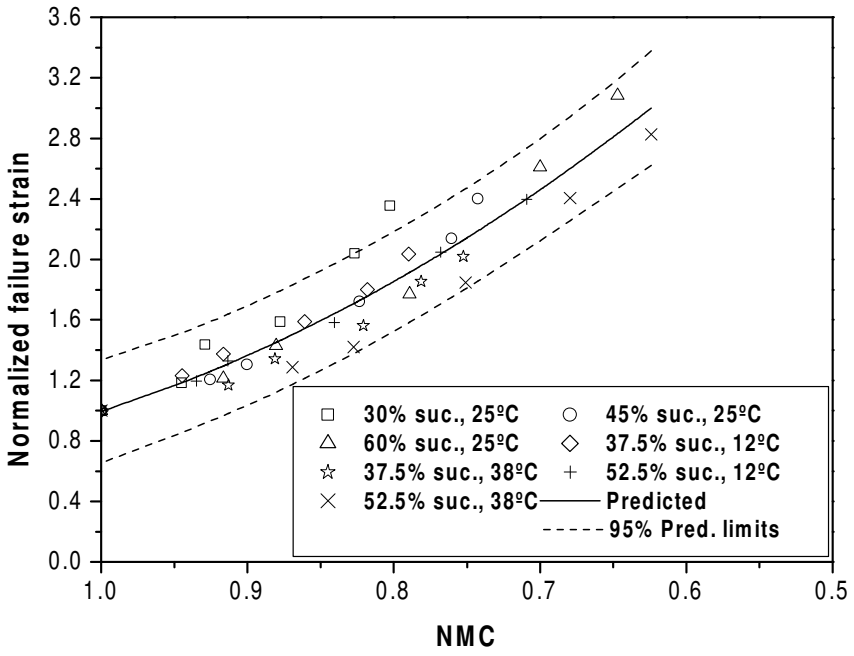

(b)

Figure 7.10. Mechanical properties of pumpkin during osmotic dehydration at different process conditions as a function of normalized moisture content (wet basis). (a) Normalized apparent elastic modulus. (b) Normalized Hencky strain at failure.

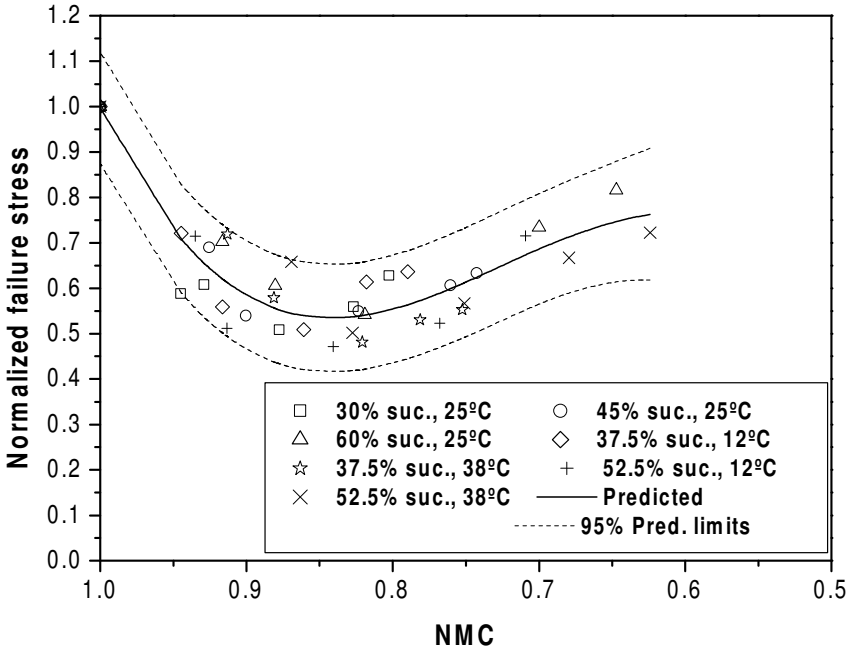

(a)

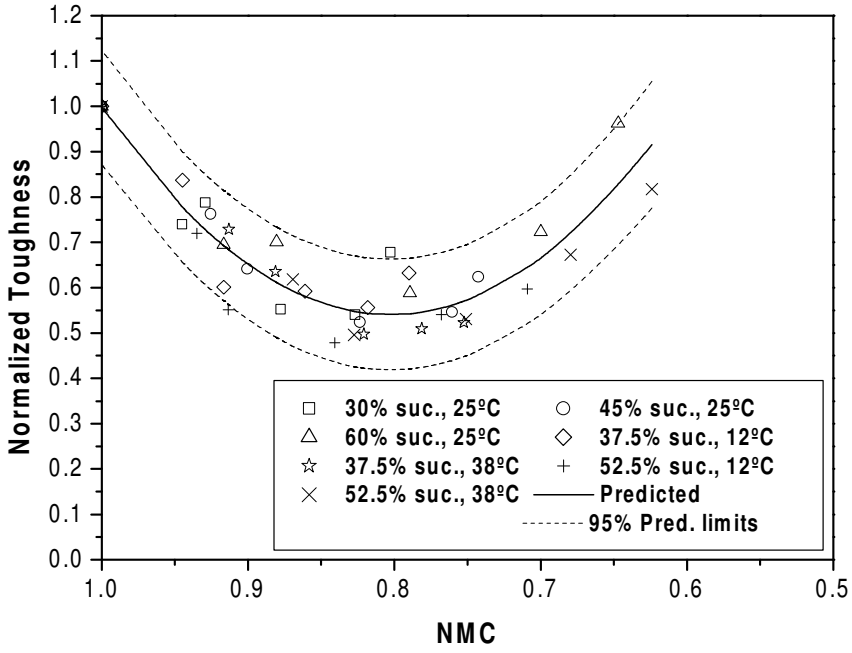

(b)

Figure 7.11. Mechanical properties of pumpkin during osmotic dehydration at different process conditions as a function of normalized moisture content (wet basis). (a) Normalized failure stress. (b) Normalized toughness.

Table 7.2. Fit results of Eq. (7.5).

Y	a_o	a_1	a_2	a_3	a_4	R^2
E_{ap}/E_{apo}	9.81	-63.30	152.18	-161.39	63.69	0.98
$\varepsilon_F/\varepsilon_{Fo}$	10.02	-14.93	5.91	-	-	0.92
σ_F/σ_{Fo}	-12.10	55.74	-78.94	36.30	-	0.90
W/W_o	8.11	-18.85	11.74	-	-	0.90

For the apparent elastic modulus (fourth degree polynomial) was obtained a very good fit, whereas for failure strain (quadratic), failure stress (cubic) and toughness (quadratic) the fits were satisfactory.

7.3.3. Water soaked samples

Figure 7.8 (b) shows the typical compression curves for fresh and water-soaked pumpkin cylinders after 9h soaking, and Figure 7.12 shows the average values of the analyzed compression parameters. As can be observed, soaked samples are firmer (more accentuated initial slope), less strong (lower failure stress) and less ductile (lower failure strain) than fresh samples. Firmness of samples increased 40%, failure strain and failure stress decreased 20% and toughness decreased 30% compared with fresh material.

Figure 7.7 (a) shows images of a water soaked cylinder during 9h. The swelling of the tissue is observed, due to the entrance of water in cells and intercellular spaces. As a consequence, turgor pressure of cells increases, and probably the internal stresses in the tissue. It is also observed that the spaces of connection of fibres are more stained, suggesting that the methylene blue solution easily entered among the fibres, as a consequence of the separation among them caused by the uptake of water, resulting in an less compacted structure than in the fresh material. This separation of the fibres can be the cause of the decrease of failure strain and failure stress compared with fresh samples.

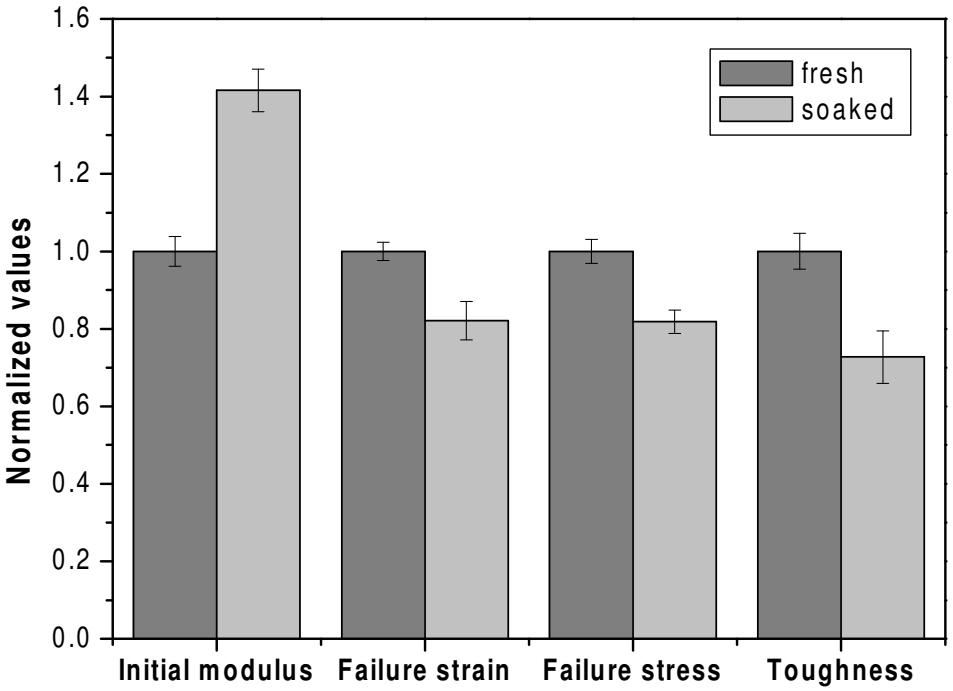

Figure 7.12. Normalized values for apparent elastic modulus, failure strain, failure stress and toughness, for fresh and water-soaked pumpkin samples.

Figure 7.13 shows a compression profile of a water soaked cylinder and online microphotographs of the compression test. In the initial linear zone of the test, it is observed the compression of fibres and cells. At higher deformations some water release starts to appear, and after that it is observed the rupture of the material by the zone of adhesion of the fibres, as in fresh and osmotically dehydrated pumpkin.

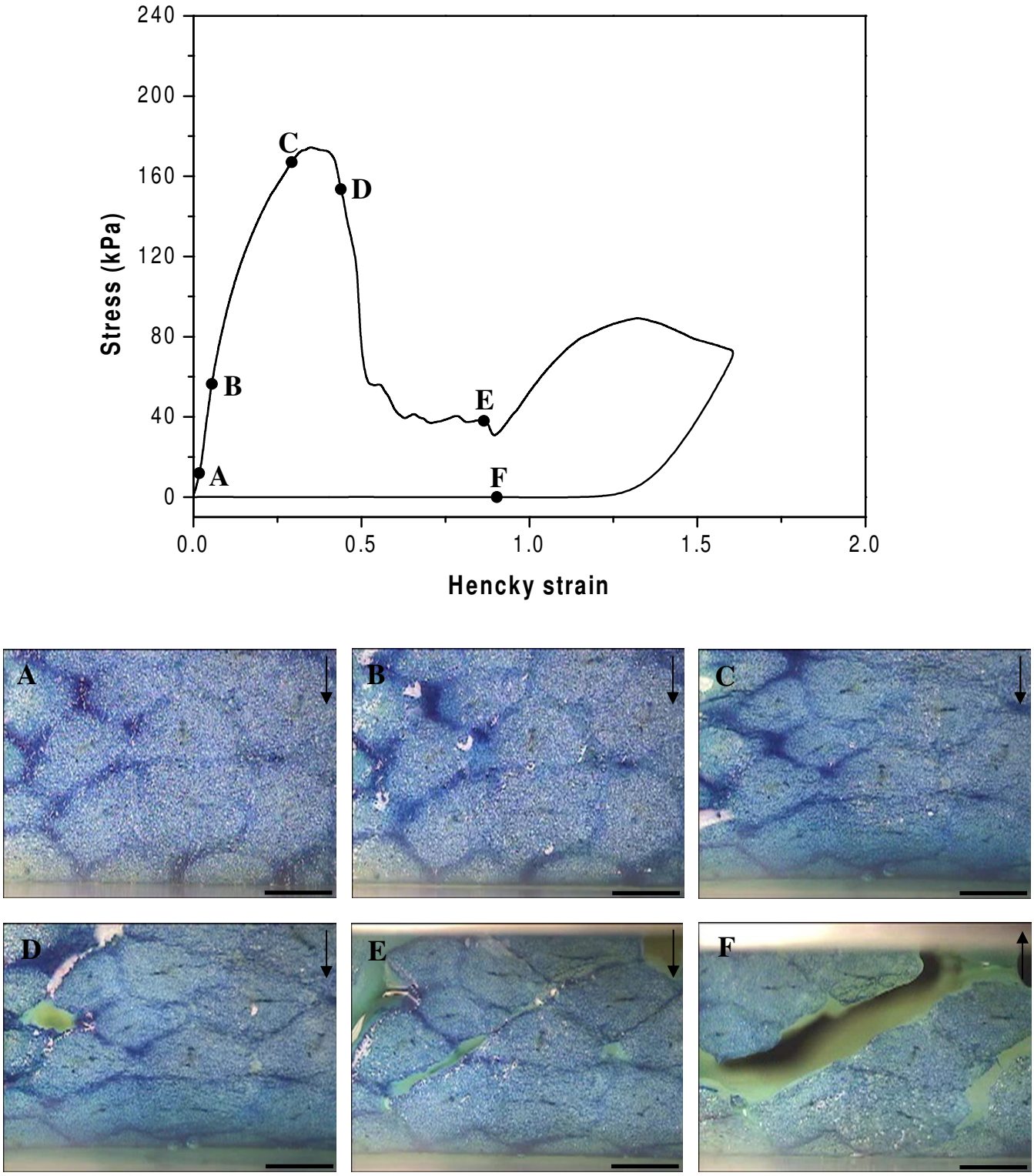

Figure 7.13. Typical compression-decompression stress-strain curve for water-soaked pumpkin after nine hours of process. A,B,C,D,E and F points in the curve correspond to A,B,C,D E and F microphotographs, respectively. The top right arrow indicates the direction of the compression probe. Bottom right horizontal line is one mm length.

7.4. Conclusions

Osmotic dehydration and water soaking produced important changes in the mechanical properties of pumpkin tissue. Initially the tissue was firm, strong and brittle. At low moisture contents, the tissue lost its firmness, keeping its strength but became more ductile. When tissue was soaked in water its firmness increased, but became less resistant to compression, decreasing failure stress and failure strain.

The mechanical properties seem to be related with different levels of structure. At low deformations, the resistance to compression is controlled by the turgor pressure of cells. The increase in turgor pressure (water soaked samples) led to the increase of the material firmness, whereas during osmotic dehydration cellular turgor pressure decreased, so did the firmness of pumpkin tissue. At higher deformations, and near the failure point, failure properties were more influenced by the strength of the adhesion among the fibres which compose the pumpkin parenchyma. In water soaked samples the fibres looked like more separated due to the entrance of water in the intercellular spaces; as a consequence the material failed at lower deformation and stress. For osmotically dehydrated samples and at low moisture content the fibres were more compacted and tissue failed at similar stress than fresh material but at higher strain.

Empirical polynomial models were used to relate the changes in the studied mechanical properties to moisture content during osmotic dehydration. Future work is needed to develop more fundamental models relating textural properties with composition and structure of fresh and dehydrated vegetable products.

CHAPTER 8

MICROSTRUCTURE CHANGES DURING OSMOTIC DEHYDRATION OF PUMPKIN FRUITS

CHAPTER 8. MICROSTRUCTURE CHANGES DURING OSMOTIC DEHYDRATION OF PUMPKIN FRUITS

8.1. Introduction

This chapter shows experimental data on microstructural changes during osmotic dehydration of pumpkin fruits. The observation of fresh and processed samples at microstructural scale was done by means of light microscopy techniques. The preparation of samples for microscopy observation was performed by two different methods, obtaining different information of the microstructural changes and complementing each other. Some mathematical models were used in order to predict the changes in microstructure during osmotic dehydration.

8.2. Materials and methods

8.2.1. Preparation of samples

The procedure explained in 3.2.1 was used in the preparation of samples for the dehydration experiments.

8.2.2. Dehydration experiments

Pumpkin cylinders were dehydrated in 45% sucrose solutions at 25ºC, as commented in 3.2.3. The samples were removed for the beakers containing the osmotic solution at different process times (0.5, 1, 3, 6 and 9 hours), then they were gently blotted with paper to remove the excess of the osmotic solution and kept in plastic boxes till experimental determinations. Nine cylinders were removed at each process time; four were used for determination of kinetic parameters and five for microscopic analysis.

8.2.3. Experimental determinations

8.2.3.1. Kinetic parameters

Weight reduction (WR), water loss (WL), solids gain (SG) and normalized moisture content (NMC) were obtained by means of the procedure explained in 3.2.4.

8.2.3.2. Microscopy

a. Sample preparation

The preparation of samples for microscopy analysis was done by two different methods. In the first method, a 0.5 mm rectangular slice was cut from fresh or dehydrated cylinders with a razor blade, as explained in 5.2.2.3. These samples were ready to be stained.

The second method, more elaborated, implies the fixation of the vegetable tissue in glutaraldehyde and then its inclusion in an acrylic resin. For a good observation in the microscope, the animal and plant tissues sometimes must be thin enough to transmit light (in histological analysis the tissue sections are often thin slices about 10 μm thick). In order to cut thin sections without producing changes in the structure of the material, the tissue is hardened and embedded in a resin. The resins usually employed have low viscosity when they are liquid, and can easily infiltrate in the tissue; after the infiltration the resin is polymerized in order to produce its solidification. In our case the resin used was LR White, an acrylic resin often used in light microscopy for the observation of vegetable tissue (Ramalho-Santos *et al*. 1997).

Initially, a slab from the fresh or dehydrated cylinder was obtained as explained in 5.2.2.3. The slab was divided in four symmetrical cuts. One on these quarters was divided in six parts, as showed in Figure 8.1. These six parts were included individually in acrylic

resin as explained above. When cylinders showed considerable shrinkage after dehydration (after six and nine hours of process), the quarters were divided in four parts.

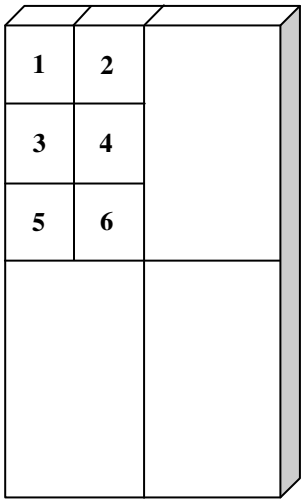

Figure 8.1. Preparation of the cuts used for fixation and inclusion of pumpkin tissue.

The total inclusion procedure has different steps:

1) Fixation. Samples were put in vials with a solution of Glutaraldehyde 2.5% and 1,4-piperazinediethanesulfonic acid (PIPES) (minimum 99%, Sigma) 1.25% at pH 7-7.2 during 24 hours, at room temperature. The fixating solution was renewed at 12 hours.

2) Washing. After fixation, the samples were rinsed with a solution of PIPES 2.5%, three times, ten minutes each time.

3) Dehydration. The interchange of water by alcohol was done progressively. The samples were introduced in a series of alcohol solutions of increasing concentration. Table 8.1 shows the dehydration procedure.

Table 8.1. Dehydration procedure for inclusion of samples in LRWhite.

Alcohol concentration	Time
25%, 35%, 50%, 70%	10 minutes each
90%	4x10 minutes
100%	6x10 minutes

4) Impregnation. The impregnation was performed with mixtures ethanol /LR White (London Resin Co., Basingstoke, UK) of increasing resin concentration. Each solution had to be impregnating the samples from 12 to 24 hours, always in the refrigerator. The mixtures used are shown in Table 8.2.

Table 8.2. Mixtures ethanol/LR White for resin impregnation.

Ethanol (volumes)	LR White (volumes)
3	1
2	1
1	1
1	2
1	3
0	1

5) Inclusion. The samples were put in gelatine capsules, and introduced in an oven at 55 ºC during 24 hours.

After the samples were included in resin, semi thin sections (0.6 µm) of the samples embedded in the resin were obtained with a microtome (mod. Reichert-Supernova, Leica, Wien, Austria).

b. Staining

For the first method of sample preparation, the samples were stained with a solution of Methylene Blue 0.1% during 15 seconds.

The sections of pumpkin tissue included in LR White were stained with an aqueous solution Azure II 0.5%, Methylene Blue 0.5%, Borax 0.5% (Ramalho-Santos *et al*., 1997) during 30 seconds. After that, they were washed with distilled water and mounted in a glass slide.

c. Microscopic observation

Microscopic observation and image acquisition/processing were performed as explained in 7.2.2.3.

8.2.3.3. Image analysis

Image analysis of some size and shape cellular parameters was performed as explained in 5.2.2.3. But in this case, the contour of the cells (instead of the sample contour) was isolated in the microphotographs as explained above.

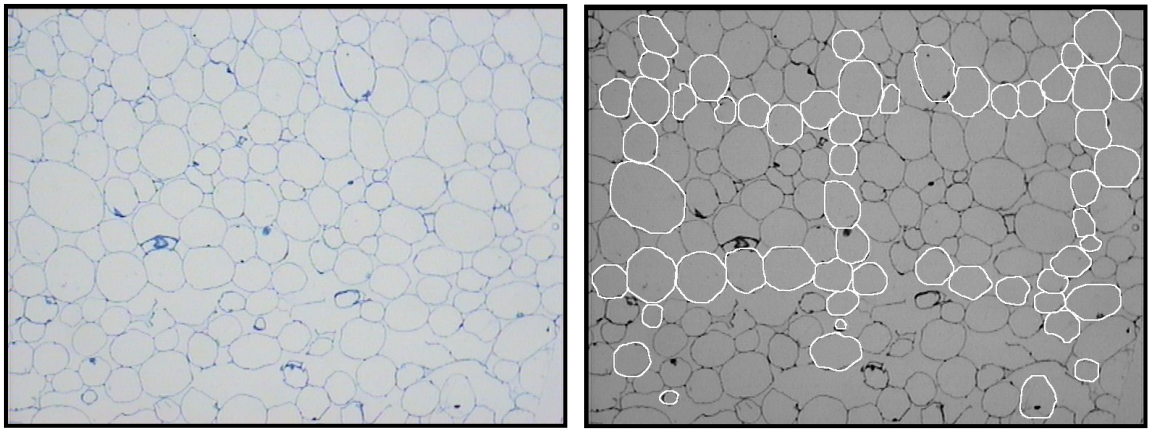

(a) **(b)**

Figure 8.2. Obtainment of the cellular contours for image analysis. (a) Image taken from the microscope. (b) Processed image with isolated cells.

From a microphotograph of the pumpkin tissue (Fig.8.2.(a)), the contour of some cells was highlighted with the software Microsoft Photo Editor 3.0 (Microsoft Corporation). This procedure was systematically done in three vertical lines and two horizontal lines of the photograph, as shown in Figure 8.2 (b). When areas close to the central zone of the fibres (see Fig. 2.5 (e)) appeared in the photographs these areas were discarded for the analysis because the sharp decrease of the cell size and because a part of the cells were not parenchymatic cells, as commented in 2.2.3. The contouring of cells allowed their isolation and later image analysis of the size and shape factors. Statistical analysis of the results was performed with the software Microsoft Excel 2003 (Microsoft Corporation).

8.3. Results and discussion

8.3.1. Fresh material

Figure 8.3 shows images of the microstructure of pumpkin parenchymatic tissue, obtained by means of the two different preparation techniques used: raw samples (Fig. 8.3 (a)) and fixed-included samples (Fig. 8.3 (b)). As can be observed, the cells present different shapes: some of them are round, others are more elongated and others have a polygonal shape. In Figure 8.3 (b) is more clearly observed the presence of intercellular spaces, which contain the air phase of the tissue and some of them can be filled with an aqueous solution. In both images the cells show a turgid aspect.

Since the tissue presents a fibre orientation (see 2.2.3), the study of the size and shape parameters was done in two directions, in order to analyze if some cellular orientation exists. For this purpose, cuts of the tissue parallel (longitudinal fibre orientation) and perpendicular (radial fibre orientation) to the longitudinal axis of the fibres were studied, with fresh non-included samples stained with methylene blue. Several samples (four for each orientation) of the same pumpkin were analyzed, totalling 437 cells.

As can be observed in Figure 8.4, no significant differences (t test, $p>0.05$ for all the parameters) were observed in the size and shape parameters between both orientations, and can be concluded that the cells are disposed in the tissue with no preferential orientation.

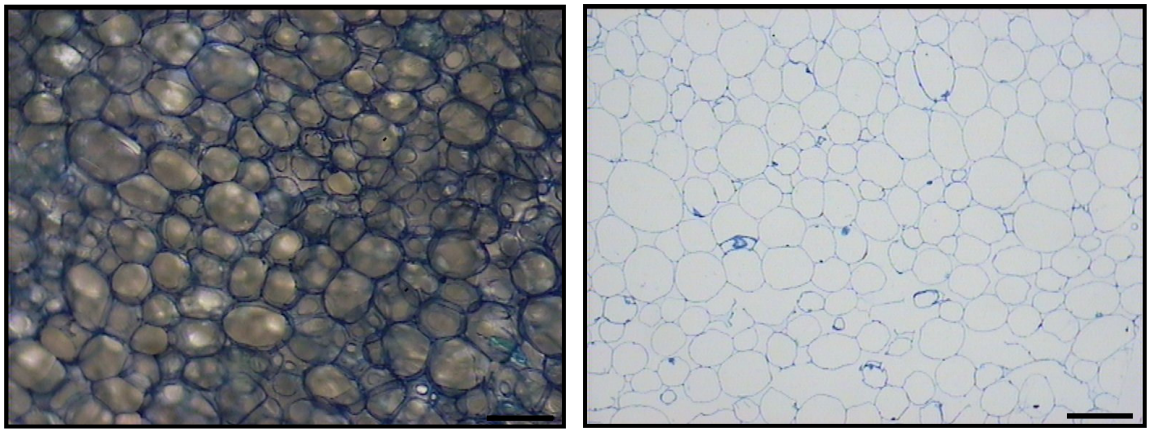

(a) **(b)**

Figure 8.3. Microscopy images of fresh pumpkin parenchymatic tissue. (a) Obtained after staining of fresh sample with methylene blue. (b) Obtained after inclusion in LR White, sectioned and stained in Azure II/Methylene blue. Horizontal bar is 0.2 mm length.

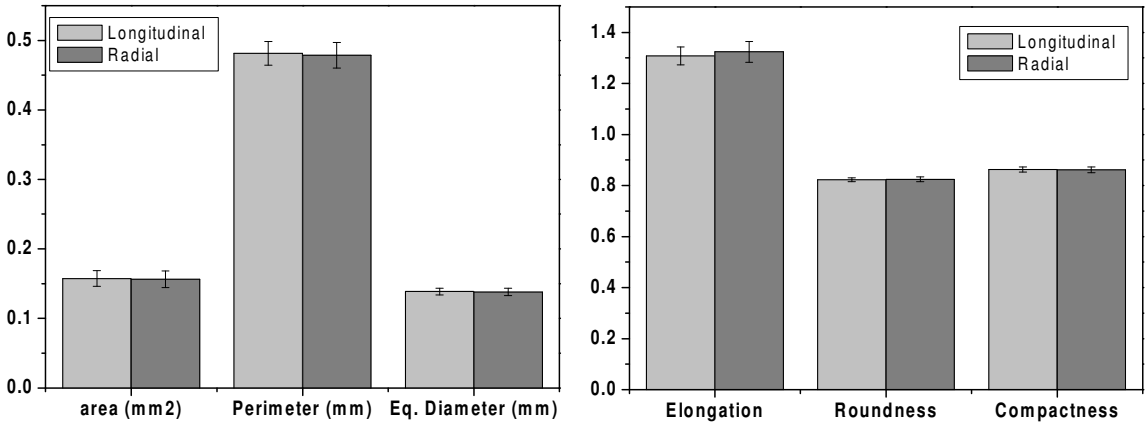

(a) **(b)**

Figure 8.4. Dimensional (a) and shape (b) parameters, for fresh pumpkin tissue, observed at two different cut-orientations: radial to the fibre and longitudinal to the fibre.

After this analysis of the cellular orientation, the effect of the preparation of samples on the cellular parameters was studied. For these purpose, several samples were obtained and analyzed from different parts of the same pumpkin, totalling 437 cells for the non-included samples and 399 cells for the included samples. In Figure 8.5 are observed the histograms of the size and shape parameters for fresh pumpkin prepared by the two explained methods. It can be observed that the size and shape of the curves is similar for all the parameters, but there is a shift in the curves corresponding to the size parameters, decreasing their values. This shift can be attributed to the "cutting effect" produced in the preparation of samples when the method of inclusion in resin is used. In this method, when the block of resin is sectioned, a shift to lower values in the average area obtained is produced, as a consequence of the random intersections of the cut through the cell. This is illustrated in Figure 8.6 (a), assuming cells are spherical. When a fresh sample is cut with a razor blade, it was observed that instead of being cut the cells are separated whole and kept intact. For this reason, the size values obtained are higher than those observed with the samples included in resin and sectioned. In accordance with the size distribution shown in Figure 8.6 (b), area value decreases to 67%, and the perimeter and equivalent diameter to 78% of the actual values. Observing Table 8.3, the decrease in the average values of the size parameters is in the order of this theoretical decrease. In this way, the values observed during observation with no inclusion of the sample are considered closer to the real values than those obtained when sections of the resin-included samples are observed.

Table 8.3 shows the average and range values for the shape and size parameters obtained from fresh stained and resin-included samples. For both types of parameters, the results are similar to those obtained in other works for other vegetables. Area values ($0.015 mm^2$) are in the range of the values found in other woks for apple (Lewicki and Pawlak, 2005; Mayor *et al*., 2005) and carrots (Lewicki and Drzewucka-Bujak, 1998), but higher than those obtained for potatoes (Zdunek and Umeda, 2005). Roundness values (0.83) are similar to those obtained for apples (Bolin and Huxsoll 1987, Lewicki and Pawlack, 2003; Mayor *et al*., 2005)

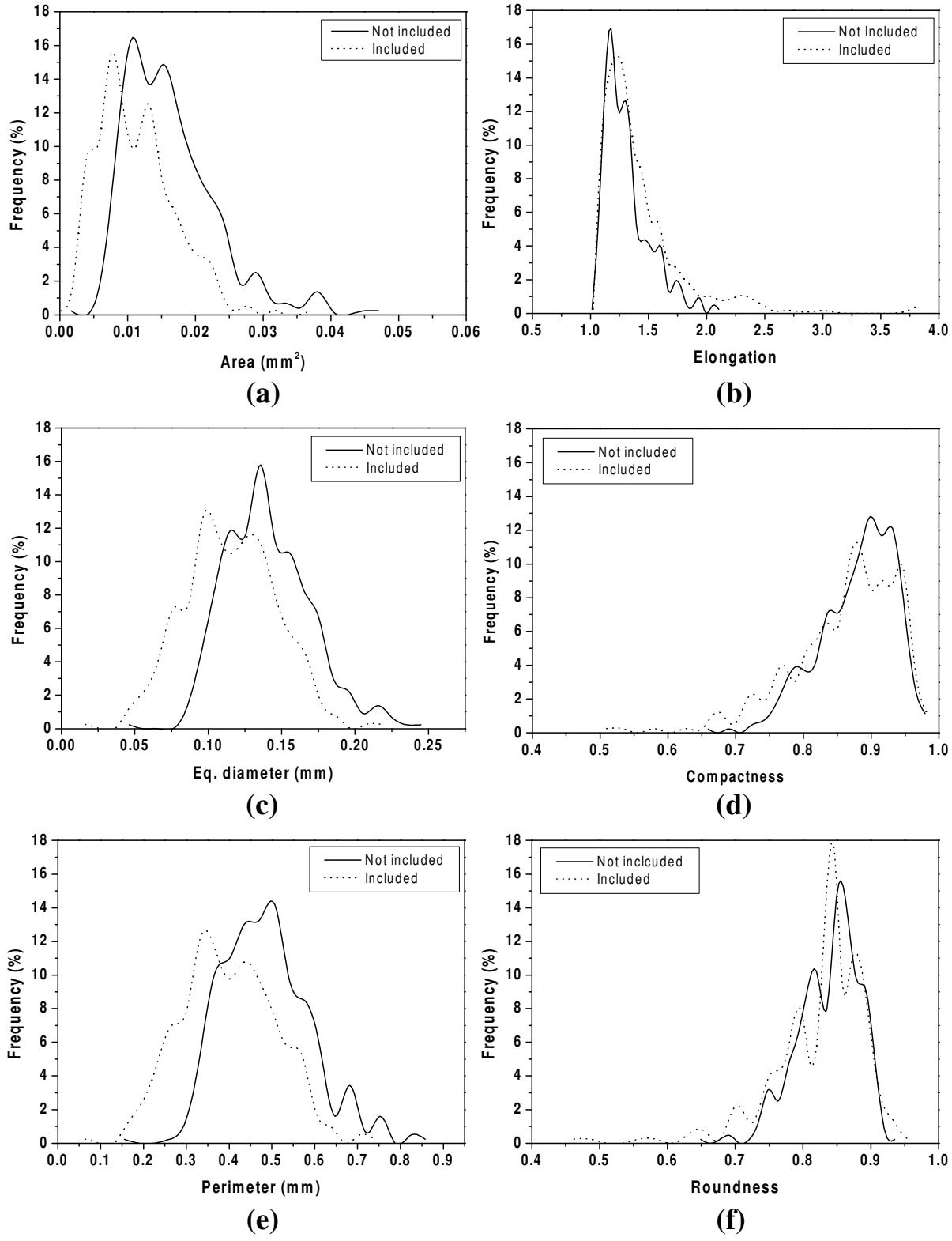

Figure 8.5. Frequency histograms for the size and shape parameters of the pumpkin cells for the two methods of sample preparation. (a) Area. (b) Elongation. (c) Perimeter. (d) Roundness. (e) Equivalent diameter. (f) Compactness.

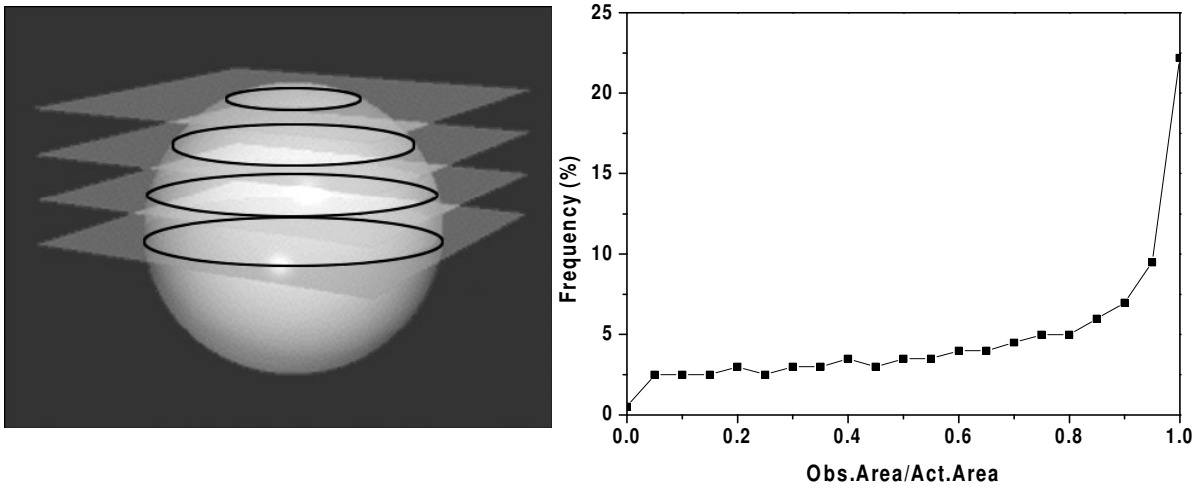

Figure 8.6. Random intersections in a sphere: (a) schematic diagram (adapted from Russ, 2004); (b) frequency distribution of the resulting areas.

Table 8.3. Size and shape parameters for pumpkin parenchymatic cells.

	Fresh cut with razor blade		Included in resin and sectioned	
Parameter	**average**	**interval**	**average**	**interval**
Area (mm^2)	0.015	0.0016-0.047	0.010	0.001-0.037
Perimeter (mm)	0.469	0.155-0.858	0.3806	0.064-0.738
Eq. Diameter (mm)	0.136	0.046-0.245	0.110	0.016-0.217
Elongation	1.299	1.013-2.104	1.358	1.024-3.835
Roundness	0.831	0.649-0.935	0.831	0.462-0.942
Compactness	0.871	0.659-0.979	0.860	0.510-0.981

Concerning the shape of the distribution curves, area, elongation compactness and roundness gave an insufficient fit to normal distributions (Kolmogorov-Smirnov tests of normality, $p<0.05$), and seem to follow a log-normal distribution. For equivalent diameter and perimeter the fit to a normal distribution was satisfactory (Kolmogorov-Smirnov test, $p>0.05$). Log-normal distributions of the cellular area have been observed for apples (Lewiki and Pawlak, 2003; Mayor *et al*., 2005), and for carrots (Lewicki and Drzewucka-

Bujak, 1998); normal distributions of cellular equivalent diameter have been observed for apple (Lewiki and Pawlak, 2003). Although all the parameters for the fresh material cannot be considered normally distributed, during the process these curves tended to normal shapes, and some part of the analysis of the data has been performed in terms of average values and standard deviations.

8.3.2. Dehydrated material.

Figure 8.7 shows cells of parenchymatic tissue with different degrees of dehydration. Initially, in the fresh material, the cells have its maximum size, and cell walls present a round and turgid aspect (Fig. 8.7 (a)).

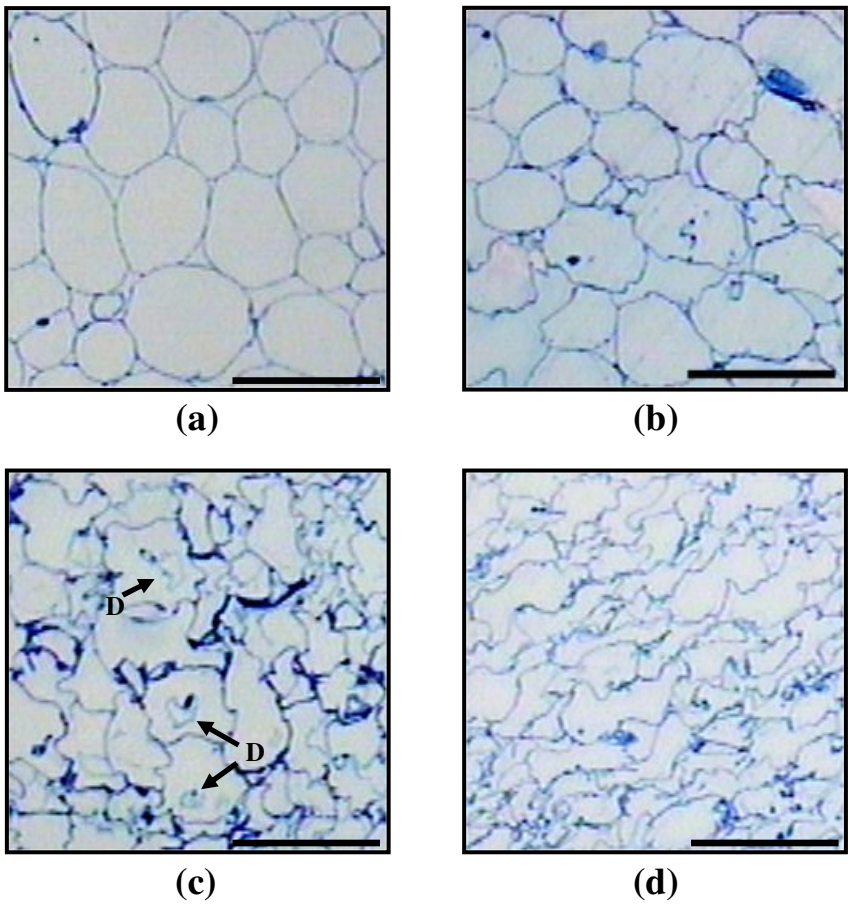

Figure 8.7. Cells of pumpkin tissue during osmotic dehydration: (a) fresh material; (b) beginning of the dehydration; (c) dehydration and plasmolysis; (d) end of the process. D= Detachment of plasma membrane (plasmolysis). Horizontal line is 0.2 mm.

Then, the samples start to dehydrate and the cell walls start to loose its initial aspect and become less round (Fig. 8.7 (b)). In a more advanced degree of dehydration, the shrinkage of cells is considerable, roundness decreases and plasmolysis is clearly observed in cells (Fig. 8.7 (c)). Very similar structural changes have been observed in light microscopy images of osmodehydrated apple in sucrose and glucose solutions (Quiles *et al.*, 2003; Nieto *et al*., 2004), showing the folding of the cell wall, plasmolysis and cellular shrinkage. In the end of the process, cells show their maximum shrinkage, maximum decrease in roundness and are highly elongated (Fig. 8.7 (d)). These different degrees of dehydration are a function of process time and the situation of the cells in the pumpkin samples, as it will be discussed in this section.

For this purpose, some samples were analyzed as commented in 8.2.3.2, in order to study the structural changes during the osmotic dehydration process. It was only possible to observe the cellular changes with the fixed-included samples, since in the not-included samples the cellular structure was not visible after the dehydration. According to this, the microphotographs of not-included samples were used to observe changes at "mesostructural" level, whereas the fixed-included samples were used to study the changes at cellular level.

Figures 8.8-8.10 show the structural changes observed during osmotic dehydration of pumpkin cylinders with 45% sucrose solutions at 25ºC. Figures 8.8 (a), 8.8 (c), 8.9 (a), 8.9 (c) and 8.10 (a) show the structural changes observed with the not included samples, whereas 8.8 (b), 8.8 (d), 8.9 (b), 8.9 (d) and 8.10 (b) show the changes observed at cellular level with the fixed-included samples.

Concerning Figures 8.8 (a), 8.8 (c), 8.9 (a), 8.9 (c) and 8.10 (a), it can be observed a dehydration front which enters in the material as the dehydration process progresses; at 0.5 hours the dehydration front is located in the external zone of the sample, whereas at nine hours of process practically the dehydration front is not observed because the entire sample has been dehydrated in all the zones of the material.

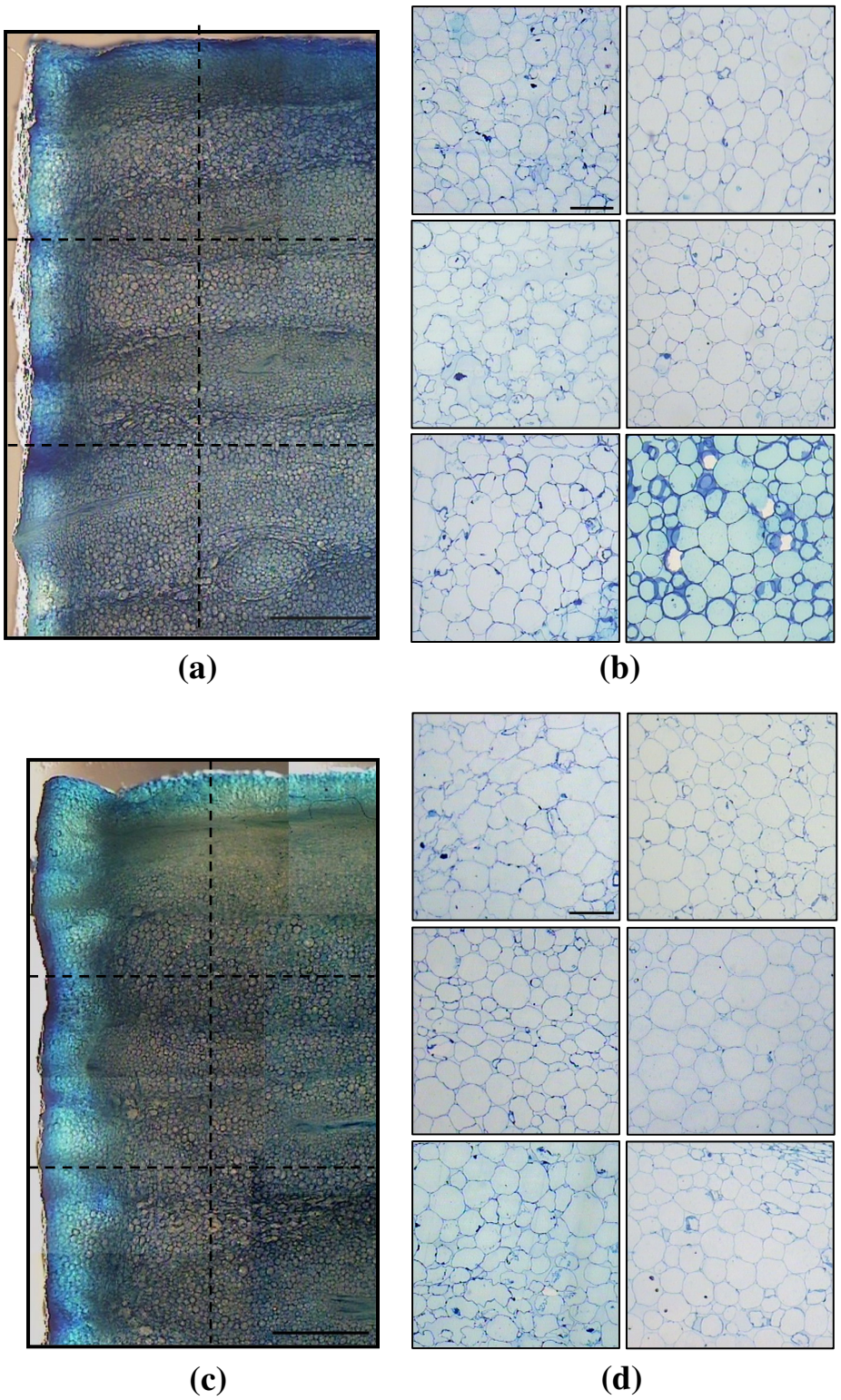

Figure 8.8. Microstructure changes during osmotic dehydration of pumpkin: (a) 0.5 hours, not included samples; (b) 0.5 hours, included samples; (c) one hour, not included samples; (d) one hour, included samples. Horizontal bar in (a) and (c) is 2 mm. Horizontal bar in (b) and (d) is 0.2 mm.

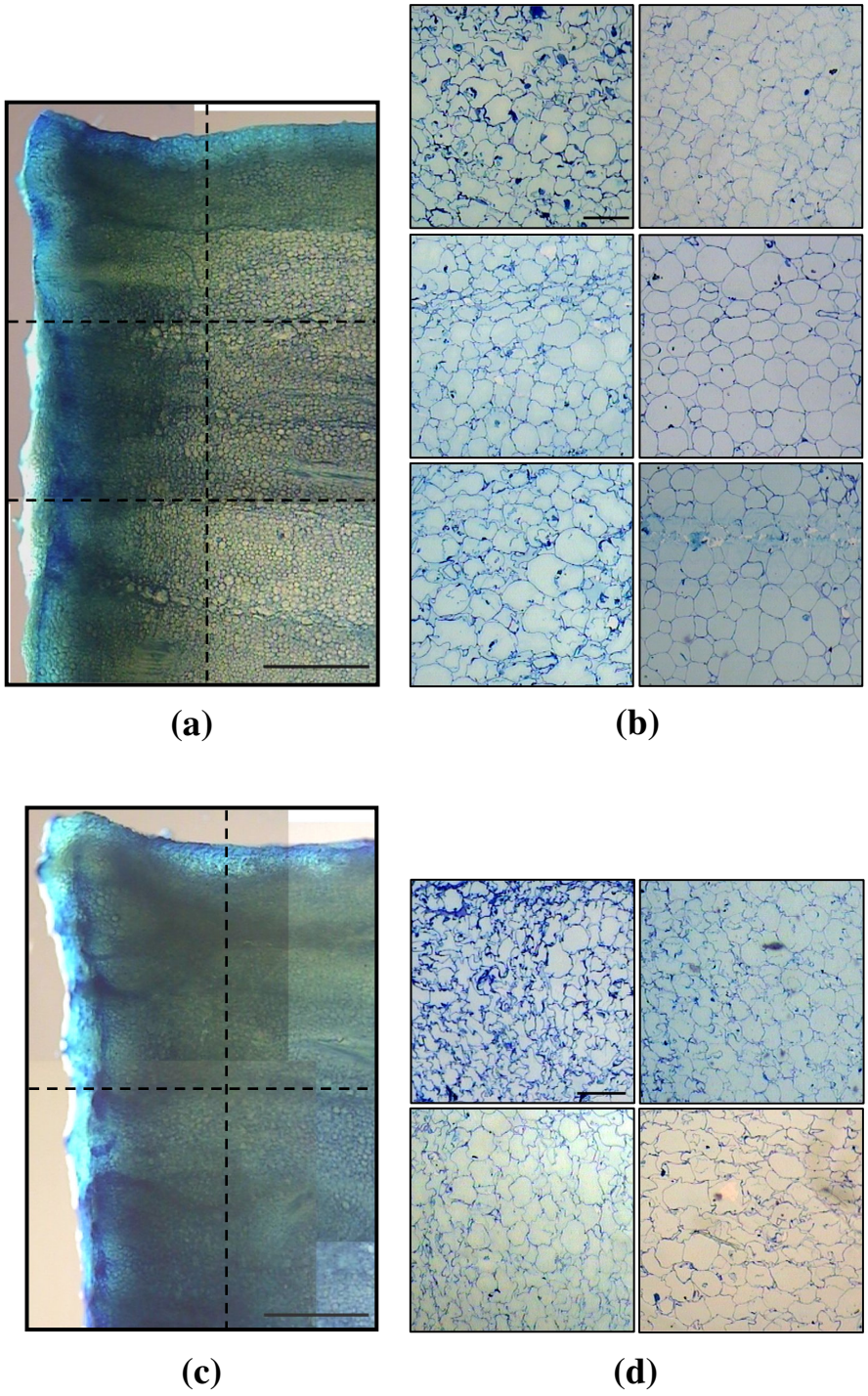

Figure 8.9. Microstructure changes during osmotic dehydration of pumpkin: (a) three hours, not included samples; (b) three hours, included samples; (c) six hours, not included samples; (d) six hours, included samples. Horizontal bar in (a) and (c) is 2 mm. Horizontal bar in (b) and (d) is 0.2 mm.

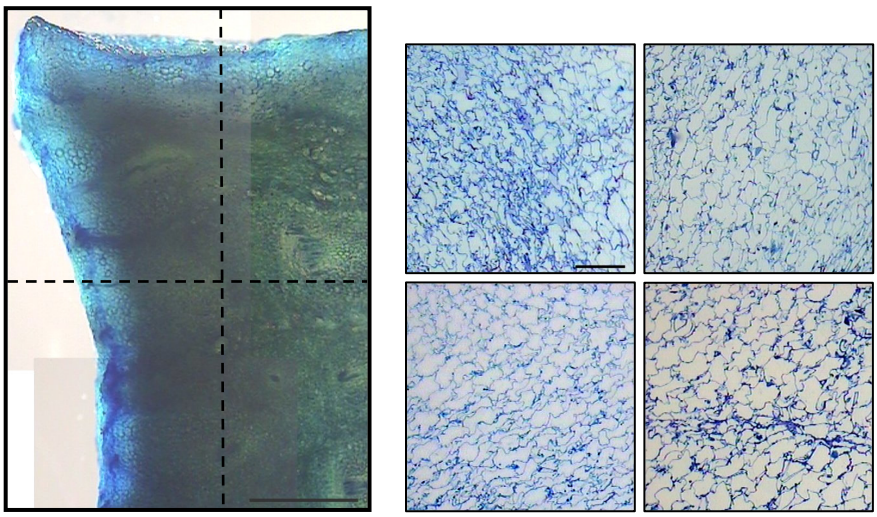

(a) (b)

Figure 8.10. Microstructure changes during osmotic dehydration of pumpkin: (a) nine hours, not included samples; (b) nine hours, included samples. Horizontal bar in (a) is 2 mm. Horizontal bar in (b) is 0.2 mm.

Observing Figures 8.8 (b), 8.8 (d), 8.9 (b), 8.9 (d) and 8.10 (b), the changes in the microstructure can be associated with the changes in the location on the dehydration front. The changes in the microstructure of the cells initially appear in the external zone of the samples, and in the inner core the cells present the characteristics observed in the fresh tissue.

At 0.5 hours and one hour of process (Figs 8.8 (b) and 8.8 (c) respectively), some slight change in cellular shape (folding of the cell walls) are observed in the external zones of the sample, whereas in the inner zones do not show alterations. At three hours of process (Fig. 8.9 (b)), shrinkage of cells, plasmolysis and folding of the cell walls are observed in the external zones of the samples, whereas the inner zones still remain unchanged, according to the existence of a no dehydrated solid core. At six hours (Fig, 8.9 (d)) the cells of the external zones are more dehydrated and the inner core starts to show some changes due to the dehydration of its cells. At nine hours (Fig. 8.10 (b)), the cells of the external zones are highly dehydrated (high degree of shrinkage, cells are wrinkled and elongated),

and the internal zone is also dehydrated but in a less accentuated way. The existence of structural profiles accompanying the compositional profiles during osmotic dehydration was also observed by Salvatori *et al.* (1998) during osmotic dehydration of apple tissue with sucrose solutions. Similarly, during convective drying of potatoes, Wang and Brennan (1995), observed that initially the changes in cellular structure (shrinkage of cells and damage of the structure) was only at the external surface of the samples; then the changes entered more in the inner of the tissue with the increase in drying time.

The analysis of shape and size parameters was performed with the microimages of fixed-included samples, since the microimages of not included samples did not allow a good observation at cellular level. Figures 8.11 and 8.12 show the histograms of frequencies and the average values obtained in the analysis of size and shape cellular parameters during dehydration, respectively. These results were obtained from the analysis of at least 400 cells at each process time. These cells comes from the six zones (four zones in the case of six and nine hours) analyzed in the sample. The same number of cells of each zone was employed in order to obtain the best representative average value of the total sample.

Concerning the size parameters (Fig. 8.11), it can be observed that the shape of the distribution curves does not change in the process. For the area and equivalent diameter, the curves suffer a shift to lower values, leading to a decrease in their average values along the process. This is in concordance with the shrinkage of the cells observed in the microphotographs. It is interesting to observe that the perimeter practically does not show change during dehydration (Fig. 8.11 (c) and (d)). Several authors have observed that the plasmatic membrane (plasmalemma) shrinks elastically during osmotic processes without folding (Segui *et al*., 2006), and it is suggested that elastic shrinkage of the cell membrane may be accompanied by an endocytosis phenomenon (Oparka *et al*., 1990). Observing the results of this work, although the cell membrane shrinks, the cell wall does not shrink during the process, and its response to the cellular shrinkage is the folding of the cell wall, affecting the shape parameters as discussed above.

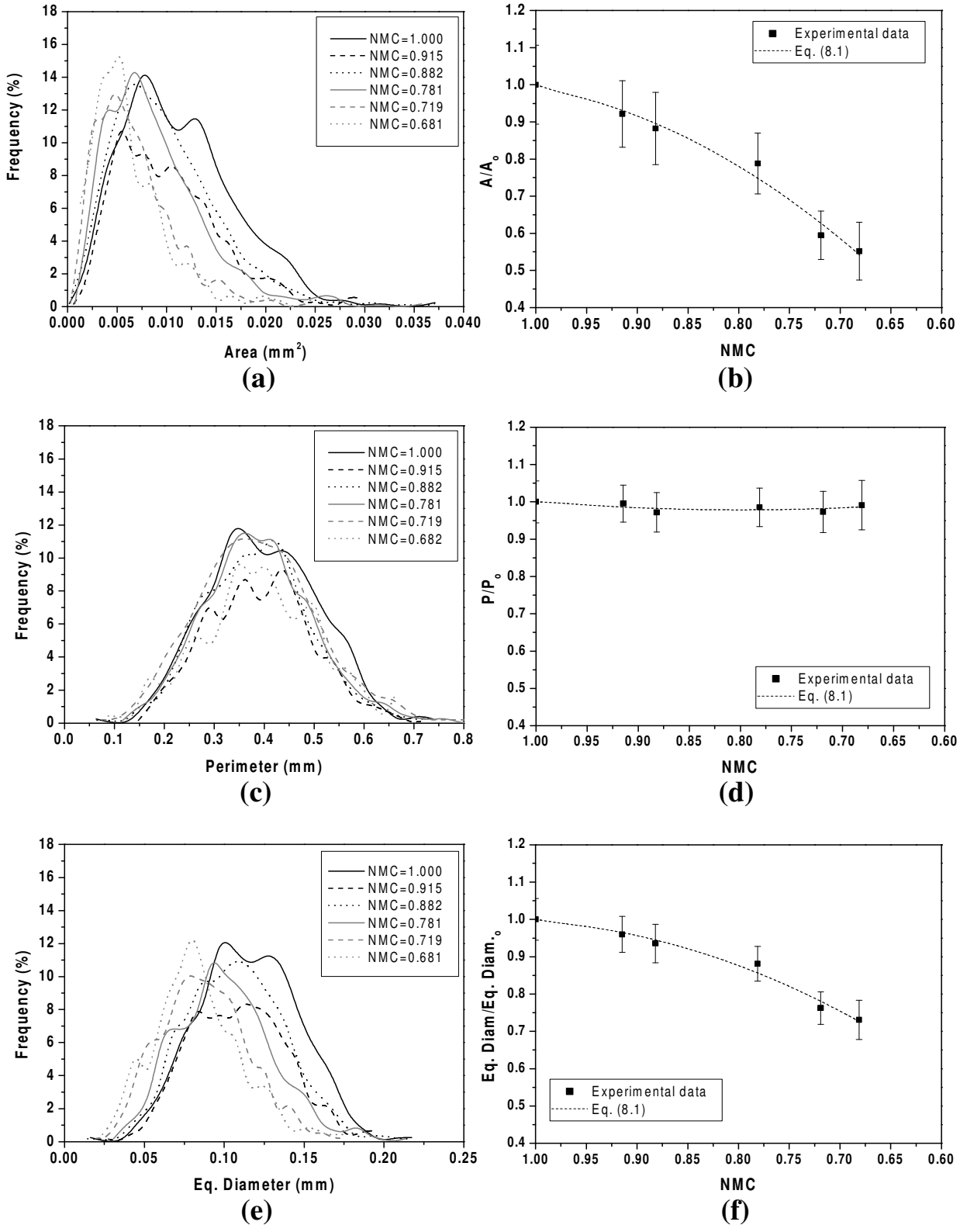

Figure 8.11. Histograms of frequencies and average values (normalized) of size parameters vs. moisture content (normalised): (a) Area histograms; (b) area averages; (c) perimeter histograms; (d) perimeter averages; (e) equivalent diameter histograms; (f) equivalent averages.

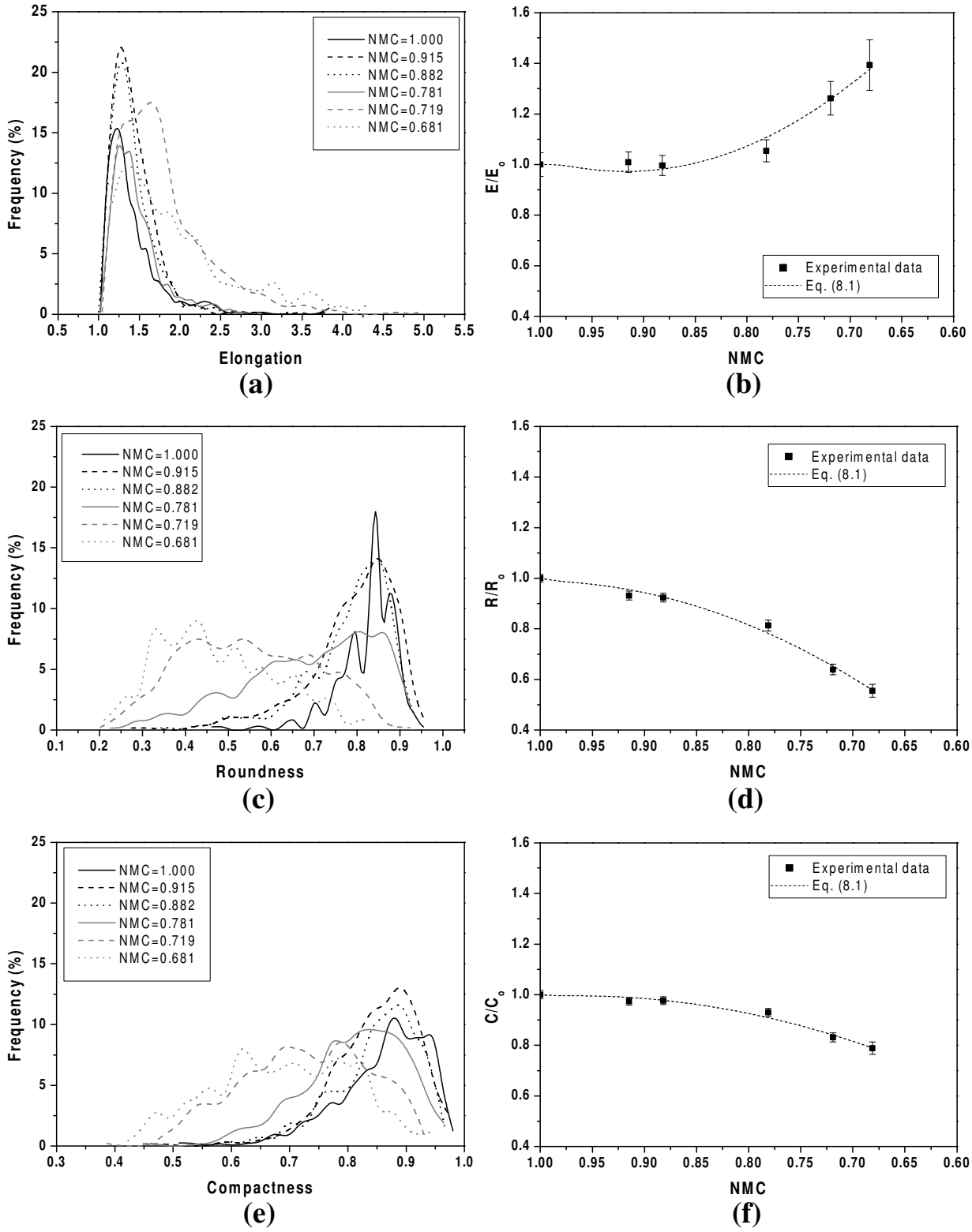

Figure 8.12. Histograms of frequencies and average values (normalized) of shape parameters vs. moisture content (normalised): (a) elongation histograms; (b) elongation averages, (c) roundness histograms; (d) roundness averages; (e) compactness histograms; (f) compactness averages.

Concerning the shape parameters (Fig. 8.12), it can be observed changes in the shape of the distribution curves and in the average values during osmotic dehydration. The values of the shape parameters are more broadly distributed when advancing in the dehydration process, changing the shape of the distribution curves to a more normal shape. The average values does not suffer important changes at the beginning of the process (up to three hours, NMC =0.882); after that, elongation increases, and roundness and compactness decrease up to the end of the process. Lewicki and Porzecka-Pawlak (2005) also observed a decrease in the roundness values of cells during osmotic dehydration of apples. Ramos *et al*. (2004) and Mayor *et al*. (2005) observed that cellular shape parameters (elongation, roundness and compactness) didn't show changes during the first stage of convective drying of grapes and apples, respectively; the last authors showed that the changes of shape factors were observed at the end of the drying process. Shrinkage of cells, folding of the cell walls and the transition from a round to an elongated shape are the cause of these changes in the shape factors.

During osmotic dehydration of food materials, it has been observed that the gain of solids is only significant in the external zones of the material (Salvatori *et al.*, 1999[b]; Mauro and Menegalli, 2003, Chenlo *et al*., 2006[b]), whereas water initially is lost in these external zones but after that attains also the inner zones of the vegetable tissue. According to this, it is expected that the changes in size and shape parameters of cells, observed in all the zones of the pumpkin tissue, are mainly due to the water loss in the material and the loss of turgor pressure of cells created by this change in the water content.

Polynomial models were employed to relate some kinetic parameters (WL, WR and NMC) with the changes in the average cellular size and shape parameters. Linear models gave a poor fit, and cubic models didn't show significant improvement in the fit compared with quadratic models, so these last ones were used for the correlation purposes. The equations used were of the type

$$Y = a + bX + cX^2 \qquad (8.1)$$

where Y is the normalized cellular factor (ratio actual value to initial value) and X is the kinetic parameter. The results of the fits are shown in Tables 8.4-8-9.

Table 8.4. Fit results of experimental data on cellular area with Eq. (8.1).

	a	b	c	R^2	ARD (%)
WL	1.00	-0.02	-1.03	0.98	2.0
WR	1.00	-0.14	-1.46	0.99	1.6
NMC	-2.43	6.37	-2.95	0.98	2.6

Table 8.5. Fit results of experimental data on cellular perimeter with Eq. (8.1).

	a	b	c	R^2	ARD (%)
WL	1.00	-0.09	0.10	0.47	0.7
WR	1.00	-0.12	0.17	0.49	0.7
NMC	1.35	-0.93	0.58	0.49	0.7

Table 8.6. Fit results of experimental data on cellular eq. diameter with Eq. (8.1).

	a	b	c	R^2	ARD (%)
WL	1.00	0.03	-0.69	0.98	1.1
WR	1.00	-0.03	-0.98	0.99	0.8
NMC	-1.27	4.36	-2.09	0.98	1.3

Table 8.7. Fit results of experimental data on cellular elongation with Eq. (8.1).

	a	b	c	R^2	ARD (%)
WL	1.00	-0.59	1.76	0.93	2.8
WR	1.00	-0.69	2.73	0.95	2.3
NMC	7.07	-13.29	7.24	0.96	2.2

Table 8.8. Fit results of experimental data on cellular roundness with Eq. (8.1).

	a	b	c	R^2	ARD (%)
WL	1.00	0.14	-1.23	0.98	2.1
WR	1.00	0.07	-1.79	0.99	1.7
NMC	-3.15	8.24	-4.09	0.99	1.7

Table 8.9. Fit results of experimental data on cellular compactness with Eq. (8.1).

	a	b	c	R^2	ARD (%)
WL	1.00	0.14	-0.70	0.97	1.2
WR	1.00	0.14	-1.05	0.98	0.9
NMC	-1.38	4.92	-2.55	0.98	1.0

In general, Eq. (8.1) shows good fits of the cellular parameters with the kinetic parameters WL, WR and NMC. The exception is the perimeter, but this is very reasonable since perimeter remains constant during the process. The quality of the fits is similar. Correlation coefficient varies from 0.93 to 0.99, and average relative deviations from 0.7 to 2.8%. Figures 8.11 and 8.12 show the predicted values of the model, when the correlations are done with normalized moisture content.

When the analysis of the cellular parameters was done in the different zones studied, some interesting results were obtained. Figure 8.13 shows the decrease in the studied parameters in the internal and the external (in contact with the osmotic solution) zones. It is observed that in the external zones the changes in all the parameters star at the beginning of the process, whereas in the internal zones the changes star only after three hours of treatment, then in both zones the changes are similar up to the end of the process.

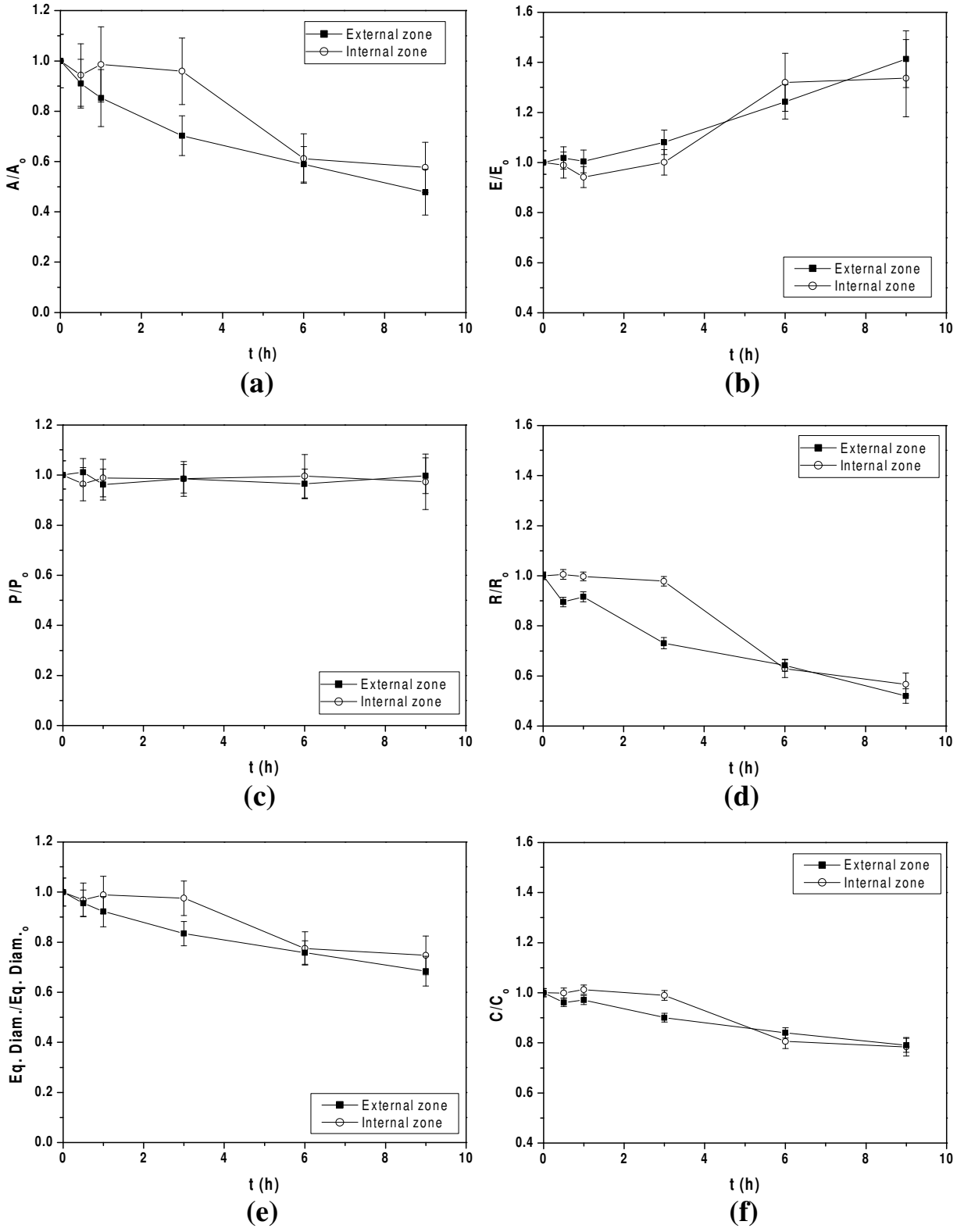

Figure 8.13. Changes in the cellular size and shape parameters in the external and internal zone of the samples during osmotic dehydration: (a) area; (b) elongation; (c) perimeter; (d) roundness; (e) equivalent diameter; (f) compactness.

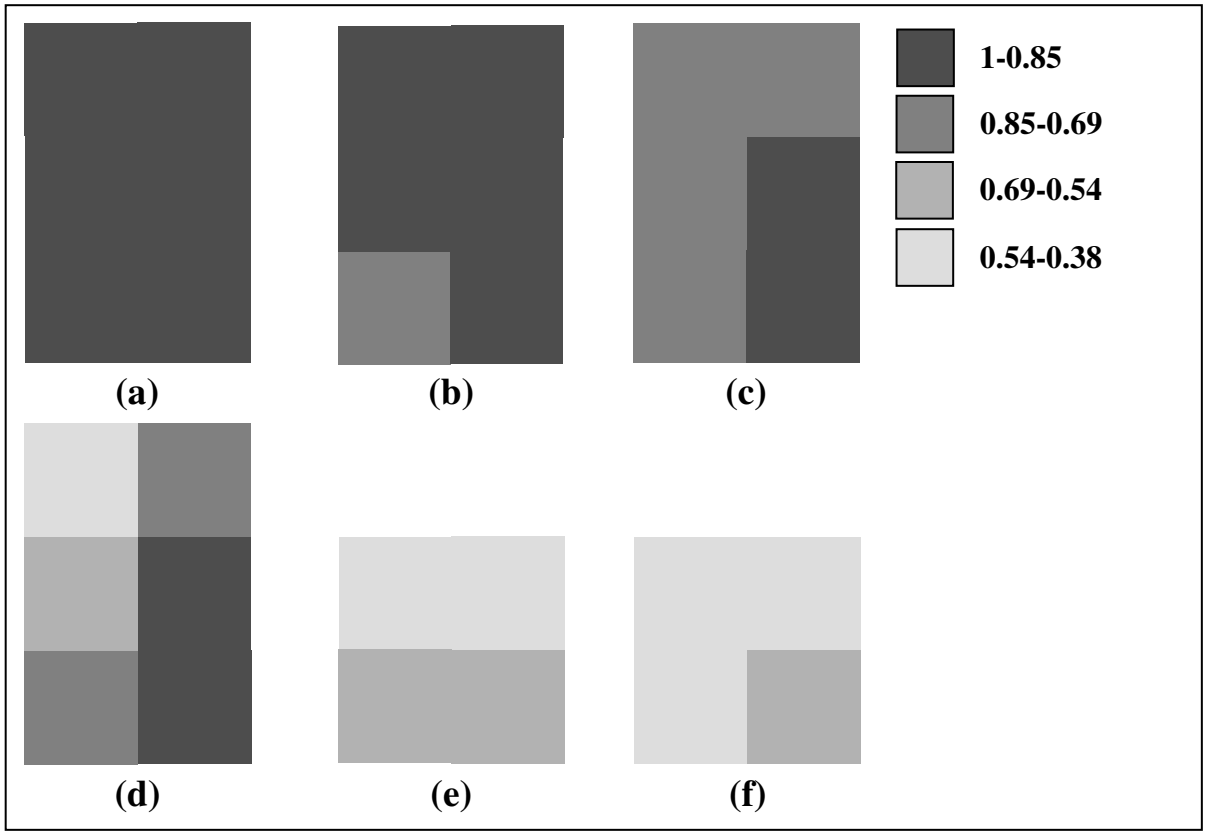

Figure 8.14. Structural profiles for the cellular area at different process times: (a) fresh material; (b) 0.5 hours; (c) one hour; (d) three hours; (e) six hours; (f) nine hours.

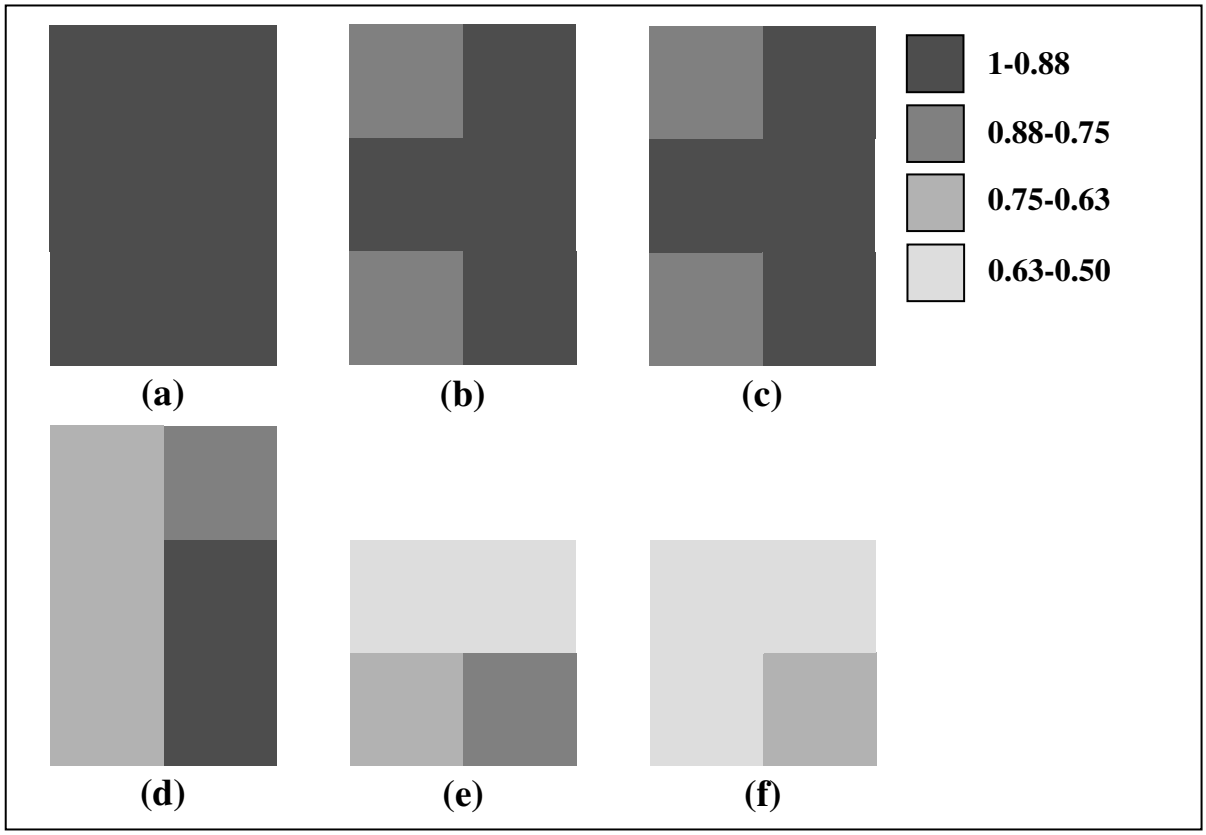

Figure 8.15. Structural profiles for the cellular roundness at different process times: (a) fresh material; (b) 0.5 hours; (c) one hour; (d) three hours; (e) six hours; (f) nine hours.

Figures 8.14 and 8.15 show the cellular area and roundness profiles at different process times, respectively. As observed before in Figure 8.13, the changes in these parameters are initially observed in the external zones of the material, and the inner solid core only suffers structural alterations after three hours of process. At nine hours, the samples have suffered changes in the entire sample, although the changes in the external zones are slightly more accentuated. As commented before, it is believed that the structural changes occur simultaneously with moisture removal. The presence of a dehydration front which enters in the material during dehydration and a solid core with the initial characteristics of the fresh material which decreases with the moisture removal is in concordance with the structural profiles observed along the dehydration process.

8.4. Conclusions

The study of the fresh parenchymatic pumpkin tissue showed that the cellular size and shape parameters are similar to those found in other vegetables, as in the case of the parenchymatic tissues of apples, carrots and potatoes. Fresh pumpkin cells show average values of 0.015 mm^2, 0.469 mm and 0.136 for cell area, cell perimeter and cell equivalent diameter, respectively; and 1.288, 0.831 and 0.871 for cellular elongation, roundness and compactness, respectively. The distribution curves for area, elongation roundness and compactness follow a lognormal distribution and those for perimeter and equivalent diameter follow a normal distribution; these curves tend to normal shapes during the dehydration process.

Osmotic dehydration causes changes in the size and shape cellular parameters of the vegetable tissue. The main phenomena observed during osmotic dehydration were shrinkage of cells, plasmolysis and folding of the cell walls. This changes lead to the decrease in cellular area, equivalent diameter, roundness and compactness; elongation of cells increased whereas the perimeter was maintained along the process.

Since sucrose penetrates only in the external zones of the tissue, it is suggested that the main cause of these microscopic changes is the water flow from the material to the osmotic solution, creating unbalances in the mechanical equilibrium of the cellular structure and decreasing the turgor pressure of the cells.

The observed changes are not homogeneously distributed in the material, and are dependent on the localization of the cells in the tissue and on the process time. It is observed that the first microstructural changes are located in the external zones of the samples in contact with the osmotic solution, whereas the inner zones of the material only suffer changes in the final stage of the process (six-nine hours). This is likely related with the moisture profiles created in the material during dehydration.

Empirical quadratic functions were used to relate the average shape and size parameters with the dehydration parameters WL, WR and NMC. The equations showed a good fit of the experimental data, leading to correlation coefficients ranging 0.93-0.99 and average relative deviations ranging 0.7 to 2.8%.

Future work has to be done to create structural models accounting for the microstructural changes during dehydration. Finite element approximations (Martins, 2006) or the use of Voronoi Tessellations (Mattea *et al*., 1989; Wenian *et al*., 1991; Mebatsion *et al*., 2006) may be some interesting approaches to this microstructural modelling. The simple empirical models obtained in this work may also be used along with the commented more complex approximations.

CHAPTER 9

CONCLUSIONS AND FUTURE WORK

CHAPTER 9. CONCLUSIONS AND FUTURE WORK

The main objective of the present work was the study and characterization of physical and structural changes of vegetable tissue during osmotic dehydration. Other objective was to predict those changes from the process conditions used. Both objectives were accomplished by the different studies presented in this work.

First of all, a material was chosen as a vegetable food model, on the basis of its availability, uniformity and typical cellular structure. The material chosen was pumpkin fruit. Additionally, the use of an osmotic process can be an interesting tool in the production of new processed products based on fresh pumpkin fruits, such as pickled vegetables or ingredients for confectionary and dairy products.

After the selection of the food model, the osmotic dehydration kinetics of pumpkin fruits were studied, varying the chemical composition of the aqueous osmotic solution (binary sucrose solutions, binary NaCl solutions and ternary sucrose/NaCl solutions), the concentration of the osmotic agents, temperature and process time. Water loss (WL), sucrose gain (SucG) and NaCl gain (NaClG) ranged from 0 to 80%, 0 to 19% and 0 to 16% of the initial sample weight, respectively, depending their value on the existing processing conditions. Ternary NaCl/sucrose solutions are preferred if the removal of water is the objective of the process, because of the high WL/SG ratio and low moisture content attained at the end of the treatment. A simple model, based on the Fick's second law of diffusion, was used to predict the changes of some kinetic parameters (water loss, solids gain (SG), weight reduction (WR) and normalized moisture content (NMC)) as a function of the process conditions (concentration and type of osmotic agent, temperature and process time). Effective coefficients of diffusion for water, sucrose and NaCl ranged from 0.29 to 4.22×10^{-9} m^2/s, 0.5 to 1.3×10^{-9} m^2/s and 0.88 to 3.3×10^{-9} m^2/s respectively, depending their value on the existing processing conditions. The experimental and predicted values showed in general a good agreement (average relative deviations lower than 8%) indicating that the model is adequate. In this way, the proposed model allows the

simulation of mass transfer processes during osmotic dehydration, and consequently it can be used as a useful tool in the design and control of the corresponding industrial operation.

This first study allowed establishing some relations between the process conditions and dehydration kinetic parameters (WL, SG, WR and NMC). This is important because the modelling of the changes in the physical properties was done as a function of this dehydration parameters in most cases (except colour changes which were related with process time), so the relation between process conditions and physical changes has to be done by means of the dehydration kinetics model.

After the dehydration kinetics, the study of the changes of some selected physical properties during osmotic dehydration was performed, namely: sorption properties, shrinkage/density/porosity, colour, mechanical properties, and microstructural changes. Sucrose solutions were used in all the studies, except in the case of shrinkage/density/porosity where binary NaCl solutions and ternary NaCl/sucrose solutions were also tested.

Concerning sorption properties, the sorption isotherms of fresh and osmotically dehydrated pumpkin samples were obtained, and experimental data was satisfactorily fitted to different models found in the literature (GAB, BET and Henderson models among others). When pumpkin parenchyma was osmotically treated, the sorption isotherm was not significantly changed compared with the non treated material. The results indicate that both products, fresh and osmotically-treated, can be stored in the same way.

A new methodology to measure the particle volume of samples with high moisture content by means of a home built gas pycnometer was developed. This technique was very important for the study of porosity changes and shrinkage during dehydration. The gas pycnometer reproducibility of 0.019%, obtained with dried porous materials, was excellent when compared with a commercial helium pycnometer. A model based on volume additivity of the material components was used to the predict particle volume of samples during dehydration, with an average relative deviation of 3%. Porosity of osmotically

dehydrated samples doubled the value for fresh samples (15%). It was possible the prediction of porosity during osmotic dehydration from predicted values of particle and bulk volume (average relative deviation of 15%).

Shrinkage (ranging from 0 to 73% of the initial volume) decreased with water loss and weight reduction during osmotic dehydration. Linear models relating the changes in bulk volume with WL and WR were successfully fitted to experimental data (average relative deviations lower than 3%). A similar relative decrease of the average values of the diameter and length of the samples along the dehydration process was observed, suggesting that shrinkage was isotropic.

Colour changes during osmotic dehydration were not very accentuated. As an average of all the tested conditions, lightness decreased ($\Delta L^* = -4.84$) whereas redness ($\Delta a^* = 2.80$), yellowness ($\Delta b^* = 4.25$) and croma ($\Delta C^* = 4.72$) increased after nine hours of treatment. Since enzymatic browning of pumpkin in contact with air was not observed, it is believed that colour changes are mainly due to pigment concentration and changes in the internal structure during dehydration. Some chemical degradation of pigments cannot be discarded. Fractional conversion models showed acceptable correlations of the changes in colour during osmotic dehydration for a*, b* and croma; the colour change rate constants for each parameter were 0.39 h^{-1}, 0.43 h^{-1} and 0.41 h^{-1} respectively. Average relative deviations were lower than 7%.

The mechanical properties of osmodehydrated pumpkin fruits were studied by means of compression tests. Fresh material showed apparent elastic modulus, failure stress and failure strain ranging from 0.96 to 2.53 MPa, 0.42 to 0.71 kPa and 250 to 630 kPa respectively. After dehydration the tissue lost its firmness (the apparent elastic modulus decreased drastically), keeping its strength (failure stress showed only a slight decrease) but became more ductile (failure strain increased). Microscopic observation before and during the compression tests allowed establishing some relations between the textural properties and the microstructure of the vegetable tissue. Firmness seems to be controlled by the turgor pressure of cells, whereas the failure properties are more related with the strength of

adhesion of the fibres composing the parenchymatic tissue. Polynomial models were used to relate the changes in the aforementioned mechanical properties with the changes in moisture content during dehydration.

.

The microstructure of fresh and osmotically dehydrated pumpkin parenchymatic tissue was studied by microscopy observation and image analysis. Fresh pumpkin cells showed average values of 0.015 mm^2, 0.47 mm and 0.14 for cell area, cell perimeter and cell equivalent diameter, respectively; and 1.29, 0.83 and 0.87 for cellular elongation, roundness and compactness, respectively. After nine hours of osmotic treatment (in 60% sucrose solutions at 25 ºC), cellular area, equivalent diameter, roundness and compactness decreased, whereas elongation of cells increased and the cellular perimeter was maintained essentially constant along the process. It was observed that the first microstructural changes are located in the external zones of the samples in contact with the osmotic solution, whereas the inner zones of the material only suffer changes in the final stage of the process (six to nine hours). This is likely related with the moisture profiles created in the material during dehydration. Quadratic functions were used to correlate the average shape and size parameters with the dehydration parameters water loss, weight reduction and normalized moisture content (average relative deviations lower than 3%).

Faced with these results, some suggestions for future work may be made:

(i) The models presented here for the physical changes are basically empirical, and depend strongly on the characteristics of the fresh product. Some efforts have to be done in order to obtain more fundamental models. Specifically, it seems interesting to model the cellular structure of plant tissue and account for this structure in the prediction of physical changes. The use of Voronoi Tessellations seems to be an interesting approach for modelling the cellular structure of plant tissues (Mattea *et al*., 1989; Mebatsion *et al*., 2006). From a polymer physics point of view, other interesting approach can be the consideration of the cellular structure as a fluid-filled foam (Georget *et al*., 2003).

(ii) Some studies can be done so as to improve the measurement of the particle volume with the presented gas pycnometer (Chapter 5). Further investigation needs to be done in order to verify the influence of the air humidity in the pressure measurements and in the sample weight loss. The operation mode of the expansion valve should as well be further investigated to assure reproducible results.

(iii) The simultaneous microscopy observation-compression test (Chapter 7) seems to be a promising technique to obtain relationships mechanical properties-structure of food materials. More work can be done with other food materials and processes in order to obtain such relations.

NOTATION

Chapter 1

a	activity	
a_w	water activity	
a*	redness	
A	food material	
b*	yellowness	
B	osmotic solution	
L*	lightness	
p_w	water vapour pressure	Pa
P	pressure	Pa
R	gas constant	J/molK
RH	relative air moisture content at equilibrium	
S	osmotic solute content	kg/kg
T	temperature	K
V	molar volume	m^3/mol
W	water content	kg/kg
x	membrane thickness	m
X	moisture content, dry basis	kg water/kg dry solid
Greek Symbols		
μ	chemical potential	J/mol
Π	osmotic pressure	Pa
Subscripts		
A	food material	
B	osmotic solution	
g	glass transition	
i	component i	
o	initial	
s	solvent	

w	water	
1	phase 1	
2	phase 2	

Superscripts

o	pure substance	

Chapter 3

a, b, c, d, e, f	empirical parameters of Eqs.(3.14), (3.15), (3.17), (3.18) and (3.19)	
ARD	average relative deviation, Eq. (3.13)	
C	concentration	kg/kg
d	diameter of the stirrer	m
D	coefficient of diffusion	m^2/s
DE	dextrose equivalent	kg/kg dry mass
E_a	activation energy	J/mol
k	constant of Eq. (3.10)	kg/kg
M	mass of substance entering or leaving the sample	kg
m	sample mass	kg
N	number of revolutions per second	s^{-1}
n	number of measurements	
NaCl	sodium chloride mass	kg
NaClG	Sodium chloride gain	kg/kg
NMC	normalized moisture content	
p	experimental and predicted values	
q	constant of Eq. (3.11)	s^{-1}
r	equivalent radius	m
R	gas constant	J/(mol·K)
R^2	square correlation coefficient	
Re	Reynolds Number	

s	solids mass	kg
SG	solids gain	kg/kg
SucG	sucrose gain	kg/kg
t	time	s
T	temperature	ºC
V	volume	m^3
v.c.	coefficient of variation	
w	water mass	kg
WL	water loss	kg/kg
WR	weight reduction	kg/kg
X	coded variable	
x	process condition, Eq. (3.12)	
y	dependent variable, Eq. (3.12)	
Greek symbols		
β	coefficient of Eq. (3.12)	
ν	kinematic viscosity	m^2/s
Subscripts		
c	calculated	
eff	effective	
eq	equilibrium	
i	experimental	
o	initial	
p	pre-exponential term	
t	at time t	
w	water	
1	sucrose concentration	
2	temperature	
3	NaCl concentration	

Chapter 4

a, b, c, d	constants of Eqs.(4.1-4.11)	
A	average residual deviation	
ARD	average relative deviation	
a_w	water activity	
n	number of measurements	
p	pressure	Pa
R	gas constant	J/(mol·K)
R^2	square correlation coefficient	
RMC	relative moisture content	
S	standard deviation	
T	temperature	K
t	time	h
X	moisture content, dry basis	kg water/kg dry solid
y	number of parameters of the model	

Subscripts

e	equilibrium
w	water

Superscripts

cal	calculated
exp	experimental
o	pure substance

Chapter 5

a	constant of Eq. (5.37)
A	defined in Eq. 5.11a
ARD	average relative deviation, Eq. (3.13)
b	constant of Eq. (5.37)
B	defined in Eq. 5.17a

c	constant of Eq. (5.37)	
D	diameter	m
E,F,G,H	defined in Eq. 5.21	
g	gravity	m/s^2
L	length	m
m	sample mass	kg
m	molality	mol/kg
M	moisture content, wet basis	kg/kg
n	number of moles	
NMC	normalized moisture content	
OD	osmotic dehydration	
p	gauge pressure	Pa
P	absolute pressure	Pa
R	universal gas constant	J/(mol/K)
R^2	square correlation coefficient	
SG	solids gain	kg/kg
T	temperature	K
V	volume	m^3
w	weight	N
WL	water loss	kg/kg
WR	weight reduction	kg/kg
Greek Symbols		
β	buoyant force	N
ε	porosity	
ρ	density	kg/m^3
σ	standard deviation	
Subscripts		
1	refers to the volume that contains the reference chamber	
2	refers to the volume that contains the sample chamber	
air	air	
atm	atmospheric	

b	bulk
cp	closed pores
e	empty
f	fluid
hep	heptane
is	insoluble solids
k	known solid volume
NaCl	sodium chloride
o	initial
om	other methods
op	open pores
p	particle
S	sample
sb	substance
sm	solid matrix
ss	initial soluble solids
suc	sucrose
T	total
w	water

Superscripts

'	refers to the measurements done with known volume solid in the sample chamber
*	refers to the measurements done with sample in the gas pycnometer

Chapter 6

a*	redness	
A	surface area	m^2
ARD	average relative deviation, Eq. (3.13)	
b*	yellowness	
C	concentration	kg/kg

C*	croma	
ΔE	total colour difference	
h*	hue	
k	colour change rate constant	h^{-1}
L*	lightness	
NMC	normalized moisture content	
r	correlation coefficient	
R^2	square correlation coefficient	
SG	solids gain	kg/kg
T	temperature	ºC
t	time	h
V	volume	m^3
v.c.	variation coefficient	
WL	water loss	kg/kg
WR	weight reduction	kg/kg
Y	colour parameter	
Subscripts		
e	equilibrium	
o	initial	

Chapter 7

a_i	regression coefficients of Eq. (7.5)	
A	contact area of compression	m^2
E_{ap}	apparent elastic modulus	Pa
F	force	N
L	height	m
NMC	normalised moisture content	
R	cylinder radius	m
R^2	square correlation coefficient	
s	cut segment for microscopy-compression tests	m

t	time	s
W	toughness	J/m^3
Y	dependent variable of Eq. (7.5)	
Greek symbols		
σ	stress	Pa
ε	Hencky strain	
Subscripts		
F	failure	
o	initial	

Chapter 8

a	constant of Eq. (8.1)	
A	area	m^2
ARD	average relative devation, Eq. (3.13)	
b	constant of Eq. (8.1)	
c	constant of Eq. (8.1)	
C	compactness	
E	elongation	
NMC	normalized moisture content	
P	perimeter	m
R^2	square correlation coefficient	
SG	solids gain	kg/kg
WL	water loss	kg/kg
WR	weight reduction	kg/kg
X	independent variable of Eq. 8.1	
Y	dependent variable of Eq. 8.1	
Subscripts		
o	initial	

REFERENCES

Acevedo, N., Schebor, C., Buera, M.P. (2006). Water-solids interactions, matrix structural properties and the rate of non-enzymatic browning. *Journal of Food Engineering, 77* (4), 1108, 1115.

Aguilera, J.M., Stanley, D.W. (1990). *Microstructural Principles of Food Processing and Engineering*. Elsevier Applied Sci. Publ.: London.

Aguilera, J.M., Cuadros, T.R., del Valle, J.M. (1998). Differential scanning calorimetry of low-moisture apple products. *Carbohydrate Polymers, 37*, 79-86.

Ahmad, S.S., Morgan, M.T., Okos, M.R. (2001). Effects of microwave on the drying, checking and mechanical strength of baked biscuits. *Journal of Food Engineering, 50*, 63-75.

Al-Muhtaseb, A.H, McMinn, W.A.M., Magee, T.R.A. (2004). Water sorption isotherms of starch powders. Part I: mathematical description of experimental data. *Journal of Food Engineering, 61* (3), 297-307.

AOAC. (1984). *Official methods of analysis*, (14th ed.). Association of Official Analytical Chemists, Virginia, USA.

Argaiz, A., Lopez-Malo, A., Palou, E., Welti, J. (1994). Osmotic dehydration of papaya with corn syrup solids. *Drying Technology, 12 (7),* 1709-1725.

Avila, I.M.L.B., Silva, C.L.M. (1999). Modelling kinetics of thermal degradation of colour in peach puree. *Journal of Food Engineering, 39*, 161-166.

Azoubel, P.M., Murr, F.E.X. (2004). Mass transfer kinetics of osmotic dehydration of cherry tomato. *Journal of Food Engineering, 61*, 291-295.

Azuara, E., Cortes, R., Garcia, H.S., Beristain, C.I. (1992). Kinetic model for osmotic dehydration and its relationship with Fick's second law. *International Journal of Food Science and Technology*, 27, 409-418.

Azuara, E., Garcia, H.S., Beristain, C.I. (1996). Effect of the centrifugal force on osmotic dehydration of potatoes and apples. *Journal of Food Engineering, 29*(2), 195-199.

Balaban, M. (1989). Effect of volume change in foods on the temperature and moisture content predictions of simultaneous heat and moisture transfer models. *Journal of Food Process Engineering, 12*, 67-88.

Barat, J.M., Fito, P., Chiralt, A. (2001). Modeling of simultaneous mass transfer and structural changes in fruit tissues. *Journal of Food Engineering, 49*, 77-85.

Bawa, A.S., Gujral, H.S. (2000). Effect of osmotic agents on the drying behaviour and product quality in raisin processing. *Journal of Scientific and Industrial Research, 59* (1), 63-66.

Bell, L.N., Labuza, T.P. (2000). Moisture sorption: *Practical aspects of isotherm measurements and use* (2nd ed.). American Association of cereal Chemists: St. Paul, MN.

Boente, G., González, H.H.L., Martínez, E.J., Pollio, M.L., Resnik, S.L. (1996). Sorption isotherms of corn. Study of mathematical models. *Journal of Food Engineering, 29*, 115-128.

Bolin, H.R., Huxsoll, C.C., Jackson, R. (1983). Effect of osmotic agents and concentration on fruit quality. *Journal of Food Science, 48* (1), 202-205.

Bolin, H.R., Huxsoll, C.C. (1987). Scanning electron microscope/image analyzer determination of dimensional postharvest changes in fruit cells. *Journal of Food Science, 52* (6), 1649-1650, 1698.

Bouhon, P., Collignan, A., Rios, G.M., Raoult-Wack, A.L. (1998). Soaking process in ternary liquids: experimental study of mass transport under natural and forced convection. *Journal of Food Engineering, 37*, 451-469.

Brennan, J.G. (1994). *Food dehydration: a dictionary and guide*. Elsevier: Oxford.

Brunauer, S., Emmett, P.H., Teller, E. (1938). Adsorption of gases in multimolecular layers. *Journal of the American Chemical Society*, *60*, 309-319.

Brunauer, S., Deming, L.S., Deming, W.E., Troller, E. (1940). On the theory of Van der Waals adsorption of gases. *Transactions of the American Society of Agricultural Engineering, 41*, 1755-1760.

Calzada, J.F., Peleg, M. (1978). Mechanical interpretation of compressive stress-strain relationships of solid foods. *Journal of Food Science, 43*, 1087-1092.

Chen, C. (2002). Sorption isotherms of sweet potato slices. *Biosystems Engineering, 83* (1), 85-95.

Cheng, J., Yang, Z.R., Chen, H.Q. (2002). Analytical solutions for the moving interface problem in freeze-drying with or without back heating. *Drying Technology, 20* (3), 553-567.

Chenlo, F., Moreira, R., Pereira, G., Ampudia, A. (2002). Viscosities of aqueous solutions of sucrose and sodium chloride of interest in osmotic dehydration processes. *Journal of Food Engineering, 54*(4), 347-352.

Chenlo, F., Moreira, R., Fernández-Herrero, C., Vázquez, G. (2006[a]). Mass transfer during osmotic dehydration of chesnut using sodium chloride solutions. *Journal of Food Engineering, 73* (2), 164-173.

Chenlo, F., Moreira, R., Fernandez-Herrero, C., Vázquez, G. (2006[b]). Experimental results and modeling of the osmotic dehydration kinetics of chesnut with glucose solutions. *Journal of Food Engineering 7*4, 324-334.

Chiralt A., Martínez-Navarrete, N., Martínez-Monzó, J., Talens, P., Moraga, G., Ayala, A., Fito, P. (2001). Changes in mechanical properties throughout osmotic processes. Cryoprotectant effect. *Journal of Food Engineering, 49*, 129-135.

Chirife, J., Boquet, R., Ferro-Fontán, C., Iglesias, H.A. (1983). A new model for describing the water sorption isotherm of foods. *Journal of Food Science*, *48* (4), 1382-1383.

Contreras, C., Martin, M.E., Martinez-Navarrete, N., Chiralt, A. (2005). Effect of vacuum impregnation and microwave application on structural changes which occurred during air-drying of apple. *LWT-Food Science and Technology, 38*, 471-477.

Corzo, O., Bracho, N. (2005). Osmotic dehydration kinetics of sardine sheets using Zugarramurdi and Lupin model. *Journal of Food Engineering, 66* (1), 51-56.

Crank, J. (1975). *The mathematics of diffusion* (2nd ed.). Oxford University Press, New York.

Cui, Z.W., Xu, S.Y., Sun, D.W. (2003). Dehydration of garlic slices by combined microwave-vacuum and air drying. *Drying Technology, 21* (7), 1173-1184.

Cunha, L.M., Oliveira, F.A.R., Aboim, A.P., Frias, J.M., Pinheiro-Torres, A. (2001). Stochastic approach to the modelling of water losses during osmotic dehydration and improved parameter estimation. *International Journal of Food Science and Technology, 36*, 253-262.

Day, L.C. (1964). A device for measuring voids in porous materials. *Agricultural Engineering*, *45*(1), 36-37.

Del Valle, J.M., Cuadros, T.R.M., Aguilera, J.M. (1998[a]). Glass transitions and shrinkage during drying and storage of osmosed apple pieces. *Food Research International, 31* (3), 191-204.

Del Valle, J.M., Aránguiz, V., Díaz, L. (1998[b]). Volumetric procedure to assess infiltration kinetics and porosity of fruits by applying a vacuum pulse. *Journal of Food Engineering*, *38*, 207-221.

Dixon, G.M., Jen, J.J. (1977). Changes of sugars and acids of osmovac-dried apple slices. *Journal of Food Science*, 42 (4), 1126-1127.

Doehlert, D.H. (1970). *Applied Statistics, 19*, 231-239.

Dullien, F.A.L. (1992). *Porous media. Fluid transport and pore structure* (2nd ed.). Academic Press: San Diego.

Edwards, M. (1999). Vegetables and fruit. In A.J. Rosenthal (Ed.), *Food texture. Measurement and Perception* (pp. 259-281). Aspen Publishers: Gaithersburg, Maryland.

Ensminger, M.E., Ensminger, A.H., Konlade, J.E., Robson, J.R.K. (1995). *The concise encyclopedia of foods and nutrition*. CRC Press: Boca Raton, Florida, USA.

Escriche, I., Garcia-Pinchi, R., Carot, J.M., Serra, J.A. (2002). Comparison of must and sucrose as osmotic solutions to obtain high quality minimally processed kiwifruit (*Actinida chinensis, P.)* slices. *International Journal of Food Science and Technology, 37*, 87-95.

Falade, K.O., Adetunji, A.I., Aworth, O.C. (2003). Adsorption isotherm and heat of sorption of fresh- and osmo-oven dried plantain slices. *European Food Research and Technology, 217*, 230-234.

FAOSTAT data (2005). FAO Statistical Databases. Available online in: http://faostat.fao.org. Last accessed June 2005.

Femenia, A., Sanchez, E.S., Simal, S., Rosello, C. (1998). Modification of cell wall composition of apricots (*Prunus armeniaca*) during drying and storage under modified atmospheres. Journal of Agricultural and Food Chemistry, 46, 5248-5253.

Fernandez, L., Castillero, C., Aguilera, J.M. (2005). An application of image analysis to dehydration of apple discs. *Journal of Food Engineering, 67*, 185-193.

Ferrando, M., Spiess, W.E.L. (2001). Cellular response of plant tissue during the osmotic treatment with sucrose, maltose, and trehalose solutions. *Journal of Food Engineering, 49*, 115-127.

Fito, P. (1994). Modelling of vacuum osmotic dehydration of food. *Journal of Food Engineering, 22* (1-4), 313-328.

Forni, E., Polesello, A., Torreggiani, D. (1993). Changes in anthocyanins in cherries (*Prunus Avium*) during osmodehydration, pasteurization and storage. *Food Chemistry*, 48 (3), 295-299.

Fortes, M., Okos, M.R. (1980). Changes in physical properties of corn during drying. *Transactions of the ASAE*, *23* (4), 1004-1008.

Francis, F.J., Clydesdale, F.M. (1975). Food colorimetry: theory and applications. The Avi Publishing Company, Inc.: Westport, Connecticut.

Francis, F.J. (2005). Colorimetric properties of foods. In M.A. Rao, S.S.H. Rizvi, A.K. Datta (Eds.), *Engineering Properties of Foods* (3rd. Ed.). Taylor and Francis Group: Boca Raton, US.

Genin, N., Rene, F. (1995). Analyse du role de la transition vitreause dans les procedes de conservation agro-alimentaire. *Journal of Food Engineering, 26*, 391-407.

Georget, D.M.R., Smith, A.C., Waldron, K.W. (2003). Modelling of carrot tissue as a fluid-filled foam. *Journal of Materials Science, 38*, 1933-1938.

Gerelt, B, Ikeuchi, Y., Suzuki, A. (2000). Meat tenderization by proteolytic enzimes after osmotic dehydration. Meat Science, 56 (3), 311-318.

Giangiacomo, R., Torreggiani, D., Abbo, E. (1987). Osmotic dehydration of fruit. Part I: sugar exchange between fruit and extracting syrup. *Journal of Food Processing and Preservation, 11*, 183-195.

Giraldo, G., Talens, P., Fito, P., Chiralt, A., (2003). Influence of sucrose solution concentration on kinetics and yield during osmotic dehydration of mango. *Journal of Food Engineering, 58* (1), 33-43.

Gogoi, B.K., Alavi, S.H., Rizvi, S.S.H. (2000). Mechanical properties of protein-stabilized starch-based supercritical fluid extrudates. *International Journal of Food Properties*, *3* (1), 37-58.

Gogus, F., Wedzicha, B.L., Lamb, J. (1998). Modelling of Maillard reaction during the drying of a model matrix. *Journal of Food Engineering, 35*, 445-458.

Greenspan, L. (1977). Humidity fixed points of binary saturated aqueous solutions. *Journal of Research of the National Bureau of Standards, 81A*, 89-96.

Greve, L.C., Shackel, K.A., Ahmadi, H., McArdle, R.N., Gohlke, J.R., Labavitch, J.M. (1994[a]). Impact of heating on carrot firmness: contribution of cellular turgor. *Journal of Agricultural and Food Chemistry, 42*, 2896-2899.

Greve, L.C., McArdle, R.N., Gohlke, J.R., Labavitch, J.M. (1994[b]). Impact of heating on carrot firmness: changes in cell wall components. *Journal of Agricultural and Food Chemistry, 42*, 2900-2906.

Gupta, P., Ahmed, J., Shivhare, U.S., Raghavan, G.S.V. (2002). Drying characteristics of red chilli. *Drying Technology, 20* (10), 1975-1987.

Haard, N.F. (1985). Characteristics of edible plant tissues. In O.R. Fennema (Ed.) *Food Chemistry* (2nd E.). Marcel Dekker, Inc.: New York.

Halsey, G. (1948). Physical adsorption on non-uniform surfaces. *Journal of Chemical Physics, 16* (10), 931-937.

Hawkes, J., Flink, J.M. (1978). Osmotic dehydration of fruit slices prior to freeze dehydration. *Journal of Food Processing and Preservation, 2*, 265-284.

Henderson, S.M. (1952). A basic concept of equilibrium moisture content. *Agricultural Engineering, 33* (2), 29-32.

Hills, B.P., Remigereau, B. (1997). NMR studies of changes in subcellular water compartmentation in parenchyma apple tissue during drying and freezing. *International Journal of Food Science and Technology*, *32*, 51-61.

Hofsetz, K., Lopes, C.C., Hubinger, M.D., Mayor, L., Sereno, A.M. (2006). Effect of high temperature on shrinkage and porosity of crispy dried bananas. In (G. Gutierrez Ed.) *Food Engineering: Integrated Approaches*. Springer: New York. (in press)

Hoover, M.W., Miller, N.C. (1975). Factors influencing impregnation of apple slices and development of a continuous process. *Journal of Food Science, 40* (4), 698-700.

Horobin, R.W., Kierman, J.A. (2002). *Conn's biological stains* (10th Ed.). BIOS Scientific Publishers: Oxford.

Hougen, O.A., Watson, K.M., Ragatz, R.A. (1954). *Chemical Process Principles. Part II: Thermodynamics* (2nd. ed.). John Wiley & Sons Inc.: New York.

Hough, G., Chirife, J., Marini, C. (1993). A simple model for osmotic dehydration of apples. *Lebensmittel Wissenschaft und Technologie, 26* (2), 151-156.

Hutchings, J.B. (1999). *Food color and appearance* (second edition). Aspen Publishers, Inc.: Maryland.

Iglesias, H.A., Chirife, J. (1982). *Handbook of food isotherms: water sorption parameters for food and food components*. Academic Press: New York.

INE data (2005). Estatísticas agrícolas 2003: Produção vegetal. Available online in: http://www.ine.pt/prodserv/quadros/quadro.asp. Last accessed June 2005.

Iyota, H., Nishimura, N., Onuma, T., Nomura T., (2001). Drying of sliced raw potatoes in superheated steam and hot air. *Drying Technology, 19* (7), 1411-1424.

Jayaraman, K. S., Das Gupta, D. K., Babu Rao, N. (1990). Effect of pretreatment with salt and sucrose on the quality and stability of dehydrated cauliflower. *International Journal of Food Science and Technology, 25*, 47–60.

Jayaraman, K.S., Das Gupta, D.K. (1992). Dehydration of fruits and vegetables: recent developments in principles and techniques. *Drying Technology*, *10* (1), 1-50.

Jayaraman, K.S., Das Gupta, D.K (1995). Drying of fruits and vegetables. In A.S. Mujumdar (Ed.), *Handbook of Industrial drying, Vol. I* (2nd Ed.) (pp. 643-690). Marcel Dekker Inc.: New York.

Jun, H.I., Lee, C.H., Song, G.S., Kim, Y.S. (2006). Characterization of the pectic polysaccharides from pumpkin peel. *LWT - Food Science and Technology*, 39 (5), 554-561.

Karathanos, V., Anglea, S., Karel, M. (1993). Collapse of structure during drying of celery. *Drying Technology, 11* (5), 1005-1023.

Keetels, C.J.A.M., Visser, K.A., van Vliet, T., Jurgens, A., Walstra, P. (1996). Structure and mechanics of starch bread. *Journal of Cereal Science, 24*, 15-26.

Keey, R.B. (1978). *Introduction to industrial drying operations*. Pergamon: New York.

Keey, R.B. (1992). *Drying of loose and particulate materials.* Hemisphere Publishing Corporation: New York.

Khraisheh, M.A.M., McMinn, W.A.M., Magee, T.R.A. (2004). Quality and structural changes in starchy foods during microwave and convective drying. *Food Research International, 37*, 497-503.

Kim, M.H., Toledo, R.T. (1987). Effect of osmotic dehydration and high temperature fluidized bed drying on properties of dehydrated rabbiteye blueberries. *Journal of Food Science, 52* (4), 980-984, 989.

Kohyama, K., Sasaki, T., Hayakawa, F., Hatakeyama, E. (2004). Effects of cross-sectional area on human bite studied with raw carrot and surimi gel. *Bioscience Biotechnology and Biochemistry, 68* (10), 2104-2110.

Kowalska, H., Lenart, A. (2001). Mass exchange during osmotic pretreatment of vegetables. *Journal of Food Engineering*, *49*, 137-140.

Krokida, M.K., Maroulis, Z.B. (1997). Effect of drying method on shrinkage and porosity. *Drying Technology, 15* (10), 2441-2458.

Krokida, M.K., Tsami, E., Maroulis, Z.B. (1998). Kinetics on color changes during drying of some fruits and vegetables. *Drying Technology, 16*, 667-685.

Krokida, M.K., Kiranoudis, C.T., Maroulis, Z.B., Marinos-Kouris, D. (2000[a]). Effect of pretreatment on color of dehydrated products. *Drying Technology, 18* (6), 1239-1250.

Krokida, M.K., Karathanos, V.T., Maroulis, Z.B. (2000[b]). Compression analysis of dehydrated agricultural products. *Drying Technology, 18* (1-2), 395-408.

Krokida, M.K., Karathanos, V.T., Maroulis, Z.B. (2000[c]). Effect of osmotic dehydration on viscoelastic properties of apple and banana. *Drying Technology, 18* (4-5), 951-966.

Krokida, M.K., Kiranoudis, C.T., Maroulis, Z.B., Marinos-Kouris, D. (2000[d]). Drying related properties of apple. *Drying Technology, 18* (6), 1251-1267.

Krokida, M.K., Karathanos, V.T., Maroulis, Z.B. (2000[e]). Effect of osmotic dehydration on color and sorption characteristics of apple and banana. *Drying Technology, 18* (4-5). 937-950.

Labuza, T.P. (1970). Properties of water as related to the keeping quality of foods. In *Proceedings of the third Intern. Conf. Food Sci. and Technol. SOS 70.* Institute of Food Technologists: Washington.

Labuza, T.P. (1980). The effect of water activity on reaction kinetics of food deterioration. *Food Technology, 4*, 36-41, 59.

Laza, M., Scanlon, M.G., Mazza, G. (2001). The effect of tuber pre-heating temperature and storage time on the mechanical properties of potatoes. *Food Research International*, 34, 659-667.

Lazarides, H.N., Katsanidis, E., Nickolaidis, A. (1995[a]). Mass transfer kinetics during osmotic preconcentration aiming at minimal solid uptake. *Journal of Food Engineering, 25*, 151-166.

Lazarides, H.N., Nickolaidis, A., Katsanidis, E. (1995[b]). Sorption changes induced by osmotic preconcentration of apple slices in different osmotic media. *Journal of Food Science, 60* (2), 348-350,359.

Lazarides, H.N., Mavroudis, N. (1996). Kinetics of osmotic dehydration of a highly shrinking vegetable tissue in a salt-free medium. *Journal of Food Engineering*, 30, 61-74.

Lazarides, H.N., Gekas, V., Mavroudis, N. (1997). Apparent mass diffusivities in fruit and vegetable tissues undergoing osmotic processing. *Journal of Food Engineering*, *31*, 315-324.

Le Maguer, M., Mazzanti, G., Fernandez, C. (2002). The cellular aproach in modeling mass transfer in fruit tissues. In J. Welti-Chanes, G.V. Barbosa-Cánovas, J.M. Aguilera (Eds.), *Engineering and food for the 21st Century* (217-234). CRC Press LLC, Boca Raton.

Lenart, A., Flink, J.M. (1984). Osmotic dehydration of potato I. Criteria for the end-point of the osmosis process. *Journal of Food Technology, 19* (1), 45-63.

Lenart, A., Lewicki, P., Karandys, S. (1993). Kinetics of osmotic dehydration of pumpkin. In *Proceedings of the 5th seminar "Properties of water in foods",* Warschau, Poland, 127-143.

Levi, G., Karel, M. (1995). Volumetric shrinkage (collapse) in freeze-dried carbohydrates above their glass transition temperature. *Food Research International, 28* (2), 145-151.

Lewicki, P.P., Lenart, A. (1995). Osmotic dehydration of fruits and vegetables. In A.S. Mujumdar (Ed.), *Handbook of Industrial drying, Vol. I* (2nd Ed.) (pp. 691-713). Marcel Dekker Inc.: New York.revisar año. Caps 1.1 y 1.2.

Lewicki, P., Wolf, W. (1995). Rheological properties of raisins: Part II. Effect of water activity. *Journal of Food Engineering, 26*, 29-43.

Lewicki, P.P., Duszczyk, E. (1998). Color change of selected vegetables during convective air drying. *International Journal of Food Properties, 1* (3), 263-273.

Lewicki, P.P., Drzewucka-Bujak, J. (1998). Effect of drying on tissue structure of selected fruits and vegetables. In *Proceedings of the 11th International Drying Symposium (IDS' 98)*, Halkidiki, Greece.

Lewicki, P.P., Pawlak, G. (2003). Effect of drying on microstructure of plant tissue. *Drying Technology*, *21* (4), 657-683.

Lewicki, P.P., Jakubczyk, E. (2004). Effect of hot air temperature on mechanical properties of dried apples. *Journal of Food Engineering, 64*, 307-314.

Lewicki, P.P., Porzecka-Pawlak, R. (2005). Effect of osmotic dewatering on apple tissue structure. *Journal of Food Engineering, 66*, 43-50.

Lide, D.R., (2005). CRC Handbook of Chemistry and Physics., 85th Edition. *CRC Press*. Boca Raton, FL., USA.

Lin, T.M., Durance, T.D., Scaman, C.H. (1998). Characterization of vacuum microwave, air and freeze dried carrot slices. *Food Research International, 31* (2), 111-117.

Lozano, J.E., Rotstein, E., Urbicain, M.J. (1980). Total porosity and open-pore porosity in the drying of fruits. *Journal of Food Science*, *45*, 1403-1407.

Lozano, J.E., Rotstein, E., Urbicain, M.J. (1983). Shrinkage, porosity and bulk density of foodstuffs at changing moisture contents. *Journal of Food Science, 48*, 1497-1502, 1553.

Lozano, J.E., Drudis-Biscarri, R., Ibarz-Ribas, A. (1994). Enzymatic browning in apple pulps. *Journal of Food Science, 59* (3), 564-567.

Luscher, C., Schlüter, O., Knorr, D. (2005). High pressure-low temperature processing of foods: impact on cell membranes, texture, color and visual appearance of potato tissue. *Innovative Food Science and Emerging Technologies, 6* (1), 59-71.

Magee, T.R.A., Hassaballah, A.A., Murphy, W.R. (1983). Internal mass transfer during osmotic dehydration of apple slices in sugar solutions. *Irish Journal of Food Science and Technology,* 7, 147-155.

Makower, B., Dye, W.B. (1956). Equilibrium moisture content and crystallization of amorphous sucrose and glucose. *Journal of Agricultural and Food Chemistry, 4* (1), 72-76.

Mandala, I.G., Anagnostaras, E.F., Oikonomou, C.K. (2005). Influence of osmotic dehydration conditions on apple air-drying kinetics and their quality characteristics. *Journal of Food Engineering, 69*, 307-316.

Mandl, A., Reich, G., Lindner, W. (1999). Detection of adulteration of pumpkin seed oil by analysis of content and composition of specific Delta 7-phytosterols. *European Food Research and Technology, 209* (6): 400-406

Marcos, B., Esteban, M.A., López, P., Alcalá, M., Gómez, R., Espejo, J., Marcos, A, (1997). Monolayer values at 30 degrees C of various spices as computed by the BET and GAB models. *Zeitschrift für Lebensmitteluntersuchung und -Forschung A, 204* (2), 109-112.

Martins, R.C. (2006). Simple finite volumes and finite elements procedures for food quality and safety simulations. *Journal of Food Engineering, 73* (4), 327-338.

Mattea, M., Urbicain, M.J., Rotstein, E. (1989). Computer model of shrinkage and deformation of cellular tissue during dehydration. *Chemical Engineering Science, 44* (12), 2853-2859.

Matuska, M., Lenart, A., Lazarides, H.N. (2006). On the use of edible coatings to monitor osmotic dehydration kinetics for mimimal solids uptake. *Journal of Food Engineering*, *72*, 85-91.

Mauro, M.A., Tavares, D.D., Menegalli, F.C. (2002). Behavior of plant tissue in osmotic solutions. *Journal of Food Engineering, 56*, 1-15.

Mauro, M.A., Menegalli, F.C. (2003). Evaluation of water and sucrose diffusion coefficients in potato tissue during osmotic concentration. *Journal of Food Engineering*, *57*, 367-374.

Mavroudis, N.E., Gekas, V., Sjöholm, I. (1998[a]). Osmotic dehydration of apples – Effects of agitation and raw material characteristics. *Journal of Food Engineering, 35* (2), 191-209.

Mavroudis, N.E., Gekas, V., Sjöholm, I. (1998[b]). Osmotic dehydration of apples. Shrinkage phenomena and the significance of initial structure on mass transfer rates *Journal of Food Engineering*, *38*, 101-123.

Mavroudis, N., Dejmek, P., Sjöholm, I. (2004). Studies on some raw material characteristics in different Swedish apple varieties. *Journal of Food Engineering, 62*, 121-129.

Mayor, L., Sereno, A.M. (2004). Modelling shrinkage during convective drying of food materials: a review. *Journal of Food Engineering, 61* (3), 373-386.

Mayor, L., Silva, M.A., Sereno, A.M. (2005). Microstructural changes during drying of apple slices. *Drying Technology 23* (9-11), 2261-2276.

Mazza, G. (1982). Moisture sorption isotherms of potato slices. *Journal of Food Technology, 17* (1), 47-54.

McMinn, W.A.M., Magee, T.R.A. (1997[a]). Physical characteristics of dehydrated potatoes-Part II. *Journal of Food Engineering, 33*, 49-55.

McMinn, W.A.M., Magee, T.R.A. (1997[b]). Kinetics of ascorbic acid degradation and non-enzymic browning of potatoes. *Food and Bioproducts Processing, 75* (C4), 223-231.

Mebatsion, H.K., Verboyen, P., Verlinden, B.E., Ho, Q.T., Nguyen, T.A., Nicolai, B.M. (2006).Microscale modeling of fruit tissue using Voronoi tessellations. *Computers and Electronics in Agriculture, 52*, 36-48.

Medina-Vivanco, M., Sobral, P.J.A., Hubinger, M.D. (2002). Osmotic dehydration of tilapia fillets in limited volume ternary solutions. *Chemical Engineering Journal, 86*, 199-205.

Mendoza, R., Schmalko, M.E. (2002). Diffusion coefficients of water and sucrose in osmotic dehydration of papaya. *International Journal of Food Properties, 5* (3), 537-546.

Mensah, J.K., Nelson, G.L., Herum, F.L., Richard, T.G. (1984). Mechanical properties related to soybean seedcoat cracking during drying. *Transactions of the ASAE, 27* (2), 550-555.

Micromeritics (1997). *AccuPyc™ 1330 Pycnometer*. Operator's Manual V2.02. Micromeritics: Norcorss, USA.

Micromeritics. Accupyc 1330 Pycnometer. Technical specifications. Norcross GA, USA: Micromeritics Instrument Corporation. Available in www.micromeritics.com/products/accupyc_specs.aspx. Access in: 27 June 2005.

Minguez-Mosquera, M.I., Hornero-Mendez, D. (1994). Comparative study of the effect of paprika processing on the carotenoids in peppers (*Capsicum annuum*) of the *bola* and *agridulce* varieties. *Journal of Agricultural and Food Chemistry*, *42*, 1555-1560.

Mohsenin, N.N. (1970). *Physical properties of plant and animal materials – structure, physical characteristics and mechanical properties*. Gordon and Breach Science Publishers: New York.

Mohsenin, N.N. (1986). *Physical properties of plant and animal materials – structure, physical characteristics and mechanical properties* (2nd ed.). Gordon and Breach Science Publishers: New York.

Monsalve-González, A., Barbosa-Cánovas, G., Cavalieri, R.P. (1993). Mass transfer and textural changes during processing of apples by combined methods. *Journal of Food Science, 58* (5), 1118-1124.

Monsalve-Gonzalez, A., Barbosa-Canovas, G.V., McEvily, A.J., Iyengar, R. (1995). Inhibition of enzymatic browning in apple products by 4-hexylresorcinol. *Food Technology, 49* (4), 110-118.

Moreira, R., Figueiredo, A., Sereno, A. (2000). Shrinkage of apple disks during drying by warm air convection and freeze drying. *Drying Technology, 18* (1-2), 279-294.

Moreira, R., Sereno, A.M. (2003). Evaluation of mass transfer coefficients and volumetric shrinkage during osmotic dehydration of apple using sucrose solutions in static and non-static conditions. *Journal of Food Engineering, 57*, 25-31.

Moreno-Castillo, E.J., Gonzalez-Garcia, R., Grajales-Lagunes, A., Ruiz-Cabrera, M.A., Abud-Archila, M. (2005). Water diffusivity and color of cactus pear fruits (Opuntia ficus indica) subjected to osmotic dehydration. *International Journal of Food Properties, 8*, 323-336.

Mujumdar, A.S. (1995*).* Preface to the first edition. In A.S. Mujumdar (Ed.), *Handbook of Industrial Drying*, *Vol. I* (2nd. Ed.). Marcel Dekker Inc.: New York.

Mujumdar, A.S., Menon, A.S. (1995). Drying of solids: principles, classification and selection of dryers. In A.S. Mujumdar (Ed.), *Handbook of Industrial drying, Vol. I* (2nd Ed.) (pp. 1-39). Marcel Dekker Inc.: New York.

Mulder, M. (1996). *Basic principles of membrane technology*. Kluwer Academic publishers: Dordretch, The Netherlands.

Mulet, A., Garcia-Reverter, J., Bon, J., Berna, A. (2000). Effect of shape on potato and cauliflower shrinkage during drying. *Drying Technology, 18* (6), 1201-1219.

Nejad, M.K., Tabil, L.G., Mortazavi, A., Kordi, A.S. (2003). Effect of drying methods on quality of pistachio nuts. *Drying Technology, 21* (5), 821-838.

Nesvabda, P. (2005). Thermal properties of unfrozen foods. In M.A. Rao, S.S.H. Rizvi, A.K. Datta (Eds.), *Engineering Properties of Foods* (3rd. Ed.). Taylor and Francis Group: Boca Raton, US.

Nieto, A.B., Salvatori, D.M., Castro, M.A., Alzamora, S.M. (2004). Structural changes in apple tissue during glucose and sucrose osmotic dehydration: shrinkage, porosity density and microscopic features. *Journal of Food Engineering*, *61*, 269-278.

Nsonzy, F., Ramaswamy, H.S. (1998). Osmotic dehydration kinetics of blueberries. *Drying Technology*, *16*(3-5), 725-741.

Oparka, K.J., Prior, D.A.M., Harris, N. (1990). Osmotic induction of fluid-phase endocytosis in onion epidermal cells. *Planta, 180* (4), 555-561.

Oswin, C.R. (1946). The kinetics of package life. *Journal of the Society of Chemical Industry-London, 65*, 419-421.

Palacha, Z., Lenart, A., Lewicki, P.P. (1997). Water vapour adsorption isotherms of pumpkin dried by osmotic-convection method. In *Proceedings of 5th Seminar of Properties of Water in Foods*. Warschau, Poland, 140-149.

Panagiotou, N.M., Karathanos, V.T., Maroulis, Z.B. (1998). Mass transfer modelling of the osmotic dehydration of some fruits. *International Journal of Food Science and Technology*, *33*, 267-284.

Park, K.J., Bin, A., Brod, F.P.R., Park, T.H.K.B. (2002). Osmotic dehydration kinetics of pear D'anjou (*Pyrus communis L.*). *Journal of Food Engineering, 52*, 293-298.

Payne, C.R., Labuza, T.P. (2005). Correlating perceived crispness intensity to physical changes in an amorphous snack food. *Drying Technology, 23*, 887-905.

Peleg, M (1993). Assessment of a semi-empirical four parameter general model for sigmoid moisture sorption isotherms. *Journal of Food Process Engineering*, 16, 21-37.

Perera, C.O. (2005). Selected quality attributes of dried foods. *Drying Technology, 23*, 717-730.

Perry, R.H., Green, D.W. (1999). *Perry's Chemical Engineers Handbook*, (7th ed.), McGraw-Hill Companies, New York.

Prestamo, G., Arroyo, G. (1998). High hydrostatic pressure effects on vegetable structure. *Journal of Food Science, 63* (5), 878-881.

Prothon, F., Ahrné, L.M., Funebo, T., Kidman, S., Langton, M., Sjöholm, I. (2001). Effects of combined osmotic and microwave dehydration of apple texture, microstructure and rehydration characteristics. *Lebensmittel Wissenschaft und Technologie, 34* (2), 95-101.

Prothon, F., Ahrné, L., Sjöholm, I. (2003). Mechanisms and prevention of plant tissue collapse during dehydration: a critical review. *Critical Reviews in Food Science and Nutrition, 43* (4), 447-479.

Ptitchkina, N.M., Danilova, I.A., Doxastakis, Kasapis, S., Morris, E.R., (1994). Pumpkin pectin: gel formation at unusually low concentration. *Carbohydrate Polymers, 23* (4), 265-273.

Quantachrome. Specifications – Automatic Gas Pycnometers. Boyton Beach, Florida, USA: Quantachrome Instruments. Available in www.quantachrome.com/Density/specifications-automatic-pycnometers.htm. Access in: 27 June 2005.

Quiles, A., Perez-Munuera, I., Hernando, I., Lluch, M.A. (2003). Impact of mass transport on microstructure of Granny Smith apple parenchyma during osmotic dehydration. *Journal of the Science of Food and Agriculture, 83*, 425-429.

Quiles, A., Hernando, I., Perez-Munuera, I., Larrea, V., Llorca, E., Lluch, M.A. (2005). Polyphenoloxidase (PPO) activity and osmotic dehydration in Granny Smith apple. *Journal of the Science of Food and Agriculture, 85*, 1017-1020.

Rahman, M.S. (2001). Toward prediction of porosity in foods during drying: a brief review. *Drying Technology, 19* (1), 1-13.

Rahman, M.S. (2003). A theoretical model to predict the formation of pores in foods during drying. *International Journal of Food Properties*, *6* (1), 61-72.

Rahman, M.S. (2005). Mass-volume-area related properties of foods. In M.A. Rao, S.S.H. Rizvi, A.K. Datta (Eds.)*, Engineering Properties of Foods* (3rd. Ed.). Taylor and Francis Group: Boca Raton, US.

Ramalho-Santos, M., Pissarra, J., Verissimo, P., Pereira, S., Salema, R., Pires, E., Faro, C.J. (1997). Cardosin A, an abundant aspartic proteinase, accumulates in protein storage vacuoles in the stigmatic papillae of *Cynara cardunculus L. Planta, 203*, 204-212.

Ramesh, M.N., Wolf, W., Tevini, D., Jung, G., (2001). Influence of processing parameters on the drying of spice paprika. *Journal of Food Engineering, 49*, 63-72.

Ramos, I.N., Silva, C.L.M., Sereno, A.M., Aguilera, J.M. (2004). Quantification of microstructural changes during first stage air drying of grape tissue. *Journal of Food Engineering, 62*, 159-164.

Rao, V.N.M., Quintero, X. (2005). Rheological properties of solid foods. In M.A. Rao, S.S.H. Rizvi, A.K. Datta (Eds.)*, Engineering Properties of Foods* (3rd. Ed.). Taylor and Francis Group: Boca Raton, US.

Raoult-Wack, A.L., Petitdemange, F., Giroux, F., Guilbert, S., Rios, G., Lebert, A. (1991[a]). Simultaneous water and solute transport in shrinking media – Part 2. A compartmental model for dewatering and impregnation soaking processes. *Drying Technology, 9* (3), 613-630.

Raoult-Wack, A.L., Guilbert, S., Le Maguer, M., Rios, G. (1991[b]). Simultaneous water and solute transport in shrinking media - Part 1. Application to dewatering and impregnation soaking process analysis (osmotic dehydration). *Drying Technology*, *9*, 589-612.

Raoult-Wack, A.L. (1994). Recent advances in the osmotic dehydration of foods. *Trends in Food Science and Technology, 5* (8), 255-260.

Rastogi, N.K., Raghavarao, K.S.M.S. (1997). Water and solute diffusion coefficients of carrot as a function of temperature and concentration during osmotic dehydration. *Journal of Food Engineering, 34*, 429-440.

Ratti, C. (1994). Shrinkage during drying of foodstuffs. *Journal of Food Engineering, 23* (1), 91-105.

Ratti, C. (2001). Hot air and freeze-drying of high-value foods: a review. *Journal of Food Engineering, 49*, 311-319.

Raven, P.H., Evert, R.F., Eichhorn, S.E. (1999). *Biology of Plants,* (6th Ed.). W.H. Freeman and Company: New York, U.S.

Rebouillat, S., Peleg, M. (1988). Selected physical and mechanical properties of commercial apple cultivars. *Journal of Texture Studies, 19*, 217-230.

Reeve, R.M. (1953). Histological investigations of texture in apples. II Structure and intercellular spaces. *Food Research , 18* (6), 604-617.

Richardson, T., Hyslop, D.B. (1985). Enzymes. In O.R. Fennema (Ed.) *Food Chemistry* (2nd Ed.). Marcel Dekker, Inc.: New York.

Riva., M., Campolongo, S., Leva, A.A., Maestrelli, A., Torreggiani, D. (2005). Structure-property relationships in osmo-air-dehydrated apricot cubes. *Food Research International, 38* (5), 533-542.

Robinson, R.W., Decker-Walters, D.S. (1997). *Cucurbits*. CAB International: Oxon, UK.

Rodrigues, A.C.C., Cunha, R.L., Hubinger, M.D. (2003). Rheological properties and colour evaluation of papaya during osmotic dehydration processing. *Journal of Food Engineering*, 59, pp. 129-135.

Roos, Y., Karel, M. (1991). Plasticizing effect of water on thermal behaviour and crystallization of amorphous food model. *Journal of Food Science, 56*, 38-43.

Rossello, C., Simal, S., SanJuan, N., Mulet, A. (1997). Nonisotropic mass transfer model for green bean drying. *Journal of Agricultural and Food Chemistry, 45*, 337-342.

Ruiz, D., Egea, J., Tomas-Barberan, F.A., Gil, M.I. (2005). Carotenoids from new apricot (*Prunus armeniaca L.*) varieties and their relationship with flesh and skin color. *Journal of Agricultural and Food Chemistry, 53*, 6368-6374.

Russ, J.C. (2004). *Image analysis of food microstructure*. CRC Press LLC.: Boca Raton, Florida.

Sa, M.M., Sereno, A.M. (1999). The kinetics of browning measured during the storage of onion and strawberry. *International Journal of Food Science and Technology, 34,* 343-349.

Salunkhe, D.K., Bolin, H.R., Reddy, N.R. (1991). *Storage, processing and nutritional quality of fruits and vegetables, vol. II* (2nd Ed.). CRC Press Inc.: Boca Raton, Florida.

Salvatori, D., Andres, A., Albors, A., Chiralt, A., Fito, P. (1998). Structural and compositional profiles in osmotically dehydrated apple. *Journal of Food Science, 63* (4), 606-610.

Salvatori, D., Andrés, A., Chiralt, A., Fito, P. (1999[a]). Osmotic dehydration progression in apple tissue II: generalized equations for concentration prediction. *Journal of Food Engineering*, *42*, 133-138.

Salvatori, D., Andrés, A., Chiralt, A., Fito, P. (1999[b]). Osmotic dehydration progression in apple tissue I: spatial distribution of solutes and moisture content. *Journal of Food Engineering*, *42*, 125-132.

Salwin, H. (1959). Defining minimum moisture contents for dehydrated foods. *Food Technology, 13* (10), 594-595.

Sanjinez-Argandona, E.J., Cunha, R.L., Menegalli, F.C., Hubinger, M.D. (2005). Evaluation of total carotenoids and ascorbic acid in osmotic pretreated guavas during convective drying. *Italian Journal of Food Science, 17* (3), 305-314.

Saputra, D. (2001). Osmotic dehydration of pineapple. *Drying Technology, 19* (2), 415-425.

Saurel, R., Raoult-Wack, A.L., Rios, G., Guilbert, S. (1994). Mass transfer phenomena during osmotic dehydration of apple I. Fresh plant tissue. *International Journal of Food Science and Technology*, 29, 531-542.

Scanlon, M.G., Pang, C.H., Biliaderis, C.G. (1996). The effect of osmotic adjustment on the mechanical properties of potato parenchyma. *Food Research International, 29* (5-6), 481-488.

Schiffmann, R.F. (1995). Microwave and dielectric drying. In A.S. Mujumdar (Ed.), *Handbook of Industrial drying, Vol. I* (2nd Ed.) (pp. 345-372). Marcel Dekker Inc.: New York.

Schrader, G.W., Litchfield, J.B. (1992). Moisture profiles in a model food gel during drying: measurement using magnetic resonance imaging and evaluation of the Fickian model. *Drying Technology, 10* (2), 295-332.

Schwartzberg, H.G., Chao, R.Y. (1982). Solute diffusivities in leaching processes. *Food Technology, February*, 73-86.

Scott, W.J. (1957). Water relations of food spoilage microorganisms. *Advances in Food Research, 7*, 83.

Segui, L., Fito, P.J., Albors, A., Fito, P. (2006). Mass transfer phenomena during osmotic dehydration of apple isolated protoplasts (*Malus domestica* var. Fuji). *Journal of Food Engineering, 77* (1), 179-187.

Sereno, A.M., Moreira, R., Martinez, E. (2001). Mass transfer coefficients during osmotic dehydration of apple in single and combined aqueous solutions of sugar and salt. *Journal of Food Engineering, 47*, 43-49.

Sherwood, T.K. (1929). The drying of solids I. *Industrial and Engineering Chemistry*, *21* (1), 12-16.

Shi, X.Q., Fito, P., Chiralt, A. (1995). Influence of vacuum treatment on mass transfer during osmotic dehydration of fruits. Food Research International, 28 (5), 445-454.

Shi, J., Le Maguer, M., Kakuda, Y., Liptay, A., Niekamp, F. (1999). Lycopene degradation and isomerization in tomato dehydration. *Food Research International, 32*, 15-21.

Shi, J., Le Maguer, M. (2002). Osmotic dehydration of foods: mass transfer and modeling aspects. *Food Reviews International, 18* (4), 305-335.

Shimada, Y., Roos, Y., Karel, M. (1991). Oxidation of methyl linoleate encapsulated in amorphous lactose based food model. *Journal of Agricultural and Food Chemistry, 39*, 637-641.

Silva, M.A., Miranda, M.N.N. (2003). Estimation of properties of ternary mixtures of solids using the mixing rule. *Powder Technology*, *134* (1-2), 16-23.

Simal, S., Rossello, C., Berna, A., Mulet, A. (1998). Drying of shrinking cylinder-shaped bodies. *Journal of Food Engineering, 37*, 423–435.

Smith, S.E. (1947). Sorption of water vapor by proteins and high polymers. *Journal of the American Chemical Society*, 69, 646-651.

Sokhansanj, S., Jayas, D.S. (1995). Drying of foodstuffs. In A.S. Mujumdar (Ed.), *Handbook of Industrial drying, Vol. I* (pp. 589-625). Marcel Dekker Inc.: New York.

Spiess, W.E.L., Behsnilian, D. (1998). Osmotic treatments in food processing. Current state and future needs. In *Proceedings of the 11th International Drying Symposium (IDS '98)*, vol. A., pp 47-56. Haldiki, Greece.

Suzuki, K., Kubota, K., Hasegawa, T., Hosaka, H. (1976). Shrinkage in dehydration of root vegetables. *Journal of Food Science, 41*, 1189-1193.

Taiwo, K.A., Angersbach, A., Ade-Omowaye, B.I.O., Knorr, D. (2001). Effects of pretreatments on the diffusion kinetics and some quality parameters of osmotically dehydrated apple slices. *Journal of Agricultural and Food Chemistry, 49* (6), 2804-2811.

Talens, P. (2002). Osmotic treatments on the cryoprotection of strawberry and kiwifruit. Ph.D. dissertation. Universidad Politecnica de Valencia: Valencia, Spain.

Telis, V.R.N., Murari, R.C.B.D.L., Yamashita, F. (2004). Diffusion coefficients during osmotic dehydration of tomatoes in ternary solutions. *Journal of Food Engineering*, *61*, 253-259.

Telis, V.R.N., Telis-Romero, J., Gabas, A.L. (2005). Solids rheology for dehydrated food and biological materials. *Drying Technology, 23*, 759-780.

Teotia, M.S. (1992). Advances in chemistry and technology of pumpkins. *Indian Food Packer, Jan-Feb,* 9-31.

Torreggiani, D. (1993). Osmotic dehydration in fruit and vegetable processing. *Food Research International*, 26, 59-68.

Torreggiani, D., Bertolo, G. (2001). Osmotic pre-treatments in fruit processing: chemical, physical and structural effects. *Journal of Food Engineering, 49*, 247-253.

Torres, J.D., Talens, P., Escriche, I., Chiralt, A. (2006). Influence of process conditions on mechanical properties of osmotically dehydrated mango. *Journal of Food Engineering*, *74* (2), 240-246.

Torriga, E., Esveld, E., Scheewe, I., van den Berg, R., Bartels, P. (2001). Osmotic dehydration as a pre-treatment before combined microwave-hot-air drying of mushrooms. *Journal of Food Engineering, 49*, 185-191.

Tregunno, N.B., Goff, H.D., (1996). Osmodehydrofreezing of apples: structural and textural effects. *Food Research International, 29* (5-6), 471-479.

Trujillo, F.J., Wiangkaew, C., Pham, Q.T. (2007). Drying modeling and water diffusivity in beef meat. *Journal of Food Engineering, 78* (1), 74-85. doi:10.1016/j.jfoodeng.2005.09.010.

Uddin, M.B., Ainsworth, P., Ibanoglu, S. (2004). Evaluation of mass exchange during osmotic dehydration of carrots using response surface methodology. *Journal of Food Engineering, 65* (4), 473-477.

Van den Berg C. (1984).Desorption of water activity of foods for engineering purposes by means of the G.A.B. model sorption. In B.M. McKenna (Ed), *Engineering and Foods* (Vol. 1, pp. 311-321). Elsevier Applied Science Publishers: New York.

van der Wel, P.G.J. (1998). Trends in powder technology. *Powder Handling & Processing*, *10*, 139-142.

Van Nieuwenhuijzen, N.H., Zareifard, M.R., Ramaswamy, H.S. (2001). Osmotic drying kinetics of cylindrical apple slices of different sizes. *Drying Technology, 19* (3-4), 525-545.

Vasconcellos, J.C. (1949). *Botânica agrícola. II Parte: Fisiologia do crescimento e da reprodução sistemática-fitogeografi*a. Livraria Sá da Costa: Lisboa, Portugal.

Vázquez, G., Chenlo, F., Moreira, R. (2003). Sorption isotherms of lupine at different temperatures. *Journal of Food Engineering, 60* (4), 449-452.

Vursavus, K., Kelebek, H., Selli, S. (2006). A study on some chemical and physico-mechanic properties of three sweet cherry varieties (*Prunus avium* L.) in Turkey. *Journal of Food Engineering*, *74* (4), 568-575.

Walde, P.M. (2002). Osmotic dehydration of cod fillet with skin in a stagnant brine. *Drying Technology, 20* (1), 157-173.

Waldron, K.W., Smith, A.C., Parr, A.J., Ng, A., Parker, M.L. (1997). New approaches to understanding and controlling cell separation in relation to fruit and vegetable texture. *Trends in Food Science and Technology*, *8* (7), 213-221.

Waliszewski, K.N., Cortes, H.D., Pardio, V.T., Garcia, M.A. (1999). Color parameter changes in banana slices during osmotic dehydration. *Drying Technology, 17* (4-5). 955-960.

Waliszewski, K.N., Pardio, V.T., Ramirez, M. (2002[a]). Effect of EDTA on color during osmotic dehydration of banana slices. *Drying Technology, 20* (6), 1291-1298.

Waliszewski, K.N., Pardio, V.T., Ramirez, M. (2002[b]). Effect of chitin on color during osmotic dehydration of banana slices. *Drying Technology, 20* (3), 719-726.

Wang, N., Brennan, J.G. (1995). Changes in structure, density and porosity of potato during dehydration. *Journal of Food Engineering, 24* (1), 61-76.

Webb, P.A., Orr, C. (1997). *Analytical methods in fine particle technology*. Micromeritics Instrument Corporation: Norcross.

Weemaes, C.A., Ooms, V., Van Loey, A.M., Hendrickx, M. E. (1999). Kinetics of chlorophyll degradation ands color loss in heated broccoli juice. *Journal of Agricultural and Food Chemistry*, 47, 2404-2409.

Weisser, H., Weber, J., Loncin, M. (1982).Wasserdampf-sorptionisothermen von zuckeraustauschtoffen im temperaturbereich von 25 bis 80ºC. *Zeirschrift für Lebensmittel-Technologie und-Verfahrenstechnik, 33*, 89-87.

Wenian, C., Duprat, F., Roudot, A.C. (1991). Evaluation of the importance of the cellular tissue geometry on the strains observed on apples after a compression or an impact. *Sciences des Aliments, 11*, 99-110.

Whistler, R.L., Daniel, J.R. (1985). Carbohydrates. In O.R. Fennema (Ed.) *Food Chemistry* (2nd E.). Marcel Dekker, Inc.: New York.

White, K. L., Bell, L. N. (1999). Glucose loss and Maillard Browning in solids as affected by porosity and collapse. *Journal of Food Science, 64* (6), 1010-1014.

Wilford, L.G., Sabarez, H., Price, W.E. (1997). Kinetics of carbohydrate change during dehydration of d'Agen prunes. *Food Chemistry, 59* (1), 149-155.

Williams, M.L., Landel, R.F., Ferry, J.D. (1955). The temperature dependence of relaxation mechanisms in amorphous polymers and other glass-forming liquids. *Journal of American Chemical Society, 77*, 3701-3707.

Wolf, W., Spiess, W.E.L., Jung, G. (1985[a]) *Sorption isotherm and water activity of food materials: a bibliography*. Science and Technology Publishers: Essex.

Wolf, W., Spiess, W.E.L., Jung, G. (1985[b]). Standarization of isotherm measurement (cost project 90 and 90 bis). In D. Simatos and J.L. Multon (Eds.)*, Properties of water in foods in relation to quality and stability* (pp. 661-669). Martinus Nijhoff Publishers: Dordrecht.

Yang, D.C., Le Maguer, M. (1992). Osmotic dehydration of strawberries in a batch recirculation system. *Journal of Food Quality, 15* (6), 387-397.

Yao, Z., Le Maguer, M. (1996). Mathematical modelling and simulation of mass transfer in osmotic dehydration processes. Part I: conceptual and mathematical models. *Journal of Food Engineering, 29*, 349-360.

Zdunek, A., Umeda, M. (2005). Influence of cell size and cell wall volume fraction on failure properties of potato and carrot tissue. *Journal of Texture Studies, 36*, 25-43.

Zogzas, N.P., Maroulis, Z.B., Marinos-Kouris, D. (1994). Densities, shrinkage and porosity of some vegetables during air drying. *Drying Technology*, *12* (7), 1653-1666.

Zogzas, N.P., Maroulis, Z.B., Marinos-Kouris, D. (1996). Moisture diffusivity data compilation in foodstuffs. *Drying Technology*, *14*(10), 2225-2253.